PRECLINICAL AND CLINICAL PHARMACOLOGY OF ORAL ANTICANCER DRUGS

ISBN/EAN 9789071382789

Cover design: Viktor Beekman, Amsterdam, www.alfred.nl
Printed by: Gildeprint Drukkerijen BV, Enschede, The Netherlands

Preclinical and clinical pharmacology of oral anticancer drugs

Preklinische en klinische farmacologie van
orale antikanker middelen
(met een samenvatting in het Nederlands)

PROEFSCHRIFT

ter verkrijging van de graad van doctor
aan de Universiteit Utrecht
op gezag van rector magnificus, prof. dr. J.C. Stoof,
ingevolge het besluit van het college voor promoties
in het openbaar te verdedigen
op woensdag 21 januari 2009 des middags te 12.45 uur

door

Roosje Lizelot Oostendorp

geboren op 6 juni 1978 te Deventer

Promotoren: Prof. dr. J.H.M. Schellens
Prof. dr. J.H. Beijnen

Co-promotor: Dr. O. van Tellingen

The research described in this thesis was performed at the Division of Experimental Therapy and the Department of Medical Oncology, The Netherlands Cancer Institute / Antoni van Leeuwenhoek Hospital and the Department of Pharmacy & Pharmacology, The Netherlands Cancer Institute / Slotervaart Hospital, Amsterdam, The Netherlands.

Publication of this thesis was financially supported by:

The Netherlands Cancer Institute, Amsterdam, The Netherlands
The Netherlands Laboratory for Anticancer Drug Formulation (NLADF), Amsterdam, The Netherlands
Boehringer Ingelheim bv, Alkmaar, The Netherlands
GlaxoSmithKline, Zeist, The Netherlands
Pfizer bv, Capelle a/d Ijssel, The Netherlands
AstraZeneca BV, Zoetermeer, The Netherlands
Bristol-Myers Squibb B.V., Woerden, The Netherlands
Merck Sharp & Dohme B.V., Haarlem, The Netherlands
Novartis Pharma B.V., Arnhem, The Netherlands
Fuji Film Manufacturing Europe B.V., Tilburg, The Netherlands

Contents

CHAPTER 1

Introduction

CHAPTER 1.1

The biological and clinical role of drug transporters at the intestinal barrier

Roos L. Oostendorp, Jos H. Beijnen, Jan H.M. Schellens

Cancer Treatment Reviews 2008 (in press);
ABC Transporters and Multidrug Resistance,
edited by Boumendjel A, Boutonnat J, Robert J,
Medicinal Research Reviews series published by Willy 2008

Abstract

Nowadays, over 25% of all anticancer drugs are developed as oral formulations and this percentage is expected to increase substantially. Oral administration of drugs can be patient convenient and practical and is preferred for many reasons. To enable oral drug therapy, adequate oral bioavailability must be achieved. Factors that have proven to be important in explaining the often variable and low oral bioavailability of many orally applied anticancer drugs is the presence of ATP-Binding Cassette drug transporters (ABC-transporters) and solute carrier (SLC) transporters. During the past two decades, significant progress has been made in understanding the pharmacological and physiological role of ABC drug efflux and SLC uptake transporters in the disposition of a broad range of drugs, toxins, endogenous compounds and their metabolites. We focus on the expression of ABC and SLC drug transporters at the intestinal barrier and the impact of these transporters on the absorption and disposition of a wide range of orally administered drugs. Furthermore, preclinical and clinical examples of modulation of the activity of intestinal transporters to increase the systemic exposure of orally administered drugs will be reviewed. Screening of test drugs, nutrients and other molecules for ABC and SLC transporter substrates or inhibitors is a useful way to predict their intestinal absorption. Recognition of the importance of intestinal transporters could guide the design and development of oral drugs.

Introduction

In general, oral administration of drugs is patient convenient and practical and has several advantageous over intravenous (i.v.) administration. Patients are able to take oral medication themselves, there is no need for expensive and frequent hospitalization, and the discomfort of an injection or infusion and risk for injection or infusion associated adverse events is absent (1, 2). Additionally, chronic exposure following repeated oral administration can have clinical benefits over intermittent therapy. However, oral administration of drugs may lead to limited and variable bioavailability (1, 3, 4). There are a number of important factors that can explain the variable and/or low oral bioavailability of drugs (5) including 1) physico-chemical properties of the drug (e.g. lipophilicity, solubility), 2) pharmaceutical factors (e.g. dosage form), and 3) physiological factors (e.g. gastric emptying rate, gastric and intestinal pH, blood flow to the intestine, metabolic enzyme activity) (6, 7). Furthermore, also the expression and activity of ATP-Binding Cassette drug transporters (ABC transporters), solute carrier (SLC) transporters and the metabolic cytochrome P450 enzymes expressed in the gastrointestinal (GI) tract have proven to limit oral bioavailability (6, 8, 9). The combined activity of drug transporters and metabolic enzymes may explain the low and variable bioavailability of a range of drugs (10). In this article we will focus on the well-characterized ABC and SLC transporters localized at the intestinal barriers. ABC transporters extrude drugs, xenobiotics and metabolites from the intestine, in an active ATP dependent manner, and thereby prevent drug and/or xenobiotic absorption into the blood or lymph circulation and protect the body against acute and chronic toxicity of toxins (11, 12). SLC transporters do not require ATP and transport substrate drugs according to their concentration gradient. Thereby SLC transporters improve the intestinal absorption of a wide range of drugs (13). Overall, ABC and SLC transporters play a pronounced role in the pharmacokinetics (i.e. absorption, tissue distribution and elimination) of a broad range of drugs, toxins, endogenous compounds and their metabolites.

Drug transporters at the intestinal barrier

Mechanism of transport through the intestinal epithelium

The human small intestine is approximately 6 m long and has an inner diameter of 2.5 to 3 cm. It is divided into three structural parts: the duodenum, jejunum and ileum, which comprise 5%, 50% and 45% of the length, respectively. The small intestine represents the principle site of absorption for any ingested compound, whether dietary, therapeutic, or

toxic. Drug absorption occurs predominantly on the outer surface of the GI epithelium (specifically enterocytes). The highly differentiated villi of these cells have an absorptive function (Fig. 1). The role of the colon in drug absorption is limited, even though it has the capacity to be an absorption site for certain types of drugs.

In the small intestine different forms of drug transport can be distinguished: paracellular (between cells) and transcellular (across cells) transport (14). Paracellular permeation is only possible for small molecules and occurs through the gaps (tight junction) in the epithelial membrane (Fig. 1). However, absorption via this route is generally low since intercellular tight junctions restrict free transepithelial movement between epithelial cells. Transcellular transport from lumen to blood requires uptake across the apical membrane, followed by transport across the cytosol, the exit across the basolateral membrane and into the blood compartment. Transcellular transport can be divided into passive diffusion, endocytosis and carrier-mediated transport. Passive diffusion is the route available for most drugs entering the systemic circulation and depends largely on the physico-chemical properties of a drug, such as lipophilicity (Fig. 1). The lipophilicity factor is commonly used to characterize the solubility of a drug in cell membranes. Endocytosis is a process by which a particle enters into a cell without passing through the cell membrane (Fig. 1). The transcellular absorption or efflux of hydrophilic drugs, toxins or metabolites can be facilitated via specific carrier-mediated transport (Fig. 1). Numerous drug transporting membrane proteins have been described in intestinal tissues, and most of them belong to two major transporter superfamilies, the ATP-binding cassette (ABC) and solute carrier (SLC) family. The ABC transporter family acts in an ATP dependent manner and can pump against a steep concentration gradient, in contrast, the SLC family of transporters does not require ATP and transports the drugs according to their concentration gradient (Fig. 1). These transport mechanisms are involved in the efficient absorption of a wide range of structurally different drugs, carcinogens and other toxins. In addition, drugs or toxic compounds that cross the apical membrane and are substrates for apical transporters, are extruded back into the lumen and thereby limiting the uptake (Fig. 1) (15). Three major subfamilies of ABC transporters, such as P-glycoprotein (MDR1; gene ABCB1), the multidrug resistance proteins (MRPs; gene ABCCs) and the breast cancer resistance protein (BCRP; gene ABCG2) are expressed at the apical or basolateral surface of epithelial cells lining the intestine (Fig. 1) (9). Drug transporter-relevant SLC members in the intestine at the apical surface of epithelial cells include, solute carrier organic anion transporter families (OATP subfamilies; gene SLCO), solute carrier peptide transporter family (PepT1; gene SLC15A1) and organic zwitterion/cation transporters (OCTNs; gene SLC22) (Fig. 1) (9). Organic anion or cation transporter families (OATs or OCTs; both SLC22 gene families) have also been identified in the

intestine, but seem to be of greater importance for transporting small endogenous molecules in the kidney. Below, the expression levels of well-characterized ABC and SLC transporters present on the three structural parts of the small intestines, i.e. the duodenum, jejunum, and ileum, are summarized.

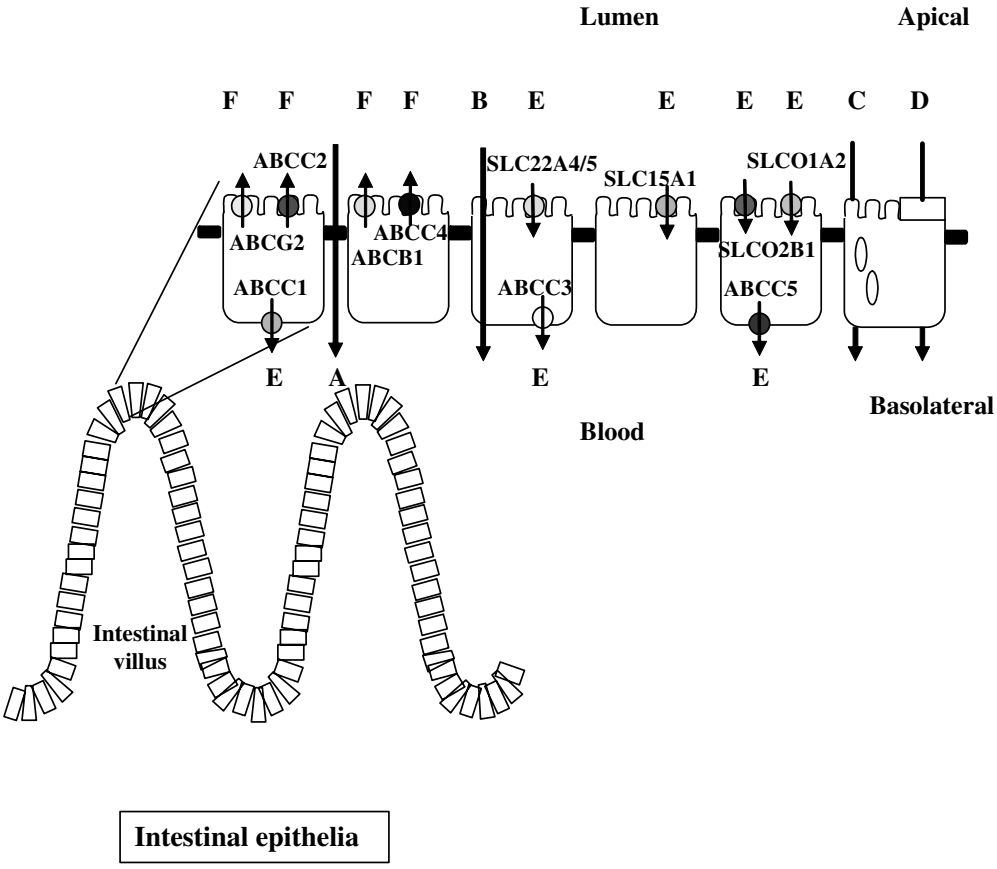

Figure 1. Mechanisms of transport through the intestinal epithelium and localization of ABC and SLC drug transporters; ABCB1, ABCG2, ABCC1-5, SLCO1A2/2B1, SLC22A4/5 and SLC15A1 A) passive diffusion via tight junctions; B) passive diffusion; C) endocytosis; D) carrier mediated transport; E) carrier mediated uptake; F) carrier mediated efflux.

ABC transporters expressed at the intestinal barrier

Different families of ABC drug transporting proteins have been described in intestinal tissues, including ABCB1 (MDR1), ABCC1-6 (MRP1-6) as well as ABCG2 (BCRP). Available data demonstrate that the expression levels of ABC transporters vary over the total length of the human GI tract. ABCB1 is expressed in the apical membrane of epithelial cells, such as enterocytes, and ABCB1 expression gradually increases from the stomach and duodenum to the colon (Fig. 2). Its messenger RNA (mRNA) level in colon tissue is similar to that in ileum tissue, which is approximately six-fold higher than in the duodenum (16-18). Moreover, characterization of the regional intestinal kinetics of drug efflux in rat and human intestine revealed that the magnitude of ABCB1-mediated efflux correlated with the expression levels of ABCB1. The efflux ratios (B-to-A permeability/A-to-B permeability; B and A denote Basolateral and Apical membrane, respectively) in the ileum are typically higher than in other regions of the intestine (19).

Besides ABCB1, other ABC transporters such as ABCC2 and ABCG2 are also expressed at the apical surface of epithelial cells throughout the small intestine and colon. ABCC2 expression is highest in the duodenum and subsequently decreases towards the terminal ileum and colon (Fig. 2) (20, 21). ABCG2 mRNA expression is also maximal in the duodenum and decreases continuously into the direction of the rectum (22). Surprisingly, ABCG2 and ABCC2 were more abundant in the jejunum than ABCB1 transcripts. Thus, the expression of a number of efflux transporters in the jejunum is equal to, or even higher than ABCB1, suggesting significant roles for these proteins (in particular ABCG2 and ABCC2) in intestinal drug efflux (23). In contrast with these apically localized transporters, ABCC1 and ABCC3 are expressed at the basolateral surface of gastrointestinal cells in the small intestine and colon (24, 25). ABCC3 expression is higher in the duodenum, ileum and colon relative to the jejunum (Fig. 2) (26). Zimmerman et al. (20) demonstrated that ABCC3 among ABCC1-5 and ABCB1 was the most abundantly expressed ABCC transporters in the duodenum and all segments of the colon, and they showed that ABCB1 had the highest level of expression in the terminal ileum. The differences in ABC transporter expression levels in the intestinal tissues between studies could be due to variability between patients and the small patient groups included. Also genetic polymorphisms in the ABC drug transporter genes could play a role on drug transporter function and could influence the bioavailability of drugs and toxins.

The expression levels of the individual ABC transporters over the total length of the GI tract, as described above, is expected to have an impact on the site of absorption of drugs. A study in humans with Cyclosporin A (CsA), an immunosuppressant drug, provides a good example of the impact of ABCB1 on oral absorption. CsA transport has been shown to be impaired by ABCB1 in a variety of ABCB1-containing *in vitro* systems (27). The influence of uneven distribution of ABCB1 in the intestine was demonstrated in a clinical study with CsA (28). CsA was given to ten volunteers at different parts of the GI tract (stomach, jejunum/ileum, and colon). The absorption of CsA increased in the order of, stomach > jejunum/ileum > colon in line with the increase in expression of ABCB1. Furthermore, Lown et al. (29) demonstrated that 30% of the variability in oral C_{max} and 17% of the variability in oral clearance of CsA in humans can be explained by the inter-individual variation in intestinal ABCB1 levels. Therefore, ABCB1 not only limits the absorption of CsA, but also contributes to the inter-individual variation in absorption and consequently to the variability in systemic exposure after oral administration.

In conclusion, preclinical and clinical studies clearly demonstrate that ABC transport-mediated intestinal efflux limits absorption of substrate drugs, and can result in variable pharmacokinetics and has a major influence on drug disposition of orally administered compounds.

SLC transporters expressed at the intestinal barrier

Different families of SLC drug transporting proteins have been described in intestinal tissues, including SLCO1A2 (OATP-A; OATP1A2), SLCO2B1 (OATP-B; OATP2B1), SLC22A4 and SLC22A5 (OCTN1 and 2) as well as SLC15A1 (PepT1) (Fig. 1) (9, 30). The expression levels of SLC transporters vary over the total length of the human GI tract (Fig. 2) (31-33). SLC15A1 was found primarily at the apical surface of epithelial cells in the small intestine and appears to have higher expression levels in the duodenum than in jejunum or ileum. Besides SLC15A1, other SLC transporters such as SLCO1A2, SLCO2B1 are probably also expressed at the apical surface of epithelial cells throughout the small intestine, however, the precise location of these transporters needs to be further studied (34). The difference in expression levels of SLC22A4 and SLC22A5 in the duodenum, jejunum or ileum was limited (9, 30).

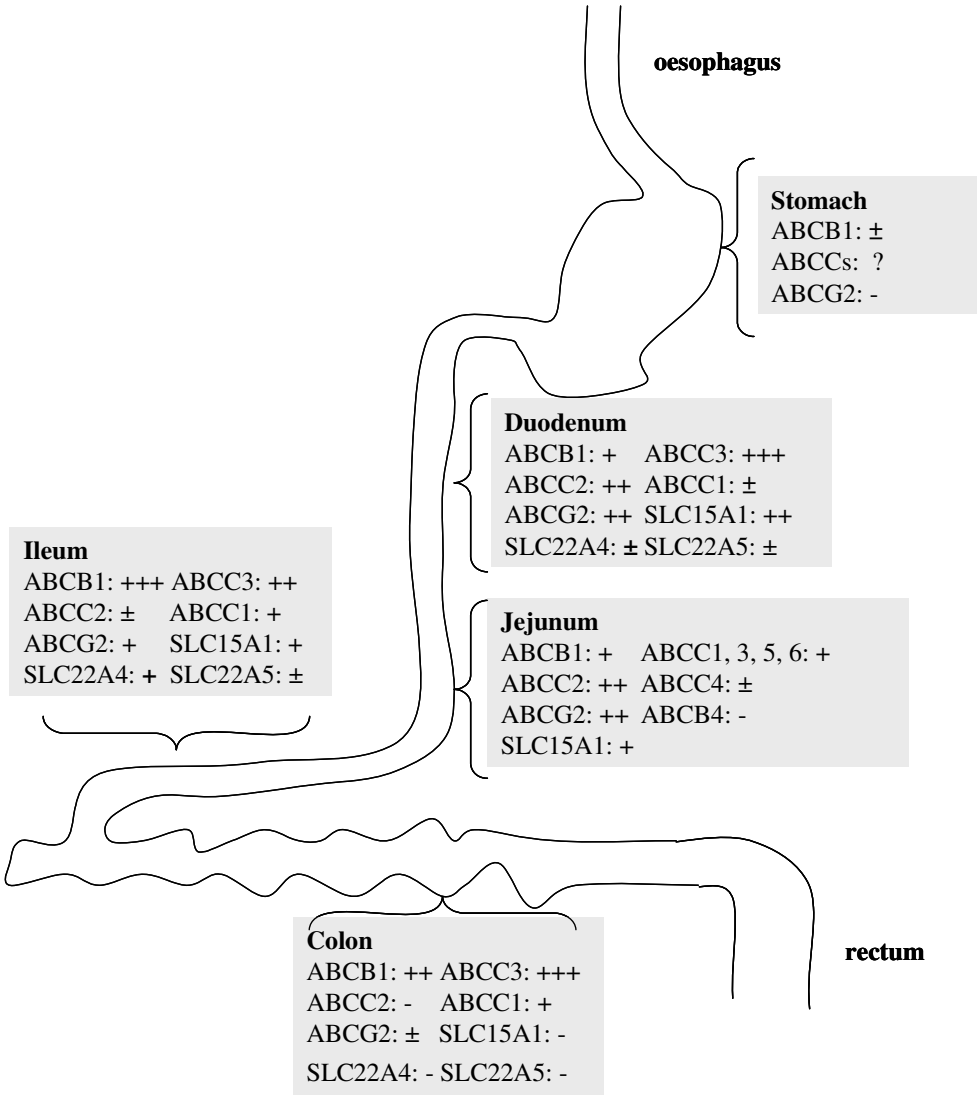

Figure 2. Expression levels of ABC and SLC transporters in different parts of the human intestine.

Impact of intestinal drug transporters on oral drug absorption

ABCB1-mediated secretory transport

ABCB1 is probably the best known secretory drug transporter in the gut. It can transport a variety of drugs of many therapeutic classes with diverse structures and pharmacological activities. The number of substrates and inhibitors for ABCB1 is continuously increasing and includes anticancer agents, antibiotics, antivirals, calcium channel blockers and immune suppressive agents (Table 1). Naturally occurring substrates for ABCB1 include biologically active compounds in normal diet, such as plant chemicals. These compounds act with ABCB1 as part of detoxification and excretion pathways.

The first evidence of the involvement of intestinal ABCB1 in drug absorption was obtained *in vitro* with human colonic adenocarcinoma (Caco-2) cells, in which ABCB1 was highly expressed at the apical domain, cultured on porous supporting materials. In these cells the intestinal B-to-A secretory transport of the anticancer drug vinblastine was 10-fold higher than the A-to-B absorptive transport (35). Moreover, the secretory transport of vinblastine could be reduced significantly when ABCB1 was inhibited by verapamil. Using similar *in vitro* approaches, numerous studies have been performed in which ABCB1 secreted several other drugs (36-38). In fact, Caco-2 cell monolayers have been widely used as an *in vitro* model of human intestinal mucosa to evaluate intestinal drug absorption of investigational new drugs (39). However, Caco-2 cells are not the ideal tool for high-throughput screening, because it is time-consuming to culture and to maintain these cells. Another major disadvantage is that Caco-2 cells have a relatively low expression of other transporters, e.g. ABCG2, while this transporter is highly abundant in the jejunum where it plays an important role in drug efflux from the systemic circulation into the feces (23, 40). This will probably result in an under estimation of the importance of ABCG2 mediated transport of orally applied drugs. Madin-Darby canine kidney II epithelial cells (MDCKII) or porcine kidney epithelial cells (LLC-PK1), transfected with various ABC drug transporters, have been helpful in demonstrating drug transporter activity (41-43). The relatively short culture time required for these cells make the LLC-PK1 and MDCKII cells excellent tools for identifying drug transporter activity. However, these cells are not able to express differentiation features characteristic of mature intestinal cells.

Direct evidence supporting a role for ABCB1 in limiting intestinal absorption was derived from *in vivo* studies with ABCB1 knockout mice (44). ABCB1 knockout mice were developed by Schinkel et al. (45), to investigate ABCB1 function *in vivo*. Mice have two mdr1 genes, mdr1a and mdr1b, which together appear to perform the same function as human MDR1 (ABCB1). Knockout mice were generated for both genes, mdr1a$^{-/-}$, mdr1b$^{-/-}$

as well as mdr1a/1b$^{-/-}$ and all display normal viability, fertility, and lifespan, with no obvious physiological abnormalities (45, 46). A good example of the contribution of ABCB1 to the disposition of paclitaxel, an anticancer agent, was a study in ABCB1 knockout and wild-type (WT) mice (6). When paclitaxel was administered orally to WT mice, the bioavailability was very low (< 10%). The systemic exposure to paclitaxel was two- and six-fold higher in the ABCB1 knockout versus WT mice after intravenous (i.v.) and oral dosing, respectively. Consequently, the apparent oral bioavailability of paclitaxel increased from 11% in the WT to 35% in the ABCB1 knockout mice. These results indicated that oral absorption of paclitaxel was effectively limited by ABCB1-mediated efflux from the intestinal epithelial cells back into the lumen. The bioavailability did not increase to 100%, probably due to other drug transporters or first-pass intestinal/hepatic extraction by metabolizing enzymes (6, 47, 48). Besides these examples, intestinal ABCB1-mediated efflux of a wide range of other drugs, such as docetaxel, vinblastine, etoposide, digoxin, indinavir, saquinavir, tacrolimus, nelfinavir and talinolol, has been demonstrated in ABCB1 knockout mice (Table 1) (38, 49-53).

Based on this observation, several studies have been initiated with ABCB1 inhibitors in combination with paclitaxel in order to enhance the oral bioavailability (Table 1). Studies in mice revealed that co-administration of PSC 833, a CsA analogue and potent ABCB1 inhibitor, and paclitaxel resulted in a 10-fold increase in systemic exposure to paclitaxel (54). A similar study was performed with CsA and paclitaxel that has shown comparable effects (55). Additionally, it was noted that the plasma levels of paclitaxel obtained in WT mice co-treated with CsA were even higher than those obtained in ABCB1 knockout mice that were treated with the same dose of oral paclitaxel alone. This can be explained by decreased elimination of paclitaxel by inhibition of the metabolic enzyme cytochrome P450 3A (CYP3A) (55, 56). However, blockade of other yet unidentified drug transporters or drug eliminating pathways cannot be ruled out. Because the use of CsA for long-term oral dosing may be complicated by potential immunosuppressive effects, an alternative, non-immunosuppressive ABCB1 blocker, GF120918 (elacridar), was explored to enhance the oral bioavailability of paclitaxel. Bardelmeijer et al. demonstrated that elacridar significantly increased the oral bioavailability of paclitaxel (57). The oral bioavailability of paclitaxel in WT mice increased from 8.5% to 40% and the pharmacokinetics of paclitaxel in WT mice receiving elacridar were similar to that found in ABCB1 knockout mice. Thus, elacridar effectively blocks ABCB1 in the intestine and most likely does not interfere with other pathways involved in paclitaxel uptake or elimination. Of note, it was demonstrated that elacridar is also an effective inhibitor of the ABC drug transporter ABCG2 (58).

Studies in mice were also performed with the anticancer agent docetaxel, another ABCB1 substrate. These studies confirmed that ABCB1 also plays an important role in the low bioavailability of docetaxel (52). In addition, co-administration of the HIV protease inhibitor, ritonavir, an effective inhibitor of CYP3A4 with minor ABCB1 inhibiting properties, was tested in combination with docetaxel in mice (52). An increase was shown in the apparent bioavailability of docetaxel from 4% to 183%: thus, extensive first-pass metabolism and inhibition of the elimination may largely contribute to the low bioavailability of oral docetaxel in mice. In addition, Herwaarden et al. (59), showed *in vivo* that expression of CYP3A4 in the intestine dramatically decreased absorption of docetaxel into the bloodstream. Inhibiting ABCB1 as well as CYP3A4 could be a successful strategy to increase the systemic exposure to oral docetaxel**.** These findings may guide the clinical development of combinations of a poorly absorbed anticancer drug plus a boosting agent, such as CsA or ritonavir.

Besides inhibitors of ABC transporters*,* clinical and preclinical findings reveal that the expression of ABCB1 is also inducible. Expression levels of ABCB1 (as well as other ABC transporters and drug-metabolizing enzymes) appear to be regulated by nuclear receptors like the pregnane X receptor (PXR), constitutive androstane receptor, and vitamin D binding receptor (60). Recent *in vitro* studies demonstrated that several drugs, including rifampicin, paclitaxel, and reserpine, can induce CYP3A4 and ABCB1 gene expression through these mechanisms and possibly can influence the absorption of drugs (61, 62). However, thus far, only rifampicin has been documented to significantly induce intestinal ABCB1 in humans: in duodenal biopsies performed in healthy volunteers after rifampicin administration, ABCB1 was induced 3.5-fold (63). Similar interactions with rifampicin have been reported for talinolol (64), fexofenadine (65), and CsA (66). For the other inducers, only *in vitro* data are available, thus raising doubts whether results obtained in cell lines can be extrapolated to human.

Table 1. The effect of absence or inhibition of ABCB1, ABCG2 and ABCC2 on the preclinical and/or clinical pharmacology of different drugs with high affinity for ABCB1, ABCG2 and ABCC2.

Oral drugs	inhibitor	Effect measured	Ref.
Preclinical studies:			
In vitro			
vinblastine	-	10-fold ↑ transport in ABCB1 over-expressing cells	(35)
vinblastine	verapamil	Reduced transport of vinblastine in ABCB1 over-expressing cells	(35)
ranitidine	-	3-fold ↑ transport in ABCB1 over-expressing cells	(37)
ranitidine	Cyclosporin A or verapamil	Reduced transport of ranitidine in ABCB1 over-expressing cells	(37)
indinavir	-	↑ transport in ABCB1 over-expressing cells	(38)
nelfinafir	-	↑ transport in ABCB1 over-expressing cells	(38)
saquinavir	-	↑ transport in ABCB1 over-expressing cells	(38)
indinavir	PSC833	Reduced transport of indinavir in ABCB1 over-expressing cells	(38)
nelfinafir	PSC833	Reduced transport of nelfinafir in ABCB1 over-expressing cells	(38)
saquinavir	PSC833	Reduced transport of saquinavir in ABCB1 over-expressing cells	(38)
topotecan	-	↑ transport in ABCG2 over-expressing cells	(68)
topotecan	GF120918	Reduced transport of topotecan in ABCG2 over-expressing cells	(68)
topotecan	Pantoprazole	Reduced transport of topotecan in ABCG2 over-expressing cells	(71)
SN-38	-	↑ resistance in ABCG2 over-expressing cells	(58)
SN-38	GF120918	Reversed resistance to SN-38 in ABCG2 over-expressing cells	(58)
SN-38	gefitinib	Reversed resistance to SN-38 in ABCG2 transduced cells	(75)
PhIP	-	↑ transport in ABCG2 over-expressing cells	(87)
In Vivo			
paclitaxel	-	↑ oral bioavailability in ABCB1 knockout mice	(6)
paclitaxel	PSC 833	↑ oral bioavailability in wild-type mice by ABCB1 inhibition	(54)
paclitaxel	Cyclosporin A	↑ oral bioavailability in wild-type mice by ABCB1 inhibition	(55)
paclitaxel	GF120918	↑ oral bioavailability in wild-type mice by ABCB1 inhibition	(57)
docetaxel	-	↑ oral bioavailability in ABCB1 knockout mice	(52)
docetaxel	Cyclosporin A	↑ oral bioavailability in wild-type mice by ABCB1 inhibition	(52)
docetaxel	ritonavir	↑ oral bioavailability in wild-type mice by ABCB1/CYP3A4 inhibition	(52)
etoposide	-	↑ oral bioavailability in ABCB1 knockout mice	(51)
etoposide	GF120918	↑ plasma levels by inhibition of ABCB1	(51)
indinavir	-	↑ oral bioavailability in ABCB1 knockout mice	(38)
nelfinafir	-	↑ oral bioavailability in ABCB1 knockout mice	(38)
saquinavir	-	↑ oral bioavailability in ABCB1 knockout mice	(38)
digoxin	-	ABCB1 contributed to direct elimination of digoxin	(50)
talinolol	verapamil	↑ oral bioavailability in wild-type rats by ABCB1 inhibition	(139)
topotecan	-	↑ oral bioavailability in ABCG2 knockout mice	(70)
topotecan	GF120918	↑ oral bioavailability in ABCG2 knockout mice	(68)
irinotecan	gefitinib	↑ oral bioavailability in wild-type mice by ABCG2 inhibition	(73)
PhIP	-	↑ oral bioavailability in ABCG2 knockout mice	(77)
PhIP	-	↑ oral bioavailability in ABCC2 deficient rats	(88)
Methotrexate	pantoprazole	↓ clearance in wildtype mice by ABCG2 inhibition	(71)
Clinical studies:			
digoxin	quinidine	↑ oral bioavailability in humans by ABCB1 inhibition	(125)
digoxin	talinolol	↑ oral bioavailability in humans by ABCB1 inhibition	(140)
paclitaxel	Cyclosporin A	↑ oral bioavailability in humans by ABCB1 inhibition	(127)
paclitaxel	GF120918	↑ oral bioavailability in humans by ABCB1 inhibition	(135)
docetaxel	Cyclosporin A	↑ oral bioavailability in humans by ABCB1 inhibition	(134)
topotecan	GF120918	↑ oral bioavailability in humans by ABCB1 inhibition	(136, 137)
Methotrexate	Omeprazole/ lansoprazole	↓ clearance in humans by ABCG2 and/or other transporter inhibition	(72)
Cyclosporin A	-	Correlation between oral exposure and ABCB1 expression/inter-individual variation	(28, 29)
talinolol	-	Correlation between oral exposure and ABCB1 expression	(141, 142)
tacrolimus	-	↓ absorption by intestinal ABCB1	(53)
digoxin	-	↓ absorption by intestinal ABCB1	(143)
fexofenadine		↓ absorption by intestinal ABCB1	(144)

Oral bioavailability indicates apparent oral bioavailability under all circumstances

ABCG2-mediated secretory transport

The ABC half-transporter ABCG2 is expressed abundantly at the apical membrane of the small intestine, in particularly the jejunum, where it limits drug absorption and/or facilitates secretion of clinically important drugs back into gut lumen (67). This has been clearly demonstrated in several studies. *In vitro* studies reveal that the anticancer drug topotecan, and other camptothecin derived topoisomerase I inhibitors, are efficiently transported by ABCG2 and have a low-affinity for ABCB1 (68, 69). Jonker et al. (70), compared the oral bioavailability of topotecan in ABCG2 knockout and WT mice and found that the systemic exposure of orally administered topotecan is about six-fold higher in BCRP knockout mice than control mice. Thus, ABCG2 appears to be a major determinant of the bioavailability of topotecan following oral administration. In ABCB1 knockout mice, topotecan was co-administered with and without elacridar, an inhibitor of ABCG2 and ABCB1 (Fig. 3A). Topotecan showed decreased plasma clearance, decreased hepatobiliary excretion, and increased re-uptake in the small intestine (68), indicating that most likely ABCG2 mediates these processes. Furthermore, the mechanism of the pharmacokinetic interaction between the antifolate drug methotrexate (MTX) and the benzimidazole drugs, e.g. pantoprazole and omeprazole, observed in patients, was investigated *in vitro* and *in vivo* (71). *In vitro* inhibition of ABCG2-mediated transport of MTX was reached at clinically relevant concentrations of benzimidazoles. In addition, the *in vitro* results also revealed that benzimidazoles are actively transported by ABCG2 themselves. *In vivo* data showed that pantoprazole significantly reduced the clearance of MTX by 1.8-fold in WT mice, and reduced it to similar levels as in ABCG2 knockout mice (71). The interaction between MTX and benzimidazoles is not frequently observed in patients: increased serum levels were only reported in cancer patients receiving high-dose MTX and omeprazole (72). Breedveld et al. showed that ABCG2 plays a significant role in the systemic clearance of high-dose MTX (500 mg/kg), but has a limited role in the systemic clearance of low-dose MTX (5 mg/kg) (71). Recently, other preclinical studies demonstrated that the oral bioavailability of the anticancer drug irinotecan could also be improved by inhibition of ABCG2 upon co-administration of the EGFR-inhibitor gefitinib (Iressa®) (73). SN38, which is the active metabolite of irinotecan, is an ABCG2 substrate drug (58, 74), and gefitinib reverses the ABCG2-mediated resistance to SN38 (73, 75). Gefitinib effectively inhibits ABCG2, although it is not a substrate for ABCG2 *in vitro* (73). At high concentrations, gefitinib also inhibits ABCB1 (76). Additionally, co-administration of oral gefitinib and oral irinotecan in non-tumor-bearing $SCID^{-/-}$ mice resulted in a 63% increase in the oral bioavailability of irinotecan compared with irinotecan administration alone (73). Whether the increased oral bioavailability is completely due to inhibition of ABCG2 is not

clear. Indeed, gefitinib may also, at least partially, increase the oral bioavailability of irinotecan by inhibiting the metabolism of irinotecan in the mouse intestine. If gefitinib or other ABCG2 inhibiting drugs are used clinically in combination with substrate drugs as irinotecan or topotecan careful drug-drug interaction studies need to be performed. Another example of limiting drug entry by ABCG2 into the body is that ABCG2 also restricts exposure to dietary carcinogens such as 2-amino-1-methyl-6-phenylimidazo[4,5-b]pyridine (PhIP). Pharmacokinetic studies by van Herwaarden et al. (77) demonstrated that the systemic exposure of oral and i.v. administration of PhIP was 2.9- and 2.2-fold higher in ABCG2 knockout mice than in WT mice, respectively. In mice with cannulated gall bladder, both hepatobiliary and direct intestinal excretion of PhIP were largely reduced in ABCG2 knockout mice compared with WT mice. The data suggest that ABCG2 effectively restricts the exposure of mice to ingested PhIP by decreasing its uptake from the small intestine and by mediating hepatobiliary and intestinal elimination. The importance of ABCG2 as a detoxification efflux transporter in the small intestine was also highlighted by Jonker et al. (70) who found that ABCG2 knockout mice are prone to developing phototoxic lesions on light-exposed areas of the skin when diet contained large amounts of chlorophyll was given. Further studies showed that ABCG2 efficiently limits the uptake of chlorophyll-breakdown product pheophorbide A, and the deficiency of ABCG2 increased the exposure of mice to pheophorbide A, leading to the high risk of protoporphyria and diet-dependent phototoxicity. This illustrates the importance of drug transporters in the protection of toxicity from normal food constituents. The preclinical data and known overlapping substrate specificity of ABCB1 (78) and ABCG2 suggest that these transporters could play a similar role in regulating absorption and disposition of substrate drugs.

ABCC-mediated secretory transport

Like ABCB1 and ABCG2, ABCCs are members of the ABC drug transporter super family and have the capacity to mediate transmembrane transport of many (conjugated) drugs and other compounds. Unfortunately, little is known about the ABCC-mediated transport process occurring at the apical or basolateral membrane of the intestinal epithelium. Thus far, it is known that ABCC1, 3 and 5 are localized at the basolateral side and ABCC2 and ABCC4 at the apical side of the membranes in the small intestines.

ABCC1

ABCC1 is localized primarily at the basolateral membrane of the crypt cells in mouse and human small intestine (25). The physiological role of ABCC1 is probably protection against toxic substrates by extruding its drugs from the cells into the blood (79). Studies in

a range of cancer cell lines demonstrated the ability of ABCC1 to confer resistance to cytotoxic drugs including daunorubicin, doxorubicin and vincristine (80-83). Additionally, ABCC1 was also shown to transport heavy metal anions, cytotoxic peptides, hydrophobic drugs and other compounds that are conjugated or complexed to the anionic tripeptide glutathione (GSH), to glucuronic acid, or to sulphate (84). Studies have shown that efficient transport of several non-anionic anticancer drugs by ABCC1 is dependent upon normal cellular supply of GSH. Transport can be facilitated either by co-transport with GSH or conjugation to GSH by glutathione S-transferase (GST) followed by transportation by ABCC1. However, the exact role of ABCC1 in intestinal drug transport has not yet been clearly established and no efficient and selective ABCC1 inhibitors are known.

ABCC2

Like ABCB1, ABCC2 is located at the apical membrane of epithelial cells of the small intestine increasing from crypt to villus (85). Compounds transported by ABCC2 show a great similarity with ABCC1 substrates, however, there is not a complete overlap in substrates. ABCC2 plays a functional role in the intestinal secretion of many drugs, e.g. both conjugated and unconjugated anionic compounds, co-transport of weakly basic drugs with GSH and/or metabolites from the small intestine (83). Experiments with ABCC2-deficient rats indicated that the protein plays a role in reducing the oral availability and biliary and intestinal excretion of the food-derived carcinogen PhIP (86, 87). Thus, components of our daily diet are also substrates for ABCC2 besides ABCG2. Using rat intestine from ABCC2-deficient and wild-type animals, ABCC2 was shown to mediate luminal excretion of the metabolite 2,4-dinitrophenyl-S-glutathione (DNP-SG) following administration of its parent compound 1-chloro-2,4-dinitrobenzene (CDNB) (88). CDNB molecules are rapidly taken up by somatic cells and are conjugated with cellular reduced glutathione to form DNP-SG, an ABCC2 substrate. Collectively, it was suggested that ABCC2 is involved in the intestinal excretion of glutathione-conjugates. Furthermore, Fromm et al. (15) described a variable inter-individual upregulation of ABCC2 by rifampicin in the apical membrane of enterocytes in the small intestine of 16 individuals. Tamoxifen influenced expression of the protein thereby influencing bioavailability, activity, and toxicity of the substrates as well *in vitro* and *in vivo* (89, 90). However, not only rifampicin or tamoxifen, but also other compounds have been reported to affect ABCC2 expression *in vitro* such as cisplatin and dexamethasone (91, 92). ABCC2 upregulation may influence the acquisition of multidrug resistance during chemotherapy (93).

It is clear that ABCC2 has some degree of overlapping substrate specificity with ABCB1, e.g. paclitaxel and doxorubicin (48, 94). The co-localization of ABCC2 and

ABCB1 at the apical membrane sites important to drug disposition (i.e. intestine, liver, and kidney) presents a barrier to drugs. Both transporters, for example, were shown to mediate the blood to lumen secretion of the fluoroquinolone antibiotic grepafloxacin by rat intestine (95), as well as by human intestinal Caco-2 cell monolayers (96) and MDCKII cell monolayers stably transfected with either ABCB1 or ABCC2 (97). Therefore, it is suggested that ABCC2 plays a significant role in mediating drug detoxification and limiting the oral absorption of their ligands by extruding them back into the intestinal lumen. In contrast with P-gp, clinical investigations regarding the influence of ABCC2 inhibition, e.g. by the ABCC2 inhibitor MK571 (98), on oral bioavailability of substrates are lacking. An explanation could be that anionic ABCC2 substrates serve as competitive inhibitors when applied in cellular *in vitro* systems and furthermore, most ABCC2 substrates are also transported by other transporters such as SLCOs. SLCOs are nowadays recognized as important uptake transporters that can have a profound impact on the systemic pharmacokinetics, tissue distribution and elimination of a wide range of drugs (43).

ABCC3

Similar to ABCC2, ABCC3 expression increases from crypt to villus tip (99). Like ABCC1, ABCC3 is localized to the basolateral membrane (100). ABCC3 shares a considerable overlap in substrate specificity with ABCC2, transporting a wide range of bile salts, non-conjugated organic anions and glucuronide-conjugates (99). The affinity of bile salts, together with its pattern of expression in the intestine, suggests a possible role for ABCC3 in mediating bile salt reabsorption, as part of the enterohepatic recirculation. Although ABCC3 has not been studied as extensively as ABCC1 and 2, it has several interesting properties. It can confer resistance to anticancer drugs such as etoposide, teniposide and MTX (101). Also, it increases efflux of toxic compounds from cells (102). Further research to elucidate the physiological function of ABCC3 is warranted.

ABCC4

ABCC4 has also been detected at low levels at the apical membrane of the jejunum. However, the exact role of ABCC4 in intestinal drug transport has not yet been clearly established. ABCC4 might limit the intestinal absorption of nucleoside phosphonate analogues, thereby contributing to their low oral bioavailability (103).

ABCC5

ABCC5 is also expressed at the intestinal barrier, including the colon (20, 104). Although the normal subcellular distribution of ABCC5 is presently unclear, human ABCC5 is routed to the basolateral membrane when stably transfected into MDCKII cells. There are

no reports at present that ABCC5 plays a role in intestinal absorption or disposition of substrate drugs.

ABCC6

Recent work using ABCC6-transfected Chinese hamster ovary cells indicated that ABCC6 can mediate the transport of several cytotoxic agents that are also substrate for ABCC1-3 (105). It is known that ABCC6 is expressed predominantly in the liver and kidney, where it localizes in the basolateral membrane of rat (106) and human hepatocytes and of proximal tubular epithelial cells (107, 108). In addition, ABCC6 shows low expression in the duodenum and colon (109). This suggests a role for ABCC6 in drug transport in tissues, including the intestinal epithelium; however thus far there are no reports available about the possible role of ABCC6 in intestinal drug absorption.

SLC-mediated absorptive transport

SLC15A1-mediated absorptive transport

The expression of SLC15A1 was found primarily in the small intestine, in particularly the duodenum (31, 32). The uptake of SLC15A1 substrates (i.e. di- and tripeptides or structurally related drugs) is mediated by a proton gradient and the membrane potential at the apical surface of epithelial cells (33). Briefly, an inward proton gradient is established at the brush border membrane by the Na^+/H^+ exchanger, and then the influx of protons back into the epithelial cells is coupled by SLC15A1 to transport its substrates, thus, the system is known as a proton-dependent cotransport system (110). SLC15A1 has generally been characterized as a low-affinity/high-capacity transporter with a wide variety of compounds as substrates. Drug molecules transported by SLC15A1 include β-lactam antibiotics such as penicillins and cephalosporins (111, 112), the anticancer agent bestatin (113), angiotensin-converting enzyme (ACE) inhibitors such as captopril, and the ester prodrugs enalapril and fosinopril (114). Prodrugs of acyclovir and L-dopa can also be recognized and transported by SLC15A1 (115, 116). While conventional approaches to enhancing the bioavailability of orally administered drugs focused on the optimization of dissolution, solubility, and passive permeability of drugs, coupling of active drugs (e.g. acyclovir and L-dopa) with an amino acid to target SLC15A1 significantly improves the intestinal absorption of the drugs by recognition and uptake via SLC15A1 (115, 117). Cephalosporins were reported to inhibit drug uptake mediated by SLC15A1 in HeLa cells (112). Clinically relevant drug interactions between substrate SLC15A1 drugs and cephalosporin may occur at the level of intestinal absorption. Clinically, drug-drug interactions that are SLC15-mediated are increasingly recognized in drug therapy and toxicology.

SLCO-mediated absorptive transport

Members of the SLCO family that have been found in the human intestine and have been relatively well studied are SLCO1A2 and SLCO2B1. SLCO1A2 was originally cloned from the human liver (118), and its transcript is found predominantly in the blood-brain barrier, and to lesser extent in the intestine (34, 119). *In vitro* and *in vivo* functional data suggest that SLCO1A2 and SLCO2B1 are localized at the apical side of the intestinal epithelial cells as an absorptive transporter (120, 121), however, the precise subcellular location and their function have not yet fully been identified. The drugs transported by SLCO1A2 include fexofenadine (120, 122), and saquinavir (123). Substrates of SLCO2B1 overlap with those of other SLCOs and transport the physiological substrates estrone-3-sulfate and xenobiotic sulfobromophtalein (34, 118).

Dresser et al. (120) studied the inhibitory activity of grapefruit, orange, and apple juice on the SLCO1A2 or ABCB1-mediated fexofenadine uptake or efflux, respectively, at the in vitro level and found that the inhibitory potency of fruit juices on SLCO1A2 is much higher than that on ABCB1. In a clinical study (120), oral administration of fexofenadine in the presence of fruit juices led to a three- to four-fold decrease in the area under the plasma concentration-time curve (AUC) and a two-fold decrease in C_{max}, while the urinary clearance of fexofenadine remained unchanged compared to administration with water. These data suggest that fruit juices may decrease the oral bioavailability of fexofenadine by inhibition of SLCO1A2-mediated drug absorption.

Few transporters belonging to the SLCO family have been identified in the GI tract to date, however, most functional characterization studies has been carried out at the cell culture level. *In vivo* data to further support the role of SLCOs on oral drug absorption are still very limited. A challenge to correlate in vitro findings with *in vivo* results is the ambiguous orthologous gene product in experimental animals such as rats or mice. For example, rat Slco1, 2, and 3 share some substrates with human SLCO1A2, but none of them represents the ortholog of human SLCO1A, because their amino acid sequence are only 67 to 73% identical to human SLCO1A2. Additionally, the tissue distribution patterns or cellular localizations of human SLCO1A2 are quite different from rat Slco1, 2, and 3.[124] *In vivo* assessment of the role of SLCOs in drug absorption is also significantly impeded by the lack of specific inhibitors for these transporters. It may be feasible to use substrates as competitive inhibitors under certain *in vitro* situations (e.g. SLCO1A2 gene transfected cells) where single transporters are present in the system, but the overlapping substrate specificity among SLCO family members makes it impossible to use this strategy for *in vivo* functional assessment of individuals SLCOs. The clinical significance of intestinal SLCOs in drug absorption needs to be established and confirmed.

Clinical examples of modulation of the activity of intestinal transporters to increase systemic exposure of orally administered drugs

In view of the importance of intestinal transporters in the absorption of drugs, efforts have been made to identify chemical inhibitors of ABC efflux transporters. These inhibitors temporarily reduce the efflux activities of the transporters and thereby can increase the oral bioavailability of some poorly absorbed drugs. Based on the preclinical results, described in the previous paragraph, numerous clinical proof-of-concept studies in humans have been initiated (Table 1) to evaluate the feasibility and the safety of the co-administration of a substrate drug and an ABC transport inhibitor.

The first example is the quinidine-digoxin interaction. Because digoxin is a ABCB1 substrate that is not metabolized (125, 126), digoxin has become a well-established model substrate to determine ABCB1 transporter activity. The absolute bioavailability of digoxin was increased in the presence of an oral dose of the ABCB1 inhibitor, quinidine. This suggests that quinidine increased the bioavailability of digoxin by inhibiting ABCB1 efflux into the intestine and possibly in the hepatobiliary excretion route.

In a clinical phase I study, five cancer patients received a safe oral dose of paclitaxel, (60 mg/m^2), and nine other patients oral paclitaxel combined with a single oral dose of the ABCB1 and CYP3A inhibitor, CsA (15 mg/kg) (127). CsA increased the systemic exposure to oral paclitaxel 8-fold, and the apparent bioavailability from 4% without CsA to 47% with CsA. In addition to ABCB1 inhibition, drug exposure was further improved by the concomitant inhibition of metabolism by CsA (128). At the highest dose level of oral paclitaxel (300 mg/m^2) in combination with CsA (15 mg/kg), the total fecal excretion was 76%, 61% of which was the parent drug. The high percentage of unabsorbed drug can be explained by the presence of the co-solvent Cremophor EL which resulted in “entrapment” of paclitaxel (129). Different oral formulations are currently being tested (130). To date several hundreds of patients have received oral paclitaxel in combination with CsA at different doses and schedules. Three phase II studies were performed to investigate activity and safety of repeated oral administration, in non small cell lung cancer, advanced gastric cancer and breast cancer, respectively (131-133). These studies show encouraging results, which may ultimately lead to application of oral paclitaxel as standard therapy in these types of cancer.

Similar results were obtained in another clinical study with docetaxel (134). Patients received one course of oral docetaxel (75 mg/kg) with or without a single dose of CsA (15 mg/kg). Pharmacokinetic results showed that co-administration of oral CsA resulted in a 7.3-fold increase of the systemic exposure to docetaxel. The apparent bioavailability of oral docetaxel in cancer patients increased from 8% without CsA to 88% in combination with

CsA. This increase can be explained by inhibition of metabolism, as well as by P-gp inhibition in the GI tract by CsA, but the magnitude of both mechanisms cannot be determined exactly. Furthermore, in another phase I study, patients received elacridar prior to oral paclitaxel (135). The increase in systemic exposure to paclitaxel was of the same magnitude as in combination with CsA.

Co-administration of elacridar also resulted in a significant increase in the systemic exposure of oral topotecan in patients (Fig. 3B) (136, 137). Previous studies reported low bioavailability (30 ± 7.7%) and moderate inter-patient variability of the i.v. formulation of topotecan administered orally (138). Elacridar increased the oral bioavailability of topotecan from 40.0% to 97.1% in eight patients and the plasma AUC increased significantly from 32.4 ± 9.6% to 78.7 ± 20.6 µg h/L. The inter-patient variability of the oral bioavailability of topotecan decreased from 17% without, to 11% with elacridar. Because topotecan is a selective substrate for ABCG2 and has low-affinity for ABCB1, these results suggest that the interaction between elacridar and topotecan is due to inhibition of ABCG2-mediated intestinal absorption. These encouraging results may have clinical implications for the oral application of topotecan and drugs with low oral bioavailability due to affinity of ABCG2 (10). It is not yet known whether the selection of a dual ABCB1 and ABCG2 inhibitor is better than the selection of a selective ABCB1 or ABCG2 inhibitor. This will depend on the affinity of the substrate drug for ABCB1 and/or ABCG2, and the toxicity profile of the combination of inhibitor and anticancer drug. Thus far, phase I clinical studies have shown that dual inhibitors, such as elacridar, can be administered to patients with only minimal side-effects. Clinical trials with third-generation modulators of ABCB1 (e.g. biricodar, zosuquidar, and laniquidar) specifically developed for MDR reversal are ongoing. The results will give insight into the possible clinical feasibility of this strategy.

A

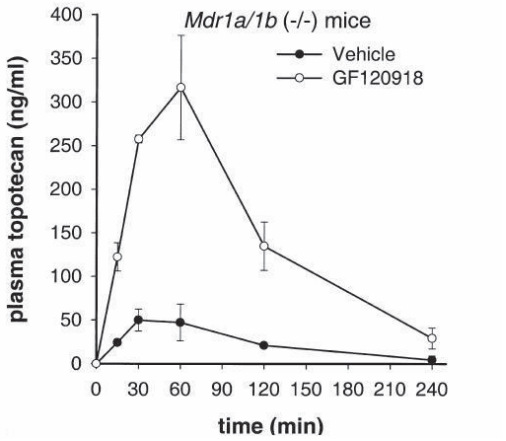

B

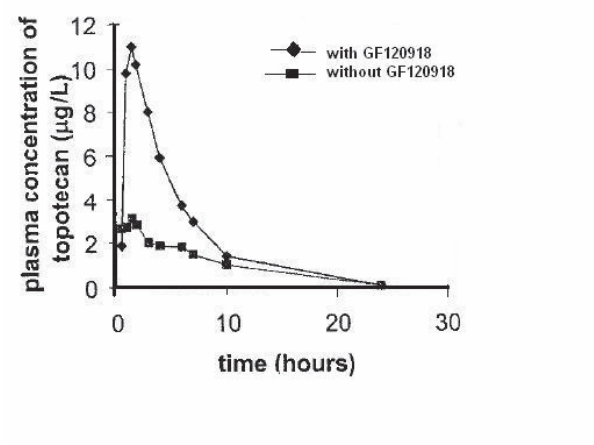

Figure 3. The effect of elacridar (GF120918) on the oral bioavailability of topotecan. A) Plasma topotecan concentration versus time curve in ABCB1 knockout mice pretreated with GF120918 or vehicle (control) (reprinted with permission) (68). B) Plasma concentration versus time curve of total topotecan in a patient cohort of 8 patients. Patients received single topotecan or in combination with GF120918 (reprinted with permission) (136).

Conclusions

During the past two decades, significant progress has been made in understanding the pharmacological and physiological role of ABC drug efflux and SLC uptake transporters. Although ABC transporters were once thought to be of relevance only in making cancer cells resistant to anticancer drugs and SLC transporters in the uptake of drugs it is now clear that they have a pronounced role in the pharmacokinetics (i.e. absorption, tissue distribution and hepatobiliary, intestinal and/or renal clearance) of a broad range of drugs, toxins, endogenous compounds and their metabolites. In this article we focused on transporters expressed in the intestinal wall. It has been demonstrated that these transporters can have a profound effect on the absorption, variability and disposition of a wide range of orally administered drugs. Furthermore, preclinical and clinical studies have shown that the oral bioavailability of drugs can be improved substantially by temporary inhibition of ABC drug transporters. Concomitant use of ABC transporter inhibitors with oral drugs is hopefully an effective and safe way that is at least as effective as standard i.v. therapy. Recognition of the importance of intestinal transporters could guide the development and design of oral drugs. Pre-screening of test drugs, nutrients and other molecules for ABC and SCL transporter substrates or inhibitors could be a useful way to predict their intestinal absorption.

References

1. DeMario MD and Ratain MJ. Oral chemotherapy: rationale and future directions. J Clin Oncol 1998;16:2557-2567.
2. Liu G, Franssen E, Fitch MI and Warner E. Patient preferences for oral versus intravenous palliative chemotherapy. J Clin Oncol 1997;15:110-115.
3. Parsons RL. Drug absorption in gastrointestinal disease with particular reference to malabsorption syndromes. Clin Pharmacokinet 1977;2:45-60.
4. Hellriegel ET, Bjornsson TD and Hauck WW. Interpatient variability in bioavailability is related to the extent of absorption: implications for bioavailability and bioequivalence studies. Clin Pharmacol Ther 1996;60:601-607.
5. Undevia SD, Gomez-Abuin G and Ratain MJ. Pharmacokinetic variability of anticancer agents. Nat Rev Cancer 2005;5:447-458.
6. Sparreboom A, van Asperen J, Mayer U, et al. Limited oral bioavailability and active epithelial excretion of paclitaxel (Taxol) caused by P-glycoprotein in the intestine. Proc Natl Acad Sci U S A 1997;94:2031-2035.
7. van Asperen J, van Tellingen O and Beijnen JH. The pharmacological role of P-glycoprotein in the intestinal epithelium. Pharmacol Res 1998;37:429-435.
8. Suzuki H and Sugiyama Y. Role of metabolic enzymes and efflux transporters in the absorption of drugs from the small intestine. Eur J Pharm Sci 2000;12:3-12.
9. Englund G, Rorsman F, Ronnblom A, et al. Regional levels of drug transporters along the human intestinal tract: co-expression of ABC and SLC transporters and comparison with Caco-2 cells. Eur J Pharm Sci 2006;29:269-277.
10. Kruijtzer CM, Beijnen JH and Schellens JH. Improvement of oral drug treatment by temporary inhibition of drug transporters and/or cytochrome P450 in the gastrointestinal tract and liver: an overview. Oncologist 2002;7:516-530.
11. Schinkel AH and Jonker JW. Mammalian drug efflux transporters of the ATP binding cassette (ABC) family: an overview. Adv Drug Deliv Rev 2003;55:3-29.

12. Ambudkar SV, Dey S, Hrycyna CA, et al. Biochemical, cellular, and pharmacological aspects of the multidrug transporter. Annu Rev Pharmacol Toxicol 1999;39:361-398.
13. Shitara Y, Horie T and Sugiyama Y. Transporters as a determinant of drug clearance and tissue distribution. Eur J Pharm Sci 2006;27:425-446.
14. Pade V and Stavchansky S. Estimation of the relative contribution of the transcellular and paracellular pathway to the transport of passively absorbed drugs in the Caco-2 cell culture model. Pharm Res 1997;14:1210-1215.
15. Fromm MF, Kauffmann HM, Fritz P, et al. The effect of rifampin treatment on intestinal expression of human MRP transporters. Am J Pathol 2000;157:1575-1580.
16. Cao X, Yu LX, Barbaciru C, et al. Permeability dominates in vivo intestinal absorption of P-gp substrate with high solubility and high permeability. Mol Pharm 2005;2:329-340.
17. Thiebaut F, Tsuruo T, Hamada H, et al. Cellular localization of the multidrug-resistance gene product P-glycoprotein in normal human tissues. Proc Natl Acad Sci U S A 1987;84:7735-7738.
18. Thorn M, Finnstrom N, Lundgren S, et al. Cytochromes P450 and MDR1 mRNA expression along the human gastrointestinal tract. Br J Clin Pharmacol 2005;60:54-60.
19. Makhey VD, Guo A, Norris DA, et al. Characterization of the regional intestinal kinetics of drug efflux in rat and human intestine and in Caco-2 cells. Pharm Res 1998;15:1160-1167.
20. Zimmermann C, Gutmann H, Hruz P, et al. Mapping of multidrug resistance gene 1 and multidrug resistance-associated protein isoform 1 to 5 mRNA expression along the human intestinal tract. Drug Metab Dispos 2005;33:219-224.
21. Dietrich CG, Geier A and Oude Elferink RP. ABC of oral bioavailability: transporters as gatekeepers in the gut. Gut 2003;52:1788-1795.
22. Gutmann H, Hruz P, Zimmermann C, et al. Distribution of breast cancer resistance protein (BCRP/ABCG2) mRNA expression along the human GI tract. Biochem Pharmacol 2005;70:695-699.
23. Taipalensuu J, Tornblom H, Lindberg G, et al. Correlation of gene expression of ten drug efflux proteins of the ATP-binding cassette transporter family in normal human jejunum and in human intestinal epithelial Caco-2 cell monolayers. J Pharmacol Exp Ther 2001;299:164-170.
24. Flens MJ, Zaman GJ, van der Valk P, et al. Tissue distribution of the multidrug resistance protein. Am J Pathol 1996;148:1237-1247.
25. Peng KC, Cluzeaud F, Bens M, et al. Tissue and cell distribution of the multidrug resistance-associated protein (MRP) in mouse intestine and kidney. J Histochem Cytochem 1999;47:757-768.
26 Rost D, Mahner S, Sugiyama Y and Stremmel W. Expression and localization of the multidrug resistance-associated protein 3 in rat small and large intestine. Am J Physiol Gastrointest Liver Physiol 2002;282:G720-G726.
27. Saeki T, Ueda K, Tanigawara Y, et al. Human P-glycoprotein transports cyclosporin A and FK506. J Biol Chem 1993;268:6077-6080.
28. Fricker G, Drewe J, Huwyler J, et al. Relevance of p-glycoprotein for the enteral absorption of cyclosporin A: in vitro-in vivo correlation. Br J Pharmacol 1996;118:1841-1847.
29. Lown KS, Mayo RR, Leichtman AB, et al. Role of intestinal P-glycoprotein (mdr1) in interpatient variation in the oral bioavailability of cyclosporine. Clin Pharmacol Ther 1997;62:248-260.
30. Meier Y, Eloranta JJ, Darimont J, et al. Regional distribution of solute carrier mRNA expression along the human intestinal tract. Drug Metab Dispos 2007;35:590-594.
31. Liang R, Fei YJ, Prasad PD, et al. Human intestinal H+/peptide cotransporter. Cloning, functional expression, and chromosomal localization. J Biol Chem 1995;270:6456-6463.
32. Herrera-Ruiz D, Wang Q, Gudmundsson OS, et al. Spatial expression patterns of peptide transporters in the human and rat gastrointestinal tracts, Caco-2 in vitro cell culture model, and multiple human tissues. AAPS PharmSci 2001;3:E9.
33. Ogihara H, Saito H, Shin BC, et al. Immuno-localization of H+/peptide cotransporter in rat digestive tract. Biochem Biophys Res Commun 1996;220:848-852.
34. Tamai I, Nezu J, Uchino H, et al. Molecular identification and characterization of novel members of the human organic anion transporter (OATP) family. Biochem Biophys Res Commun 2000;273:251-260.
35. Hunter J, Jepson MA, Tsuruo T, et al. Functional expression of P-glycoprotein in apical membranes of human intestinal Caco-2 cells. Kinetics of vinblastine secretion and interaction with modulators. J Biol Chem 1993;268:14991-14997.
36. Adachi Y, Suzuki H and Sugiyama Y. Comparative studies on in vitro methods for evaluating in vivo function of MDR1 P-glycoprotein. Pharm Res 2001;18:1660-1668.

37. Collett A, Higgs NB, Sims E, et al. Modulation of the permeability of H2 receptor antagonists cimetidine and ranitidine by P-glycoprotein in rat intestine and the human colonic cell line Caco-2. J Pharmacol Exp Ther 1999;288:171-178.
38. Kim RB, Fromm MF, Wandel C, et al. The drug transporter P-glycoprotein limits oral absorption and brain entry of HIV-1 protease inhibitors. J Clin Invest 1998;101:289-294.
39. Artursson P and Karlsson J. Correlation between oral drug absorption in humans and apparent drug permeability coefficients in human intestinal epithelial (Caco-2) cells. Biochem Biophys Res Commun 1991;175:880-885.
40. Breedveld P, Beijnen JH and Schellens JH. Use of P-glycoprotein and BCRP inhibitors to improve oral bioavailability and CNS penetration of anticancer drugs. Trends Pharmacol Sci 2006;27:17-24.
41. Evers R, Zaman GJ, van Deemter L, et al. Basolateral localization and export activity of the human multidrug resistance-associated protein in polarized pig kidney cells. J Clin Invest 1996;97:1211-1218.
42. Evers R, Kool M, van Deemter L, et al. Drug export activity of the human canalicular multispecific organic anion transporter in polarized kidney MDCK cells expressing cMOAT (MRP2) cDNA. J Clin Invest 1998;101:1310-1319.
43. Sasaki M, Suzuki H, Ito K, et al. Transcellular transport of organic anions across a double-transfected Madin-Darby canine kidney II cell monolayer expressing both human organic anion-transporting polypeptide (OATP2/SLC21A6) and Multidrug resistance-associated protein 2 (MRP2/ABCC2). J Biol Chem 2002;277:6497-6503.
44. Borst P and Schinkel AH. What have we learnt thus far from mice with disrupted P-glycoprotein genes?. Eur J Cancer 1996;32A:985-990.
45. Schinkel AH, Smit JJ, van Tellingen O, et al. Disruption of the mouse mdr1a P-glycoprotein gene leads to a deficiency in the blood-brain barrier and to increased sensitivity to drugs. Cell 1994;77:491-502.
46. Schinkel AH, Mayer U, Wagenaar E, et al. Normal viability and altered pharmacokinetics in mice lacking mdr1-type (drug-transporting) P-glycoproteins. Proc Natl Acad Sci U S A 1997;94:4028-4033.
47. Sparreboom A, van Tellingen O, Nooijen WJ and Beijnen JH. Preclinical pharmacokinetics of paclitaxel and docetaxel. Anticancer Drugs 1998;9:1-17.
48. Lagas JS, Vlaming ML, van Tellingen O, et al. Multidrug resistance protein 2 is an important determinant of paclitaxel pharmacokinetics. Clin Cancer Res 2006;12:6125-6132.
49. van Asperen J, Schinkel AH, Beijnen JH, et al. Altered pharmacokinetics of vinblastine in Mdr1a P-glycoprotein-deficient Mice. J Natl Cancer Inst 1996;88:994-999.
50. Mayer U, Wagenaar E, Beijnen JH, et al. Substantial excretion of digoxin via the intestinal mucosa and prevention of long-term digoxin accumulation in the brain by the mdr 1a P-glycoprotein. Br J Pharmacol 1996;119:1038-1044.
51. Allen JD, Van Dort SC, Buitelaar M, et al. Mouse breast cancer resistance protein (Bcrp1/Abcg2) mediates etoposide resistance and transport, but etoposide oral availability is limited primarily by P-glycoprotein. Cancer Res 2003;63:1339-1344.
52. Bardelmeijer HA, Ouwehand M, Buckle T, et al. Low systemic exposure of oral docetaxel in mice resulting from extensive first-pass metabolism is boosted by ritonavir. Cancer Res 2002;62:6158-6164.
53. Hebert MF. Contributions of hepatic and intestinal metabolism and P-glycoprotein to cyclosporine and tacrolimus oral drug delivery. Adv Drug Deliv Rev 1997;27:201-214.
54. van Asperen J, van Tellingen O, Sparreboom A, et al. Enhanced oral bioavailability of paclitaxel in mice treated with the P-glycoprotein blocker SDZ PSC 833. Br J Cancer 1997;76:1181-1183.
55. van Asperen J, van Tellingen O, Van Der Valk MA, et al. Enhanced oral absorption and decreased elimination of paclitaxel in mice cotreated with cyclosporin A. Clin Cancer Res 1998;4:2293-2297.
56. Harris JW, Rahman A, Kim BR, et al. Metabolism of taxol by human hepatic microsomes and liver slices: participation of cytochrome P450 3A4 and an unknown P450 enzyme. Cancer Res 1994;54:4026-4035.
57. Bardelmeijer HA, Beijnen JH, Brouwer KR, et al. Increased oral bioavailability of paclitaxel by GF120918 in mice through selective modulation of P-glycoprotein. Clin Cancer Res 2000;6:4416-4421.
58. Maliepaard M, van Gastelen MA, Tohgo A, et al. Circumvention of breast cancer resistance protein (BCRP)-mediated resistance to camptothecins in vitro using non-substrate drugs or the BCRP inhibitor GF120918. Clin Cancer Res 2001;7:935-941.
59. van Herwaarden AE, Wagenaar E, van der Kruijssen CM, et al. Knockout of cytochrome P450 3A yields new mouse models for understanding xenobiotic metabolism. J Clin Invest 2007;117:3583-3592.
60. Xu C, Li CY and Kong AN. Induction of phase I, II and III drug metabolism/transport by xenobiotics. Arch Pharm Res 2005;28:249-268.

61. Schuetz EG, Beck WT and Schuetz JD. Modulators and substrates of P-glycoprotein and cytochrome P4503A coordinately up-regulate these proteins in human colon carcinoma cells. Mol Pharmacol 1996;49:311-318.
62. Geick A, Eichelbaum M and Burk O. Nuclear receptor response elements mediate induction of intestinal MDR1 by rifampin. J Biol Chem 2001;276:14581-14587.
63. Greiner B, Eichelbaum M, Fritz P, et al. The role of intestinal P-glycoprotein in the interaction of digoxin and rifampin. J Clin Invest 1999;104:147-153.
64. Westphal K, Weinbrenner A, Zschiesche M, et al. Induction of P-glycoprotein by rifampin increases intestinal secretion of talinolol in human beings: a new type of drug/drug interaction. Clin Pharmacol Ther 2000;68:345-355.
65. Hamman MA, Bruce MA, Haehner-Daniels BD and Hall SD. The effect of rifampin administration on the disposition of fexofenadine. Clin Pharmacol Ther 2001;69:114-121.
66. Hebert MF, Roberts JP, Prueksaritanont T and Benet LZ. Bioavailability of cyclosporine with concomitant rifampin administration is markedly less than predicted by hepatic enzyme induction. Clin Pharmacol Ther 1992;52:453-457.
67. Maliepaard M, Scheffer GL, Faneyte IF, et al. Subcellular localization and distribution of the breast cancer resistance protein transporter in normal human tissues. Cancer Res 2001;61:3458-3464.
68. Jonker JW, Smit JW, Brinkhuis RF, et al. Role of breast cancer resistance protein in the bioavailability and fetal penetration of topotecan. J Natl Cancer Inst 2000; 92:1651-1656.
69. Maliepaard M, van Gastelen MA, de Jong LA, et al. Overexpression of the BCRP/MXR/ABCP gene in a topotecan-selected ovarian tumor cell line. Cancer Res 1999;59:4559-4563.
70. Jonker JW, Buitelaar M, Wagenaar E, et al. The breast cancer resistance protein protects against a major chlorophyll-derived dietary phototoxin and protoporphyria. Proc Natl Acad Sci U S A 2002;99:15649-15654.
71. Breedveld P, Zelcer N, Pluim D, et al. Mechanism of the pharmacokinetic interaction between methotrexate and benzimidazoles: potential role for breast cancer resistance protein in clinical drug-drug interactions. Cancer Res 2004;64:5804-5811.
72. Joerger M, Huitema AD, van den Bongard HJ, et al. Determinants of the elimination of methotrexate and 7-hydroxy-methotrexate following high-dose infusional therapy to cancer patients. Br J Clin Pharmacol 2006;62:71-80.
73. Stewart CF, Leggas M, Schuetz JD, et al. Gefitinib enhances the antitumor activity and oral bioavailability of irinotecan in mice. Cancer Res 2004;64:7491-7499.
74. Nakatomi K, Yoshikawa M, Oka M, et al. Transport of 7-ethyl-10-hydroxycamptothecin (SN-38) by breast cancer resistance protein ABCG2 in human lung cancer cells. Biochem Biophys Res Commun 2001;288:827-832.
75. Yanase K, Tsukahara S, Asada S, et al. Gefitinib reverses breast cancer resistance protein-mediated drug resistance. Mol Cancer Ther 2004;3:1119-1125.
76. Ozvegy-Laczka C, Hegedus T, Varady G, et al. High-affinity interaction of tyrosine kinase inhibitors with the ABCG2 multidrug transporter. Mol Pharmacol 2004;65:1485-1495.
77. van Herwaarden AE, Jonker JW, Wagenaar E, et al. The breast cancer resistance protein (Bcrp1/Abcg2) restricts exposure to the dietary carcinogen 2-amino-1-methyl-6-phenylimidazo[4,5-b]pyridine. Cancer Res 2003;63:6447-6452.
78. Allen JD, Brinkhuis RF, Wijnholds J and Schinkel AH. The mouse Bcrp1/Mxr/Abcp gene: amplification and overexpression in cell lines selected for resistance to topotecan, mitoxantrone, or doxorubicin. Cancer Res 1999;59:4237-4241.
79. Allen JD, Brinkhuis RF, van Deemter L, et al. Extensive contribution of the multidrug transporters P-glycoprotein and Mrp1 to basal drug resistance. Cancer Res 2000;60:5761-5766.
80. Cole SP, Sparks KE, Fraser K, et al. Pharmacological characterization of multidrug resistant MRP-transfected human tumor cells. Cancer Res 1994;54:5902-5910.
81. de Jong MC, Slootstra JW, Scheffer GL, et al. Peptide transport by the multidrug resistance protein MRP1. Cancer Res 2001;61:2552-2557.
82. Leslie EM, Deeley RG and Cole SP. Toxicological relevance of the multidrug resistance protein 1, MRP1 (ABCC1) and related transporters. Toxicology 2001;167:3-23.
83. Jedlitschky G, Leier I, Buchholz U, et al. ATP-dependent transport of bilirubin glucuronides by the multidrug resistance protein MRP1 and its hepatocyte canalicular isoform MRP2. Biochem J 1997;327:305-310.
84. Zaman GJ, Lankelma J, van Tellingen O, et al. Role of glutathione in the export of compounds from cells by the multidrug-resistance-associated protein. Proc Natl Acad Sci U S A 1995;92:7690-7694.

85. Hirohashi T, Suzuki H, Chu XY, et al. Function and expression of multidrug resistance-associated protein family in human colon adenocarcinoma cells (Caco-2). J Pharmacol Exp Ther 2000;292:265-270.
86. Dietrich CG, de Waart DR, Ottenhoff R, et al. Mrp2-deficiency in the rat impairs biliary and intestinal excretion and influences metabolism and disposition of the food-derived carcinogen 2-amino-1-methyl-6-phenylimidazo. Carcinogenesis 2001;22:805-811.
87. Dietrich CG, de Waart DR, Ottenhoff R, et al. Increased bioavailability of the food-derived carcinogen 2-amino-1-methyl-6-phenylimidazo[4,5-b]pyridine in MRP2-deficient rats. Mol Pharmacol 2001;59:974-980.
88. Gotoh Y, Suzuki H, Kinoshita S, et al. Involvement of an organic anion transporter (canalicular multispecific organic anion transporter/multidrug resistance-associated protein 2) in gastrointestinal secretion of glutathione conjugates in rats. J Pharmacol Exp Ther 2000;292:433-439.
89. Naruhashi K, Tamai I, Inoue N, et al. Active intestinal secretion of new quinolone antimicrobials and the partial contribution of P-glycoprotein. J Pharm Pharmacol 2001;53:699-709.
90. Kauffmann HM, Keppler D, Gant TW and Schrenk D. Induction of hepatic mrp2 (cmrp/cmoat) gene expression in nonhuman primates treated with rifampicin or tamoxifen. Arch Toxicol 1998;72:763-768.
91. Okudaira N, Komiya I and Sugiyama Y. Polarized efflux of mono- and diacid metabolites of ME3229, an ester-type prodrug of a glycoprotein IIb/IIIa receptor antagonist, in rat small intestine. J Pharmacol Exp Ther 2000;295:717-723.
92. Kauffmann HM, Keppler D, Kartenbeck J and Schrenk D. Induction of cMrp/cMoat gene expression by cisplatin, 2-acetylaminofluorene, or cycloheximide in rat hepatocytes. Hepatology 1997;26:980-985.
93. Borst P, Evers R, Kool M and Wijnholds J. A family of drug transporters: the multidrug resistance-associated proteins. J Natl Cancer Inst 2000;92:1295-1302.
94. Vlaming ML, Mohrmann K, Wagenaar E, et al. Carcinogen and anticancer drug transport by Mrp2 in vivo: studies using Mrp2 (Abcc2) knockout mice. J Pharmacol Exp Ther 2006;318:319-327.
95. Naruhashi K, Tamai I, Inoue N, et al. Involvement of multidrug resistance-associated protein 2 in intestinal secretion of grepafloxacin in rats. Antimicrob Agents Chemother 2002;46:344-349.
96. Lowes S and Simmons NL. Multiple pathways for fluoroquinolone secretion by human intestinal epithelial (Caco-2) cells. Br J Pharmacol 2002;135:1263-1275.
97. Mottino AD, Hoffman T, Jennes L and Vore M. Expression and localization of multidrug resistant protein mrp2 in rat small intestine. J Pharmacol Exp Ther 2000;293:717-723.
98. Bow DA, Perry JL, Miller DS, et al. Localization of P-gp (Abcb1) and Mrp2 (Abcc2) in Freshly Isolated Rat Hepatocytes. Drug Metab Dispos 2008;36:198-202.
99. Kool M, van der Linden M, de Haas M, et al. MRP3, an organic anion transporter able to transport anti-cancer drugs. Proc Natl Acad Sci U S A 1999;96:6914-6919.
100. Zeng H, Liu G, Rea PA and Kruh GD. Transport of amphipathic anions by human multidrug resistance protein 3. Cancer Res 2000;60:4779-4784.
101. Zeng H, Chen ZS, Belinsky MG, et al. Transport of methotrexate (MTX) and folates by multidrug resistance protein (MRP) 3 and MRP1: effect of polyglutamylation on MTX transport. Cancer Res 2001;61:7225-7232.
102. Kool M, de Haas M, Scheffer GL, et al. Analysis of expression of cMOAT (MRP2), MRP3, MRP4, and MRP5, homologues of the multidrug resistance-associated protein gene (MRP1), in human cancer cell lines. Cancer Res 1997;57:3537-3547.
103. Belinsky MG, Guo P, Lee K, et al. Multidrug resistance protein 4 protects bone marrow, thymus, spleen, and intestine from nucleotide analogue-induced damage. Cancer Res 2007;67:262-268.
104. Wijnholds J, Mol CA, van Deemter L, et al. Multidrug-resistance protein 5 is a multispecific organic anion transporter able to transport nucleotide analogs. Proc Natl Acad Sci U S A 2000;97:7476-7481.
105. Belinsky MG, Chen ZS, Shchaveleva I, et al. Characterization of the drug resistance and transport properties of multidrug resistance protein 6 (MRP6, ABCC6). Cancer Res 2002;62:6172-6177.
106. Madon J, Hagenbuch B, Landmann L, et al. Transport function and hepatocellular localization of mrp6 in rat liver. Mol Pharmacol 2000;57:634-641.
107. Scheffer GL, Hu X, Pijnenborg AC, et al. MRP6 (ABCC6) detection in normal human tissues and tumors. Lab Invest 2002;82:515-518.
108. Beck K, Hayashi K, Dang K, et al. Analysis of ABCC6 (MRP6) in normal human tissues. Histochem Cell Biol 2005;123:517-528.
109. Kool M, van der Linden M, de Haas M, et al. Expression of human MRP6, a homologue of the multidrug resistance protein gene MRP1, in tissues and cancer cells. Cancer Res 1999;59:175-182.

110. Adibi SA. The oligopeptide transporter (Pept-1) in human intestine: biology and function. Gastroenterology 1997;113:332-340.
111. Terada T, Saito H and Inui K. Interaction of beta-lactam antibiotics with histidine residue of rat H+/peptide cotransporters, PEPT1 and PEPT2. J Biol Chem 1998;273:5582-5585.
112. Ganapathy ME, Prasad PD, Mackenzie B, et al. Interaction of anionic cephalosporins with the intestinal and renal peptide transporters PEPT 1 and PEPT 2. Biochim Biophys Acta 1997;1324:296-308. 1997.
113. Gonzalez DE, Covitz KM, Sadee W and Mrsny RJ. An oligopeptide transporter is expressed at high levels in the pancreatic carcinoma cell lines AsPc-1 and Capan-2, Cancer Res 1998;58:519-525.
114. Zhu T, Chen XZ, Steel A, et al. Differential recognition of ACE inhibitors in Xenopus laevis oocytes expressing rat PEPT1 and PEPT2. Pharm Res 2000;17:526-532.
115. Balimane PV, Tamai I, Guo A, et al. Direct evidence for peptide transporter (PepT1)-mediated uptake of a nonpeptide prodrug, valacyclovir. Biochem Biophys Res Commun 1998;250:246-251.
116. Tamai I, Nakanishi T, Nakahara H, et al. Improvement of L-dopa absorption by dipeptidyl derivation, utilizing peptide transporter PepT1. J Pharm Sci 1998;87:1542-1546.
117. Han H, de Vrueh RL, Rhie JK, et al. 5'-Amino acid esters of antiviral nucleosides, acyclovir, and AZT are absorbed by the intestinal PEPT1 peptide transporter. Pharm Res 1998;15:1154-1159.
118. Kullak-Ublick GA, Hagenbuch B, Stieger B, et al. Molecular and functional characterization of an organic anion transporting polypeptide cloned from human liver. Gastroenterology 1995;109:1274-1282.
119. Gao B, Hagenbuch B, Kullak-Ublick GA, et al. Organic anion-transporting polypeptides mediate transport of opioid peptides across blood-brain barrier. J Pharmacol Exp Ther 2000;294:73-79.
120. Dresser GK, Bailey DG, Leake BF, et al. Fruit juices inhibit organic anion transporting polypeptide-mediated drug uptake to decrease the oral availability of fexofenadine. Clin Pharmacol Ther 2002;71:11-20.
121. Kobayashi D, Nozawa T, Imai K, et al. Involvement of human organic anion transporting polypeptide OATP-B (SLC21A9) in pH-dependent transport across intestinal apical membrane. J Pharmacol Exp Ther 2003;306:703-708.
122. Cvetkovic M, Leake B, Fromm MF, et al. OATP and P-glycoprotein transporters mediate the cellular uptake and excretion of fexofenadine. Drug Metab Dispos 1999;27:866-871.
123. Su Y, Zhang X and Sinko PJ. Human organic anion-transporting polypeptide OATP-A (SLC21A3) acts in concert with P-glycoprotein and multidrug resistance protein 2 in the vectorial transport of Saquinavir in Hep G2 cells. Mol Pharm 2004;1:49-56.
124. Kullak-Ublick GA, Ismair MG, Stieger B, et al. Organic anion-transporting polypeptide B (OATP-B) and its functional comparison with three other OATPs of human liver. Gastroenterology 2001;120:525-533.
125. Doering W. Quinidine-digoxin interaction: Pharmacokinetics, underlying mechanism and clinical implications. N Engl J Med 1979;301:400-404.
126. Hinderling PH and Hartmann D. Pharmacokinetics of digoxin and main metabolites/derivatives in healthy humans. Ther Drug Monit 1991;13:381-401.
127. Meerum Terwogt JM, Malingre MM, Beijnen JH, et al. Coadministration of oral cyclosporin A enables oral therapy with paclitaxel. Clin Cancer Res 1999;5:3379-3384.
128. Malingre MM, Schellens JH, van Tellingen O, et al. Metabolism and excretion of paclitaxel after oral administration in combination with cyclosporin A and after i.v. administration. Anticancer Drugs 2000;11:813-820.
129. Bardelmeijer HA, Ouwehand M, Malingre MM, et al. Entrapment by Cremophor EL decreases the absorption of paclitaxel from the gut. Cancer Chemother Pharmacol 2002;49:119-125.
130. Veltkamp SA, Rosing H, Huitema AD, et al. Novel paclitaxel formulations for oral application: a phase I pharmacokinetic study in patients with solid tumours. Cancer Chemother Pharmacol 2007;60:635-642.
131. Helgason HH, Kruijtzer CM, Huitema AD, et al. Phase II and pharmacological study of oral paclitaxel (Paxoral) plus ciclosporin in anthracycline-pretreated metastatic breast cancer. Br J Cancer 2006;95:794-800.
132. Kruijtzer CM, Boot H, Beijnen JH, et al. Weekly oral paclitaxel as first-line treatment in patients with advanced gastric cancer. Ann Oncol 2003;14:197-204.
133. Kruijtzer CM, Schellens JH, Mezger J, et al. Phase II and pharmacologic study of weekly oral paclitaxel plus cyclosporine in patients with advanced non-small-cell lung cancer. J Clin Oncol 2002;20:4508-4516.

134. Malingre MM, Richel DJ, Beijnen JH, et al. Coadministration of cyclosporine strongly enhances the oral bioavailability of docetaxel. J Clin Oncol 2001;19:1160-1166.
135. Malingre MM, Beijnen JH, Rosing H, et al. Co-administration of GF120918 significantly increases the systemic exposure to oral paclitaxel in cancer patients. Br J Cancer 2001;84:42-47.
136. Kruijtzer CM, Beijnen JH, Rosing H, et al. Increased oral bioavailability of topotecan in combination with the breast cancer resistance protein and P-glycoprotein inhibitor GF120918. J Clin Oncol 2002;20:2943-2950.
137. Kuppens IE, Witteveen EO, Jewell RC, et al. A phase I, randomized, open-label, parallel-cohort, dose-finding study of elacridar (GF120918) and oral topotecan in cancer patients. Clin Cancer Res 2007;13:3276-3285.
138. Schellens JH, Creemers GJ, Beijnen JH, et al. Bioavailability and pharmacokinetics of oral topotecan: a new topoisomerase I inhibitor. Br J Cancer 1996;73:1268-1271.
139. Spahn-Langguth H, Baktir G, Radschuweit A, et al. P-glycoprotein transporters and the gastrointestinal tract: evaluation of the potential in vivo relevance of in vitro data employing talinolol as model compound. Int J Clin Pharmacol Ther 1998;36:16-24.
140. Westphal K, Weinbrenner A, Giessmann T, et al. Oral bioavailability of digoxin is enhanced by talinolol: evidence for involvement of intestinal P-glycoprotein. Clin Pharmacol Ther 2000;68:6-12.
141. Gramatte T, Oertel R, Terhaag B and Kirch W. Direct demonstration of small intestinal secretion and site-dependent absorption of the beta-blocker talinolol in humans. Clin Pharmacol Ther 1996;59:541-549.
142. Wetterich U, Spahn-Langguth H, Mutschler E, et al. Evidence for intestinal secretion as an additional clearance pathway of talinolol enantiomers: concentration- and dose-dependent absorption in vitro and in vivo. Pharm Res 1996;13:514-522.
143. Hoffmeyer S, Burk O, von Richter O, et al. Functional polymorphisms of the human multidrug-resistance gene: multiple sequence variations and correlation of one allele with P-glycoprotein expression and activity in vivo. Proc Natl Acad Sci U S A 2000;97:3473-3478.
144. Robbins DK, Castles MA, Pack DJ, et al. Dose proportionality and comparison of single and multiple dose pharmacokinetics of fexofenadine (MDL 16455) and its enantiomers in healthy male volunteers. Biopharm Drug Dispos 1998;19:455-463.

CHAPTER 2

Preclinical pharmacological studies on imatinib

CHAPTER 2.1

The effect of P-gp (Mdr1a/1b), BCRP (Bcrp1) and P-gp/BCRP inhibitors on the *in vivo* absorption, distribution, metabolism and excretion of imatinib

Roos L. Oostendorp, Tessa Buckle, Jos H. Beijnen, Olaf van Tellingen, Jan H.M. Schellens

Investigational New Drugs 2008 (in press)

Abstract

Imatinib is transported by P-glycoprotein (P-gp) and Breast Cancer Resistance Protein (BCRP), however, the exact impact of these transporters on absorption, distribution, metabolism and excretion (ADME) of imatinib is not fully understood due to incomplete data. We have performed a comprehensive ADME study of imatinib given as single agent or in combination with the well known BCRP/P-gp inhibitors, elacridar and pantoprazole, in wild-type and P-gp and/or BCRP knockout mice. The absence of P-gp and BCRP together resulted in a significantly higher area under the plasma concentration-time curve (AUC) after i.v. administration, whereas the AUC after oral dosing was unaltered. Both elacridar and pantoprazole significantly increased the AUC of orally administered imatinib in wild-type but also in P-gp/BCRP knockout mice. The lower clearance was not due to a (further) reduction in biliary excretion. Fecal excretion was significantly reduced in P-gp and P-gp/BCRP knockout but not in BCRP knockout mice, whereas the brain penetration was significantly higher in P-gp/BCRP knockout mice compared to single P-gp or BCRP knockout or wild-type mice. In conclusion, P-gp and BCRP have only a modest effect on the ADME of imatinib in comparison to metabolic elimination. P-gp is the most prevalent factor for systemic clearance and limiting the brain penetration. The considerable drug-drug interaction observed with elacridar or pantoprazole is only partly mediated by inhibition of P-gp and BCRP and far more by the inhibition of other elimination pathways.

Introduction

Imatinib mesylate (Glivec®, formerly STI-571; Novartis, Basel, Switzerland) is an orally active tyrosine kinase inhibitor that is approved for use in BCR/ABL positive chronic myeloid leukemia (CML) (1, 2) and in gastrointestinal stromal tumors (GIST) that harbor c-KIT mutations (3). It is now being tested for the treatment of a number of other malignancies alone (4, 5) or in combination with other agents (6, 7).

In spite of the excellent response of newly diagnosed CML and GIST patients, patients develop resistance to imatinib therapy. Several potential resistance mechanisms have been described, including the presence of point mutations in the kinase domain, amplification of the gene and imatinib binding to α_1-acid glycoprotein (8-12). In addition, changes or variations in pharmacokinetics of imatinib that may affect therapeutic efficacy have also been observed. For instance, despite the high oral bioavailability (98%) of imatinib (13, 14), preliminary data revealed a reduced systemic exposure to imatinib in GIST patients when given for prolonged periods of time (15). Furthermore, the systemic exposure of imatinib shows wide inter-individual variability (coefficient of variation ranging from 40% to 60% in CML and GIST patients) (15, 16), which may cause differences in compliance and attribute to variation in absorption, distribution, metabolism and excretion (ADME) between patients. It is known that the major mechanism of elimination of imatinib involves metabolism in the gut wall and liver. Cytochrome P450 (CYP) 3A accounts for most of the biotransformation of imatinib and to a lesser exent CYP1A1/2, 1B1, 2C8/9 and 2D6 (17, 18). In patients, one major imatinib metabolite, N-desmethyl-imatinib (CGP74588), has been identified and was shown to have comparable activity as the parent compound (19). Furthermore, some other metabolites were also found in plasma and characterized as hydroxy-, *N*-oxide-, deaminated-, and glucoroconjugate metabolites (20). The wide variability of CYP activity between individuals may contribute to the observed interindividual variation in pharmacokinetic parameters. However, *in vitro* and *in vivo* experiments have shown that imatinib is a substrate for the drug-efflux transporters P-glycoprotein (P-gp; rodent Mdr1a/1b) and Breast Cancer Resistance Protein (BCRP; rodent Bcrp1) (21-29) and therefore P-gp and BCRP might also affect the ADME of imatinib. Previous studies were not conclusive (24, 25, 29) and more complex investigations were deemed necessary to assess the role of these transporters in the ADME of imatinib in more detail. In part this was due to the fact that, most of these previous studies have relied on measurement of total radioactivity following administration of radiolabeled imatinib for determination of drug levels. However, Dai et al. and Bihorel et al. (25, 29), have shown that imatinib is extensively metabolized with unchanged drug representing only 25% of plasma radioactivity.

We have now performed a comprehensive pharmacokinetic study in wild-type, P-gp and BCRP single knockout mice, and P-gp/BCRP combined knockout mice to unequivocally establish the role of these drug transporters on the disposition of imatinib. Both intact drug and its metabolite CGP74588 were measured by high-performance liquid chromatography (HPLC) and total radioactivity was determined. Moreover, we studied the effects of the P-gp and BCRP inhibitors, elacridar and pantoprazole, on the disposition of imatinib in order to demonstrate potential drug-drug interactions when imatinib is combined with inhibitors of P-gp and BCRP.

Materials and Methods

Chemicals and reagents

Imatinib (STI-571) and [^{14}C]imatinib (both as mesylate salt) were kindly provided by Novartis Pharma AG (Basel, Switzerland). Elacridar (GF120918) was a generous gift from GlaxoSmithKline (Research Triangle Park, NC). Pantoprazole (Pantozol® 40 mg i.v., Altana pharma, Hoofddorp, The Netherlands) was obtained from the pharmacy of the Netherlands Cancer institute. Hypnorm (fentanyl 0.2 mg/ml and fluanisone 10 mg/ml) was obtained from VetaPharma Ltd (Leeds, UK), Dormicum (midazolam 5 mg/ml) was provided by Rôche Nederland (Mijdrecht, The Netherlands) and methoxyflurane (Metofane®) was from Medical Development Australia (Springvale, Victoria, Australia). Bovine serum albumin (BSA), Fraction V, was from Roche (Mannheim, Germany). Methanol, acetonitrile (both high-performance liquid chromatography (HPLC) grade) were from Merck (Darmstadt, Germany). Drug-free human plasma was obtained from the Central Laboratory of the Blood Transfusion Service (Sanquin, Amsterdam, The Netherlands).

Animals

Mice were housed and handled according to institutional guidelines complying with Dutch legislation. Animals used in all experiments were female Mdr1a/1b$^{-/-}$ (P-gp knockout), Bcrp1$^{-/-}$ (BCRP knockout), Mdr1a/1b/Bcrp1$^{-/-}$ (P-gp/BCRP knockout), and wild-type (WT) mice of a comparable genetic background (FVB) between 9 and 14 weeks of age. Animals were kept in a temperature-controlled environment with a 12-hour light/12-hour dark cycle. They received a standard diet (AM-II, Hope Farms, Woerden, The Netherlands) and acidified water *ad libitum.*

Drug solutions

Imatinib alone or a mixture of imatinib and [^{14}C]imatinib (~ 0.5 μCi/animal) was diluted with glucose 5% to a final concentration of 10 mg/mL for oral (p.o.) or 5 mg/mL for i.v. administration. Elacridar was suspended at 10 mg/mL in a mixture of hydroxypropylmethylcellulose (10 g/L)/2% Tween 80/H_2O) (0.5:1:98.5 [v/v/v]) for p.o. administration. A vial of pantoprazole was diluted with NaCl 0.9% to a final concentration of 4 mg/mL for p.o. administration.

Plasma pharmacokinetics and oral bioavailability

WT and Mdr1a/1b/Bcrp1$^{-/-}$ mice received imatinib either by i.v administration in the tail vein at a dose of 50 mg/kg or by p.o. administration at a dose of 100 mg/kg. In the combination studies mice were pretreated with elacridar (100 mg/kg) 2 hours (h) before i.v. or 20 min before p.o. imatinib and pantoprazole (40 mg/kg) 30 min before i.v. or p.o. imatinib. To minimize variation in absorption, mice were fasted for 3 h before oral imatinib was administered by gavage into the stomach. Blood samples (~ 30 μl) were collected from the tail vein at 5, and 30 min and 1, 2, 4, 8 and 24 h after i.v. administration of imatinib, or at 15 and 30 min and 1, 2, 4, 8, 10 or 24 h after p.o. administration of imatinib using heparinized capillary tubes (Oxford Labware, St. Louis, MO). The plasma fraction of the blood samples was collected after centrifugation at 2,100 x *g* for 10 min at 4°C, and stored at -20°C until HPLC analysis.

Urinary and fecal excretion

WT, Mdr1a/1b$^{-/-}$, Bcrp1$^{-/-}$ and Mdr1a/1b/Bcrp1$^{-/-}$ mice were individually housed in Ruco Type M/1 metabolic cage (Valkenswaard, The Netherlands). They were first accustomed to the cages for 2 days before 50 mg/kg i.v. or 100 mg/kg p.o. imatinib, supplemented with [^{14}C]imatinib (~0.5 μCi/animal), was administered with or without prior oral co-administration of elacridar (100 mg/kg) or pantoprazole (40 mg/kg). Feces and urine were collected in fractions of 0-8, 8-24, 24-48, 48-72 and 72-96 h after drug administration. Feces were homogenized in 4% (w/v) BSA and urine was diluted up to 10-fold with human plasma. An aliquot of the sample was used to determine the levels of radioactivity by liquid scintillation counting (Tri-Carb® 2100 CA Liquid Scintillation analyzer, Canberra Packard, Groningen, The Netherlands); the rest was stored at -20°C until HPLC analysis.

Hepato-biliary excretion

In gall bladder cannulation experiments, WT and Mdr1a/1b/Bcrp1$^{-/-}$ mice were anesthesized with 5 mL/kg of intraperitoneally administered Hypnorm/Dormicum/water (1:1:2, v/v/v).

After opening the abdominal cavity and distal ligation of the common bile duct, a polythene catheter (Portex Ltd., Hythe, United Kingdom), with an inner diameter of 0.28 mm, was inserted into the gall bladder and fixed with an additional ligation. Bile was collected at 5, 15, 30, 60, 90 and 150 min after i.v. injection of 50 mg/kg imatinib, supplemented with [^{14}C]imatinib (~0.5 μCi/animal), with or without prior oral co-administration of elacridar (100 mg/kg). At the end of the experiment, the WT and Mdr1a/1b/Bcrp1$^{-/-}$ mice were sacrificed by cervical dislocation. The bile samples were stored at -20°C until HPLC analysis.

Tissue distribution

To study the impact of Mdr1a/1b and/or Bcrp1 on tissue distribution of imatinib, WT, Mdr1a/1b$^{-/-}$, Bcrp1$^{-/-}$ and Mdr1a/1b/Bcrp1$^{-/-}$ mice received oral imatinib at a dose of 100 mg/kg with or without prior oral co-administration of elacridar (100 mg/kg) or pantoprazole (40 mg/kg). At 1 and 4 h after imatinib administration animals were anaesthetized with methoxyflurane, their blood was collected by cardiac puncture, they were sacrificed by cervical dislocation and brain, liver and kidneys were removed. Tissues were homogenized in 4% (w/v) BSA using a polytron PT1200 (Kinematica AG, Littau, Switzerland) and tissue homogenates and plasma were stored at -20°C until HPLC analysis. The tissue penetration of oral imatinib was calculated by determining the absolute tissue concentration (ng/g tissue) at t = 1 and 4 h. To correct for the differences in plasma concentration between some groups, the imatinib tissue concentration relative to the plasma imatinib concentration at the same time points was calculated.

Drug analysis

Amounts of imatinib and its main active metabolite CGP74588 in all murine samples were determined using a previously described reversed-phase HPLC assay with a lower limit of quantification of 10 ng/mL (30).

Pharmacokinetic and statistical analysis

Pharmacokinetic parameters were calculated per mouse by the noncompartmental trapezoidal method using the software package WinNonlin Professional (version 5.0, Pharsight, Mountain View, CA, USA). The area under the plasma concentration-time curve (AUC) was calculated from time 0 up to 24 h and with extrapolation to infinity ($AUC_{0\text{-}inf}$). The maximal plasma concentration (C_{max}) is reported as observed values. Plasma clearance (Cl) after i.v. imatinib administration was calculated by the formula Cl = dose / $AUC_{i.v}$ and the volume of distribution (V_d) during the elimination phase, also known as β- phase, was

performed by Cl divided by the rate of elimination (β). The oral bioavailability (F) was calculated by the formula $F = (AUC_{oral} \times dose_{i.v.}) / (AUC_{i.v.} \times dose_{oral}) \times 100\%$. Elimination half-lives ($t_{1/2}$) were calculated by linear regression analysis of the log-linear part of the plasma concentration-time curves. Statistical analyses were performed by ANOVA using Bonferroni post-hoc test for multiple comparisons. All values are given as average ± standard deviation (SD). Differences were considered statistically significant when $p < 0.05$.

Results

Plasma pharmacokinetics of oral and i.v. imatinib in WT and Mdr1a/1b/Bcrp1$^{-/-}$ mice

To investigate the role of P-gp and BCRP in ADME of unchanged imatinib *in vivo*, we studied oral and i.v. plasma pharmacokinetics in WT and Mdr1a/1b/Bcrp1$^{-/-}$ mice over a 24-hour time period. We observed that within 15 min after oral administration, at a dose of 100 mg/kg imatinib, the plasma imatinib levels had already reached its maximum in both WT and Mdr1a/1b/Bcrp1$^{-/-}$ mice, suggesting rapid absorption from the intestine (Fig. 1A). Plasma CGP74588 levels reached on average 3-6% of the imatinib plasma levels (data not shown). The $AUC_{0\text{-inf}}$, C_{max} and $t_{1/2}$ for oral imatinib were not significantly different between Mdr1a/1b/Bcrp1$^{-/-}$ and WT mice ($p > 0.05$; Table 1). Plasma imatinib concentrations also declined rapidly after i.v. administration (Fig. 1B), given at a dose of 50 mg/kg (a dose of 100 mg/kg i.v. was too toxic). The $AUC_{0\text{-inf}}$ for i.v. imatinib was 1.6-fold higher in Mdr1a/1b/Bcrp1$^{-/-}$ compared with WT mice (Table 1; $p < 0.05$). Furthermore, plasma Cl in Mdr1a/1b/Bcrp1$^{-/-}$ mice was significantly lower, $t_{1/2}$ significantly longer, however V_d was not significantly different compared with WT mice. The calculated oral bioavailability of imatinib was 48.9 ± 2.9% in Mdr1a/1b/Bcrp1$^{-/-}$ and 70.6 ± 3.5% in WT mice, respectively ($p < 0.05$). Overall, these results show that Mdr1a/1b and Bcrp1 together play a significant role in the Cl of i.v. imatinib, but they do not affect Cl/F of oral imatinib.

We administered an oral or i.v. dose of imatinib (100 mg/kg and 50 mg/kg, respectively) to WT and Mdr1a/1b/Bcrp1$^{-/-}$ mice, which were pretreated with p.o. elacridar (100 mg/kg) or p.o. pantoprazole (40 mg/kg). Interestingly, co-administration of elacridar increased the $(AUC_{0\text{-inf}})_{oral}$ and $(AUC_{0\text{-inf}})_{i.v.}$ by 3.3- and 2.0-fold, respectively, in WT and 2.7- and 1.3-fold in Mdr1a/1b/Bcrp1$^{-/-}$ mice ($p < 0.05$; Fig. 1; Table 1). In addition, co-administration of pantoprazole increased the $(AUC_{0\text{-inf}})_{oral}$ and $(AUC_{0\text{-inf}})_{i.v.}$ as well 3.4- and 3.5-fold, respectively, in WT and 3.6- and 3.0-fold in Mdr1a/1b/Bcrp1$^{-/-}$ mice ($p < 0.05$; Fig. 1; Table 1). The oral bioavailability of imatinib co-administered with elacridar was 105 ± 4.6% and 102 ± 7.6% in WT and Mdr1a/1b/Bcrp1$^{-/-}$ mice, respectively, and 67.7 ± 7.2% and 60.0 ± 4.9% when pantoprazole was co-administered. These results suggest that

besides Mdr1a/1b and Bcrp1 also other mechanisms, such as interaction with other drug transporters or drug metabolizing enzymes by which elacridar or pantoprazole could influence imatinib disposition, are involved.

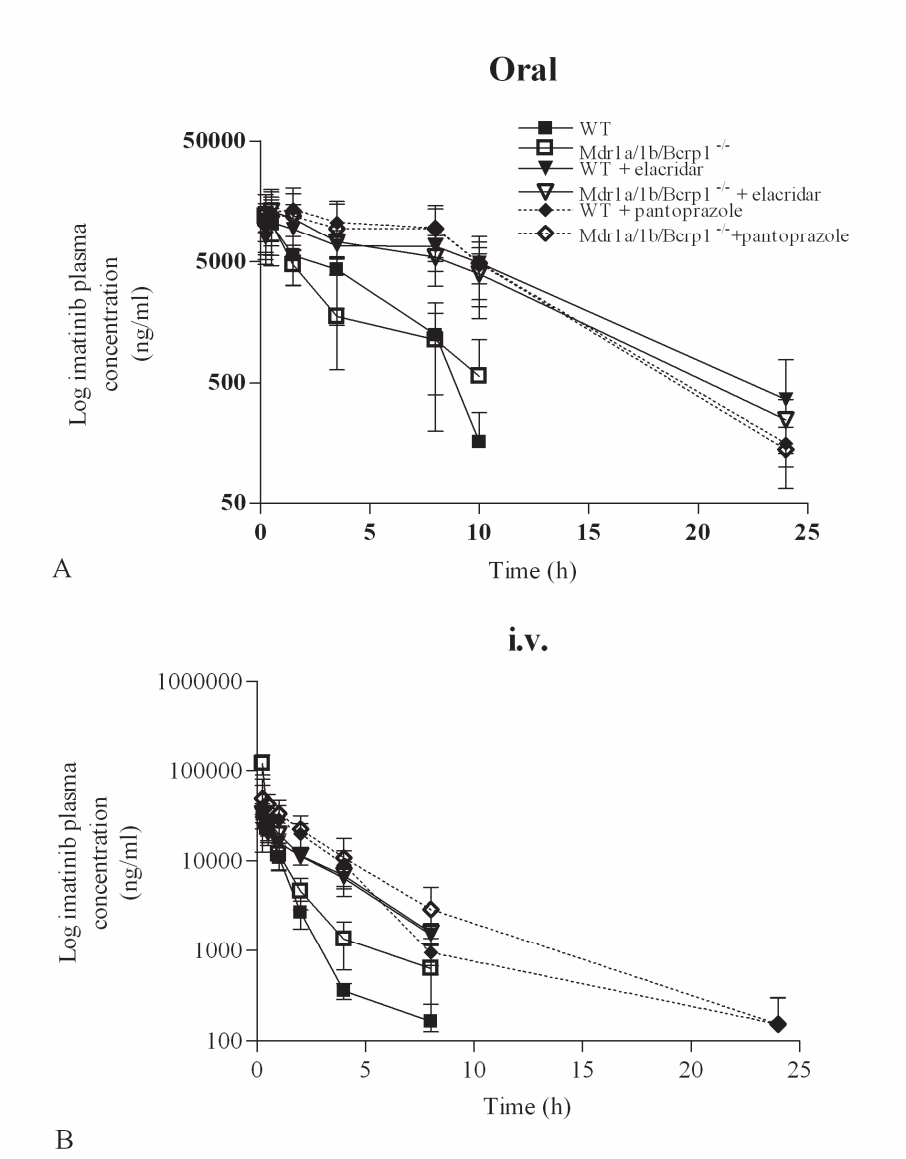

Figure 1. Plasma concentration-time curves of oral (100 mg/kg) (A) and i.v. (50 mg/kg) (B) imatinib in female FVB wild-type (WT) mice (black squares), Mdr1a/1b/Bcrp1$^{-/-}$ mice (open squares), WT or Mdr1a/1b/Bcrp1$^{-/-}$ mice pre-treated with elacridar (100 mg/kg) (black triangles or open triangles, respectively) and WT or Mdr1a/1b/Bcrp1$^{-/-}$ mice pre-treated with pantoprazole (40 mg/kg) (black diamond or open diamond, respectively). (A) Effect of the P-gp/BCRP inhibitors elacridar and pantoprazole on the pharmacokinetics of oral imatinib.

(B) Effect of elacridar and pantoprazole on the pharmacokinetics of i.v. imatinib. Plasma levels of imatinib were determined by a validated HPLC method with lower limit of quantification of 10 ng/mL. Data points are expressed as mean concentrations for oral (n = 6) and i.v. (n = 4) administration; error bars indicate SD.

Table 1. Plasma pharmacokinetic parameters after oral (100 mg/kg) and i.v. (50 mg/kg) administration of imatinib in wild-type and Mdr1a/1b/Bcrp1$^{-/-}$ mice with or without pretreatment of elacridar or pantoprazole.

	Oral administration			i.v. administration					
Strain	**$AUC_{0\text{-inf}}$ (mg*h/L)**	**C_{max} (mg/L)**	**$t_{1/2}$ (h)**	**$AUC_{0\text{-inf}}$ (mg*h/L)**	**C_{max} (mg/L)**	**$t_{1/2}$ (h)**	**Cl (mL/h)**	**V (mL)**	**F %**
wild-type	30.0 ± 5.0	10.8 ± 2.8	2.0 ± 0.8	42.5 ± 6.4	52.4 ± 23.2	1.4 ± 0.2	58.7 ± 16.2	119 ± 39.7	70.6 ± 3.5
Mdr1a/1b/Bcrp1$^{-/-}$	33.9 ± 5.9	12.1 ± 4.6	3.5 ± 1.8	69.2* ± 9.2	116* ± 24.6	2.5* ± 0.3	32.7* ± 3.6	77.2 ± 16.3	48.9* ± 2.9
wild-type + elacridar	99.3$^{*\#}$ ± 14.0	11.8 ± 3.0	4.1 ± 1.8	94.8* ± 11.8	29.0$^{\#}$ ± 10.5	2.6* ± 0.3	26.3* ± 4.2	97.6 ± 17.7	105$^{*\#}$ ± 4.6
Mdr1a/1b/Bcrp1$^{-/-}$ + elacridar	92.9$^{*\#}$ ± 18.9	17.4* ± 2.8	3.6 ± 0.7	90.7* ± 11.5	36.6$^{\#}$ ± 9.3	2.5* ± 0.3	23.3* ± 4.3	85.3 ± 17.6	102$^{*\#}$ ± 7.6
wild-type + pantoprazole	101$^{*\#}$ ± 29.8	18.1* ± 3.4	3.2 ± 0.6	150$^{*\#\$}$ ± 20.6	63.9$^{\#}$ ± 26.2	1.2$^{\#\$}$ ± 0.2	17.1$^{*\#\$}$ ± 1.5	30.2$^{*\#\$}$ ± 7.0	67.7$^{\#\$}$ ± 7.2
Mdr1a/1b/Bcrp1$^{-/-}$ +pantoprazole	123$^{*\#}$ ± 33.1	16.7 ± 3.4	3.3 ± 0.4	205$^{*\#\$}$ ± 18.9	65.6$^{\#\$}$ ± 13.9	2.3$^{\&}$ ± 0.7	11.7$^{*\#\$}$ ± 1.3	39.4$^{*\#\$}$ ± 12.3	60.0$^{\#\$}$ ± 4.9

Note: Dose corrected AUC values. Data are mean ± SD, n = 6 for oral and n = 4 for i.v. administration. Abbreviation: $AUC_{0\text{-inf}}$, Area under the concentration time curve from 0 to infinity; C_{max}, the maximal plasma concentration; $t_{1/2}$, elimination halve-life; Cl, total plasma clearance; V, volume of distribution; F, oral bioavailability. * $p < 0.05$, compared with WT mice; # $p < 0.05$, compared with Mdr1a/1b/Bcrp1$^{-/-}$ mice;
\$ $p < 0.05$, compared with WT and Mdr1a/1b/Bcrp1$^{-/-}$ mice pretreated with elacridar; & $p < 0.05$, compared with WT mice pretreated with pantoprazole.

Fecal and urinary excretion of oral and i.v. imatinib and CGP74588

[^{14}C]imatinib was administered orally (100 mg/kg) or i.v. (50 mg/kg) with or without co-administration of elacridar or pantoprazole to WT and Mdr1a/1b$^{-/-}$ and/or Bcrp1$^{-/-}$ mice. The cumulative excretion of total fecal and urinary radioactivity as well as unchanged imatinib and CGP74588 were measured. Most of the radioactivity in feces and urine was excreted during the first 48 h. In the 48-96 h feces and urine portions, radioactivity was low (~ 1% additional excretion; data not shown). In WT mice after administration of oral [^{14}C]imatinib, 44.6% ± 3.3% of the given radioactivity was recovered from the feces and 38.6% ± 4.2% from urine (Fig. 2A). HPLC analyses showed that fecal excretion of unmodified imatinib and CGP74588 was 24.9% ± 5.8% and 1.3 ± 0.1%, respectively, and

urinary excretion accounted for 1.4 ± 0.5% and 0.1% ± 0.01% of the administered dose in WT mice (Fig. 2A). This indicates that unchanged imatinib is mainly excreted in the feces and that it is extensively metabolized to other metabolites besides CGP74588. These metabolites are found both in feces and urine. The fecal excretion of unmodified imatinib diminished 5.2-fold in Mdr1a/1b/Bcrp1$^{-/-}$, 3.4-fold in Mdr1a/1b$^{-/-}$, but was not significantly different in Bcrp1$^{-/-}$ mice compared with control WT mice (Fig. 2A). The effect of elacridar on the fecal excretion of oral imatinib showed also a reduction of 3.3-fold in WT and 2.8-fold in Mdr1a/1b/Bcrp1$^{-/-}$ mice. In contrast, WT mice pretreated with pantoprazole showed no significant difference compared with WT mice, however in Mdr1a/1b/Bcrp1$^{-/-}$ mice pretreated with pantoprazole a 2.7-fold reduction was shown. Similar differences between the different genotypes were found after i.v. dosing of imatinib. This suggests a prominent role for Mdr1a/1b in the fecal excretion of imatinib. Inhibition of both Mdr1a/1b and Bcrp1 is more effective than inhibition of Mdr1a/1b alone, which means that Bcrp1 has an effect on the fecal excretion of imatinib as well. Elacridar reduced the fecal excretion by inhibition of Mdr1a/1b and Bcrp1, in contrast with pantoprazole.

As noted above, the urinary excretion of unchanged imatinib and CGP74588 was very low in WT mice. For urinary excretion an increase of 2.7- and 3.8-fold was found in WT and Mdr1a/1b/Bcrp1$^{-/-}$ mice, respectively, pretreated with elacridar and 2.7-fold in Mdr1a/1b/Bcrp1$^{-/-}$ mice pretreated with pantoprazole compared with WT mice ($p < 0.05$; Fig. 2A). This suggests that in these mice the imatinib excretion shifts towards the urinary route. This is in line with the observed three times higher plasma levels in WT and Mdr1a/1b/Bcrp1 mice pretreated with elacridar or pantoprazole as described above. Urinary excretion was not significantly different in any of the genotypes and WT mice pretreated with pantoprazole compared to control mice. CGP74588 levels in feces and urine in all knockout mice were < 1%. The fecal and urinary excretion of unchanged imatinib and CGP74588 after i.v. administration of [^{14}C]imatinib showed a similar excretory pattern as the orally treated mice (Fig. 2B). Together, the data suggests that the absence or inhibition of Mdr1a/1b and to a lesser extent Bcrp1 by elacridar mainly reduces the fecal excretion and, thus, most likely the hepatic/biliary elimination of imatinib in mice. Furthermore, elacridar increases the urinary excretion; however pantoprazole had no effect on the fecal and urinary excretion.

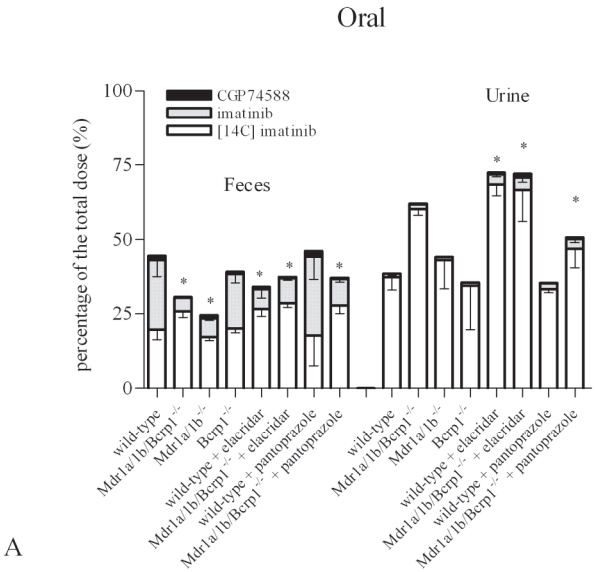

A

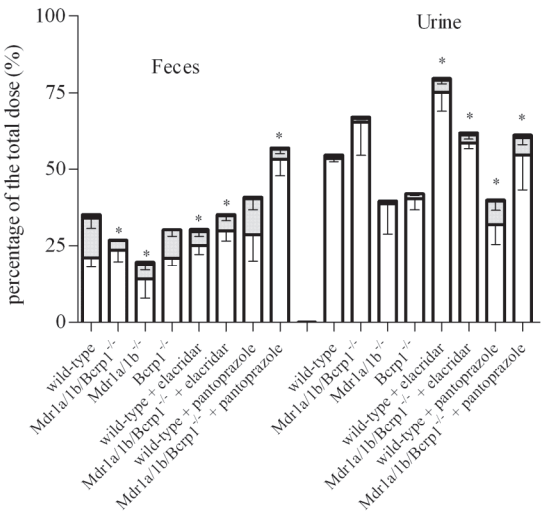

B

Figure 2. Fecal and urinary excretion of imatinib in Mdr1a/1b/Bcrp1$^{-/-}$, Mdr1a/1b$^{-/-}$, Bcrp1$^{-/-}$ and WT mice with or without elacridar or pantoprazole. The mice were housed in metabolic cages and were treated with 100 mg/kg p.o. imatinib or 50 mg/kg i.v., supplemented with a tracer dose of [^{14}C]imatinib (~0.5 μCi/animal), with or without co-administration of one oral dose of elacridar (100 mg/kg) or one oral dose of pantoprazole (40 mg/kg). (A) Role of Mdr1a/1b and Bcrp1 and the effect of elacridar or pantoprazole in the mass balance of oral imatinib. (B) Role of

Mdr1a/1b and Bcrp1 and the effect of elacridar or pantoprazole in the mass balance of i.v. imatinib. Radioactivity was measured in feces and urine excreted between 0-48 h. Unmodified imatinib and CGP74588 was measured using a validated HPLC method. Results are expressed as percentage of the given dose; Bars ± SD (n = 4). * $p < 0.05$ is the significant difference of the percentage of unchanged imatinib in the different knockout mice compared with wild-type mice.

Hepatobiliary excretion of i.v. imatinib in gall bladder-cannulated mice

To further investigate the role of Mdr1a/1b and Bcrp1 and the effect of elacridar on the hepatobiliary excretion of imatinib, we administered [^{14}C]imatinib (50 mg/kg) i.v. with or without pretreatment of elacridar to WT and Mdr1a/1b/Bcrp1$^{-/-}$ mice with a cannulated gall bladder and ligated common bile duct. At 150 min after i.v. administration, the cumulative unchanged imatinib and CGP74588 excretion, as percentage of the dose, was 4.3 ± 0.9% and 0.3 ± 0.08%, respectively, in WT mice (Fig. 3). Due to the low bile volume, we were not able to measure the radioactivity in individual bile fractions. Compared with WT mice, the biliary excretion of imatinib and CGP74588 in Mdr1a/1b/Bcrp1$^{-/-}$ mice was significantly reduced 8.1- and 7.2-fold, respectively. Co-administration of elacridar decreased the biliary excretion of imatinib and CGP74588 to the same levels observed in Mdr1a/1b/Bcrp1$^{-/-}$ mice (Fig. 3). We conclude from this experiment that the hepatobiliary elimination of imatinib and CGP74588 in mice is dominated by Mdr1a/1b and Bcrp1 and that elacridar can significantly inhibit the Mdr1a/1b/Bcrp1 mediated hepatobiliary excretion of imatinib and CGP74588.

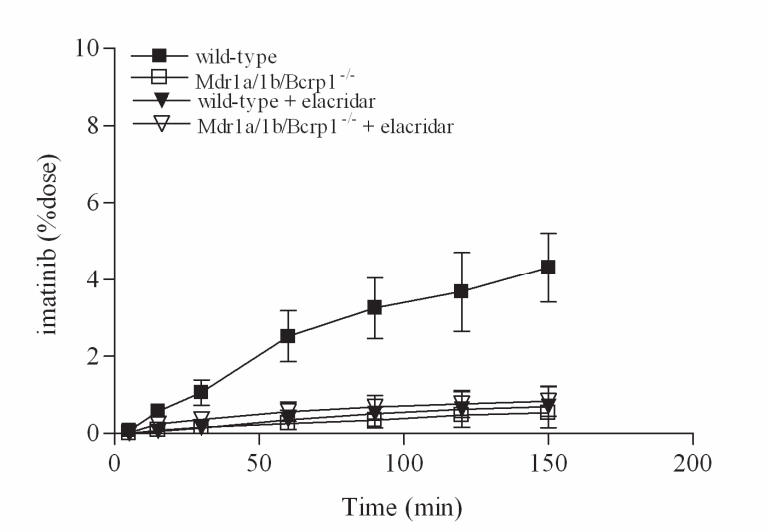

A

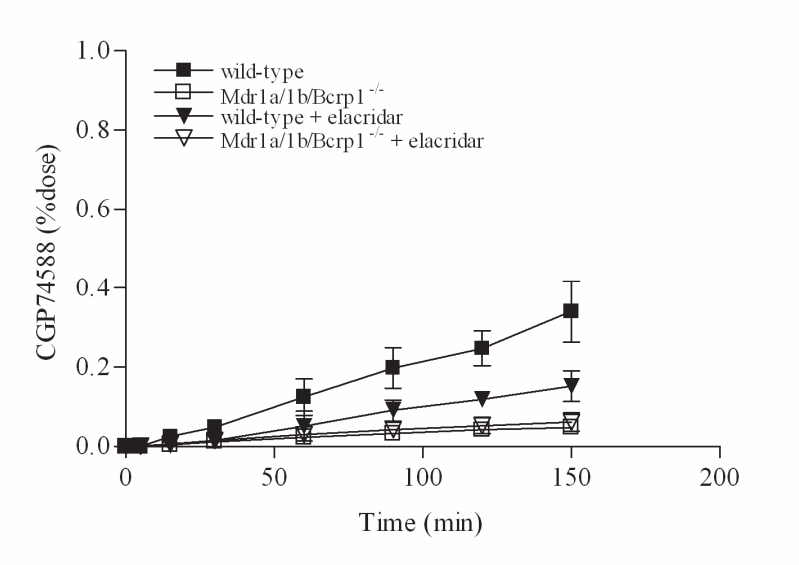

B

Figure 3. Cumulative hepatobiliary excretion of (A) imatinib and (B) CGP74588 in wild-type and Mdr1a/1b/Bcrp1$^{-/-}$ mice. [^{14}C]imatinib was administered i.v. (50 mg/kg) with or without pretreatment of elacridar (100 mg/kg) to mice with a cannulated gall bladder. Unchanged imatinib and CGP74588 were measured by HPLC in bile fractions of wild-type (black squares), Mdr1a/1b/Bcrp1$^{-/-}$ (open squares), wild-type + elacridar (black triangle) and Mdr1a/1b/Bcrp1$^{-/-}$ + elacridar (open triangle) mice. Data are expressed as percentage of the dose ± SD (n = 4-5; at all time points).

Liver and kidney distribution of oral imatinib

Furthermore, we investigated the role of Mdr1a/1b and Bcrp1 and the effect of elacridar or pantoprazole on the accumulation of imatinib in the liver and kidney. The liver and kidney accumulation of imatinib at t = 1 h (but not at t = 4 h) was significantly increased in WT and Mdr1a/1b/Bcrp1$^{-/-}$ mice co-administered with elacridar ($p < 0.05$) compared with WT mice (data not shown). However, when corrected for the plasma concentration at t = 1 and 4 h, the accumulation of imatinib in liver and kidney in these mice was not significantly different compared to WT controls, even when elacridar was co-administered (Fig. 4A and B). This suggests that the liver and kidney drug levels in these mice are in dose equilibrium with plasma.

Brain penetration of oral imatinib

Finally, we investigated the role of Mdr1a/1b and Bcrp1 and the effect of elacridar or pantoprazole on the imatinib accumulation in the brain after oral administration. As shown in figure 4C, the brain penetration of unchanged imatinib, corrected for the plasma

concentration, after 1 and 4 h was increased 13.3- and 12.6-fold ($p < 0.001$), respectively, in Mdr1a/1b/Bcrp1$^{-/-}$ mice and 2.3-fold ($p < 0.05$) after 1 h in Mdr1a/1b$^{-/-}$ mice compared with WT mice. There was no significant difference (1.0-fold) after 4 h in Mdr1a/1b$^{-/-}$ mice and at both time points in Bcrp1$^{-/-}$ mice compared with WT mice ($p > 0.05$). Co-administration of elacridar in WT mice increased the brain penetration of oral imatinib after 1 and 4 h 5.0- and 3.0-fold, respectively, and in Mdr1a/1b/Bcrp1$^{-/-}$ 7.9- and 6.4-fold ($p < 0.001$). Pantoprazole enhanced the brain penetration of oral imatinib to a lesser extent in WT mice after 1 and 4 h, 1.2- and 1.8-fold ($p < 0.05$), respectively, and in Mdr1a/1b/Bcrp1$^{-/-}$ 10.3- and 6.0-fold ($p < 0.001$) compared with WT mice. Our results show that the absence or inhibition of both Mdr1a/1b and Bcrp1 on the central nervous system accumulation of imatinib in mice is much more effective than inhibition of Mdr1a/1b or Bcrp1 alone. The brain penetration can be substantially improved by co-administration of elacridar and to a lesser extent by co-administration of pantoprazole.

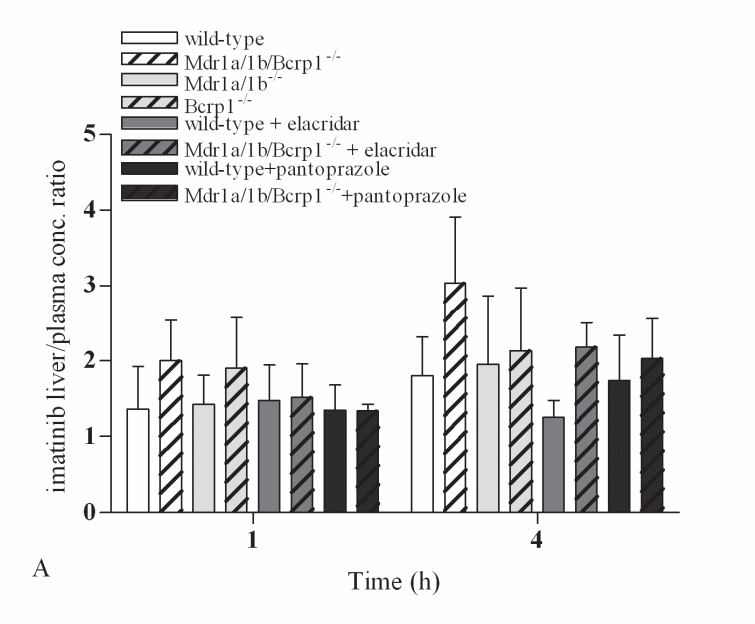

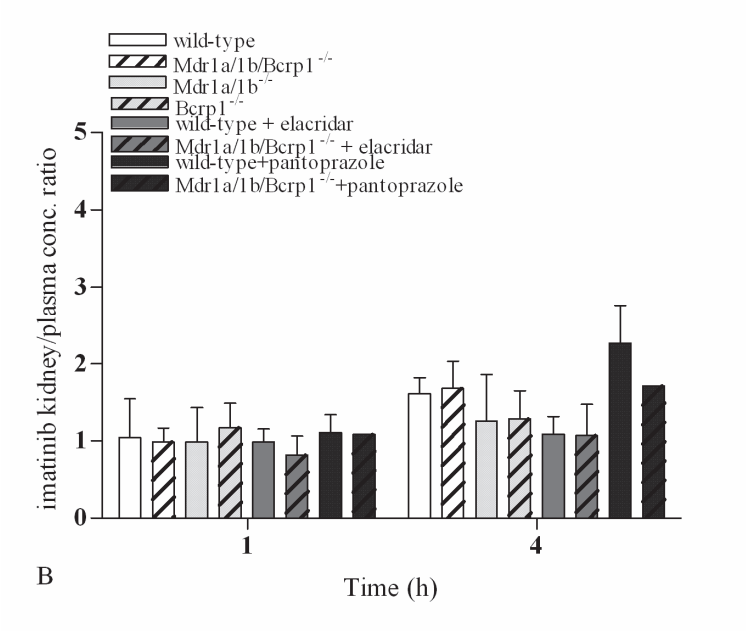

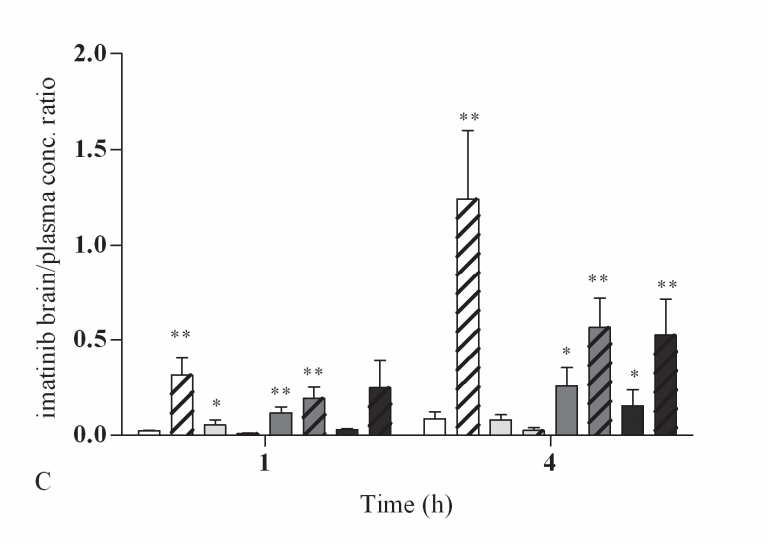

Figure 4. Imatinib (100 mg/kg) liver, kidney and brain penetration in wild-type, Mdr1a/1b$^{-/-}$, Bcrp1$^{-/-}$ and Mdr1a/1b/Bcrp1$^{-/-}$ with or without pre-treatment of elacridar (100 mg/kg) or pantoprazole (40 mg/kg). At t = 1 and 4 h, blood, liver, kidneys and brain were collected and concentrations of imatinib were measured by HPLC. Results are expressed as the imatinib tissue to plasma concentration ratio (Liver A, Kidney B, Brain C). Values shown are the means (columns) of 5 mice per group ± SD (bars). * $p < 0.05$ and ** $p < 0.001$ are the significant differences of the imatinib tissue/plasma conc. ratio in the different knockout mice compared with wild-type mice.

Discussion

This study shows that P-gp and BCRP are both involved in the ADME of imatinib. Although their combined deficiency reduced hepatobiliary-fecal excretion significantly, this had just a modest effect on the systemic drug exposure after i.v. or oral drug administration. The effect of these drug transporters on the brain penetration of imatinib was most evident in the P-gp/BCRP knockout mice, since the presence of either P-gp or BCRP alone was already sufficient to reduce the brain:plasma concentration ratio close to the levels found in WT mice.

In order to study the role of P-gp and BCRP we made use of the P-gp/BCRP knockout mouse model that has recently become available (31, 32). Previous studies have been carried out using single BCRP or P-gp knockout mice receiving imatinib with or without co-administration of inhibitors (24, 25, 29). However, a major problem is that the effects of these inhibitors on other systems involved in ADME of imatinib are largely unknown making it hard to draw firm conclusions. For example, Bihorel et al. (29) reported that the imatinib blood levels increased by 3.3- to 3.8-fold in WT mice when given in combination with valspodar or elacridar. Our results in P-gp/BCRP knockout mice clearly show that these increased levels are only partly due to inhibition of P-gp and BCRP, as the plasma level was only 1.6-fold higher in these mice. Although, compensatory mechanisms in knockout mice may conceal some of the effect of the absence of these transporters, we were able to show the non-selective effects of inhibitors, elacridar and pantoprazole, by giving them to P-gp/BCRP knockout mice. Their co-administration should not have led to increased plasma levels of imatinib if they would have been selective for P-gp and/or BCRP. Instead, however, we found that the plasma levels increased significantly to levels observed in WT mice receiving imatinib and the inhibitor. The moderate 1.6-fold reduction in the Cl of imatinib by the absence of P-gp and BCRP and the more pronounced effects by the inhibitors suggest that other elimination routes are more important. Indeed, it is known that metabolic degradation is an important component in the elimination of imatinib from the body (25, 29) and this was clearly confirmed by the results obtained in our mouse models. The fecal excretion of unchanged drug and CGP74588 in WT mice receiving i.v. imatinib was about 14.0% and < 1.0%, respectively, whereas radioactivity measurements showed that most of the drug left the organism in feces or urine as unknown metabolites. The absence of P-gp but not BCRP alone reduced the fecal excretion of imatinib significantly showing that the Pgp is more important for the fecal excretion. However, the combined absence of P-gp and BCRP resulted in a greater reduction than inhibition of P-gp alone, suggesting that, BCRP does play a role in the fecal excretion of imatinib. This could not be shown in BCRP single knockout mice, most likely due to the action of P-gp. In a

bile cannulation experiment we clearly confirmed that the P-gp and BCRP inhibitor, elacridar, appeared to fully inhibit P-gp and BCRP in the liver, showing that, no other transporters besides P-gp and BCRP were inhibited in the hepatobiliary excretion route.

Whereas the tissue to plasma ratios in liver and kidney were not affected by the absence or inhibition of P-gp and/or BCRP in the different mouse strains, the brain penetration was significantly higher in P-gp knockout mice. This shows that P-gp is an important factor in the brain penetration of imatinib, in line with previous reports (25, 26, 29). In contrast to our previous results (24), the absence of BCRP alone had no distinct effect on the brain penetration of imatinib. Whereas the reason for this discrepancy is conjecture, it may be related to the fact that these previous results were based on the determination of total radioactivity instead of unchanged drug levels as used in this study. Moreover, whereas in studies imatinib was given i.v., we have now used oral dosing since this route is the commonly applied route for treatment of patients. A major difference between the two routes is that the very high plasma levels that occur immediately after i.v. dosing do not occur after oral dosing. Our current results with imatinib given as single agent to WT, P-gp and BCRP knockout mice are in line with those reported by Bihorel et al. (29). What becomes very clear from the P-gp/BCRP knockout mice is that combined absence of P-gp and BCRP was much more effective on the brain penetration than the absence of P-gp or BCRP alone.

Although the mechanism behind the additional effect of elacridar or pantoprazole on the systemic exposure of imatinib is not clear, we speculate that this is due to inhibition of metabolic degradation. The reason, that this does not result in a significantly higher excretion of unchanged drug, most likely results from the fact that elacridar or pantoprazole at the same time inhibit the excretion of unchanged drug. Overall, this dual inhibition of both excretion and metabolism just causes a delay in the elimination of imatinib. This hypothesis, however, is in conflict with previous reports suggesting that elacridar is not an inhibitor of the Cyp3a isoenzymes that may also be involved in the metabolism of imatinib (33). Whereas it is certainly possible that elacridar could have an effect on other efflux transporters as suggested by Lee et al. (34), it seems unlikely that this could have such a profound effect on the plasma level of imatinib. The fraction of unchanged drug that is excreted in P-gp/BCRP knockout mice is already very low, and a further reduction by a few percent cannot explain the more than 3-fold reduction in clearance. In addition, previous experiments showed already that imatinib was not a substrate for Multidrug Resistance Protein 1 (MRP1) and MRP2 (24, 35) and elacridar does not seem to modulate the transport activity of MRP1 and MRP2 (36). Another option would be the inhibition of drug influx transporters such as Organic Cation Transporters (OCTs) and Organic Anion Transporting Polypeptides (OATPs) (37-39). We have shown *in vitro* that elacridar and pantoprazole

inhibited both human OCT1 and OATP1B1 (submitted). Furthermore, the V_d of imatinib in WT and P-gp/BCRP knockout mice co-administered with pantoprazole was significantly lower compared with WT and P-gp/BCRP knockout mice, which is possibly due to inhibition of a drug influx transporter by pantoprazole. Recent *in vitro* studies have shown that human OCT1 mediated influx is a key determinant of the intracellular accumulation of imatinib (40-42). In CML patients, it has recently been found that the OCT1 transcript levels are lower in imatinib non-responders than in imatinib responders (43, 44). Thus inhibition of influx transporters could also provide a reasonable explanation for the reduced plasma Cl.

In summary, our results reveal that in mice P-gp and BCRP have only modest effects on the ADME of imatinib in comparison to metabolic elimination. Of these two drug transporters P-gp is the most prevalent factor for systemic clearance and the most important for limiting the brain penetration. Interestingly, coadministration of the P-gp/BCRP inhibitors, elacridar or pantoprazole, significantly increased the systemic exposure to imatinib in the presence or absence of P-gp/BCRP in mice. This suggests that besides P-gp and BCRP other elimination pathways are involved in the drug-drug interaction between imatinib-elacridar/pantoprazole.

Acknowledgement

We are grateful to Lianne Asschert (Novartis Pharma B.V., Arnhem, The Netherlands) for providing us with imatinib mesylate and its metabolite CGP74588 (Novartis Pharma AG, Basel, Switzerland). We would like to thank Alfred Schinkel (Department of Experimental Therapy, The Netherlands Cancer Institute, The Netherlands), Irma Meijerman (Faculty of Science, Utrecht University, The Netherlands) and Alwin D.R. Huitema (Department of Pharmacy & Pharmacology, Slotervaart Hospital, The Netherlands) for scientific input.

References

1. Capdeville R, Buchdunger E, Zimmermann J et al. Glivec (STI571, imatinib), a rationally developed, targeted anticancer drug. Nat Rev Drug Discov 2002;1:493–502.
2. Druker BJ, Talpaz M, Resta DJ, et al. Efficacy and safety of a specific inhibitor of the BCR-ABL tyrosine kinase in chronic myeloid leukaemia. N Engl J Med 2001;344:1031–1037.
3. Demetri GD, von Mehren M, Blanke CD, et al. Efficacy and safety of imatinib mesylate in advanced gastrointestinal stromal tumors. N Engl J Med 2002;347:472–480.
4. Johnson BE, Fischer T, Fischer B, et al. Phase II study of imatinib in patients with small cell lung cancer. Clin Cancer Res 2003;9:5880–5887.
5. Rao K, Goodin S, Levitt MJ, et al. A phase II trial of imatinib mesylate in patients with prostate specific antigen progression after local therapy for prostate cancer. Prostate 2005;62:115–122.
6. Reardon DA, Egorin MJ, Quinn JA, et al. Phase II study of imatinib mesylate plus hydroxyurea in adults with recurrent glioblastoma multiforme. J Clin Oncol 2005;23:9359–9368.
7. Dresemann G. Imatinib and hydroxyurea in pretreated progressive glioblastoma multiforme: a patient series. Ann Oncol 2005;16:1702–1708.
8. Shannon KM. Resistance in the land of molecular cancer therapeutics. Cancer Cell 2002;2:99–102.

9. McCormick F. New-age drug meets resistance. Nature 2001;412:281–282.
10. Heinrich MC, Corless CL, Blanke CD, et al. Molecular correlates of imatinib resistance in gastrointestinal stromal tumors. J Clin Oncol 2006;24:4764–4774.
11. Sleijfer S, Wiemer E, Seynaeve C, et al. Improved insight into resistance mechanisms to imatinib in gastrointestinal stromal tumors: a basis for novel approaches and individualization of treatment. Oncologist 2007;12:719–726.
12. Gambacorti-Passerini C, Zucchetti M, Russo D, et al. Alpha1 acid glycoprotein binds to imatinib (STI571) and substantially alters its pharmacokinetics in chronic myeloid leukemia patients. Clin Cancer Res 2003;9:625–632.
13. Cohen MH, Williams G, Johnson JR, et al. Approval summary for imatinib mesylate capsules in the treatment of chronic myelogenous leukaemia. Clin Cancer Res 2002;8:935–942.
14. Peng B, Dutreix C, Mehring G, et al. Absolute bioavailability of imatinib (Glivec) orally versus intravenous infusion. J Clin Pharmacol 2004;44:158–162.
15. Judson I, Ma P, Peng B, et al. Imatinib pharmacokinetics in patients with gastrointestinal stromal tumour: a retrospective population pharmacokinetic study over time. EORTC Soft Tissue and Bone Sarcoma Group. Cancer Chemother Pharmacol 2005;55:379–386.
16. Peng B, Hayes M, Resta D, et al. Pharmacokinetics and pharmacodynamics of imatinib in a phase I trial with chronic myeloid leukemia patients. J Clin Oncol 2004;22:935–942.
17. Peng B, Lloyd P, Schran H. Clinical pharmacokinetics of imatinib. Clin Pharmacokinet 2005;44:879–894.
18. Rochat B. Role of cytochrome P450 activity in the fate of anticancer agents and in drug resistance: focus on tamoxifen, paclitaxel and imatinib metabolism. Clin Pharmacokinet 2005;44:349–366.
19. Gschwind HP, Pfaar U, Waldmeier F, et al. Metabolism and disposition of imatinib mesylate in healthy volunteers. Drug Metab Dispos 2005;33:1503–1512.
20. Marull M, Rochat B. Fragmentation study of imatinib and characterization of new imatinib metabolites by liquid chromatography-triple-quadrupole and linear ion trap mass spectrometers. J Mass Spectrom 2006; 41:390–404.
21. Hamada A, Miyano H, Watanabe H, et al. Interaction of imatinib mesilate with human P-glycoprotein. J Pharmacol Exp Ther 2003;307:824–828.
22. Burger H, van Tol H, Boersma AW, et al. Imatinib mesylate (STI571) is a substrate for the breast cancer resistance protein (BCRP)/ABCG2 drug pump. Blood 2004;104:2940–2942.
23. Houghton PJ, Germain GS, Harwood FC, et al. Imatinib mesylate is a potent inhibitor of the ABCG2 (BCRP) transporter and reverses resistance to topotecan and SN-38 in vitro. Cancer Res 2004;64:2333–2337.
24. Breedveld P, Pluim D, Cipriani G, et al. The effect of Bcrp1 (Abcg2) on the in vivo pharmacokinetics and brain penetration of imatinib mesylate (Gleevec): implications for the use of breast cancer resistance protein and P-glycoprotein inhibitors to enable the brain penetration of imatinib in patients. Cancer Res 2005;65:2577–2582.
25. Dai H, Marbach P, Lemaire M, et al. Distribution of STI-571 to the brain is limited by P-glycoprotein-mediated efflux. J Pharmacol Exp Ther 2003;304:1085–1092.
26. Bihorel S, Camenisch G, Lemaire M, et al. Influence of breast cancer resistance protein (Abcg2) and p-glycoprotein (Abcb1a) on the transport of imatinib mesylate (Gleevec®) across the mouse blood-brain barrier. J Neurochem 2007;102:1749–1757.
27. Mahon FX, Belloc F, Lagarde V, et al. MDR1 gene overexpression confers resistance to imatinib mesylate in leukemia cell line models. Blood 2003;101:2368–2373.
28. Nakanishi T, Shiozawa K, Hassel BA, et al. Complex interaction of BCRP/ABCG2 and imatinib in BCR-ABL-expressing cells: BCRP-mediated resistance to imatinib is attenuated by imatinib-induced reduction of BCRP expression. Blood 2006;108:678–684.
29. Bihorel S, Camenisch G, Lemaire M, et al. Modulation of the brain distribution of imatinib and its metabolites in mice by valspodar, zosuquidar and elacridar. Pharm Res 2007;24:1720–1728.
30. Oostendorp RL, Beijnen JH, Schellens JH, et al. Determination of imatinib mesylate and its main metabolite (CGP74588) in human plasma and murine specimens by ion-pairing reversed-phase high-performance liquid chromatography. Biomed Chromatogr 2007;21:747–754.
31. Jonker JW, Freeman J, Bolscher E, et al. Contribution of the ABC transporters Bcrp1 and Mdr1a/1b to the side population phenotype in mammary gland and bone marrow of mice. Stem Cells 2005;23:1059–1065.
32. de Vries NA, Zhao J, Kroon E, et al. P-glycoprotein and breast cancer resistance protein: two dominant transporters working together in limiting the brain penetration of topotecan. Clin Cancer Res 2007;13:6440–6449.

33. Lam JL, Benet LZ. Hepatic microsome studies are insufficient to characterize in vivo hepatic metabolic clearance and metabolic drug-drug interactions: studies of digoxin metabolism in primary rat hepatocytes versus microsomes. Drug Metab Dispos 2004;32:1311–1316.
34. Lee YJ, Kusuhara H, Jonker JW, et al. Investigation of efflux transport of dehydroepiandrosterone sulfate and mitoxantrone at the mouse blood-brain barrier: a minor role of breast cancer resistance protein. J Pharmacol Exp Ther 2005;312:44–52.
35. Ozvegy-Laczka C, Hegedus T, Varady G, et al. High-affinity interaction of tyrosine kinase inhibitors with the ABCG2 multidrug transporter. Mol Pharmacol 2004;65:1485-1495.
36. Evers R, Kool M, Smith AJ, et al. Inhibitory effect of the reversal agents V-104, GF120918 and Pluronic L61 on MDR1 Pgp-, MRP1- and MRP2-mediated transport. Br J Cancer 2000;83:366-374.
37. Endres CJ, Hsiao P, Chung FS, et al. The role of transporters in drug interactions. Eur J Pharm Sci 2006;27:501-517.
38. Borst P, Elferink RO. Mammalian ABC transporters in health and disease. Annu Rev Biochem 2002;71:537-592.
39. Shitara Y, Horie T, Sugiyama Y. Transporters as a determinant of drug clearance and tissue distribution. Eur J Pharm Sci 2006;27:425-446.
40. White DL, Saunders VA, Dang P, et al. OCT-1-mediated influx is a key determinant of the intracellular uptake of imatinib but not nilotinib (AMN107): reduced OCT-1 activity is the cause of low in vitro sensitivity to imatinib. Blood 2006;108:697-704.
41. Jiang X, Zhao Y, Smith C, et al. Chronic myeloid leukemia stem cells possess multiple unique features of resistance to BCR-ABL targeted therapies. Leukemia 2007;21:926-935.
42. Thomas J, Wang L, Clark RE, et al. Active transport of imatinib into and out of cells: implications for drug resistance. Blood 2004;104:3739-3745.
43. Crossman LC, Druker BJ, Deininger MW, et al. hOCT 1 and resistance to imatinib. Blood 2005;106:1133-1134.
44. Wang L, Giannoudis A, Lane S, et al. Expression of the Uptake Drug Transporter hOCT1 is an Important Clinical Determinant of the Response to Imatinib in Chronic Myeloid Leukemia. Clin Pharmacol Ther 2008;83:258-264.

CHAPTER 2.2

The role of Organic Cation Transporter 1 and 2 in the *in vivo* pharmacokinetics of imatinib

Roos L. Oostendorp, Tessa Buckle, Alfred H. Schinkel, Jos H. Beijnen, Olaf van Tellingen, Jan H.M. Schellens

Submitted for publication

Abstract

Previous *in vivo* studies concerning the pharmacokinetics of oral imatinib indicated that the breast cancer resistance protein (BCRP; ABCG2)/ P-glycoprotein (P-gp; ABCB1) inhibitor, elacridar, could inhibit transporters other than BCRP and P-gp. Imatinib has recently been described to be transported by the organic cation transporter 1 (OCT1) *in vitro*. In this study we investigated the inhibitory effect of elacridar on the OCT1 mediated transport of imatinib *in vitro*, and the possible role of OCT1 and 2 and the effect of elacridar on the oral absorption, tissue distribution and elimination of imatinib in mice. In HEK293 cells, elacridar was found to be an inhibitor of the OCT1 mediated transport of imatinib. In OCT1/2 knockout mice a moderately but significantly higher area under the plasma concentration-time curve (AUC) after oral and i.v. administration of imatinib was shown. Elacridar in combination with imatinib significantly increased the AUC of orally administered imatinib in wild-type but also in OCT1/2 knockout mice. The hepatobiliary excretion and liver accumulation of imatinib was not significantly different between wild-type and OCT1/2 knockout mice, whereas elacridar reduced the hepatobiliary excretion. In conclusion, OCT1/2 has a modest, albeit statistically significant, effect on the systemic exposure of imatinib *in vivo*. The considerable drug-drug interaction observed with elacridar is only partly mediated by inhibition of OCT1/2 and furthermore by the inhibition of other elimination pathways.

Introduction

Imatinib mesylate (Gleevec) is an orally administered tyrosine kinase inhibitor that is FDA and EMEA approved for the treatment of Bcr-Abl positive chronic myeloid leukemia (CML) (1) and c-KIT-positive metastatic and unresectable gastrointestinal stromal tumors (GIST) (2). This drug is currently also under intensive investigation in other tumor types as single agent (3) or in combination with other agents (4). Changes or variations in the pharmacokinetics of imatinib that may compromise therapeutic efficacy in patients with CML or GIST have been observed, but are not well-understood (5). Whereas imatinib has an oral bioavailability of 98% (6), a reduced systemic exposure to imatinib over prolonged time periods was shown (7). Furthermore, wide interindividual variability (variation coefficient ranging from 40% to 60%) in the systemic exposure was shown in patients with CML and GIST (7, 8), which may cause differences in compliance and attribute to variation in absorption, distribution, metabolism and excretion (ADME) between patients. It is known that imatinib is extensively metabolized by Cytochrome P450s (CYPs) in liver (9, 10). N-desmethyl-imatinib (CGP74588), primarily formed in the liver by CYP3A4, has been identified as a major metabolite of imatinib and has comparable activity as the parent compound (10), whereas a number of other CYPs are involved in the formation of minor metabolites (11). Besides drug metabolizing enzymes, *in vitro* and *in vivo* studies have shown that imatinib interacts with the drug-efflux transporters breast cancer resistance protein (BCRP; rodent Bcrp1) and P-glycoprotein (P-gp; rodent Mdr1a/1b) and tumor expression of these transporters probably influences the antitumor response to imatinib in patients (12-16). However, recently we have found that BCRP and P-gp have only modest effects on the ADME of imatinib *in vivo* (17). Interestingly, co-administration of the BCRP/P-gp inhibitor, elacridar, significantly increased the systemic exposure to oral imatinib 3-fold in the presence or absence of BCRP/P-gp in mice (17). This suggests that besides BCRP and P-gp other elimination pathways are involved in the drug-drug interaction between oral imatinib and elacridar. *In vitro* studies have shown that human organic cation transporter 1 (OCT1; rodent Oct1) is involved in the cellular uptake of imatinib in a variety of leukemia cells (18-20). OCT1 is a highly expressed solute carrier in the basolateral membrane of hepatocytes (21). Furthermore, in CML patients it has been found that the OCT1 transcript levels in tumor cells are lower in imatinib non-responders than in imatinib responders (20, 22, 23). In contrast to these earlier studies, Hu et al. (24) recently showed only a minor contribution of OCT1 to the transport of imatinib. In the present study, we performed a pharmacokinetic study in wild-type and OCT1 and 2 double knockout mice to establish the role of OCT1 in the pharmacokinetics of imatinib *in vivo*. We have chosen this OCT1/2 double knockout mouse model (25) as imatinib might also

have affinity for OCT2 besides OCT1. Moreover, we also studied the effect of elacridar on the disposition of imatinib *in vitro* and *in vivo* in order to demonstrate whether OCT1/2 is involved in the drug-drug interaction between imatinib and elacridar.

Material and Methods

Chemicals and reagents

Imatinib (STI-571) and [^{14}C]imatinib (both as mesylate salt) were kindly provided by Novartis Pharma AG (Basel, Switzerland). Elacridar (GF120918) was a generous gift from GlaxoSmithKline (Research Triangle Park, NC). [^{3}H]MPP^{+} iodide (N-[methyl-^{3}H]-4-phenylpyridinium iodide; 80 Ci/mmol) was purchased from PerkinElmer Life Science Products (Boston, MA). Hypnorm (fentanyl 0.2 mg/ml and fluanisone 10 mg/ml) was obtained from VetaPharma Ltd (Leeds, UK), midazolam (Dormicum® 5 mg/ml) was from Rôche Nederland (Mijdrecht, The Netherlands) and methoxyflurane (Metofane®) was from Medical Development Australia (Springvale, Victoria, Australia). Bovine serum albumin (BSA), Fraction V, was from Roche (Mannheim, Germany). Methanol, acetonitril (both high-performance liquid chromatography (HPLC) grade) were from Merck (Darmstadt, Germany). Drug-free human plasma was obtained from the Central Laboratory of the Blood Transfusion Service (Sanquin, Amsterdam, The Netherlands). Other chemicals and drugs were from Sigma (St Louis, MO).

Cell lines

Human embryonic kidney (HEK293) cells, stably expressing hOCT1, were kindly provided by Dr. H. Bönisch (Institute of Pharmacology and Toxicology, University of Bonn, Bonn, Germany) and were cultured as described previously (26).

In vitro transport study

HEK293-parental and -OCT1 cells (2 x 10^{5} cells/well) were grown in 24 well plates precoated with 0.1 g l^{-1} poly-L-ornithine in 0.15 M sodium borate (pH 8.4). After 2 days in culture, the cells were used for uptake experiments as described by Hayer-Zillgen et al. (26). [^{3}H]MPP^{+} (25 nM) was used as OCT1 substrate and procainamide (100 µM) as OCT1 inhibitor. [^{14}C]imatinib and the BCRP and/or Pgp inhibitor elacridar (5 µM), were tested in this assay. The concentrations we used for the different compounds are based on comprehensive experience with these compounds (26, 27).

Animals

Mice were housed and handled according to institutional guidelines complying with Dutch legislation. Animals used in all experiments were female FVB wild-type (WT) and Oct1/2$^{-/-}$ (OCT1/2 knockout) mice and were between 9 and 14 weeks of age. Animals were kept in a temperature-controlled environment with a 12-hour light/12-hour dark cycle. They received a standard diet (AM-II, Hope Farms, Woerden, The Netherlands) and acidified water *ad libitum.*

Drug solutions

Imatinib was diluted with glucose 5% to a final concentration of 10 mg/mL for oral (p.o.) or 5 mg/mL for i.v. administration in mice. Elacridar was suspended at 10 mg/mL in a mixture of hydroxypropylmethylcellulose (10 g/L)/2% Tween 80/H_2O) (0.5:1:98.5 [v/v/v]) for p.o. administration in mice.

Plasma pharmacokinetics

WT and Oct1/2$^{-/-}$ mice received imatinib either by i.v. administration in the tail vein at a dose of 50 mg/kg or by oral administration at a dose of 100 mg/kg. In the combination studies mice were pretreated with oral elacridar (100 mg/kg) 20 min before p.o. imatinib. To minimize variation in oral absorption, mice were fasted for 3 h before oral imatinib was administered by gavage into the stomach. Blood samples (~ 30 µl) were collected from the tail vein at 5, and 30 min and 1, 4, 8 and 24 h after i.v. administration of imatinib, or at 15 and 30 min and 1, 4, 8, or 24 h after p.o. administration of imatinib using heparinized capillary tubes (Oxford Labware, St. Louis, MO). The plasma fraction of the blood samples was collected after centrifugation at 2,100 x *g* for 10 min at 4°C, and stored at -20°C until HPLC analysis.

Hepato-biliary excretion

In gall bladder cannulation experiments, WT and Oct1/2$^{-/-}$ mice were anesthesized with 5 mL/kg of intraperitoneally (i.p.) administered Hypnorm/Dormicum/water (1:1:2, v/v/v). After opening the abdominal cavity and distal ligation of the common bile duct, a polythene catheter (Portex Ltd., Hythe, United Kingdom), with an inner diameter of 0.28 mm, was inserted into the gall bladder and fixed with an additional ligation. Bile was collected at 5, 15, 30, 60 and 90 min after i.v. injection of 50 mg/kg imatinib, with or without prior oral co-administration of elacridar (100 mg/kg). At the end of the experiment, the WT and Oct1/2$^{-/-}$ mice were anaesthetized with methoxyflurane, their blood was collected by cardiac puncture, they were sacrificed by cervical dislocation and the liver was removed

and homogenized in 4% (w/v) BSA by a polytron PT1200 (Kinematica AG, Littau, Switzerland). The bile samples, tissue homogenate and plasma were stored at -20°C until HPLC analysis. The tissue penetration of i.v. imatinib was calculated by determining the absolute tissue concentration (ng/g tissue) at t = 90 min. To correct for the differences in plasma concentration between groups, the imatinib tissue concentration relative to the plasma imatinib concentration at the same time points was calculated.

Drug analysis

Concentrations of imatinib and its main active metabolite CGP74588 in all murine samples were determined using a previously described reversed-phase HPLC assay with a lower limit of quantification of 10 ng/mL using 100 µl of sample (28).

Pharmacokinetic and statistical analysis

Pharmacokinetic parameters were calculated per mouse by the noncompartmental trapezoidal method using the software package WinNonlin Professional (version 5.0, Pharsight, Mountain View, CA, USA). The area under the plasma concentration-time curve (AUC) was calculated from time 0 up to the last measured time point ($AUC_{0\text{-}last}$) and with extrapolation to infinity ($AUC_{0\text{-}inf}$). The maximal plasma concentration (C_{max}) is reported as observed values. Plasma clearance (Cl) after i.v. imatinib administration was calculated by the formula Cl = dose / $AUC_{i.v}$ and the volume of distribution (V_d) was calculated by the formula $V_d = Cl / \beta$. The oral bioavailability (F) was calculated by the formula $F = AUC_{oral} / AUC_{i.v.} \times 100\%$ at a dose of 100 mg/kg. Elimination half-lives ($t_{1/2}$) were calculated by linear regression analysis of the log-linear part of the plasma concentration-time curves. Statistical analyses were performed by ANOVA using Bonferroni post-hoc test for multiple comparisons. All values are given as average ± standard deviation (SD). Differences were considered statistically significant when $p < 0.05$.

Results

The effect of elacridar on the uptake of imatinib by hOCT1 *in vitro*

We investigated the effect of the BCRP/P-gp inhibitor, elacridar, on the uptake of imatinib by hOCT1 *in vitro,* employing HEK293 cells stably expressing hOCT1 (Fig. 1). We used MPP^+, a known hOCT1 substrate, and procainamide, a known hOCT1 inhibitor, as positive controls. OCT1 expression resulted in a significantly 3.9- and 1.2-fold ($P < 0.05$) increased uptake of MPP^+ and imatinib, respectively, compared with the uptake in HEK293-parental cells. Procainamide and elacridar reduced the uptake of MPP^+ and imatinib by hOCT1 completely to the level observed in HEK293-parental cells.

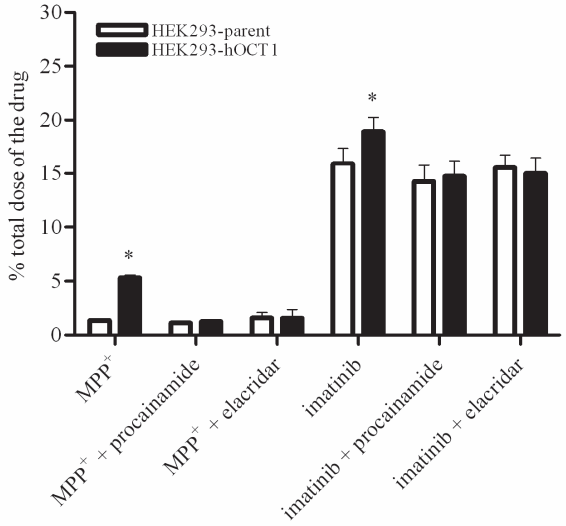

Figure 1. Uptake of N-[methyl-^{3}H]4-phenylpyridinium iodide (MPP^+) and imatinib by hOCT1 in the absence or presence of procainamide (100 µM) or elacridar (5 µM). HEK293-parental (white bars) and HEK293-hOCT1 cells (black bars) were pre-incubated for 15 min with and without one of the inhibitors in Krebs-Ringer-HEPES (KRH) buffer. 25 nM of [^{3}H]MPP^+ and the indicated concentration of the inhibitors were applied at t = 0 and after 10 min uptake was stopped by ice cold KRH buffer. * $p < 0.05$ is the significant difference of MPP^+ and imatinib uptake in HEK293-hOCT1 cells compared with the MPP^+ and imatinib uptake in HEK293-parental cells. All bars represent the mean of each experiment in triplicate ± SD.

Plasma pharmacokinetics of oral and i.v. imatinib in WT and Oct1/2$^{-/-}$ mice

We studied oral and i.v. plasma pharmacokinetics of imatinib in WT and Oct1/2$^{-/-}$ mice over a 24-h time period. We observed that within 15-30 min after oral administration of a dose of 100 mg/kg imatinib the plasma imatinib levels had already reached their maximum in both WT and Oct1/2$^{-/-}$ mice, suggesting rapid absorption (Fig. 2A). Plasma CGP74588 levels reached on average 3-6% of the plasma levels of imatinib (data not shown). The $AUC_{0\text{-inf}}$ and C_{max} of imatinib after oral administration was significantly increased by 1.6- and 1.4-fold, respectively, in Oct1/2$^{-/-}$ compared with WT mice ($p < 0.05$; Table 1; Fig. 2A). Plasma imatinib concentrations declined rapidly after i.v. administration (Fig. 2B), given at a dose of 50 mg/kg (a dose of 100 mg/kg i.v. was too toxic). The $AUC_{0\text{-inf}}$ of imatinib after i.v. administration was significantly higher (1.3-fold) in Oct1/2$^{-/-}$ versus WT mice ($p < 0.05$; Table 1; Fig. 2B). Calculating the $AUC_{0\text{-last}}$ using the linear trapezoidal rule yielded analogous results (approximately 95% of the total $AUC_{0\text{-inf}}$; Table 1). Furthermore, total plasma Cl and V_d were significantly lower in Oct1/2$^{-/-}$ mice, however, C_{max} was not significantly different compared with WT mice. The calculated oral bioavailability of

imatinib was 58.1 ± 7.4 and 45.9 ± 5.5 for Oct1/2$^{-/-}$ and WT mice, respectively, *i.e.*, moderately but significantly ($P < 0.05$) increased in Oct1/2$^{-/-}$ mice. Overall these results show that OCT1/2 has a modest but significant effect on the systemic exposure after oral or i.v. administration of imatinib.

Table 1. Plasma pharmacokinetic parameters of imatinib after oral (100 mg/kg) and i.v. (50 mg/kg) administration of imatinib in wild-type and Oct1/2$^{-/-}$ mice with or without pretreatment of elacridar.

	Oral administration			i.v. administration					
Strain	**Imatinib $AUC_{0\text{-inf}}$ (mgxh/L)**	**Imatinib $AUC_{0\text{-last}}$ (mgxh/L)**	**Imatinib C_{max} (mg/L)**	**Imatinib $AUC_{0\text{-inf}}$ (mgxh/L)**	**Imatinib $AUC_{0\text{-last}}$ (mgxh/L)**	**Imatinib C_{max} (mg/L)**	**Imatinib Cl (mL/h)**	**Imatinib V_d (mL)**	**F %**
wild-type	28.8 ± 4.0	27.2 ± 4.5	11.0 ± 1.9	30.7 ± 4.8	30.4 ± 4.8	29.9 ± 3.8	37.3 ± 5.6	51.5 ± 7.8	45.9 ± 5.5
Oct1/2$^{-/-}$	46.6* ± 8.6	44.4* ± 8.2	15.5* ± 3.1	41.2* ± 5.9	40.6* ± 6.1	33.7 ± 5.7	26.3* ± 4.4	41.3* ± 5.6	58.1* ± 7.4
wild-type + elacridar	98.2*,** ± 21.6	94.7*,** ± 20.9	11.8 ± 3.0						
Oct1/2$^{-/-}$ + elacridar	92.3*,** ± 26.5	92.1*,** ± 26.5	14.9* ± 0.8						

Dose corrected Area under the plasma concentration-time curve (AUC) values. Data are mean ± SD, n = 12 for oral and n = 6 for i.v. administration. Abbreviation: $AUC_{0\text{-inf}}$ Area under the plasma concentration-time curve from 0 to infinity; $AUC_{0\text{-last}}$ Area under the plasma concentration-time curve from 0 to last measurable time point; C_{max} the maximal plasma concentration; $t_{1/2}$ elimination half-life; Cl total plasma clearance; V_d volume of distribution; F oral bioavailability. * $p < 0.05$, compared with wild-type mice; ** $p < 0.05$, compared with Oct1/2$^{-/-}$ mice.

To assess the effect of elacridar on the plasma pharmacokinetics of oral imatinib in WT and Oct1/2$^{-/-}$ mice, we administered an oral dose of imatinib (100 mg/kg) to WT and Oct1/2$^{-/-}$ mice, which were pretreated with oral elacridar (100 mg/kg).

No experiments were performed with i.v. imatinib co-administered with elacridar, because the effect of elacridar on the systemic clearance of i.v. imatinib was expected to be small, consistent with our previous *in vivo* experiments with imatinib and topotecan (17, 29). Interestingly, co-administration of elacridar increased the ($AUC_{0\text{-inf}}$) of oral imatinib 3.4- and 2.0-fold in WT and Oct1/2$^{-/-}$ mice, respectively ($p < 0.05$; Fig. 2A; Table 1). The data of $AUC_{0\text{-last}}$ showed the same pattern as the $AUC_{0\text{-inf}}$ (Table 1). These results suggest that co-administration of elacridar significantly affected the pharmacokinetics of oral imatinib, which could partly be due to inhibition of OCT1/2 activity, based on the *in vitro* data and the results of the Oct1/2$^{-/-}$ mice treated with a single dose of imatinib described above. However, the additional effect of elacridar on the $AUC_{0\text{-inf}}$ of imatinib observed in Oct1/2$^{-/-}$

mice after oral administration indicates that other mechanisms, such as interaction with other drug transporters besides OCT1/2, or drug metabolizing enzymes by which elacridar could influence imatinib absorption and elimination are involved.

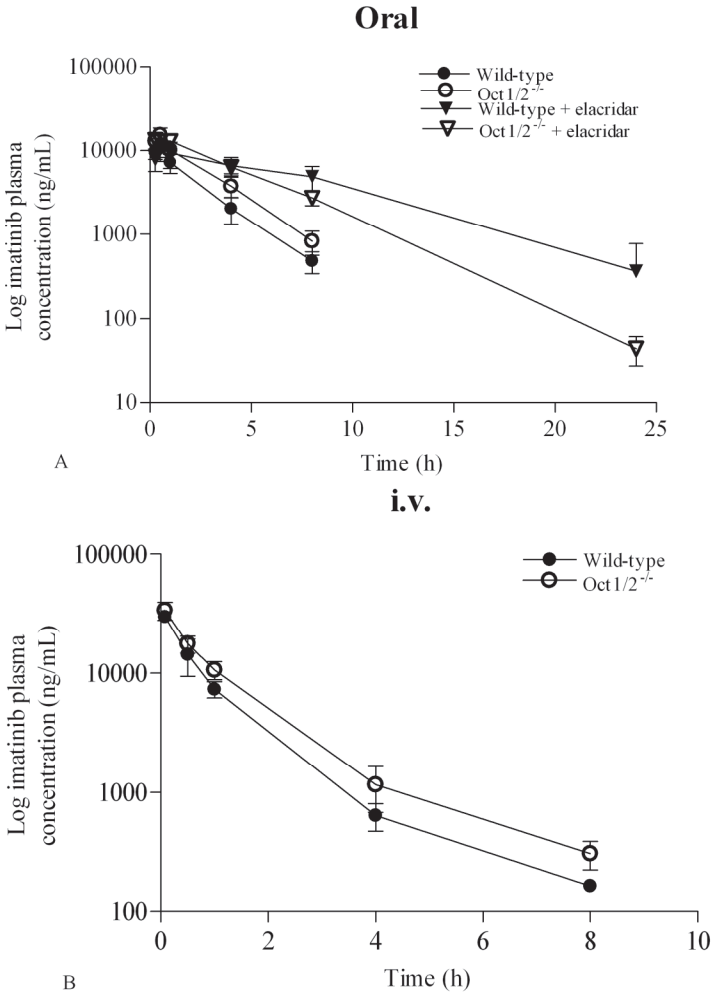

Figure 2. Plasma concentration-time curves of oral (100 mg/kg) (A) and i.v. (50 mg/kg) (B) imatinib in female FVB wild-type (WT) mice (black circles), Oct1/2$^{-/-}$ mice (open circles), WT or Oct1/2$^{-/-}$ mice pre-treated with elacridar (100 mg/kg; black triangles or open triangles, respectively). (A) Effect of OCT1/2 and the BCRP/P-gp inhibitor elacridar on the pharmacokinetics of oral imatinib. (B) Effect of OCT1/2 on the pharmacokinetics of i.v. imatinib. Plasma levels of imatinib were determined by a validated HPLC method with lower limit of quantification of 10 ng/mL. Data points are expressed as mean concentrations for oral (n = 12) and i.v. (n = 6) administration; error bars indicate SD.

Hepatobiliary excretion of i.v. imatinib in gall bladder-cannulated mice

To further investigate the role of OCT1/2 and the effect of elacridar in the hepatobiliary excretion of imatinib, we administered imatinib (50 mg/kg) i.v. with or without pretreatment of elacridar to WT and Oct1/2$^{-/-}$ mice with a cannulated gall bladder and ligated common bile duct. At 90 min after i.v. administration, the cumulative unchanged imatinib and CGP74588 excretion, as percentage of the dose, was 2.2 ± 0.9% and 0.3 ± 0.1%, respectively, in WT mice (Fig. 3). Compared with WT mice, the biliary excretion of imatinib and CGP74588 in Oct1/2$^{-/-}$ mice was not significantly reduced. However, co-administration of elacridar decreased the biliary excretion of imatinib and CGP74588 3.7- and 2.1-fold, respectively, in WT and 2.9- and 2.2-fold in Oct1/2$^{-/-}$ mice (Fig. 3). Furthermore, in the same bile cannulation experiment described above, we investigated the role of OCT1/2 and the effect of elacridar on the accumulation of i.v. imatinib in the liver. The liver accumulation of imatinib at t = 90 min was significantly increased in WT and Oct1/2$^{-/-}$ mice co-administered with elacridar ($p < 0.05$), but not in Oct1/2$^{-/-}$ mice compared with WT mice (Fig. 4A). However, when corrected for the plasma concentration at t = 90 min, the accumulation of imatinib in the liver in these mice, which also were treated with elacridar was not significantly different compared to WT controls (Fig. 4B). This suggests that the drug levels in the livers of these mice are a direct reflection of the plasma concentrations. Overall, elacridar has less effect on the liver-uptake instead of the hepato-biliary excretion of imatinib.

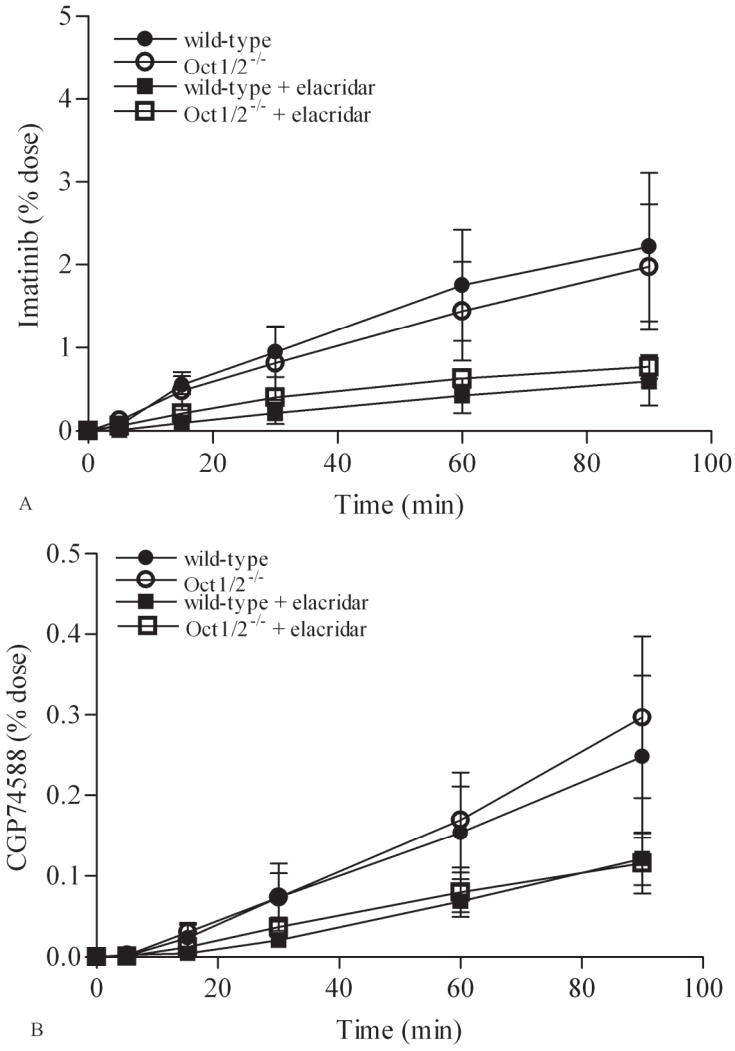

Figure 3. Cumulative hepatobiliary excretion of (A) imatinib and (B) CGP74588 in wild-type and Oct1/2$^{-/-}$ mice. Imatinib was administered i.v. (50 mg/kg) with or without pretreatment of elacridar (100 mg/kg) to mice with a cannulated gall bladder. Unchanged imatinib and CGP74588 were measured by HPLC in bile fractions of wild-type (black circles), Oct1/2$^{-/-}$ (open circles), wild-type + elacridar (black squares) and Oct1/2$^{-/-}$ + elacridar (open squares) mice. Data are expressed as percentage of the dose ± SD (n = 5-6; at all time points).

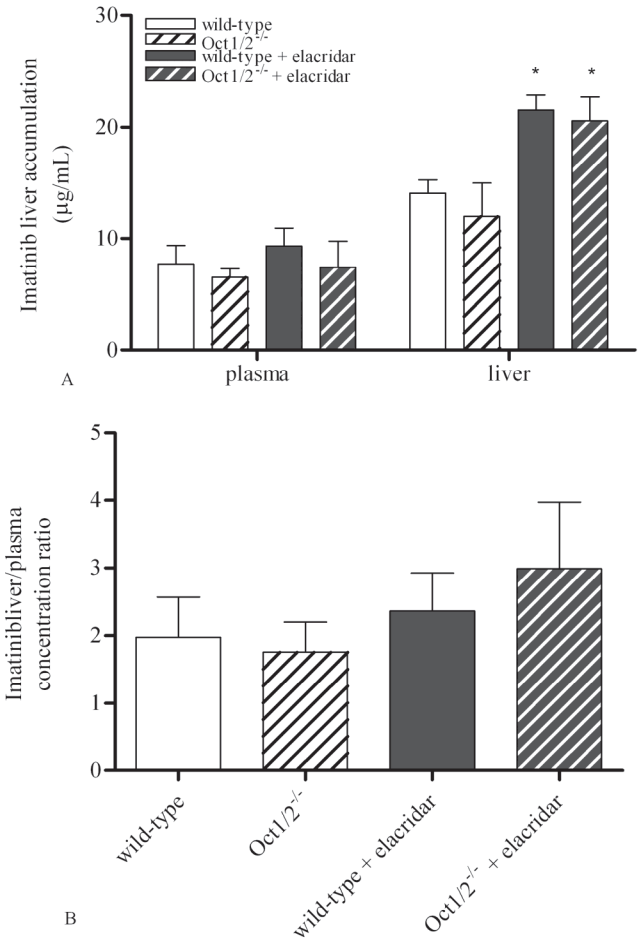

Figure 4. Imatinib plasma concentrations and liver accumulation levels (A) and the imatinib liver/plasma concentration ratio (B) in wild-type and Oct1/2$^{-/-}$ mice with or without pre-treatment of elacridar. Imatinib was administered i.v. (50 mg/kg) with or without pretreatment of elacridar (100 mg/kg) to mice with a cannulated gall bladder. At t = 90 min, blood and liver were collected and the concentration of imatinib was measured by HPLC. Values shown are the means (columns) of 5-6 mice per group ± SD (error bars). * $p < 0.05$ is the significant difference of the plasma concentrations, liver accumulation levels and the imatinib tissue/plasma concentration ratio in the knockout and elacridar pretreated mice compared with wild-type mice.

Discussion

The present study shows that OCT1/2 is significantly, but moderately, involved in the pharmacokinetics of imatinib. Although their combined deficiency resulted in a significant effect on the systemic exposure to imatinib after oral or i.v. administration, OCT1/2 had no significant effect on the hepatobiliary excretion and liver accumulation of imatinib. The BCRP/P-gp inhibitor elacridar had an inhibitory effect on the OCT1 mediated transport of imatinib *in vitro.* The pre-treatment of elacridar further reduced the total plasma clearance and hepatobiliary excretion of oral imatinib in both WT and OCT1/2 knockout mice.

In order to study the role of OCT1/2 in the disposition of imatinib, we used the OCT1/2 knockout mouse model (25). This model was chosen because imatinib is probably also a substrate for OCT2, which could compensate in part for the role of OCT1 in the OCT1 knockout mouse model. In *in vitro* studies no affinity of imatinib for OCT2 was observed (19, 24), however *in vitro* and *in vivo* systems may show discrepant results. In the knockout mice, we found that OCT1/2 only had a moderate effect on the systemic exposure of oral and i.v. imatinib and no significant effect on the hepatobiliary excretion and liver accumulation of imatinib. This is in contrast with previous *in vitro* studies that revealed that OCT1 mediates the cellular accumulation of imatinib in a variety of leukemia cells (18, 19). However, our *in vivo* experiments are in line with the recently published *in vitro* data by Hu et al. (24) and our *in vitro* results presented in this manuscript (Fig. 1), which showed that OCT1 has a limited contribution to the transport and pharmacokinetics of imatinib. In spite of our observation, results obtained in a number of recent clinical studies seem to indicate that the expression of OCT1 is an important determinant for activity of imatinib in CML patients (20, 22, 23). Although compensatory mechanisms in our knockout mice may conceal some of the effects of the absence of these transporters, Hu et al. (24) hypothesized that the high expression of OCT1 in leukemic target cells directly controls local drug levels and thereby alters the pharmacodynamic effects of imatinib without affecting its systemic exposure.

Furthermore, we studied the effect of elacridar on the disposition of imatinib in order to unravel whether OCT1 is involved in the drug-drug interaction of imatinib and elacridar. Our previously published results illustrate that elacridar is a non-selective inhibitor of drug transporters (17). The inhibitory effect of elacridar on the OCT1 transport of imatinib and MPP^+ *in vitro* and the moderate 1.6-fold increase in the AUC of orally administered imatinib by the absence of OCT1/2 could explain in part the interaction of imatinib and elacridar. Other elimination routes besides OCT1/2 are also important as co-administration of elacridar led to a further 3.0-fold increase in the AUC of imatinib. Preliminary data obtained in our group have shown that elacridar inhibited also OATP1B1,

however, recently it was found that imatinib was not transported by OATP1B1 (24). Furthermore, in the bile cannulation experiment we clearly confirmed our previously published data (17) wherein elacridar appeared to fully inhibit BCRP- and P-gp-mediated biliary excretion of imatinib.

Recently, Hu et al. (24) found, by using an *in vitro* screen of expressed *Xenopus laevis* oocytes and transfected HEK293 cells, that imatinib is also transported by the human uptake transporter OCTN2 (CT1;(30, 31)) and, to a modest extent by OATP1B3 (LST-2, OATP8; (32)). Preliminary *in vivo* studies provide evidence that the cellular uptake of imatinib is mediated by OATP1A2 (24). Other transporters localized at the human basolateral membrane of hepatocytes such as OAT2 and OATP1B1 (LST-1, OATP-C, OATP2) were not found to transport this anticancer drug. Human transporters that are predominantly expressed in other organs such as the kidney, including the OAT1, OAT3, and OCT2, also did not transport imatinib, which is consistent with the relatively low renal clearance of the drug (5). Additional single or combined drug efflux/uptake transporter and CYP enzyme knockout mice models are needed, to identify other important uptake and elimination pathways of imatinib, which are important in the observed drug-drug interaction of imatinib and elacridar. Furthermore, these uptake and elimination pathways can be important to explain the observed variability in the pharmacokinetics of imatinib that may compromise therapeutic efficacy in patients with CML and GIST.

In summary, our results reveal that OCT1/2 has a significant effect on the pharmacokinetics of imatinib in mice, however, in comparison to other drug transporters and/or metabolic elimination pathways the magnitude of the effect appears to be modest. Interestingly, co-administration of the BCRP/P-gp inhibitor, elacridar, significantly increased the systemic exposure to imatinib in the presence or absence of OCT1/2. This suggests that besides OCT1/2, other elimination pathways are involved in the drug-drug interaction between imatinib and elacridar.

Acknowledgement

We are grateful to Lianne Asschert (Novartis Pharma B.V., Arnhem, The Netherlands) for providing us with imatinib mesylate and its metabolite CGP74588 (Novartis Pharma AG, Basel, Switzerland). We would like to thank Els Wagenaar (Department of Experimental Therapy, The Netherlands Cancer Institute, The Netherlands) for providing us with OCT1/2 knockout mice.

References

1. Druker BJ, Talpaz M, Resta DJ, et al. Efficacy and safety of a specific inhibitor of the BCR-ABL tyrosine kinase in chronic myeloid leukemia. N Engl J Med 2001;344:1031-1037.
2. Demetri GD, von Mehren M, Blanke CD, et al. Efficacy and safety of imatinib mesylate in advanced gastrointestinal stromal tumors. N Engl J Med 2002;347:472-480.
3. Rao K, Goodin S, Levitt MJ, et al. A phase II trial of imatinib mesylate in patients with prostate specific antigen progression after local therapy for prostate cancer. Prostate 2005;62:115-122.
4. Reardon DA, Egorin MJ, Quinn JA, et al. Phase II study of imatinib mesylate plus hydroxyurea in adults with recurrent glioblastoma multiforme. J Clin Oncol 2005;23:9359-9368.
5. Peng B, Lloyd P, Schran H. Clinical pharmacokinetics of imatinib. Clin Pharmacokinet 2005;44:879-894.
6. Peng B, Dutreix C, Mehring G, et al. Absolute bioavailability of imatinib (Glivec) orally versus intravenous infusion. J Clin Pharmacol 2004;44:158-162.
7. Judson I, Ma P, Peng B, et al. Imatinib pharmacokinetics in patients with gastrointestinal stromal tumour: a retrospective population pharmacokinetic study over time. EORTC Soft Tissue and Bone Sarcoma Group. Cancer Chemother Pharmacol 2005;55:379-386.
8. Peng B, Hayes M, Resta D, et al. Pharmacokinetics and pharmacodynamics of imatinib in a phase I trial with chronic myeloid leukemia patients. J Clin Oncol 2004;22:935-942.
9. Rochat B. Role of cytochrome P450 activity in the fate of anticancer agents and in drug resistance: focus on tamoxifen, paclitaxel and imatinib metabolism. Clin Pharmacokinet 2005;44:349-366.
10. Gschwind HP, Pfaar U, Waldmeier F, et al. Metabolism and disposition of imatinib mesylate in healthy volunteers. Drug Metab Dispos 2005;33:1503-1512.
11. van Erp NP, Gelderblom H, Karlsson MO, et al. Influence of CYP3A4 inhibition on the steady-state pharmacokinetics of imatinib. Clin Cancer Res 2007;13:7394-7400.
12. Hamada A, Miyano H, Watanabe H, Saito H. Interaction of imatinib mesilate with human P-glycoprotein. J Pharmacol Exp Ther 2003;307:824-828.
13. Burger H, van Tol H, Boersma AW, et al. Imatinib mesylate (STI571) is a substrate for the breast cancer resistance protein (BCRP)/ABCG2 drug pump. Blood 2004;104:2940-2942.
14. Breedveld P, Pluim D, Cipriani G, et al. The effect of Bcrp1 (Abcg2) on the in vivo pharmacokinetics and brain penetration of imatinib mesylate (Gleevec): implications for the use of breast cancer resistance protein and P-glycoprotein inhibitors to enable the brain penetration of imatinib in patients. Cancer Res 2005;65:2577-2582.
15. Dai H, Marbach P, Lemaire M, Hayes M, Elmquist WF. Distribution of STI-571 to the brain is limited by P-glycoprotein-mediated efflux. J Pharmacol Exp Ther 2003;304:1085-1092.
16. Bihorel S, Camenisch G, Lemaire M, Scherrmann JM. Modulation of the brain distribution of imatinib and its metabolites in mice by valspodar, zosuquidar and elacridar. Pharm Res 2007;24:1720-1728.
17. Oostendorp RL, Buckle T, Beijnen JH, van Tellingen O, Schellens JH. The effect of P-gp (Mdr1a/1b), BCRP (Bcrp1) and P-gp/BCRP inhibitors on the in vivo absorption, distribution, metabolism and excretion of imatinib. Invest New Drugs 2008 (in press).
18. White DL, Saunders VA, Dang P, et al. OCT-1-mediated influx is a key determinant of the intracellular uptake of imatinib but not nilotinib (AMN107): reduced OCT-1 activity is the cause of low in vitro sensitivity to imatinib. Blood 2006;108:697-704.
19. Thomas J, Wang L, Clark RE, Pirmohamed M. Active transport of imatinib into and out of cells: implications for drug resistance. Blood 2004;104:3739-3745.
20. Wang L, Giannoudis A, Lane S, Williamson P, Pirmohamed M, Clark RE. Expression of the Uptake Drug Transporter hOCT1 is an Important Clinical Determinant of the Response to Imatinib in Chronic Myeloid Leukemia. Clin Pharmacol Ther 2008;83(2):258-64.
21. Zhang L, Dresser MJ, Gray AT, Yost SC, Terashita S, Giacomini KM. Cloning and functional expression of a human liver organic cation transporter. Mol Pharmacol 1997;51:913-921.
22. Crossman LC, Druker BJ, Deininger MW, Pirmohamed M, Wang L, Clark RE. hOCT 1 and resistance to imatinib, Blood 2005;106:1133-1134.
23. White DL, Saunders VA, Dang P, et al. Most CML patients who have a suboptimal response to imatinib have low OCT-1 activity: higher doses of imatinib may overcome the negative impact of low OCT-1 activity. Blood 2007;110:4064-4072.
24. Hu S, Franke RM, Filipski KK, et al. Interaction of imatinib with human organic ion carriers. Clin Cancer Res 2008;14:3141-3148.
25. Jonker JW, Wagenaar E, Van Eijl S, Schinkel AH. Deficiency in the organic cation transporters 1 and 2 (Oct1/Oct2 [Slc22a1/Slc22a2]) in mice abolishes renal secretion of organic cations. Mol Cell Biol 2003;23:7902-7908.

26. Hayer-Zillgen M, Bruss M, Bonisch H. Expression and pharmacological profile of the human organic cation transporters hOCT1, hOCT2 and hOCT3. Br J Pharmacol 2002;136:829-836.
27. Bardelmeijer HA, Ouwehand M, Beijnen JH, Schellens JH, van Tellingen O. Efficacy of novel P-glycoprotein inhibitors to increase the oral uptake of paclitaxel in mice. Invest New Drugs 2004;22:219-229.
28. Oostendorp RL, Beijnen JH, Schellens JH, Tellingen O. Determination of imatinib mesylate and its main metabolite (CGP74588) in human plasma and murine specimens by ion-pairing reversed-phase high-performance liquid chromatography. Biomed Chromatogr 2007;21:747-754.
29. Jonker JW, Smit JW, Brinkhuis RF, et al. Role of breast cancer resistance protein in the bioavailability and fetal penetration of topotecan. J Natl Cancer Inst 2000;92:1651-1656.
30. Tamai I, Ohashi R, Nezu J, et al. Molecular and functional identification of sodium ion-dependent, high affinity human carnitine transporter OCTN2. J Biol Chem 1998;273:20378-20382.
31. Wu X, Prasad PD, Leibach FH, Ganapathy V. cDNA sequence, transport function, and genomic organization of human OCTN2, a new member of the organic cation transporter family. Biochem Biophys Res Commun 1998;246:589-595.
32. Abe T, Unno M, Onogawa T, et al. LST-2, a human liver-specific organic anion transporter, determines methotrexate sensitivity in gastrointestinal cancers. Gastroenterology 2001;120:1689-1699.

CHAPTER 2.3

The effect of hydroxyurea on P-glycoprotein/BCRP-mediated transport and CYP3A metabolism of imatinib mesylate

Roos L. Oostendorp, Serena Marchetti, Jos H. Beijnen, R. Mazzanti, Jan H.M. Schellens

Cancer Chemotherapy and Pharmacology 2007;59:855-860

Abstract

It has been reported that combination therapy of imatinib mesylate, a tyrosine kinase inhibitor, plus hydroxyurea, a ribonucleotide reductase inhibitor, is associated with remarkable antitumor activity in patients with recurrent glioblastoma multiforme. However, the mechanism of the added activity of hydroxyurea to imatinib is not known. The purpose of this study was to investigate *in vitro*, whether hydroxyurea could enhance the central nervous system penetration of imatinib, by inhibition of the ATP-dependent transporter proteins P-glycoprotein (ABCB1; MDR1; Pgp) and Breast Cancer Resistance Protein (ABCG2; BCRP), or by inhibition of cytochrome P450 3A (CYP3A) metabolism of imatinib. The effect of hydroxyurea on the Pgp and BCRP mediated transport of imatinib was investigated by the sulforhodamine-B (SRB) drug cytotoxicity assay and transepithelial transport assay. *In vitro* biotransformation studies with supersomes expressing human CYP3A4 were performed to investigate whether hydroxyurea inhibited CYP3A4. In both *in vitro* cytotoxicity and transport assays, hydroxyurea did not affect Pgp and BCRP mediated transport of imatinib. In a biotransformation assay, hydroxyurea had no influence on the metabolic degradation of imatinib either. The results indicate that hydroxyurea does not interact with imatinib by inhibition of Pgp and BCRP mediated transport or by CYP3A4 mediated metabolism of imatinib.

Introduction

Imatinib mesylate (STI-571, Gleevec®, imatinib), a potent and selective receptor tyrosine kinase inhibitor was shown to be clinically effective and well tolerated in Bcr/Abl-expressing chronic myeloid leukemia (1) and c-Kit-expressing gastro-intestinal stromal tumors (GIST) (2). In addition, imatinib effectively inhibits platelet-derived growth factor (PDGF)-induced glioblastoma cell growth preclinically (3). However, trials with imatinib in patients with recurrent glioblastoma multiforme showed limited penetration of imatinib into the central nervous system and modest antitumor activity (4, 5). A plausible explanation for this low efficacy of imatinib is the efficient protection of the brain against drugs by the blood-brain barrier, containing various efflux transporters, including P-glycoprotein (ABCB1; MDR1; Pgp) and Breast Cancer Resistance Protein (ABCG2; BCRP). Pgp and BCRP are located in apical membranes of epithelia and vascular endothelial cells, which can actively extrude a variety of structurally diverse drugs and drug metabolites from the central nervous system and from tumor cells into the blood circulation (6, 7). *In vitro* and *in vivo* studies have shown that Pgp and BCRP play an important role in the transport of imatinib and limit the distribution of imatinib to the brain (8, 9). Furthermore, effective Pgp and/or BCRP inhibitors, such as elacridar (GF120918), zosuquidar (LY335979) and pantoprazole, significantly improved the brain accumulation of imatinib (8, 9). This concept raises the possibility that co-administration of a transport inhibitor improves therapy with imatinib.

Two recent reports suggested that the combination of imatinib plus hydroxyurea, a ribonucleoside reductase inhibitor, is a safe and effective therapy for a subpopulation of glioblastoma multiforme patients who have experienced disease progression after prior radiotherapy and at least temozolomide-based chemotherapy (10, 11). This is the first report that a signal transduction inhibitor combined with a chemotherapeutic agent has activity in glioblastoma multiforme. However, the mechanism of action underlying the activity of this regimen is unknown. Based on the preclinical results of Dai et al. (8) and Breedveld et al. (9), we hypothesized that hydroxyurea interferes with the penetration of imatinib through the blood-brain barrier by inhibition of the efflux transporters Pgp and/or BCRP or by inhibition of cytochrome P450 3A (CYP3A) metabolism of imatinib.

Materials and methods

Chemicals

Imatinib, [^{14}C]imatinib (both as the mesylate salt) and its main metabolite N-desmethyl-STI (CGP74588) were kindly provided by Novartis Pharma AG (Basel, Switzerland). Pantoprazole (Pantozol®, Altana Pharma, Hoofddorp, The Netherlands) was obtained from the pharmacy of the Netherlands Cancer Institute. Zosuquidar trihydrochloride (LY335979) was kindly provided by Eli Lilly (Indianapolis, USA). Ritonavir was provided by Abbott (Chicago, IL, USA). Hydroxyurea was purchased from Sigma (St. Louis, MO).

Cell lines and culture conditions

The Madin-Darby Canine Kidney II (MDCKII) epithelial cells were cultured in Dulbecco's modified Eagle's Medium (DMEM) supplemented with 10% fetal calf serum (FCS) and 100 units penicillin/streptomycin per ml (12). Cells were grown at 37°C with 5% CO_2 under humidifying conditions. Polarized MDCKII cells stably expressing human MDR1 (ABCB1) or murine Bcrp1 (ABCG2) cDNA have been described previously (13, 14).

Cytotoxicity assay

MDCKII-parental, -MDR1 and -Bcrp1 cells were cultured as described above and used in a sulforhodamine B (SRB) drug cytotoxicity assay for single and combination experiments as described by Ma et al. (15). Briefly, 1000 exponentially growing MDCKII cells/200 µl/ well in 96-well plates were allowed to attach for 1 day followed by imatinib administration in the presence or absence of hydroxyurea for 3 more days.

Transport across MDCKII monolayers

MDCKII-parental, -MDR1 and -Bcrp1 cells were seeded on microporous polycarbonate membrane filters at a density of 1 x 10^6 cells/well in complete medium. Transepithelial transport assays were performed as described previously (16). To exclude any contribution of Pgp in the MDCKII-Bcrp1 and MDCKII-parental cells, LY335979 was added. As the expression of BCRP in the MDCKII-parental and -MDR1 cells is negligible, co-administration of a BCRP inhibitor is redundant.

Biotransformation assay

The main metabolite of imatinib, CGP74588, was formed in *in vitro* incubations with supersomes that contained cDNA expressing human CYP3A4. Supersomal incubations (final volume = 50 µl) were performed at 37°C according to the BD Gentest

procedure/catalogue (BD Bioscience, Erembodegem, Belgium) and contained, per incubation: supersomes CYP3A4 (10 pmol), NADPH regenerating solutions A (2.5 µl) and B (0.5 µl) from BD Gentest/Bioscience, 0.1 M phosphate buffer, water and imatinib 20 µM in the presence or absence of hydroxyurea 300 µM or the known CYP3A4 inhibitor ritonavir 100 µM. Supersomal incubations were started by the addition of imatinib in water. Control incubations were performed on ice instead of 37°C. Incubations were performed for 1h and stopped by the addition of 50 µl acetonitrile. Protein precipitations were obtained by the centrifugation of the incubates (8000 rpm for 10 min). Supernatants were transferred and injected into the analytical column (method described below).

HPLC analysis of imatinib and CGP74588

Imatinib, CGP74588 and the internal standard 4-hydroxybenzophenone were separated using a narrow bore (2.1 x 150 mm) stainless steel packed column packed with 3.5 µm Symmetry C-18 material and detection was accomplished with a UV detector set at excitation and emission wavelengths of 265 nm and 460 nm, respectively. The mobile phase consisted of 28% (v/v) acetonitrile in 50 mM ammonium acetate buffer pH 6.8 containing 0.005 M 1-octane sulfonic acid and was delivered at 0.2 ml/min.

Statistical analysis

Statistical evaluation was performed using the two-sided unpaired Student's *t*-test to assess the statistical significance of difference between two sets of data. Differences were considered to be statistically significant when $P < 0.05$.

Results

The effect of hydroxyurea on the cytotoxicity of imatinib

In the first part of this study we investigated *in vitro* the effect of hydroxyurea on the cytotoxicity of imatinib in parental MDCKII and MDCKII cells stably transfected with human Pgp or BCRP, for which we used the mouse homolog Bcrp1 (MDCKII-MDR1 or MDCKII-Bcrp1, respectively). Hydroxyurea and imatinib alone were not less cytotoxic to the MDCKII-MDR1 and MDCKII-Bcrp1 cells compared to parental MDCKII cells ($P>0.05$; Table 1). Furthermore, the cytotoxicity of imatinib was not significantly affected by co-incubation with a non-toxic dose of 50 or 100 µM hydroxyurea ($P > 0.05$; Table 1).

Table 1. Cytotoxicity of imatinib in MDCKII-parental, -Bcrp1 and -MDR1 cell lines in the absence or presence of hydroxyurea. Inhibiting concentrations of 50% (IC_{50}, in μM) of 3 day incubations are shown as mean ± SD from > 3 independent experiments.

Drugs	MDCKII-parental IC_{50} (μM)	MDCKII-Bcrp1 IC_{50} (μM)	MDCKII-MDR1 IC_{50} (μM)
Hydroxyurea	740 ± 66	679 ± 69	698 ± 60
Imatinib	8.0 ± 0.2	9.1± 1.3	8.5 ± 0.9
Imatinib + Hydroxyurea 50 μM	8.4 ± 0.6	9.3 ± 2.0	8.4 ± 0.8
Imatinib + Hydroxyurea 100 μM	8.2 ± 0.4	9.2 ± 1.7	8.9 ± 1.6

The effect of hydroyurea on the active transport of imatinib by Pgp and Bcrp1

Secondly, we investigated *in vitro,* employing polarized MDCKII-parental, -MDR1 and -Bcrp1 monolayers, whether hydroxyurea is capable of inhibiting the active transport of imatinib by Pgp and Bcrp1. Imatinib alone resulted in an increased transport by Pgp and Bcrp1 from the basolateral to the apical side (BA) compared with the transport from the apical to the basolateral side (AB), i.e. active transport (BA/AB is 10.3 and 20.4, respectively) (Fig. 1A and B). These results are comparable to those shown previously by Dai et al. (8) and Breedveld et al (9). Furthermore, the effect of hydroxyurea and the Pgp and BCRP inhibitors, LY335979 and pantoprazole as positive controls, on the active transport of imatinib by Pgp and Bcrp1 were investigated. LY335979 and pantoprazole inhibited the MDR1 and Bcrp1-mediated transport of imatinib, respectively, as upon co-incubation the transport from BA was approximately equal to the transport from AB, i.e. no active transport. In contrast, hydroxyurea did not affect Pgp and Bcrp1-mediated transport of imatinib (BA/AB is 12.0 and 18.5, respectively) (Fig. 1A and B).

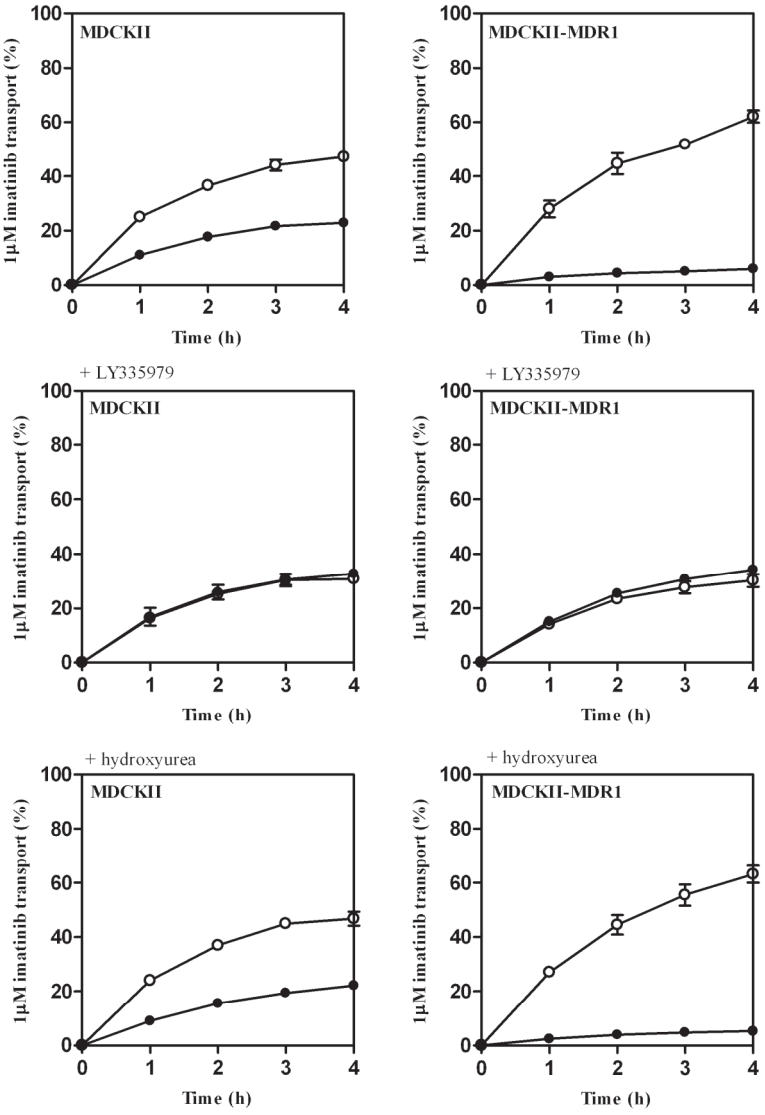
MDCKII
MDCKII-MDR1
+ LY335979
+ hydroxyurea
1µM imatinib transport (%)
Time (h)
0
20
40
60
80
100
0
1
2
3
4

A

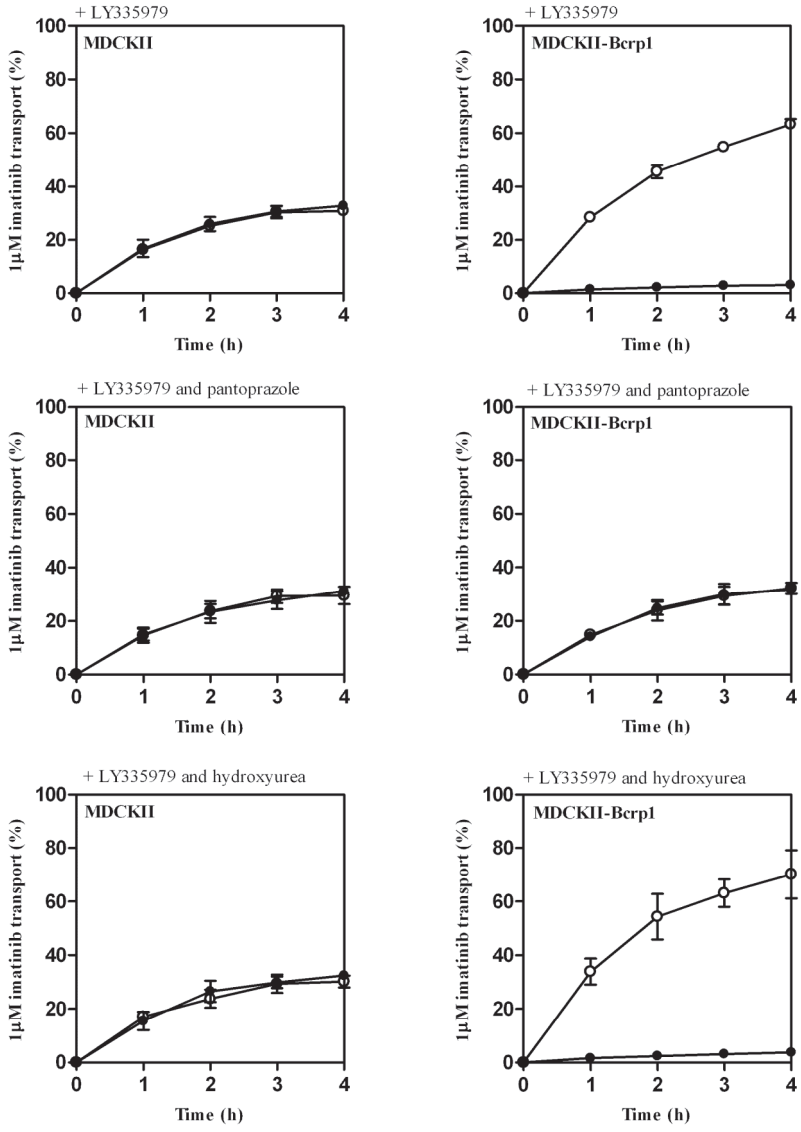

B

Figure 1. Transport of imatinib by MDR1 (Fig. 1A) and Bcrp1 (Fig. 1B) in the absence or presence of hydroxyurea, LY335979 and pantoprazole. A, MDCKII parental and MDCKII-MDR1 cells were pre-incubated for 2 hours with and without (control) 5 µM LY335979 or 30 mM hydroxyurea. One µM of [^{14}C]imatinib and the indicated concentration of LY335979 or hydroxyurea were applied at t = 0 to the apical or basal side and the

amount of [^{14}C]imatinib appearing in the opposite basal compartment (AB; closed symbols) or apical compartment (BA; open symbols) was determined. Samples were taken at t = 1, 2, 3 and 4 h. Points, means of each experiment in triplicate; bars, SD. B MDCKII parental and MDCKII-Bcrp1 cells were pre-incubated for 2 h with 5 μM LY335979, and without (control) or with 500 μM pantoprazole or 30 mM hydroxyurea. One μM of [^{14}C]imatinib and the indicated concentration of LY335979 or hydroxyurea were applied at t = 0 to the apical or basal side and the amount of [^{14}C]imatinib appearing in the opposite basal compartment (AB; closed symbols) or apical compartment (BA; open symbols) was determined. Samples were taken at t = 1, 2, 3 and 4 h. Points, means of each experiment in triplicate; bars, SD.

Imatinib biotransformation by human CYP3A supersomes in the absence and presence of hydroxyurea

We then tested whether hydroxyurea inhibited cytochrome P450 3A (CYP3A). Although hydroxyurea is not a known CYP substrate, recent studies of the 5-lipoxygenase inhibitor, zileuton, the structure of which includes a hydroxyurea moiety, indicate that it inhibits CYPs, including CYP3A, which isozyme is mainly responsible for the biotransformation of imatinib (17, 18). We performed *in vitro* biotransformation studies with supersomes expressing human CYP3A4. The CYP3A4 supersomes metabolized 12.3 ± 1.2% of imatinib to its main metabolite CGP74588 over 1h of incubation. Subsequently, we incubated imatinib with hydroxyurea or ritonavir; the latter is a known CYP3A4 inhibitor. Ritonavir was able to inhibit imatinib biotransformation completely. In contrast, hydroxyurea had no inhibitory effect on the biotransformation of imatinib. The CYP3A4 supersomes metabolized 11.8 ± 0.9% of imatinib to CGP74588 in the presence of hydroxyurea, which is not significantly different from the rate of biotransformation of imatinib in the absence of hydroxyurea ($P > 0.05$).

Discussion

The combination therapy of imatinib plus hydroxyurea is associated with remarkable antitumor activity in patients with recurrent glioblastoma. Thus far the mechanism of the added activity of hydroxyurea to imatinib is unknown. We hypothesized that the effect could be due to increased exposure of the tumor to imatinib. As imatinib is a high affinity substrate drug for Pgp and BCRP and is extensively metabolized by CYP3A, we investigated the effect of hydroxyurea on Pgp/BCRP mediated transport and CYP3A metabolism of imatinib. This study shows for the first time that hydroxyurea does not interact with imatinib by inhibition of Pgp and BCRP mediated transport or by CYP3A mediated metabolism of imatinib.

There are several other possible mechanisms of action that have to be investigated and could underlie the positive activity of this regimen. First, preclinical studies support that imatinib may enhance hydroxyurea mediated cytotoxicity by improving its delivery to

the tumor microenvironment (19, 20). Imatinib can diminish the tumor interstitial pressure. This could lead to increased capillary-to-interstitium transport and enhanced chemotherapy delivery, e.g. of hydroxyurea (21). A clinical trial of imatinib with temozolomide, a cytotoxic agent with more established single-agent activity against glioblastoma multiforme than hydroxyurea, may be of interest in this respect.

Imatinib can also diminish tumor cell DNA repair after radiotherapy or chemotherapy by reducing Rad51 expression. Rad51 is an essential component of the DNA double-strand break pathway and has been implicated as a determinant of cellular radiosensitivity (22). Imatinib-related decreased DNA repair may potentiate the cytotoxicity of hydroxyurea.

A final potential mechanism of action may be that PDGFR inhibitors exhibit significant antiangiogenic activity primarily by targeting perivascular cells, as shown in preclinical models (23, 24). Furthermore, several chemotherapeutic agents suppress tumor angiogenesis and enhance the antitumor activity of vascular endothelial growth factor inhibitors. Therefore, PDGFR inhibition by imatinib combined with chemotherapy e.g. hydroxyurea may provide complementary antiangiogenic activity, thereby limiting tumor growth, e.g. in glioblastoma multiforme.

In conclusion, hydroxyurea and imatinib do not interact at the level of Pgp, BCRP and CYP3A4 and further research is needed to clarify the beneficial activity against glioblastoma multiforme of the combination of hydroxyurea and imatinib.

References

1. Druker BJ, Talpaz M, Resta DJ, et al. Efficacy and safety of a specific inhibitor of the BCR-ABL tyrosine kinase in chronic myeloid leukemia. N Engl J Med 2001;344:1031-1037.
2. Demetri GD, von Mehren M, Blanke CD, et al. Efficacy and safety of imatinib mesylate in advanced gastrointestinal stromal tumors. N Engl J Med 2002;347:472-480.
3. Kilic T, Alberta JA, Zdunek PR, et al. Intracranial inhibition of platelet-derived growth factor-mediated glioblastoma cell growth by an orally active kinase inhibitor of the 2-phenylaminopyrimidine class. Cancer Res 2000;60:5143-5150.
4. Raymond E, Brandes A, Van Oosterom A, et al. Multicentre phase II study of imatinib mesylate in patients with recurrent glioblastoma: An EORTC: NDDG/BTG Intergroup Study. *In*: Anonymousp 2004;107 Proc ASCO.
5. Wen PYWLK. PhaseI/II study of imatinib mesylate (STI571) for patients with recurrent malignant gliomas. *In*: Anonymousp 2004;383 Proc ASCO.
6. Schinkel AH, Smit JJ, van Tellingen O, et al. Disruption of the mouse mdr1a P-glycoprotein gene leads to a deficiency in the blood-brain barrier and to increased sensitivity to drugs. Cell 1994;77:491-502.
7. Eisenblatter T, Huwel S and Galla HJ. Characterisation of the brain multidrug resistance protein (BMDP/ABCG2/BCRP) expressed at the blood-brain barrier. Brain Res 2003;971:221-231.
8. Dai H, Marbach P, Lemaire M, et al. Distribution of STI-571 to the brain is limited by P-glycoprotein-mediated efflux. J Pharmacol Exp Ther 2003;304:1085-1092.
9. Breedveld P, Pluim D, Cipriani G, et al. The effect of Bcrp1 (Abcg2) on the in vivo pharmacokinetics and brain penetration of imatinib mesylate (Gleevec): implications for the use of breast cancer resistance protein and P-glycoprotein inhibitors to enable the brain penetration of imatinib in patients. Cancer Res 2005;65:2577-2582.

10. Dresemann G. Imatinib and hydroxyurea in pretreated progressive glioblastoma multiforme: a patient series. Ann Oncol 2005;16:1702-1708.
11. Reardon DA, Egorin MJ, Quinn JA, et al. Phase II Study of Imatinib Mesylate Plus Hydroxyurea in Adults With Recurrent Glioblastoma Multiforme. J Clin Oncol 2005;23:9359-9368.
12. Louvard D. Apical membrane aminopeptidase appears at site of cell-cell contact in cultured kidney epithelial cells. Proc Natl Acad Sci U S A 1980;77:4132-4136.
13. Evers R, Kool M, Smith AJ, et al. Inhibitory effect of the reversal agents V-104, GF120918 and Pluronic L61 on MDR1 Pgp-, MRP1- and MRP2-mediated transport. Br J Cancer 2000;83:366-374.
14. Jonker JW, Smit JW, Brinkhuis RF, et al. Role of breast cancer resistance protein in the bioavailability and fetal penetration of topotecan. J Natl Cancer Inst 2000;92:1651-1656.
15. Ma J, Maliepaard M, Nooter K, et al. Synergistic cytotoxicity of cisplatin and topotecan or SN-38 in a panel of eight solid-tumor cell lines in vitro. Cancer Chemother Pharmacol 1998;41:307-316.
16. Breedveld P, Zelcer N, Pluim D, et al. Mechanism of the pharmacokinetic interaction between methotrexate and benzimidazoles: potential role for breast cancer resistance protein in clinical drug-drug interactions. Cancer Res 2004;64:5804-5811.
17. Lu P, Schrag ML, Slaughter DE, et al. Mechanism-based inhibition of human liver microsomal cytochrome P450 1A2 by zileuton, a 5-lipoxygenase inhibitor. Drug Metab Dispos 2003;31:1352-1360.
18. Peng B, Lloyd P and Schran H. Clinical pharmacokinetics of imatinib. Clin Pharmacokinet 2005;44:879-894.
19 Hwang RF, Yokoi K, Bucana CD, et al. Inhibition of platelet-derived growth factor receptor phosphorylation by STI571 (Gleevec) reduces growth and metastasis of human pancreatic carcinoma in an orthotopic nude mouse model. Clin Cancer Res 2003;9:6534-6544.
20. Pietras K, Rubin K, Sjoblom T, et al. Inhibition of PDGF receptor signaling in tumor stroma enhances antitumor effect of chemotherapy. Cancer Res 2002;62:5476-5484.
21. Pietras K, Ostman A, Sjoquist M, et al. Inhibition of platelet-derived growth factor receptors reduces interstitial hypertension and increases transcapillary transport in tumors. Cancer Res 2001;*61:*2929-2934.
22. Russell JS, Brady K, Burgan WE, et al. Gleevec-mediated inhibition of Rad51 expression and enhancement of tumor cell radiosensitivity. Cancer Res 2003;63:7377-7383.
23. Laird AD, Vajkoczy P, Shawver LK, et al. SU6668 is a potent antiangiogenic and antitumor agent that induces regression of established tumors. Cancer Res 2000;60:4152-4160.
24. Shaheen RM, Tseng WW, Davis DW, et al. Tyrosine kinase inhibition of multiple angiogenic growth factor receptors improves survival in mice bearing colon cancer liver metastases by inhibition of endothelial cell survival mechanisms. Cancer Res 2001;61:1464-1468.

CHAPTER 2.4

Determination of imatinib mesylate and its main metabolite (CGP74588) in human plasma and murine specimens by ion-pairing reversed-phase High-Performance Liquid Chromatography

Roos L. Oostendorp, Jos H. Beijnen, Jan H.M. Schellens and Olaf van Tellingen

Biomedical Chromatography 2007;21:747-754

Abstract

A sensitive reversed-phase high performance liquid chromatographic (HPLC) method has been developed and validated for the determination of imatinib, a tyrosine kinase inhibitor, and its main metabolite N-desmethyl-imatinib (CGP74588) in human plasma and relevant murine biological matrices. A simple HPLC assay for the individual quantification of imatinib and CGP74588 in murine specimens has not been reported to date. Sample pre-treatment involved liquid-liquid extraction with *tert*-butyl-methyl ether. Imatinib, CGP74588 (metabolite) and the internal standard 4-hydroxybenzophenone were separated using a narrow bore (2.1 x 150 mm) stainless steel Symmetry C-18 column and detected by UV at 265 nm. The mobile phase consisted of 28% (v/v) acetonitrile in 50 mM ammonium acetate buffer pH 6.8 containing 0.005 M 1-octane sulfonic acid and was delivered at 0.2 ml/min. The calibration curve was prepared in blank human plasma and was linear over the dynamic range (10 ng/ml to 10 µg/ml). The accuracy was close to 100% and the within-day and between-day precision was within the generally accepted 15% range. The validation results showed that the assay was selective and reproducible. This method was applied to study the pharmacokinetics of imatinib and its main metabolite in human and mice.

Introduction

Imatinib mesylate (STI-571, Gleevec®, imatinib) (Fig. 1), a tyrosine kinase inhibitor, is one of the first examples of rationally designed molecularly targeted agents that is successfully used for treatment in cancer patients (1). Specifically, it is a potent small molecule inhibitor of several non-receptor protein-tyrosine kinases c- ABL, c-ARG, and the related oncogene BCR-ABL (2, 3), and the receptor kinases c-KIT (4, 5) and PDGFR (4, 6). Imatinib is approved for use in BCR/ABL positive chronic myeloid leukemia (CML) (7) and gastrointestinal stromal (GIST) tumors that harbor c-KIT mutations (8). Its usefulness in the treatment of a number of other tumor types (9, 10) and its utility when combined with other agents is currently under investigation (11-13). Unfortunately, in many patients, resistance to imatinib therapy due to alterations in the target kinase has been described (14, 15). Moreover, preclinical *in vitro* and *in vivo* studies have shown that imatinib is a substrate of P-glycoprotein (ABCB1) and Breast Cancer Resistance Protein (ABCG2) and these drug efflux transporter proteins may also play an important role in the pharmacokinetics and efficacy of imatinib (16-18).

The biotransformation of imatinib occurs mainly by the human cytochrome P450 enzyme CYP3A4 and to a lesser extent by CYP1A1/2, 1B1, 2C8/9 and 2D6 (19-21). Thus far one major imatinib metabolite, N-desmethyl-imatinib (CGP74588) (Fig. 1), has been identified in plasma samples of healthy individuals and patients with CML/GIST and/or other tumor types receiving imatinib and has comparable activity as the parent compound (22, 23). However, some other metabolites were also identified in plasma and characterized as hydroxy-, *N*-oxide-, deaminated-, and glucoroconjugate metabolites (21).

In order to support our preclinical and clinical pharmacokinetic studies with imatinib, we developed and validated a simple and sensitive bioanalytical HPLC assay for the drug and its main metabolite CGP74588. Previously described analytical methods (24-32) for the determination of imatinib and CGP74588 were only tested and validated for human/monkey plasma, human urine, patient tumor tissue, erythrocytes, cerebrospinal fluid, culture medium and cell preparations. Mouse plasma is only available in small quantities, thus demanding better mass-sensitivity. Moreover, our studies require the determination of imatinib and CGP74588 in a variety of murine biological matrices. Since the performance of an analytical assay may be strongly dependent on the biological matrix, it is important to investigate the accuracy and precision of an analytical assay for all relevant specimens. Therefore the aim of this study was to develop and validate a sensitive HPLC assay for imatinib and CGP74588 in human plasma and a range of biological matrices of mice that are relevant for clinical and preclinical investigations.

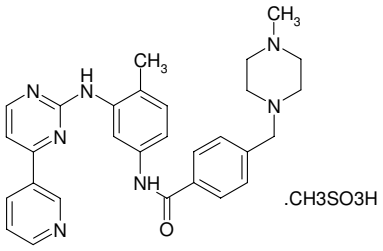

Imatinib

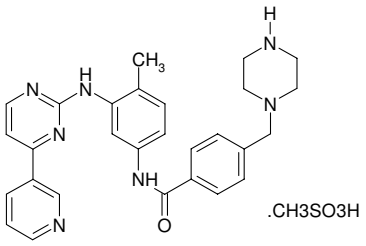

GCP74588

Figure 1. Molecular structure of imatinib and CGP74588

Experimental

Materials

Imatinib mesylate (chemical purity of 99%) and its metabolite CGP74588 were kindly provided by Novartis Pharma AG (Basel, Switzerland). 4-hydroxybenzophenone and Bovine serum albumine (BSA) were obtained from Sigma (St. Louis, MO, USA). PIC-B8 (1-octane sulfonic acid) was purchased from Waters (Milford, MA, USA). All other chemicals were of analytical or Lichrosolv gradient grade and were purchased from E. Merck (Darmstadt, Germany). Water was purified by the Milli-Q Plus system (Millipore, Milford, MA, USA). Blank human plasma was obtained from the Central Laboratory of the Blood Transfusion Service (Sanquin, Amsterdam, The Netherlands).

Experimental Procedures

Preparation of stock solutions

Stock solutions of imatinib and CGP74588 were prepared by accurately weighing of approximately 5 mg pure substance and dissolving this in exactly the volume of purified water to obtain 1.00 mg/ml (corresponding to 1.46 and 1.49 mM, respectively). Aliquots of these solutions were stored at -20°C. The imatinib working solution of 100 µg/ml was prepared by diluting 1 ml of the imatinib stock solution (1.00 mg/ml) with drug-free human plasma to 10 ml. 4-hydroxybenzophenone was used as internal standard and a 1 mg/ml stock solution was prepared by dissolving 5 mg of accurately weighed 4–hydroxybenzophenone in 5 ml of methanol. This stock solution was stored at -20°C and with each run further diluted with methanol to a 50 µg/ml internal working solution.

Collection of murine specimens

All handlings involving animals were approved by the animal experiment committee of the Institute and carried out in accordance with Dutch law. Male and female FVB mice between 9 and 14 weeks of age were anaesthetized with methoxyflurane, their blood was collected by cardiac puncture, and they were sacrified by cervical dislocation. Furthermore, the following tissues were dissected: brain, liver, kidney, lung, heart and spleen. The blank tissues were homogenized with a Polytron tissue homogenizer (Kinematica AG, Littau, Switzerland) in 4% (w/v) BSA in water resulting in final concentrations of approximately 0.05-0.2 g tissue per ml. Feces and urine were obtained from mice housed in metabolic cages. Feces were homogenized in 4% (w/v) BSA in water (0.03-0.1 g faeces per ml) according to the procedure described above for tissue specimens.

Preparation of calibration standards and quality control samples

Prior to each run, an aliquot of the 100 µg/ml imatinib working solution was used to prepare a set of calibration samples in drug-free human plasma. Calibration standards contained 10, 50, 100, 500 ng/ml and 1, 5, 10 µg/ml of imatinib and were processed and analyzed in duplicate. Quality control samples in human plasma were prepared by dilution of the independently prepared 100 µg/ml imatinib working solution in drug-free human plasma to final concentrations of 15, 500 ng/ml and 5 µg/ml of imatinib (low, medium and high). All human plasma quality control samples were aliquoted and stored at -20°C. Quality control samples in murine specimens were prepared by dilution of the 1.00 mg/ml imatinib stock solution in the different homogenized murine tissues to final concentrations of 150 ng/ml, 5 and 50 µg/ml. These quality control samples were stored at -20°C. Prior to each run, these were diluted 10-fold in drug-free human plasma to final concentrations of 15, 500 ng/ml and 5 µg/ml of imatinib (low, medium and high) prior to further sample pre-treatment.

Sample pre-treatment

Frozen samples were thawed at room temperature and thorougly mixed by vortexing. Dilutions of murine plasma (2- to 10-fold), feces homogenate (10-fold) and urine (10-fold) were prepared in blank human plasma, dilutions of murine tissues (10-fold) were prepared in 4% BSA, whereas human plasma was used without further dilution. Of each sample 100 µl was pipetted into a 2 ml eppendorf vial. Volumes of 50 µl of internal standard solution (50 µg/ml) and 1 ml of *tert*-butyl methylether were added and the vials were mixed vigorously for 5 min. After centrifugation for 5 min at 5000 rpm, the aqueous layer was frozen in a bath of ethanol-dry ice. The organic layer was decanted into a 1.5 ml HPLC

eppendorf vial. After evaporation in a Speed-Vac Plus SC210A (Savant, Farmingdale, NY, USA) at 43°C, the residue was reconstituted in 100 µl acetonitrile-50 mM ammonium acetate buffer (20:80, v/v) by sonification for 5 minutes, vortex mixing, centrifugation at 14000 rpm for 3 min and the vials were placed in the HPLC autosampler. 50 µl was injected into the sample loop using the sample pick-up mode of the autosampler.

HPLC instrumentation conditions

The HPLC system consisted of a model P680 HPLC pump (Dionex Corp. Sunnyvale, CA, USA), a Midas autosampler (Spark Holland, Emmen, The Netherlands), provided with a 100 µl sample loop and a Model SF757 UV detector (Kratos, Ramsey, NJ, USA) operating at a wavelength of 265 nm. Separation of imatinib, CGP74588 and the internal standard was performed using a narrow bore stainless steel column (150 X 2.1 mm I.D.) packed with 3.5 µm Symmetry C_{18} material (Waters, Milford, MA, USA) and a mobile phase consisting of acetonitrile-50 mM ammonium acetate buffer pH 6.8 (28:72, v/v) plus one vial of PIC B-8 (Waters) resulting in a final concentration of 5 mM 1-octane sulfonic acid. The flow rate was 0.2 ml/min. Chromatographic data acquisition and reprocessing was performed using Chromeleon version 6.60 (Dionex Corp. Sunnyvale, CA, USA). Ratios of peak areas of imatinib and CGP74588 versus the internal standard were used for quantitative calculations.

Method validation

Validation of the analysis of imatinib was performed in human plasma and murine specimens. The statistical analyses were done with the computer program SPSS for Windows (version 12.0; SPSS, Chicago, IL, USA).

Calibration curves and linearity

Calibration curves were computed using linear regression analysis of the peak ratios of imatinib, CGP74588 and internal standard versus concentration. Weighting by $1/x^2$ (reciprocal of the square of the concentration) was used. The *F*-test for lack of fit ($\alpha = 0.05$) was used to evaluate the linearity of the calibration curves.

Accuracy and precision

Full validation was performed in human plasma. Quality controls (15, 500 ng/ml and 5 µg/ml imatinib) were analyzed in 6-fold in three separate analytical runs for evaluation of accuracy and between-day/within-day precision. Subsequently, a limited validation was done in all murine specimens. Quality controls (15, 500 ng/ml and 5 µg/ml imatinib) were

analyzed in a single analytical run in 5-fold for evaluation of accuracy and within-day precision. The accuracy was calculated by dividing the observed concentration and the nominal concentration and multiplied by 100%. The between-day precision was calculated by one-way analysis of variance (ANOVA) for each control sample using the run day as the classification variable. The day mean square (DayMS), error mean square (ErrMS) and the grand mean (GM) of the observed concentrations across run days were used. The within-day precision (WDP %) and the between-day precision (BPD %) for each quality control sample was calculated using the formulas:

WDP %= $(\text{ErrMS})^{0.5}$ / GM. 100%

BDP % = $[(\text{DayMS} - \text{ErrMS})/n]^{0.5}$ /GM.100%

(Where n = number of replicates within each run)

Selectivity

Blank human plasma from six different healthy donors and pooled blank plasma from twelve untreated FVB-mice were processed and analyzed to determine whether endogenous plasma peaks co-eluted with imatinib, CGP74588 or the internal standard.

Lower limit of quantification

To determine the lower limit of quantification (LLQ), we spiked blank human and mouse plasma of nine and eleven different subjects, respectively, with imatinib at concentrations of 5, 10, 15 ng/ml. The LLQ was established when the accuracy was within the 100 ± 20% range and the WDP % was smaller than 20%.

Recovery

To determine the extraction recovery of imatinib, CGP74588 and the internal standard, non-processed samples were prepared in mobile phase solution, acetonitrile-50mM ammonium acetate buffer, pH 6.8 (20:80 v/v), at concentrations corresponding with those used for the calibration curves in plasma. The recovery was determined by calculating the ratio of the slopes of the processed versus unprocessed calibration curves.

Stability

The stability of imatinib was tested at a concentration of 500 ng/ml in human and mice plasma. Aliquots were stored at 4°C and at room temperature (22-26°C) for 24 h. Furthermore, the stability during four freeze-thaw cycles was also determined in the aliquots. The long-term stability of imatinib in human plasma at concentrations of 15, 500 ng/ml and 5 µg/ml under storage conditions of -20°C was determined for up to 9 months.

The stability of imatinib in the processed specimens while standing at room temperature in the autosampler was checked up to 96 h. Data were compared by one-way ANOVA in order to evaluate the stability of the drug in plasma.

Demonstration of applicability to biological samples of human and mice

Pharmacokinetic plasma samples of a GIST patient were used to quantify concentrations of imatinib and CGP74588 to demonstrate the applicability of this HPLC method. In the study, after informed consent, we collected steady state blood levels of imatinib into heparinized tubes at t = 0, 1, 2, 3, 4, 5, 6, 8 and 10 h after an oral dose of 400 mg imatinib. Each sample was centrifuged at 5000 rpm for 10 min, and the plasma was stored at -20°C until analyzed with the procedure described above.

Blood samples of female FVB mice after receiving orally administered imatinib (100 mg/kg) were collected into EDTA tubes at t = 0.25, 0.5, 1.5, 3.5 and 8 h, which were centrifuged (10 min, 4200g, 4°C) to separate the plasma fraction and analyzed with the procedure described above.

Results and Discussion

Optimization of Chromatographic separation and sample pre-treatment

A number of analytical methods for imatinib and its main metabolite CGP74588 in human plasma using HPLC-UV or liquid chromatographic-mass spectrometry (LC-MS) have been reported, previously (24-30). Since we aimed to determine imatinib and CGP74588 in a variety of murine biological matrices and because murine plasma is only available in small quantities, we first developed this simple and sensitive validated HPLC-UV assay for human plasma and, next, validated it for all relevant murine specimens. We selected a narrow bore (2.1; ID x 150 mm) column, which was packed with 3.5 µm Symmetry C_{18} material packing material. This column increased the intrinsic sensitivity of the system due to a reduction in the peak dilution and reduced mobile phase consumption compared to a normal bore (4.6 mm ID) column. We first tried a simple mobile phase consisting of 0.02 M potassium phosphate buffer-acetonitrile pH 4.0 (70:30, v/v), but this resulted in broad peaks for imatinib, which is not uncommon for a compound containing basic (nitrogen) moieties. We then checked different other packing materials, however, without much improvement in the peak shape. Modification of the mobile phase composition, acetonitrile- ammonium acetate buffer pH 4.2 (28:72, v/v) and 0.005 M of 1-octane sulfonic acid as a negatively charged counter ion, markedly improved the peak shape of imatinib. After slight further adjustments of the mobile phase the retention time of the positively charged imatinib and internal standard, 4-hydroxybenzophenone, was 10.5 and

19.5 min, respectively, yielding a good separation. However, under these conditions the retention times of CGP74588 and imatinib were virtually overlapping. We managed to improve the separation between imatinib and CGP74588 by changing the pH of the mobile phase buffer to pH 6.8. Under these conditions, there was sufficient resolution between CGP74588, imatinib and 4-hydroxybenzophenone with retention times of 10.5, 11.3 and 20.5 min, respectively (Fig. 2). The final composition of the mobile phase with acceptable selectivity of imatinib and CGP74588 was acetonitrile-50mM ammonium acetate buffer pH 6.8 (28:72, v/v) plus 1-octane sulfonic acid 0.005 M.

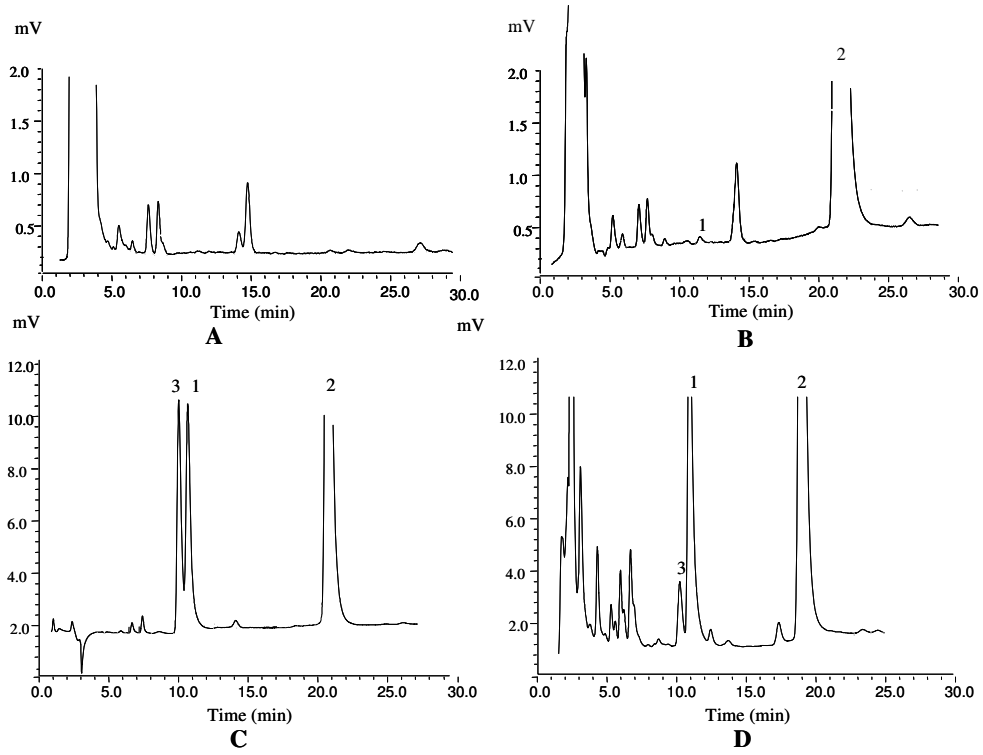

Figure 2. Typical chromatograms of blank human plasma (A), human plasma spiked with 10 ng/ml (LLQ) (B), human plasma spiked with 1 µg/ml imatinib and CGP74588 (C) and plasma sample from a female mouse obtained at 4 h after 100 mg/kg oral administered imatinib, resulting in a concentration of 2.2 µg/ml imatinib and 318 ng/ml CGP74588 (D). Peaks are labelled with 1 = imatinib, 2 = 4-hydroxybenzophenone (internal standard), 3 = CGP74588.

Sample pre-treatment by liquid-liquid extraction with *tert*-butyl methyl ether was tested, since this method can be uniformly applied to all biological matrices including tissue and feces homogenates. Chloroform, isopropanol and methanol were also tested, however the recovery of the analytes in these solvents was less than the recoveries with *tert*-butyl methyl ether. The recovery of di-ethyl ether showed similar results than the recovery of *tert*-butyl methyl ether in human/mouse plasma. However the recovery from the biological matrices after di-ethyl ether extraction was less. Human plasma and murine specimens extractions with *tert*-butyl methyl ether resulted in high CGP74588, imatinib and 4-hydroxybenzophenone recoveries of 87 to 99% in all biological matrices.

In blank human and mouse plasma no interfering endogenous peaks were found (Fig. 2). All other specimens were also free of interfering peaks. Chromatograms of blank murine liver and liver from a female mouse obtained at 1 h after 100 mg/kg oral administered imatinib are shown in figure 3. To purge late-eluting compounds from the column, the column was flushed for 10 min with a mobile phase containing acetonitrile-50 mM ammonium acetate buffer pH 6.8 (60:40, v/v) plus 0.005 M of 1-octane sulfonic acid. Next, the mobile phase was returned to its original composition and maintained for 15 min prior to injection of the next sample. The total analysis time was 50 min per sample.

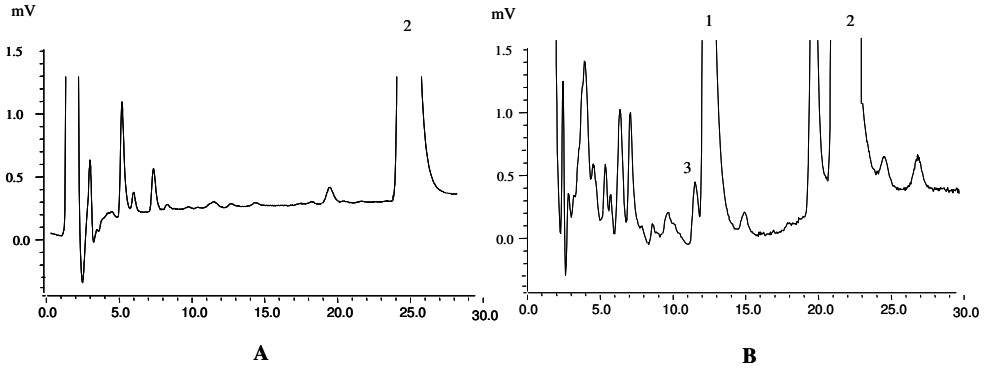

Figure 3. Chromatograms of (A) blank murine liver; (B) liver of female mouse, 1 h after oral administration of 100 mg/kg imatinib, resulting in a concentration of 6.1 µg/ml imatinib and 181 ng/ml CGP74588. Peaks are labelled with 1 = imatinib, 2 = 4-hydroxybenzophenone (internal standard), 3 = CGP74588.

Method validation

Lower limit of quantification

The LLQ in human plasma was established by spiking blank human plasma from five different individuals at concentrations of 5, 10 and 15 ng/ml. At a concentration of 10 ng/ml the accuracy and precision met the requirements (within 20%) (Table 1). Thus the LLQ in human plasma is 10 ng/ml (Fig. 2B). This LLQ was more sensitive or in the same range as the LLQ of several LC-MS analytical assays (26, 28-30). Since a similar procedure to establish the LLQ in mouse plasma from individual animals is not possible due to the small sample size, we have chosen to use pooled mouse plasma spiked at concentrations of 5, 10 and 15 ng/ml (Table 1). The LLQ in pooled mouse plasma was similar as in human plasma and within the generally accepted ranges for bio-analytical assays (33). The results show that it is possible to read concentrations of imatinib in mouse plasma samples from a calibration curve prepared in human plasma. This is advantageous, because of the limited availability of blank mouse plasma.

Table 1. Assay validation: Determination of the lower limit of quantification (LLQ).

	Nominal concentration (ng/ml)	Measured concentration (ng/ml)	Accuracy (%)	Within-day precision (%)
human	5	6.6	132	32.4
	10	9.9	99	0.4
	20	18.4	92	8.3
mouse	5	6.4	128	29.1
	10	10.2	102	2.5
	20	18.9	95	5.7

Calibration curves and linearity

Calibration curves in human plasma were linear over a concentration range of 10 ng/ml to 10 µg/ml. This range was considered acceptable for our pharmacokinetic studies. The optimum weighting factor for the calibration curve was $1/x^2$ (reciprocal of the squared concentration).

Accuracy and precision

Within the linear dynamic range of the assay the accuracy of quality control samples (15, 500 ng/ml and 5 µg/ml) in human plasma were close to 100% (Table 2). Additional, the accuracy of the quality control samples under storage conditions of -20°C up to 9 months measured in every run was also close to 100% (Table 3). The within-day precision and between-day precision were within the generally accepted 15% range. However, the quality control data obtained from homogenized mice tissues spiked at 15, 500 ng/ml and 5 µg/ml did not meet the requirements for accuracy and within-day precision, viz. 42-78% and 20-45%, respectively. These results using spiked mouse tissue homogenates clearly demonstrate the importance of validation in all relevant specimens, since the accuracy and precision were highly matrix-dependent. To improve the accuracy in spiked murine tissue samples, these samples were first diluted 10-fold with blank human plasma (Table 4). Under these conditions, the validation results showed that the assay was selective and reproducible for spiked and treated human plasma and mice specimens.

Although this modification increases the LLQ in tissue homogenate by 10-fold, the sensitivity of the assay was still sufficient to analyze imatinib in all tested tissues up to at least 8 h after administration of 100 mg/kg.

Table 2. Assay validation: quality control data of the assay for imatinib in human plasma represented by the accuracy, the within-run precision and the between-run precision.

	Nominal concentration (ng/ml)	Measured concentration (ng/ml)	Accuracy (%)	Within-day precision (%)	Between-day precision (%)
human	15	14.9	99.8	7.8	7.6
	500	496.8	99.4	2.9	1.5
	5000	5032.5	100.7	1.3	1.1

Table 3. Assay validation: Human plasma spiked with 15, 500 ng/ml and 5 µg/ml under storage conditions of -20°C up to 9 months represented by the accuracy, the within-run precision and the between-run precision.

	Nominal concentration (ng/ml)	Measured concentration (ng/ml)	Accuracy (%)	Within-day precision (%)	Between-day precision (%)
human	15	15.6	104	10.8	3.1
	500	483.8	96.8	6.2	8.3
	5000	5252.9	105	6.6	6.1

Stability

Imatinib was stable in human and mouse plasma kept at room temperature (22-26°C) and 4°C for at least 24 h and four freeze-thaw cycles had no effect on the imatinib levels. The long-term stability of imatinib levels in human plasma under storage conditions of -20°C for up to 9 months was also acceptable. Processed samples were stable at ambient temperature for at least 96 h.

Table 4. Assay validation: Quality control data of the assay for imatinib in murine specimens represented by the accuracy and the within-run precision. Data were determined in 5-fold using freshly prepared tissue homogenate sample spiked at three different concentrations. Samples were diluted 10-fold.

Murine Specimen	Nominal concentration (ng/ml)	Nominal concentration (ng/g)*	Measured concentration (ng/ml)	Accuracy (%)	Within-day precision (%)
Brain	150	1271	150	100	5.9
	5000	42373	4357	87.1	4.4
	50000	423729	44590	89.2	6.8
Liver	150	775	149	99.3	3.1
	5000	25833	4525	90.5	5.7
	50000	258333	44680	89.4	3.9
Kidney	150	2150	153	102	3.7
	5000	71667	4090	81.8	10.6
	50000	716667	49480	98.9	3.6
Lung	150	2293	152	101	3.7
	5000	76429	5215	104.3	4.3
	50000	764286	47860	95.7	4.5
Heart	150	3150	149.5	99.7	2.0
	5000	105000	4899	98	10.1
	50000	1050000	48990	97.9	7.2
Spleen	150	3483	156	104	4.4
	5000	116111	4520	90.4	6.8
	50000	1161111	43090	86.2	7.6
Feces	150		149	99.3	5.5
	5000		4591	91.8	7.5
	50000		54730	109	1.8
Urine	150		153	102	4.3
	5000		4914	98	4.7
	50000		51900	104	8.1

* Tissue homogenates were spiked at 3 levels. As the tissues had been homogenized in 3 (brain), 5 (liver) and 2 ml (kidney, lung, spleen, heart) of BSA solution, the approximate corresponding concentrations in ng/g of tissue are depicted in the second column.

Applicability

The applicability of the assay was demonstrated in samples from a GIST patient and female mice receiving 400 mg and 100 mg/kg imatinib, respectively, by oral administration (Fig. 4). The concentrations of imatinib and CGP74588 in both species were within the dynamic range of the assay.

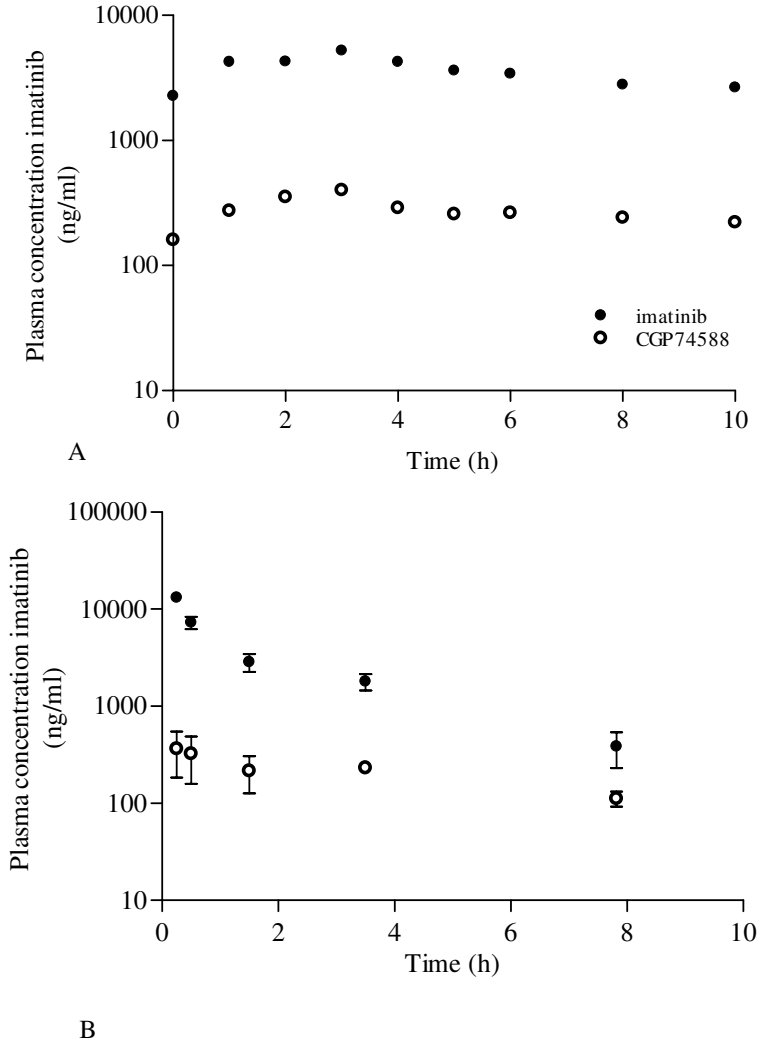

Figure 4. Time course for imatinib and CGP74588 in plasma of a GIST patient given 400 mg of imatinib orally (A) and female FVB mice receiving 100 mg/kg of imatinib orally (B) (Data of the mice are shown as the mean of four mice ± standard deviation).

Conclusion

In conclusion, a simple sensitive HPLC method with UV detection has been developed and validated for the quantification of imatinib and its main metabolite CGP74588 in microvolumes of human and mice plasma and a range of other biological matrices of mice.

References

1. Capdeville R, Buchdunger E, Zimmermann J and Matter A. Glivec (STI571, imatinib), a rationally developed, targeted anticancer drug. Nat Rev Drug Discov 2002;1:493-502.
2. Beran M, Cao X, Estrov Z, et al. Selective inhibition of cell proliferation and BCR-ABL phosphorylation in acute lymphoblastic leukemia cells expressing Mr 190,000 BCR-ABL protein by a tyrosine kinase inhibitor (CGP-57148). Clin Cancer Res 1998;4:1661-1672.
3. Carroll M, Ohno-Jones S, Tamura S, et al. CGP 57148, a tyrosine kinase inhibitor, inhibits the growth of cells expressing BCR-ABL, TEL-ABL, and TEL-PDGFR fusion proteins. Blood 1997;90:4947-4952.
4. Buchdunger E, Cioffi CL, Law N, et al. Abl protein-tyrosine kinase inhibitor STI571 inhibits in vitro signal transduction mediated by c-kit and platelet-derived growth factor receptors. J Pharmacol Exp Ther 2000;295:139-145.
5. Heinrich MC, Griffith DJ, Druker BJ, et al. Inhibition of c-kit receptor tyrosine kinase activity by STI 571, a selective tyrosine kinase inhibitor. Blood 2000;96:925-932.
6. Druker BJ and Lydon NB. Lessons learned from the development of an abl tyrosine kinase inhibitor for chronic myelogenous leukemia. J Clin Invest 2000;105:3-7.
7. Druker BJ, Talpaz M, Resta DJ, et al. Efficacy and safety of a specific inhibitor of the BCR-ABL tyrosine kinase in chronic myeloid leukemia. N Engl J Med 2001;344:1031-1037.
8. Demetri GD, von Mehren M, Blanke CD, et al. Efficacy and safety of imatinib mesylate in advanced gastrointestinal stromal tumors. N Engl J Med 2002;347:472-480.
9. Johnson BE, Fischer T, Fischer B, et al. Phase II study of imatinib in patients with small cell lung cancer. Clin Cancer Res 2003;9:5880-5887.
10. Rao K, Goodin S, Levitt MJ, et al. A phase II trial of imatinib mesylate in patients with prostate specific antigen progression after local therapy for prostate cancer. Prostate 2005;62:115-122.
11. Reardon DA, Egorin MJ, Quinn JA, et al. Phase II Study of Imatinib Mesylate Plus Hydroxyurea in Adults With Recurrent Glioblastoma Multiforme. J Clin Oncol 2005;23:9359-9368.
12. Dresemann G. Imatinib and hydroxyurea in pretreated progressive glioblastoma multiforme: a patient series. Ann Oncol 2005;16:1702-1708.
13. Mohi MG, Boulton C, Gu TL, et al. Combination of rapamycin and protein tyrosine kinase (PTK) inhibitors for the treatment of leukemias caused by oncogenic PTKs. Proc Natl Acad Sci USA 2004;101:3130-3135.
14. Shannon KM. Resistance in the land of molecular cancer therapeutics. Cancer Cell 2002;2:99-102.
15. McCormick F. New-age drug meets resistance. Nature 2001;19;412:281-282.
16. Hamada A, Miyano H, Watanabe H and Saito H. Interaction of imatinib mesilate with human P-glycoprotein. J Pharmacol Exp Ther 2003;307:824-828.
17. Dai H, Marbach P, Lemaire M, et al. Distribution of STI-571 to the brain is limited by P-glycoprotein-mediated efflux. J Pharmacol Exp Ther 2003;304:1085-1092.
18. Breedveld P, Pluim D, Cipriani G, et al. The effect of Bcrp1 (Abcg2) on the in vivo pharmacokinetics and brain penetration of imatinib mesylate (Gleevec): implications for the use of breast cancer resistance protein and P-glycoprotein inhibitors to enable the brain penetration of imatinib in patients. Cancer Res 2005;65:2577-2582.
19. Peng B, Lloyd P and Schran H. Clinical pharmacokinetics of imatinib. Clin Pharmacokinet 2005;44:879-894.
20. Rochat B. Role of cytochrome P450 activity in the fate of anticancer agents and in drug resistance: focus on tamoxifen, paclitaxel and imatinib metabolism. Clin Pharmacokinet 2005;44:349-366.
21. Marull M and Rochat B. Fragmentation study of imatinib and characterization of new imatinib metabolites by liquid chromatography-triple-quadrupole and linear ion trap mass spectrometers. J Mass Spectrom 2006;41:390-404.
22. Gschwind HP, Pfaar U, Waldmeier F, et al. Metabolism and disposition of imatinib mesylate in healthy volunteers. Drug Metab Dispos 2005;33:1503-1512.

23. Ramalingam S, Lagattuta TF, Egorin MJ, et al. Biliary excretion of imatinib mesylate and its metabolite CGP 74588 in humans. Pharmacotherapy 2004;24:1232-1235.
24. Velpandian T, Mathur R, Agarwal NK, et al. Development and validation of a simple liquid chromatographic method with ultraviolet detection for the determination of imatinib in biological samples. J Chromatogr B Analyt Technol Biomed Life Sci 2004;804:431-434.
25. Schleyer E, Pursche S, Kohne CH, et al. Liquid chromatographic method for detection and quantitation of STI-571 and its main metabolite N-desmethyl-STI in plasma, urine, cerebrospinal fluid, culture medium and cell preparations. J Chromatogr B Analyt Technol Biomed Life Sci 2004;799:23-36.
26. Parise RA, Ramanathan RK, Hayes MJ and Egorin MJ. Liquid chromatographic-mass spectrometric assay for quantitation of imatinib and its main metabolite (CGP 74588) in plasma. J Chromatogr B Analyt Technol Biomed Life Sci 2003;791:39-44.
27. Widmer N, Beguin A, Rochat B, et al. Determination of imatinib (Gleevec) in human plasma by solid-phase extraction-liquid chromatography-ultraviolet absorbance detection. J Chromatogr B Analyt Technol Biomed Life Sci 2004;803:285-292.
28. Titier K, Picard S, Ducint D, et al. Quantification of imatinib in human plasma by high-performance liquid chromatography-tandem mass spectrometry. Ther Drug Monit 2005;27:634-640.
29. Bakhtiar R, Lohne J, Ramos L, et al. High-throughput quantification of the anti-leukemia drug STI571 (Gleevec) and its main metabolite (CGP 74588) in human plasma using liquid chromatography-tandem mass spectrometry. J Chromatogr B Analyt Technol Biomed Life Sci 2002;768:325-340.
30. Bakhtiar R, Khemani L, Hayes M, et al. Quantification of the anti-leukemia drug STI571 (Gleevec) and its metabolite (CGP 74588) in monkey plasma using a semi-automated solid phase extraction procedure and liquid chromatography-tandem mass spectrometry. J Pharm Biomed Anal 2002;28:1183-1194.
31. Guetens G, Prenen H, De Boeck G, et al. Imatinib (Gleevec, Glivec) tumour tissue analysis by measurement of sediment and by liquid chromatography tandem mass spectrometry. J Sep Sci 2006;29:453-459.
32. Guetens G, De Boeck G, Highley M, et al. Quantification of the anticancer agent STI-571 in erythrocytes and plasma by measurement of sediment technology and liquid chromatography-tandem mass spectrometry. J Chromatogr A 2003;1020:27-34.
33. Shah VP, Midha KK, Findlay JW, et al. Bioanalytical method validation--a revisit with a decade of progress. Pharm Res 2000;17:1551-1557.

CHAPTER 3

Preclinical and clinical pharmacological studies on camptothecins

CHAPTER 3.1

In vitro transport of gimatecan (7-t-butoxyiminomethylcamptothecin) by BCRP, P-gp and MRP2

Serena Marchetti, Roos L. Oostendorp, Dick Pluim, Monique van Eijndhoven, Olaf van Tellingen, Alfred H. Schinkel, Richard Versace, Jos H. Beijnen, Roberto Mazzanti, Jan H.M. Schellens

Molecular Cancer Therapeutics 2007; 6:3307-3313

Abstract

Lipophilic campthothecin derivatives are considered to have negligible affinity for Breast Cancer Resistance Protein (BCRP; ABCG2). Gimatecan, a new orally available 7-t-butoxyiminomethyl substituted lipophilic camptothecin derivative, has been previously reported to be not a substrate for BCRP. Using a panel of *in vitro* models, we tested whether gimatecan is a substrate for BCRP as well as for P-glycoprotein (P-gp, MDR1) or Multidrug Resistance Protein 2 (MRP2, ABCC2), ABC-drug efflux transporters involved in anti-cancer drug resistance and able to affect the pharmacokinetics of substrate drugs.

Cell survival, drug transport, accumulation and efflux were studied in IGROV1 and (human BCRP-overexpressing) T8 cells, MDCKII (WT, -Bcrp1, -MDR1, –MRP2) and LLCPK (WT, –MDR1) cells. Competition with methotrexate uptake was studied in Sf9-BCRP membrane vesicles.

In vitro, expression of BCRP resulted in 8-10 fold resistance to gimatecan. In transwell experiments gimatecan was transported by Bcrp1 and transport was inhibited by the BCRP/P-gp inhibitors elacridar and pantoprazole. Efflux of gimatecan from MDCKII-Bcrp1 cells was faster than in WT cells. In Sf9-BCRP membrane vesicles gimatecan significantly inhibited BCRP-mediated transport of Methotrexate. In contrast, gimatecan was not transported by MDR1 or MRP2.

Gimatecan is transported by BCRP/Bcrp1 *in vitro,* although to a lesser extent than the campthothecin analogue topotecan. Implications of BCRP expression in the gut for the oral development of gimatecan and the interaction between gimatecan and other BCRP substrate drugs and/or inhibitors warrant further clinical investigation.

Introduction

The ATP-binding cassette (ABC) drug efflux transporters, breast cancer resistance protein (BCRP, ABCG2) (1), P-glycoprotein (P-gp, MDR1, ABCB1), and the Multidrug Resistance Proteins (MRP) 1-5 (ABCC1-5) are involved in resistance against anticancer drugs (2, 3). Besides expression in various tumor tissues, these drug transporters are expressed in a number of normal tissues where they exert partly overlapping physiological functions. P-gp and BCRP are highly expressed at the luminal side of the intestinal epithelial cells, in the bile canalicular membrane, the syncytiotrophoblast and at the vascular endothelial side of the blood brain barrier (BBB) (4, 5). These drug transporters mediate the active, i.e. ATP-dependent, efflux of a wide range of chemical compounds with different physico-chemical characteristics. In the intestine, BBB and placenta these transporters have a protective role as they limit uptake from the intestinal lumen into the body, the penetration of compounds into the central nervous system (CNS), or the exposure of the fetus by limiting penetration through the placenta (4).

The camptothecin derived topoisomerase I (topI) inhibitors are substrates for BCRP and P-gp (6). The affinity of the camptothecins for BCRP is for most compounds significantly higher than for P-gp. Usually, low cross-resistance is found with classical P-gp substrate drugs such as paclitaxel and docetaxel (7). However, the affinity for BCRP can vary substantially among the different derivatives of camptothecin (6). Topotecan and irinotecan, but especially SN38, the pharmacologically active metabolite of irinotecan, have high affinity for BCRP. They also have moderate affinity for P-gp. We previously reported that the camptothecin derivatives, which are substituted at the 7 position of the planar aromatic five-ring structure resulting in a more lipophilic molecule (such as lurtotecan (GI147211, NX211) and exatecan mesylate (DX-8951f)), have less affinity for BCRP than topotecan and SN38 (6). It was suggested by others that the 7-oxyiminomethyl substituted more lipophilic camptothecin derivative gimatecan (ST1481, LBQ707) is not a substrate for BCRP (8, 9). However, based on our experience with a range of other camptothecin derivatives we hypothesized that gimatecan might also be a substrate for BCRP. We tested this hypothesis in a panel of well-defined *in vitro* models, including the BCRP-overexpressing human ovarian cancer cell line T8 (10), the Madin-Darby canine kidney II (MDCKII) epithelial cells stably expressing mouse Bcrp1 (11) and Sf9-BCRP membrane vesicles. We used elacridar and pantoprazole as inhibitors of BCRP and topotecan as positive control.

Moreover, we investigated whether gimatecan is a substrate of MRP2 and P-glycoprotein (P-gp, MDR1) *in vitro*. Affinity of gimatecan for BCRP could be clinically

relevant as oral bioavailability may be reduced by BCRP as shown for topotecan (12) and especially after oral administration drug-drug interactions with other BCRP substrate drugs may take place.

Material and Methods

Chemicals and reagents

[^{3}H]-inulin (0.78 Ci/mmol), [^{14}C]inulin carboxylic acid (54 mCi/mmol), [^{14}C]topotecan (SK&F 104864, 48 mCi/mmol) and [^{3}H]MTX (methotrexate, 5.9 Ci/mmol) were purchased from Amersham Biosciences (Little Chalfont, UK). Topotecan (Hycamtin®) was obtained from GlaxoSmithKline (GSK) Pharmaceuticals (King of Prussia, PA). Gimatecan (STI1481; LBQ707) and [^{3}H]gimatecan (40 µCi/mg) were provided by Novartis Pharmaceuticals Inc. (East Hanover, NJ). Pantoprazole (Pantozol® 40 mg, Altana Pharma, Zwanenburg, The Netherlands) was obtained from the pharmacy of the Netherlands Cancer Institute. Elacridar (GF120918) was kindly provided by GSK (Research Triangle Park, NC) and zosuquidar (LY335979), was a generous gift from Dr P Multani (Kanisa Pharmaceuticals, San Diego, CA). All other chemicals and reagents were from Sigma (St Louis, MO) and of analytical grade or better.

Cell lines

Polarized MDCKII (Madin-Darby canine kidney II) cells wild-type (WT) and transfected subclones stably expressing human MRP2 (ABCC2), human MDR1 (P-gp, ABCB1) or mouse Bcrp1 (Abcg2) cDNA were kindly provided by Dr AH Schinkel (The Netherlands Cancer Institute, Amsterdam, The Netherlands) and were described previously (11, 13). They were cultured in Dulbecco's Modified Eagle's Medium (DMEM) with Glutamax (Life Technologies, Breda, The Netherlands) supplemented with 100 IU/ml penicillin G, 100 µg/ml streptomycin sulphate and 10% fetal calf serum (MP Biochemicals, ICN Biomedicals Inc.). Bcrp1, MDR1 and MRP2 expression in the various transfected MDCKII sublines was checked by Western Blot. The IGROV1 human ovarian adenocarcinoma and the IGROV1-derived resistant T8 cell lines were cultured in RPMI 1640 Medium supplemented with 25 mM HEPES, L-Glutamine, 10% fetal calf serum, 100 IU/ml penicillin and 100 µg/ml streptomycin. T8 cells were exposed to 950 nM concentration of topotecan weekly for 1 h, which keeps the resistance level in T8 constant for at least 25 weeks (10, 14). The polarized porcine kidney epithelial cells LLC-PK -WT and -MDR1, which were a generous gift from Dr P Borst (The Netherlands Cancer Institute, Amsterdam, The Netherlands), were described previously (15). They were cultured in M199 medium with L-glutamine (Life Technologies, Inc., Breda, The Netherlands) and supplemented with

penicillin G (100 IU/ml), streptomycin (100 µg/ml) and 10% (v/v) fetal bovine serum (MP Biochemicals, ICN Biomedicals Inc.). All cell lines were grown at 37°C with 5% CO_2 under humidifying conditions.

Cytotoxicity Assays

Exponentially growing-cells were plated (1000 cells/200 µl per well for the MDCKII-WT, -Bcrp1 and -MRP2 cells; 1500 cells/200 µl per well for the MDCKII-MDR1 cells; 5000 cells/200 µl per well for the IGROV1 and T8 cells) in 96-well microplates (Costar Corporation, Cambridge, Mass., USA) and allowed to attach for 24 h at 37°C under 5% CO_2. After this attachment period, 100 µl of drug solution (diluted in culture medium), were added to the wells, and cells were incubated for 72 h at 37°C under 5% CO_2. Subsequently, the cytotoxicity was determined using the SRB method as described previously (16). In the combination experiments elacridar (used as inhibitor of BCRP, however it is also known as a P-gp inhibitor) (17) was added 30 min prior to adding gimatecan or topotecan, to obtain a final concentration of 500 nM and 2 µM in the MDCKII and IGROV1/T8 cell lines, respectively. The concentration of elacridar was lower than that in the transport experiments (5 µM) to circumvent toxicity, but sufficient to inhibit BCRP- and P-gp-mediated transport. Each agent (and combination) was tested in quadruplicate in at least three independent experiments.

Transport across MDCKII and LLCPK monolayers

Transepithelial transport assays were performed in Costar transwell plates with 3-µm-pore membranes (Transwell 3414, Costar, Corning, NY) as described previously (18, 19). In brief, cells (MDCKII -WT, -Bcrp1, -MRP2, -MDR1, LLCPK -WT and -MDR1) were seeded at a density of 1 x 10^6 in 2 ml of complete medium. Cells were grown for three days and allowed to form tight monolayers, with medium replacement every day. Two hours before the start of the experiment, complete medium at both sides of the monolayer (apical and basolateral compartments) was replaced by 2.5 ml of (serum-free) Optimem medium (Life Technologies, Inc. Ltd., Paisley, Scotland) containing the appropriate concentration of transport modulator (5 µM zosuquidar to inhibit endogenous P-gp levels and/or 500 µM of pantoprazole or 5 µM of elacridar to inhibit endogenous P-gp and BCRP).

At t = 0, 2.5 mL of transport medium supplemented with zosuquidar (5 µM) and without (control) or with elacridar (5 µM) or pantoprazole (500 µM) were applied at both sides of the monolayers, whereas radiolabeled drug ([^{3}H]gimatecan (1 µM) or [^{14}C]topotecan (5 µM)) and radiolabeled inulin ([^{14}C]inulin or [^{3}H]inulin) (to check the integrity of the monolayer), were added to the apical or basal side of the monolayer in different wells.

After 1 and 4 hours samples of 500 µL were taken and the amount of [^{3}H]gimatecan or [^{14}C]topotecan appearing in the compartment (apical or basal) opposite to which the labeled drug was added, was measured by liquid scintillation counting (tri-Carb 2100 CA Liquid Scintillation Analyzer; Canberra Packard, Groningen, The Netherlands). Trans-epithelial transport of the drug and paracellular inulin flux through the monolayer was expressed as percentage of total radioactivity added at the beginning of the experiment. Inulin leakage was tolerated up to 2% of the total radioactivity over 4 hours.

Accumulation and Efflux studies

Intracellular accumulation and efflux of gimatecan were measured in MDCKII-WT and -Bcrp1 cell lines. Cells were seeded at a density of 1 x10^{6} in cell culturing plates (ø 4.8 cm, Costar Corning, NY) in 5 ml of complete medium and grown to about 80-90% confluence. Then plates were incubated for 30 min at 37^{o}C with 5 ml of complete medium buffered with HEPES (25 mM), adjusted to pH 7.0 and containing 0, 1, 1.5, 2 µM of [^{3}H]gimatecan. After incubation, cells were washed twice with ice-cold PBS, scraped immediately, collected in plastic tubes and centrifuged (2 min, 1300 rpm, 0^{o}C). Subsequently, the cells were resuspended in 1 ml of acetic acid 0.1%, to lyse the cells. Protein concentrations were determined using the Bio-Rad assay based on the Bradford method (20). The concentration of gimatecan in the samples was determined by scintillation counting. For efflux studies, MDCKII-WT and -Bcrp1 cells were loaded with 1.5 µM and 2 µM of [^{3}H]gimatecan, respectively, for 30 min at 37^{o}C to obtain approximately equal intracellular concentrations of the drug. After loading the cells, medium was removed and replaced by fresh medium. Directly after incubation and at several following time points intracellular concentrations of gimatecan were determined.
Efflux experiments were also performed in the presence of elacridar (5 µM). Accumulation and efflux of gimatecan were determined in at least three independent experiments.

Preparation of membrane vesicles and competition experiments

Inside-out membrane vesicles from Spodoptera frugiperda (Sf9) cells were prepared as described previously (18). Using Sf9- WT and -BCRP membrane vesicles, we evaluated the effect of gimatecan on the transport of 0.31 µM methotrexate (MTX), a well known BCRP substrate, in the presence of 4 mM ATP. Sf9-WT and -BCRP membrane vesicles were incubated with 0.31 µM [^{3}H]-MTX for 5 min at 37°C in the presence or absence of different concentrations (0.01, 0.1 and 2 µM) of gimatecan. The ATP-dependent transport is plotted as percentage of the control value. Of note, all the experiments were performed in absence and absence of ATP.

Statistical analysis

Statistical analysis was performed using Student's *t*-test (2-tailed, unpaired). Differences between 2 sets of data were considered statistically significant at $p < 0.05$.

Results

Reduced cytotoxicity of gimatecan by BCRP expression

A significant difference in IC_{50} of gimatecan was found between MDCKII-WT and -Bcrp1 cells, with a RI (resistance index) of 8.4 ($p < 0.005$). A significant difference in IC_{50} with a RI of 10.4 ($p < 0.005$) was also seen in the same assay using the IGROV1 and T8 cell lines, indicating that BCRP expression resulted in resistance to gimatecan. Topotecan was chosen as reference drug (9, 10). The RI of topotecan in MDCKII-Bcrp1 was 83 and in the T8 cell line 148, in line with previous publications (10), and substantially higher than the RI of gimatecan in these cell lines. In the applied cell lines gimatecan showed a markedly higher cytotoxicity than topotecan (Table 1).

To further demonstrate the role of BCRP/Bcrp1 in the resistance to gimatecan, the cytotoxicity assays were repeated in the presence of elacridar, an inhibitor of BCRP as well as of P-gp (6, 17). The cytotoxicity of gimatecan in the MDCKII-WT and IGROV1 was not significantly ($p > 0.05$) affected by co-incubation with a non-toxic dose of elacridar (500 nM and 2 µM, respectively). In contrast, co-incubation with elacridar resulted in a partial reversal of resistance of gimatecan in the MDCKII-Bcrp1 and T8 cell lines, yielding an IC_{50} ratio without/with elacridar of 6.5 and 3, respectively ($p < 0.05$, Table 1).

Table 1. Cytotoxicity of gimatecan in IGROV1, T8 and MDCKII cell lines ± elacridar

	IGROV1		T8		MDCKII-WT		MDCKII-Bcrp1		MDCKII-MDR1		MDCKII-MRP2	
	IC_{50} (nM)[a]	RI[b]	IC_{50} (nM)[a]	RI[b]	IC_{50} (nM)[a]	RI[b]	IC_{50} (nM)[a]	RI[b]	IC_{50} (nM)[a]	RI[b]	IC_{50} (nM)[a]	RI[b]
Topotecan	33 ± 5	NA	4867 ± 337	148*[c]	122 ± 11	NA	10135 ± 1736	83*[c]	251 ± 23	2*	122 ± 7	1*
Gimatecan	3 ± 1	NA	33 ± 4	10.4*[c]	8.6 ± 3.6	NA	72 ± 19	8.4*[c]	7 ± 4	0.8*	10 ± 4	1.2*
Topotecan + elacridar	42 ± 11	0.8[#]	152 ± 21	32[#c]	143 ± 43	0.85[#]	177 ± 19	57[#c]	NA	NA	NA	NA
Gimatecan + elacridar	3.8 ± 1.7	0.8[#]	10.9 ± 1	3[#c]	9.2 ± 2	0.9[#]	11 ± 0.5	6.5[#c]	NA	NA	NA	NA

[a] Assessed by SRB cytotoxicity assay after 72 h of drug exposure. Values are the mean ± SD of at least three experiments. [b] RI, resistance index: ratio between the IC_{50} values of the resistant and WT cell lines (*) or ratio between the IC_{50} values in absence and presence of elacridar ([#]). [c] Significant difference ($p < 0.05$). NA: Not Applicable.

Cytotoxicity of gimatecan is not affected by P-gp and MRP2

In contrast to the results obtained in BCRP/Bcrp1 over-expressing cells, no significant difference in IC_{50} of gimatecan was found between MDCKII-WT, -MDR1 and -MRP2 cell lines ($p > 0.05$, Table1).

Transport of gimatecan across MDCKII monolayers

Transport of gimatecan by Bcrp1 was studied in MDCKII-WT and -Bcrp1 cell monolayers. To exclude any contribution of P-gp, the P-gp inhibitor zosuquidar (LY335979, 5 μM) was added. An increased transport of gimatecan (1 μM) from the basolateral to the apical compartments (BA) compared with the transport from the apical to the basolateral compartments (AB) (i.e. active transport (BA/AB is 3.1 ± 0.46)) was observed in MDCKII-Bcrp1 compared to the WT cell line (BA/AB is 0.94 ± 0.08) (Fig. 1). Moreover, gimatecan transport was completely abolished in MDCKII-Bcrp1 monolayers in the presence of the BCRP/P-gp inhibitors elacridar (5 μM) or pantoprazole (500 μM) (6, 18, 21) (Fig. 1). Transwell experiments using topotecan as control drug have also been performed: the results were in line with previous publications (11) and showed active transport of topotecan (data not shown). The magnitude of topotecan transport was of the same order as of gimatecan. In contrast, no transport was found for gimatecan in transwell experiments performed with MDCKII-MRP2 and -MDR1, LLCPK-WT and -MDR1 monolayers (data not shown).

Accumulation and efflux of gimatecan in Bcrp1 overexpressing cell lines

To further elucidate the effect of BCRP/Bcrp1 overexpression on cellular transport of gimatecan we performed accumulation and efflux experiments in MDCKII-WT and -Bcrp1 cell lines. The accumulation and efflux of gimatecan could not be tested at concentrations higher than 2 μM due to limited drug solubility. Accumulation of gimatecan was approximately 1.5-fold reduced in the MDCKII-Bcrp1 compared with WT cell line (data not shown). In efflux studies, a significantly increased initial efflux rate of gimatecan was observed in the MDCKII-Bcrp1 cells (~90%) within 1 minute compared with WT cells (~30%) (Fig. 2). Co-incubation of the cells with elacridar (5 μM) completely restored the intracellular accumulation and efflux of gimatecan in MDCKII-Bcrp1 cells to the intracellular levels observed in the WT cell line. Efflux of gimatecan was not affected by co-incubation with elacridar in MDCKII-WT cells (Fig. 2).

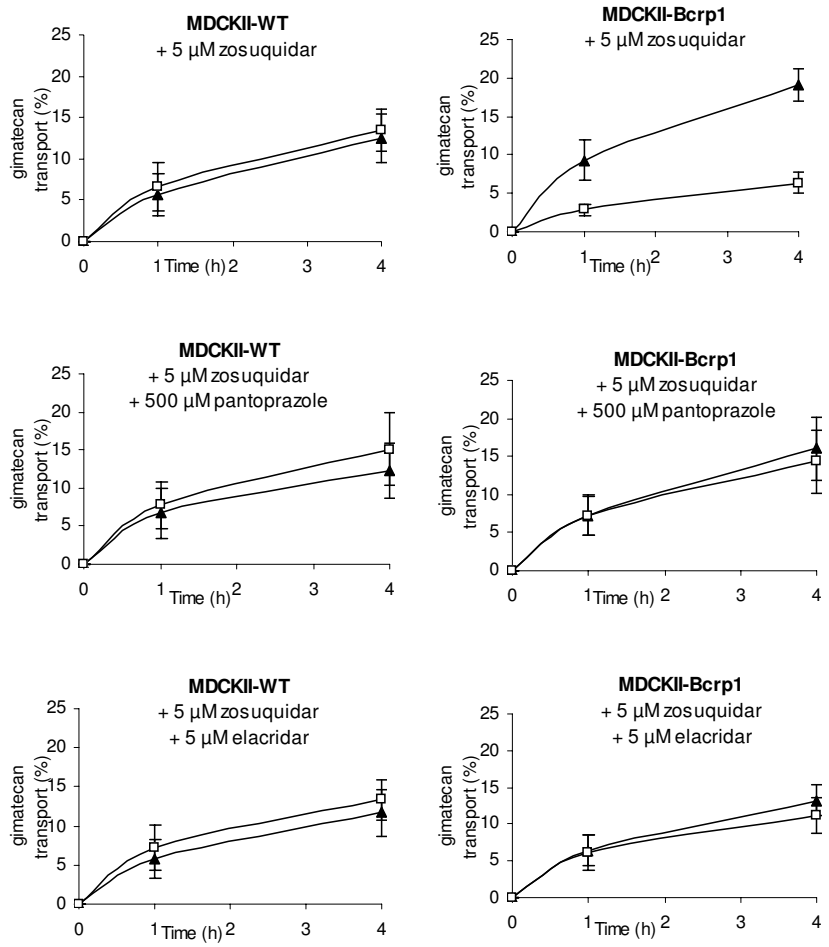

Figure 1. Transport of [^{3}H]gimatecan (1 µM) across MDCKII-WT and -Bcrp1 cell monolayers in absence or presence of pantoprazole (500 µM) or elacridar (5 µM). Active transport of gimatecan is evidenced by an overall increased appearance of the drug in the apical compartment, as a result of an increased transport from the basolateral to the apical compartment and, as a consequence, a reduced translocation of the drug from the apical to the basolateral compartment. (▲)Translocation from basal to apical compartments; (□) translocation from apical to basolateral compartments. Points are mean ± SD of at least three experiments.

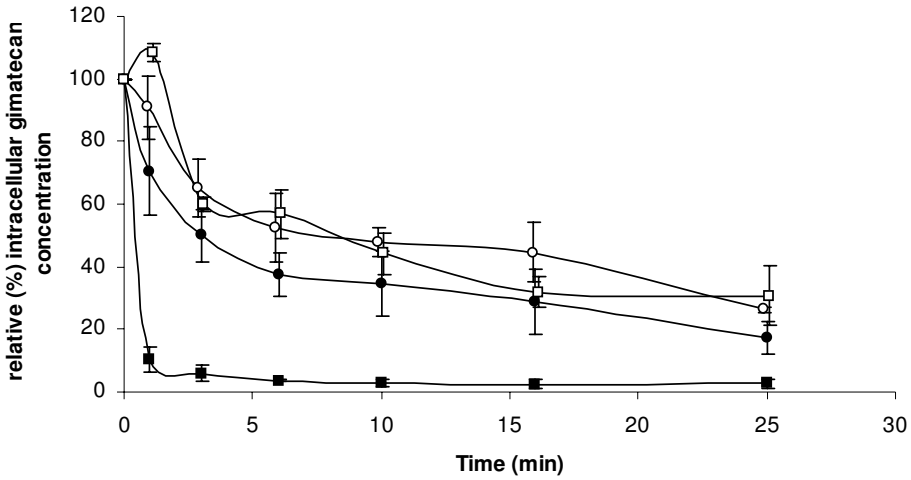

Figure 2. Efflux of gimatecan from MDCKII-WT (●) and -Bcrp1(■) overexpressing cells with (○,□ respectively) or without (●,■ respectively) 2 h pre-incubation with elacridar (5 μM). MDCKII-WT and -Bcrp1 cells were loaded for 30 min at 37°C with 1.5 and 2 μM [^{3}H]gimatecan respectively. Subsequently, efflux of gimatecan from the cells was determined. Data are means of three independent experiments; *bars*, SD.

Effect of gimatecan on BCRP-mediated MTX transport in Sf9 membrane vesicles

Using Sf9-BCRP and Sf9-WT membrane vesicles we studied the effect of different concentrations of gimatecan on the transport of 0.31 μM of [^{3}H]MTX. The ATP-dependent transport of MTX by human BCRP was inhibited by gimatecan in a concentration-dependent manner, demonstrating competition between gimatecan and MTX for BCRP-mediated transport (Fig. 3). Control experiments have been performed in Sf9-WT vesicles as well as in Sf9-BCRP and WT vesicles in the presence of pantoprazole, a competitive BCRP transport inhibitor; the results observed were in line with previous publications (18) and further supported the competition of gimatecan for BCRP- mediated transport of MTX (data not shown).

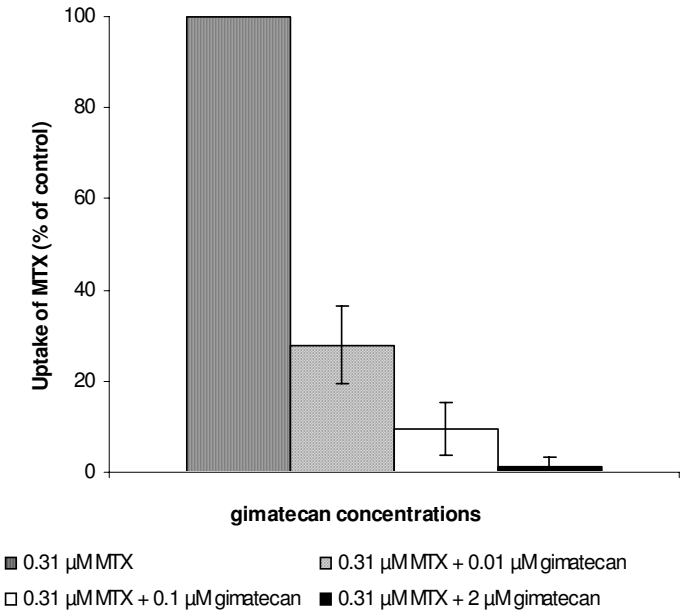

Figure 3. Effect of gimatecan on ATP-dependent transport of MTX by BCRP. Sf9-BCRP membrane vesicles were incubated with [^{3}H]MTX (0.31 µM) for 5 min at 37°C in the absence or presence of increasing concentrations of gimatecan (0, 0.1, 0.01, 2 µM). The ATP-dependent transport of MTX is plotted as percentage of the control value. *Columns*, means of three independent experiments; *bars*, SD.

Discussion

We tested the hypothesis that gimatecan is a substrate drug for BCRP/Bcrp1, P-gp and MRP2 *in vitro.* The first indication for affinity of BCRP/Bcrp1 for gimatecan was obtained in the cell survival studies using T8 and MDCKII-Bcrp1 cells. Compared with their parental counterparts the BCRP expressing cells showed 8.4-fold (T8) and 10.4-fold (MDCKII-Bcrp1) resistance to gimatecan. However, this resistance index is clearly lower than the resistance factor for topotecan of 148 in T8 and 83 in MDCKII-Bcrp1, respectively. Furthermore, co-incubation with a non-toxic concentration of elacridar resulted in a partial reversal of the resistance to gimatecan. This suggests that BCRP/Bcrp1 is involved in the resistance to gimatecan in the two cell systems.

Results obtained in the transport studies with MDCKII-Bcrp1 versus WT cells reveal that there is active Bcrp1-mediated transport of gimatecan. The magnitude of the difference in basolateral to apical (BA) versus apical to basolateral (AB) transport of gimatecan was in the order of topotecan, which was used as control substrate drug for BCRP. This shows that the difference in the level of resistance to gimatecan and topotecan

in the cell survival studies is not the same as the difference in the level of active transport in the MDCKII monolayer experiments. Further proof of active Bcrp1-mediated transport was obtained in the transport studies by co-incubation with elacridar or pantoprazole, which collapsed the B-A/A-B curves completely.

Similar experiments conducted with LLCPK-MDR1, MDCKII-MDR1 and MDCKII-MRP2 showed that MDR1 and MRP2 do not mediate transport of gimatecan at detectable levels. In addition, we determined the rate of efflux of gimatecan from loaded MDCKII-Bcrp1 and WT cells. The results support that Bcrp1 mediates the efflux of gimatecan: the Bcrp1 expressing cells extruded gimatecan significantly faster than the parental cells. Finally, we tested the affinity of gimatecan for human BCRP in competition experiments using Sf9-BCRP vesicles. We could not test gimatecan itself in transport experiments in vesicles, because gimatecan is a highly lipophilic drug. Consequently, it sticks to the applied filters in the assay. In competition experiments we tested the ability of gimatecan to compete with MTX for transport mediated by BCRP. Our results showed that gimatecan inhibited the ATP-mediated transport of MTX by BCRP in a concentration-dependent manner. Therefore, the applied *in vitro* assays revealed that BCRP is involved in resistance to and transport of gimatecan.

It is of interest that others have not found that gimatecan is transported by BCRP (8). However, in this previous study another cell system was employed, consisting of a human colon carcinoma cell line (HT29/MIT), selected by exposure of the parental (HT29) cell line to increasing concentrations of mitoxantrone, a well-known BCRP substrate. Although the selected HT29/MIT subline was checked for expression, along of BCRP, also of MDR1 and MRP1, expression of other ABC transporters and other mechanisms of resistance could have been induced as well. An overlap in substrate specificities between different ABC transporters induced by mitoxantrone may potentially have affected the reported resistance of the HT29/MIT cell line. For instance, MRP2 and MRP4 (not identified yet at the time that the previous experiments were performed) have recently been reported to transport mitoxantrone and several campthothecins (in particular topotecan, irinotecan and its metabolite SN38), respectively (22, 23). Moreover, in the previous studies, control experiments with BCRP inhibitors to reverse resistance and/or drug transport have not been performed. This is relevant considering that recently it has been reported that inhibition of BCRP was not able to restore mitoxantrone sensitivity in irinotecan-selected human leukemia CPT-K5 cells (24). These findings support the hypothesis that induction of other transporters or other mechanisms besides the up-regulation of BCRP may contribute to the multidrug resistance phenotype of resistant cell sublines selected by increased exposure to substrate drugs. In our experiments we used subclones of MDCKII cell stably transfected with the cDNA of Bcrp1, MDR1 and MRP2,

respectively, making the expression of other transporters unlikely. Moreover, we have performed control experiments employing elacridar and/or pantoprazole as BCRP inhibitors: in the cytotoxicity (applying MDCKII-Bcrp1 and T8 cells) and transwell (in MDCKII-Bcrp1 monolayers) assays the BCRP inhibitors (elacridar and pantoprazole) were able to reverse the resistance and transport of gimatecan, respectively.

Moreover, the parental cells in the earlier experiments (8) appear to be much less sensitive to gimatecan than those used in our study and this could explain why in the previous studies the overexpression of BCRP had relatively little effect. Another reason for the discrepancy between our results and the results of other authors can be that the expression level of BCRP in the cell systems used was different. This hypothesis is supported by the relatively higher resistance index of topotecan observed in our cytotoxicity experiments in Bcrp1/BCRP overexpressing cells (RI in MDCKII-Bcrp1 cells: 83; RI in T8 cells: 148) compared with the previous study (RI in HT29/MIT: 13.2) (8). A lower BCRP expression in the HT29/MIT cells compared with our cell systems may have contributed to the different results. Finally, the authors in the previous study did not explore the efflux kinetics, which might have shown a significant difference between the resistant and parental cells, nor have they studied transport in detail in monolayers of stably Bcrp1 overexpressing cells as the MDCKII cells that we developed and used.

In a subsequent article Croce et al. (9) evaluated accumulation and efflux of gimatecan from parental and BCRP overexpressing cells, but the experiments have been conducted at a high concentration (22 μM) that most likely have resulted in precipitation of the drug. Moreover, the authors did not mention at which pH the experiments where performed: this is relevant as the transport activity of BCRP has been recently reported to be affected by the pH (25). In our accumulation and efflux experiments the medium with drug solution used was buffered with HEPES and the pH was adjusted. Finally, as hypothesized also for the other previous studies, a difference in expression of BCRP between the cell systems employed may have also contributed to the discrepancy in results.

Conclusions

Our results reveal that *in vitro* gimatecan is a moderate substrate drug for mouse Bcrp1 as well as for human BCRP. The affinity for BCRP/Bcrp1 appears to be less than for topotecan that was used as control substrate drug.

Implications of BCRP expression in the gut for the oral development of gimatecan may be limited but need to be explored. The interaction between oral gimatecan and other BCRP substrate drugs and/or inhibitors warrants further clinical investigation.

References

1. Doyle LA, Yang W, Abruzzo LV, et al. A multidrug resistance transporter from human MCF-7 breast cancer cells. Proc Natl Acad Sci U S A 1998;95:15665-70.
2. Borst P, Oude Elferink R. Mammalian ABC Transporters in Health and Disease. Annu Rev Biochem 2002;71:537-93.
3. Kruh GD, Belinsky MG. The MRP family of drug efflux pumps. Oncogene 2003;22:7537-52.
4. Schinkel AH, Jonker JW. Mammalian drug efflux transporters of the ATP binding cassette (ABC) family: an overview. Adv Drug Deliv Rev 2003;55:3-29.
5. Breedveld P, Beijnen JH, Schellens JH. Use of P-glycoprotein and BCRP inhibitors to improve oral bioavailability and CNS penetration of anticancer drugs. Trends Pharmacol Sci 2006;27:17-24.
6. Maliepaard M, van Gastelen MA, Tohgo A, Hausheer FH, van Waardenburg RC, de Jong LA, Pluim D, Beijnen JH, Schellens JH. Circumvention of breast cancer resistance protein (BCRP)-mediated resistance to camptothecins in vitro using non-substrate drugs or the BCRP inhibitor GF120918. Clin Cancer Res 2001;7:935-41.
7. Mattern MR, Hofmann GA, Polsky RM, Funk LR, McCabe FL, Johnson RK. In vitro and in vivo effects of clinically important camptothecin analogues on multidrug-resistant cells. Oncol Res 1993;5:467-74.
8. Perego P, De Cesare M, De Isabella P, et al. A novel 7-modified camptothecin analog overcomes breast cancer resistance protein-associated resistance in a mitoxantrone-selected colon carcinoma cell line. Cancer Res 2001;61:6034-7.
9. Croce AC, Bottiroli G, Supino R, Favini R, Zuco V, Zunino F. Subcellular localization of the camptothecin analogues, topotecan and gimatecan. Biochem Pharmacol 2004;67:1035-45.
10. Maliepaard M, van Gastelen MA, de Jong LA, et al. Overexpression of the BCRP/MXR/ABCP gene in a topotecan-selected ovarian tumor cell line. Cancer Res 1999;59:4559-63.
11. Jonker JW, Smit JW, Brinkhuis RF, et al. Role of breast cancer resistance protein in the bioavailability and fetal penetration of topotecan. J Natl Cancer Inst 2000;92:1651-6.
12. Kruijtzer CM, Beijnen JH, Rosing H, et al. Increased oral bioavailability of topotecan in combination with the breast cancer resistance protein and P-glycoprotein inhibitor GF120918. J Clin Oncol 2002;20:2943-50.
13. Evers R, Kool M, van Deemter L, et al. Drug export activity of the human canalicular multispecific organic anion transporter in polarized kidney MDCK cells expressing cMOAT (MRP2) cDNA. J Clin Invest 1998;101:1310-9.
14. Schellens JH, Maliepaard M, Scheper RJ, et al. Transport of topoisomerase I inhibitors by the breast cancer resistance protein. Potential clinical implications. Ann N Y Acad Sci 2000;922:188-94.
15. Schinkel AH, Wagenaar E, van Deemter L, Mol CA, Borst P. Absence of the mdr1a P-Glycoprotein in mice affects tissue distribution and pharmacokinetics of dexamethasone, digoxin, and cyclosporin A. J Clin Invest 1995;96:1698-705.
16. Mistry P, Kelland LR, Abel G, Sidhal S, Harrap KR. The relationships between glutathione, glutathione-S-transferase and cytotoxicity of platinum drugs and melphalan in eight ovarian carcinoma cell lines. Br J Cancer 1991;64:215-220.
17. de Bruin M, Miyake K, Litman K, Robey R, Bates SE. Reversal of resistance by GF120918 in cell lines expressing the half-transporter, MXR. Cancer Lett 1999;146:117-26.
18. Breedveld P, Zelcer N, Pluim D, et al. Mechanism of the pharmacokinetic interaction between methotrexate and benzimidazoles: potential role for breast cancer resistance protein in clinical drug-drug interactions. Cancer Res 2004;64:5804-11.
19. Horio M, Chin KV, Currier SJ, et al. Transepithelial transport of drugs by the multidrug transporter in cultured Madin-Darby canine kidney cell epithelia. J Biol Chem 1989;264:14880-4.
20. Bradford MM. A rapid and sensitive method for the quantitation of microgram quantities of protein utilizing the principle of protein-dye binding. Anal Biochem 1976;72:248-54.
21. Pauli-Magnus C, Rekersbrink S, Klotz U, Fromm MF. Interaction of omeprazole, lansoprazole and pantoprazole with P-glycoprotein. Arch Pharmacol 2001;364:551-7.
22. Tian Q, Zhang J, Chan SY, et al. Topotecan is a substrate for multidrug resistance associated protein 4. Curr Drug Metab 2006;7:105-18.
23. Tian Q, Zhang J, Tan TM, et al. Human multidrug resistance associated protein 4 confers resistance to camptothecins. Pharm Res 2005;22:1837-53.
24. Su Y, Lee SH, Sinko PJ.Inhibition of efflux transporter ABCG2/BCRP does not restore mitoxantrone sensitivity in irinotecan-selected human leukemia CPT-K5 cells: evidence for multifactorial multidrug resistance. Eur J Pharm Sci 2006;29:102-10.

25. Breedveld P, Pluim D, Cipriani G, et al. The effect of low pH on breast cancer resistance protein (ABCG2)-mediated transport of methotrexate, 7-hydroxymethotrexate, methotrexate diglutamate, folic acid, mitoxantrone, topotecan, and resveratrol in in vitro drug transport models. Mol Pharmacol 2007;71:240-9.

CHAPTER 3.2

In vivo implications of BCRP/P-gp deletion on the pharmacokinetics of gimatecan (7-t-butoxyiminomethylcamptothecin)

Serena Marchetti, Roos L. Oostendorp, Dick Pluim, Olaf van Tellingen, Richard Versace, Jos H. Beijnen, Roberto Mazzanti, Jan H.M. Schellens

Submitted for publication

Abstract

We previously reported that the 7-t-butoxyiminomethyl substituted lipophilic camptothecin derivative gimatecan is a substrate for BCRP *in vitro.* In order to assess the potential *in vivo* implications of such transport, we tested the pharmacokinetics and tissue distribution of gimatecan in wild-type (WT) and Bcrp1/Mdr1a/1b$^{-/-}$ mice, and the effect of the co-administration of elacridar and pantoprazole, well known BCRP/P-gp inhibitors.

Oral and i.v. pharmacokinetics and tissue accumulation were studied in WT and in Bcrp1/Mdr1a/1b$^{-/-}$ mice, in presence or absence of pantoprazole or elacridar.

Systemic exposure to gimatecan after oral administration in Bcrp1/Mdr1a/1b$^{-/-}$ mice was 1.4-fold higher than in WT mice ($p < 0.01$). Elacridar significantly increased systemic exposure to oral gimatecan in WT, but also in Bcrp1/Mdr1a/1b$^{-/-}$ mice, whereas pantoprazole did not significantly affect the pharmacokinetics of gimatecan. Brain accumulation of gimatecan after i.v. administration was increased in Bcrp1/Mdr1a/1b$^{-/-}$ versus WT mice, whereas the concentration of the drug in the kidney was slightly reduced in Bcrp1/Mdr1a/1b$^{-/-}$ versus WT mice. In the other tissues examined (liver, lung, heart and spleen) the concentration of gimatecan was not significantly different in WT compared with knockout mice even when elacridar was co-administered.

In vivo, absence of Bcrp1/Mdr1a/1b resulted in increased systemic exposure to gimatecan and increased accumulation into the brain. The *in vivo* interaction between elacridar and gimatecan is partly mediated by other drug transporters than BCRP/Bcrp1.

Introduction

Gimatecan (ST1481; 7-[(E)-tert-butyloxyiminomethyl]-camptothecin) is a new oral camptothecin analogue selected for clinical development on the basis of a promising preclinical antitumor activity and a favorable pharmacological profile. Actually gimatecan is tested in clinical phase I/II and an orphan designation has recently been granted by the European Commission for gimatecan for the treatment of glioma (1).

Previously, we reported that gimatecan is transported *in vitro* by human BCRP (Breast Cancer Resistance Protein, ABCG2) and by the murine homologous Bcrp1 (Abcg2), but not by human P-gp (P-glycoprotein, MDR1, ABCB1) and MRP2 (Multidrug Resistance Protein 2, ABCC2) (2). BCRP, P-gp and MRP2 are ATP-binding cassette (ABC) drug efflux transporters originally involved in tumor resistance against anticancer drugs (3, 4). The localization of these transporters in tissues important for absorption (e.g., gut), metabolism and elimination (liver and kidney) of xenobiotics and in tissues involved in maintaining the barrier function of sanctuary sites (e.g., blood-brain barrier, blood-cerebral spinal fluid barrier, blood-testis barrier and the maternal-fetal barrier or placenta) suggests for these transporters a physiological protective role for the body against xenotoxins. Similarly, they are increasingly recognized for their ability to modulate the absorption, distribution, metabolism, excretion, and toxicity of substrate drugs (5).

The camptothecin derived topoisomerase I inhibitors have been reported as substrates for BCRP and P-gp, although their affinity for such transporters vary substantially between the different derivatives (6). In particular topotecan, irinotecan and its active metabolite SN38 have high affinity for BCRP and moderate affinity for P-gp (7, 8). BCRP expression/activity has been shown to affect the bioavailability after oral administration and the brain penetration of topotecan (8-11) and genotype variants of BCRP have recently been suggested to affect the pharmacokinetics of topotecan (12, 13).

Although it has been suggested that the 7-substituted camptothecin derivatives (i.e., lurtotecan and exatecan mesylate), have less affinity for BCRP than other analogues (6), we previously demonstrated that gimatecan (7-[(E)-tert-butyloxyiminomethyl]-camptothecin) is transported *in vitro* by BCRP (2). In order to test the potential *in vivo* implications of such transport for the clinical development of the drug, we evaluated the pharmacokinetics and the tissue distribution of gimatecan in WT and in Bcrp1/Mdr1a/1b$^{-/-}$ mice, obtained by cross breading of the Bcrp1$^{-/-}$ (BCRP knockout) (14) and Mdr1a/1b$^{-/-}$ (P-gp knockout) mice (15). Although in our previous *in vitro* experiments no transport of gimatecan by MDR1 was detected, we chose this triple knockout mouse model in order to exclude any potential effect of P-gp, also because some camptothecin derived top I

inhibitors have low affinity for P-gp (6). Moreover, we used elacridar and pantoprazole as BCRP/P-gp inhibitors (16-19).

Affinity of gimatecan for BCRP could be clinically relevant as, similar to the camptothecin analogue topotecan (10, 20, 21), the oral bioavailability and the brain penetration of the drug might be significantly affected by BCRP. Moreover, clinically relevant drug-drug interactions with other BCRP substrate drugs and/or inhibitors may take place.

Materials and Methods

Chemicals and reagents

Gimatecan (STI1481; LBQ707) and [^{3}H]gimatecan (40 μCi/mg) were provided by Novartis Pharmaceuticals Inc. (East Hanover, NJ). Pantoprazole (Pantozol® 40 mg, Altana Pharma, Zwanenburg, The Netherlands) was obtained from the pharmacy of the Netherlands Cancer Institute. Elacridar (GF120918) was kindly provided by GSK (Research Triangle Park, NC).

Animals

Animals used in this study were female WT and Bcrp1/Mdr1a/1b$^{-/-}$ mice, all with a > 99% FVB genetic background between 10 and 14 weeks of age. Mice were housed and handled according to institutional guidelines complying with Dutch legislation. Animals were kept in a temperature-controlled environment with a 12-hours light/12-hours dark cycle and received a standard diet (AM-II; Hope Farms, Woerden, the Netherlands) and acidified water *ad libitum*.

Drug preparation, administration and plasma analysis

For intravenous (i.v.) administration, gimatecan was dissolved in DMSO (2 mg/ml). For oral (p.o.) administration, gimatecan was dissolved in a microemulsion solution, provided by Novartis Pharmaceuticals Inc. (East Hanover, NJ) at 0.5 mg/ml. The microemulsion was stored in the darkness at 0^{o}C and equilibrated before use for at least 1 h at room temperature in the darkness. Elacridar was suspended at 10 mg/ml in a mixture of hydroxypropylmethylcellulose (10 g/L)/2% Tween 80/H_2O (0.5:1:98.5 [v/v/v] for p.o. administration. A vial of pantoprazole (Pantozol® 40 mg) was diluted with NaCl 0.9% to a final concentration of 4 mg/ml for p.o. administration. WT and Bcrp1/Mdr1a/1b$^{-/-}$ mice received gimatecan either by i.v. (in the tail vein) or p.o. administration at a dose of 2 mg/kg with or without co-administration of one oral dose of elacridar (25 mg/kg) 2 h and 20 min before i.v. and p.o. gimatecan, respectively, or pantoprazole (40 mg/kg) 30 min

before i.v. and p.o. gimatecan. The 25 mg/kg oral dose of elacridar was applied in these studies because in previous experiments it was sufficient to efficiently block BCRP at the intestinal level. To minimize variation in absorption, mice were fasted for 4 h before gimatecan was administered orally. Multiple blood samples (~30 µl each) were collected from the tail vein at 5 min and at 0.5, 2, 4, 8, 24 and 48 h after i.v. administration, or at 0.5, 1, 2, 4, 8, 24 and 48 h after p.o. administration of gimatecan using heparinized capillary tubes (Oxford Labware, St. Louis, MO). The plasma fraction of the blood samples was collected after centrifugation at 3,000 x *g* for 10 min at 4°C, and stored at -20°C until analysis according to a validated high performance liquid chromatography (HPLC) method as described below.

Tissue distribution of gimatecan

To study the impact of Bcrp1 on the tissue distribution of gimatecan, WT and Bcrp1/Mdr1a/1b$^{-/-}$ mice were injected i.v. with 2 mg/kg of gimatecan +/- pretreatment (2 h in advance) with one dose of oral elacridar (100 mg/kg). At 1, 4, 8 h after gimatecan injection animals were anaesthetized with methoxyflurane, their blood was collected by cardiac puncture, they were sacrificed by cervical dislocation and several tissues (brain, liver, kidneys, lungs, spleen, heart) were removed and homogenized in 1% bovine serum albumine by a polytron PT1200 (kinematica AG, Littau, Switzerland). Plasma and tissue homogenates were stored at -20°C until HPLC analysis. All samples were processed and measured in the darkness due to the high light sensitivity of the drug.

HPLC analysis

Amounts of gimatecan, as the ring-open carboxylate form, were determined in small mouse plasma and tissue samples by using an HPLC fluorimetric method. The HPLC system consisted of a model 300 isocratic pump (Gyncotek 300c, Germering, Germany), a Basic Marathon autosampler (Spark, The Netherlands), provided with a 50 µl sample loop and a Model FP-920 fluorescence detector (Jasco, Hachioju City, Japan) operating at excitation and emission wavelengths of 380 and 527 nm, respectively. Chromatographic separations were carried out using a narrow bore stainless steel column (2.1 x 150 mm I.D.) packed with 3.5 µm Symmetry C_{18} material (Waters, Milford, MA, USA). The mobile phase consisted of acetonitrile-50 mM ammonium acetate buffer pH 6.8 (30:70, v/v) and the flow rate was set at 0.2 ml/min. Chromatographic data acquisition and reprocessing was performed using Chromeleon version 6.60 (Dionex Corp. Sunnyvale, CA, USA). Volumes of 50 µl of calibration and quality control samples in human plasma sample or 5 to 20 µl of mouse plasma sample supplemented with blank human plasma to a total volume of 100 µl

were vortexed with 200 µl of methanol. After centrifugation (14000 rpm, 5 min, 4°C), 200 µl of supernatant was mixed with 300 µl 0.01 M Borax (di-Natriumtetraborat-decahydrat, Merck) solution with complete conversion of gimatecan in its hydroxyl-acid form. The samples were vortexed and centrifuged again (14000 rpm, 5 min, 4°C) and 100 µl of the clear solution was injected into the HPLC system. Calibration samples ranged from 2 to 2000 ng/ml and were prepared in drug free human plasma. Quality Control samples containing 2, 10 and 1000 ng/ml prepared in blank human plasma showed that the accuracy and precision were within the acceptable ranges of 85% to 115% and ± 15%, respectively.

Pharmacokinetic and statistical analysis

Pharmacokinetic parameters of gimatecan were calculated by the noncompartmental trapezoidal method using WinNonlin Professional (version 5.0, Pharsight, Mountain View, CA, USA). The pharmacokinetic parameters of gimatecan were determined as follows:
$AUC_{0\text{-}24}$ as area under the curve (AUC) from time 0 up to 24 h (ng*h/ml), using the linear trapezoidal rule, $AUC_{0\text{-}inf}$ as AUC from time 0 extrapolated to infinity (ng*h/ml).
The apparent oral bioavailability (F) was calculated by the following formula: $F = AUC_{oral} / AUC_{iv} \times 100\%$. Statistical analysis was performed using Student's *t*-test (2-tailed, unpaired). Differences between 2 sets of data were considered statistically significant at $p < 0.05$.

Results

***In vivo* plasma pharmacokinetics of gimatecan in WT and Bcrp1/Mdr1a/1b$^{-/-}$ mice**

To assess whether the *in vitro* observed BCRP mediated transport of gimatecan is also relevant *in vivo*, we tested the oral uptake of gimatecan in WT and Bcrp1/Mdr1a/1b$^{-/-}$ mice. At a dose of 2 mg/kg, the $AUC_{0\text{-}inf}$ of gimatecan after p.o. administration was 1.4-fold higher in Bcrp1/Mdr1a/1b$^{-/-}$ compared with WT mice ($p < 0.01$; Table 1; Fig. 1A). The $AUC_{0\text{-}inf}$ of gimatecan after i.v. administration was not significantly different (1.03-fold) in Bcrp1/Mdr1a/1b$^{-/-}$ *versus* WT mice ($p > 0.05$; Table 1; Fig. 1B). Considering the high contribution of the extrapolated area to the $AUC_{0\text{-}inf}$ observed in several mice treated we calculated also the $AUC_{0\text{-}24h}$ using the linear trapezoidal rule, obtaining however analogous results. The calculated apparent oral availability was 48 ± 4.4% and 35 ± 2.9% for Bcrp1/Mdr1a/1b$^{-/-}$ and WT mice respectively, i.e. moderately but significantly ($p < 0.05$) increased in Bcrp1/Mdr1a/1b$^{-/-}$ mice. Also the mean (± SD) maximum plasma concentration (C_{max}) of gimatecan after p.o. administration was significantly higher in Bcrp1/Mdr1a/1b$^{-/-}$ compared with WT mice (368 ± 173 vs. 205 ± 80 ng/ml; $p < 0.05$), but not after i.v. administration (1323 ± 145 vs 1178 ± 137 ng/ml, $p > 0.05$).

Table 1. Pharmacokinetic parameters of gimatecan after p.o. and i.v. administration in WT and Bcrp1/Mdr1a/1b$^{-/-}$ mice ± pantoprazole or elacridar.

	p.o. administration			i.v. administration	
	$AUC_{0\text{-}24h}$[a] (ng*h/ml)	$AUC_{0\text{-}inf}$[b] (ng*h/ml)		$AUC_{0\text{-}24h}$[a] (ng*h/ml)	$AUC_{0\text{-}inf}$[b] (ng*h/ml)
WT[c]	2042 ± 464	2583 ± 405	*, #	7207 ± 1004	7346 ± 1018
WT[c]+pantoprazole	2556 ± 565	3087 ± 649		10172 ± 5171	10657 ± 5458
WT[c]+elacridar	3541 ± 1179	4714 ± 961		13155 ± 2477	13683 ± 2520
TKO[d]	3011 ± 608	3648 ± 464		7462 ± 1417	7599 ± 1420
TKO[d]+pantoprazole	2804 ± 854	3425 ± 903		9249 ± 1520	9469 ± 1512
TKO[d]+elacridar	4154 ± 343	5862 ± 836	$	16715 ± 3973	16890 ± 3935

[a] Area under the concentration-time curve from 0 to 24 h. [b] Area under the concentration-time curve from 0 to infinity. [c] WT: wild-type mice. [d]TKO: Bcrp1/Mdr1a/1b$^{-/-}$(triple knockout) mice. * $p < 0.01$ WT vs. WT + elacridar. # $p < 0.01$ WT vs. TKO. $ $p < 0.01$ TKO vs. TKO + elacridar. Data are presented as mean ± SD.

Effect of elacridar or pantoprazole on the plasma pharmacokinetics of gimatecan in WT and Bcrp1/Mdr1a/1b$^{-/-}$ mice

We administered an oral or i.v. dose of gimatecan (2 mg/kg) to WT and Bcrp1/Mdr1a/1b$^{-/-}$ mice pretreated with p.o. elacridar (25 mg/kg) or pantoprazole (40 mg/kg). As shown in table 1 co-administration of elacridar increased the $AUC_{0\text{-}inf}$ p.o. and the $AUC_{0\text{-}inf}$ i.v. 1.8- and 1.9-fold, respectively, in WT and 1.6- and 2.2-fold, respectively, in Bcrp1/Mdr1a/1b$^{-/-}$ mice ($p < 0.001$). The pharmacokinetic data of $AUC_{0\text{-}24}$ showed the same pattern as the $AUC_{0\text{-}inf}$ (Table 1). These results suggest that co-administration of elacridar significantly affects the pharmacokinetics of p.o. and i.v. gimatecan, which could in part take place by inhibition of BCRP and P-gp activity. However, the additional effect of elacridar on the $AUC_{0\text{-}inf}$ of gimatecan observed in Bcrp1/Mdr1a/1b$^{-/-}$ mice after p.o. and i.v. administration indicates that other mechanisms, such as interaction with other drug transporters or drug metabolizing enzymes by which elacridar could influence gimatecan absorption and disposition are involved. In contrast, p.o. pantoprazole at the applied dosage (40 mg/kg) in this animal model did not significantly affect the p.o. and i.v. pharmacokinetics of gimatecan (Table 1).

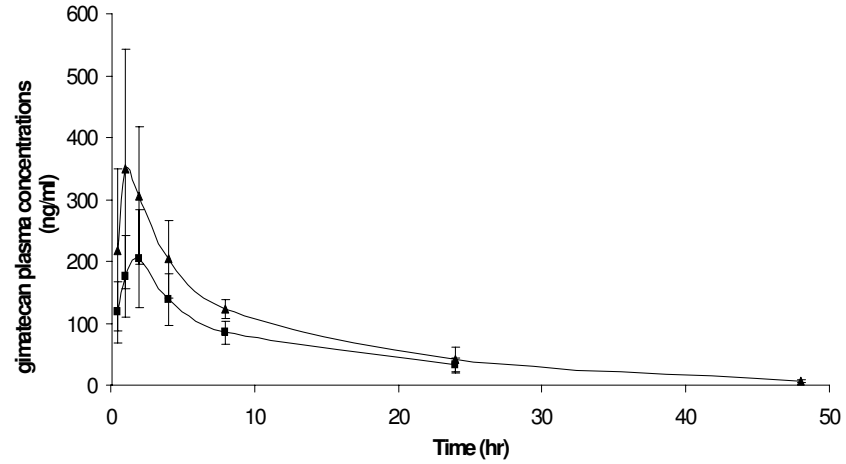

A

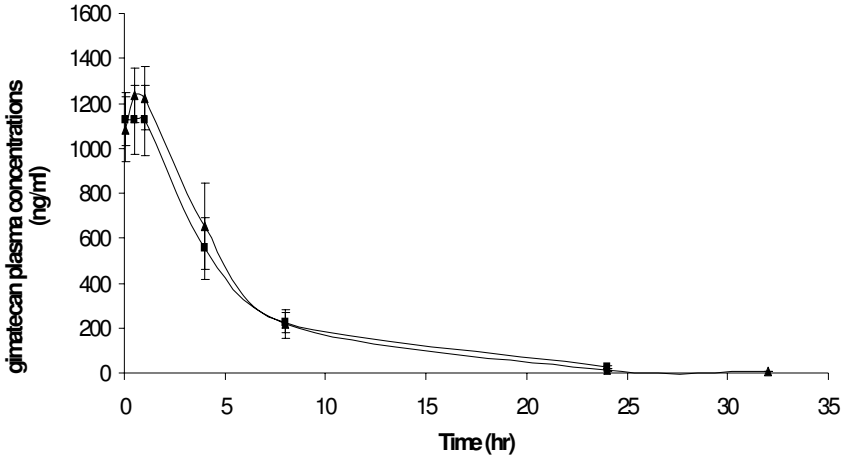

B

Figure 1. Plasma concentration time curves in WT(■) and Bcrp1/Mdr1a/1b$^{-/-}$ (▲) mice after oral (A) and i.v. (B) administration of gimatecan (2 mg/kg). At least 6 mice for each group were used. Points mean concentrations for oral and i.v. administration ($n \geq 6$) ± SD.

Brain penetration of gimatecan in Bcrp1/Mdr1a/1b$^{-/-}$ and WT mice and effect of elacridar

The CNS penetration of i.v. gimatecan was calculated by determining the absolute gimatecan brain concentration (ng/g tissue) at t = 1, 4 and 8 h after administration and the gimatecan brain concentration relative to the plasma gimatecan concentration at the same

time points. As shown in figure 2, the brain concentrations after i.v. gimatecan (absolute and corrected for plasma values) in Bcrp1/Mdr1a/1b$^{-/-}$ were significantly increased compared with WT mice ($p < 0.05$). To further evaluate the effect of a P-gp and BCRP inhibitor on the brain penetration of gimatecan, WT and Bcrp1/Mdr1a/1b$^{-/-}$ mice were treated with p.o. elacridar (100 mg/kg) 2 h before an i.v. dose of gimatecan (2 mg/kg). Co-administration of elacridar in WT mice significantly increased the absolute brain concentration of gimatecan after t = 4 and 8 h ($p < 0.05$; Fig. 2A Brain). However, when corrected for the plasma concentrations, the brain penetration of gimatecan was not significantly different in WT mice in presence or absence of elacridar ($p > 0.05$; Fig. 2B Brain), suggesting that the increased brain penetration at t = 4 and 8 h is a reflection of the higher gimatecan plasma levels. Also, no significant additional effect of elacridar was found on brain accumulation of gimatecan in Bcrp1/Mdr1a/1b$^{-/-}$ mice.

Brain

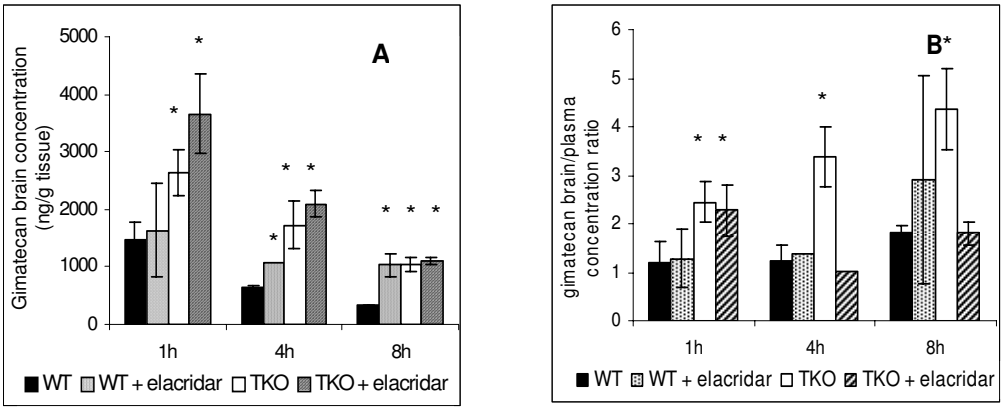

A

Kidney

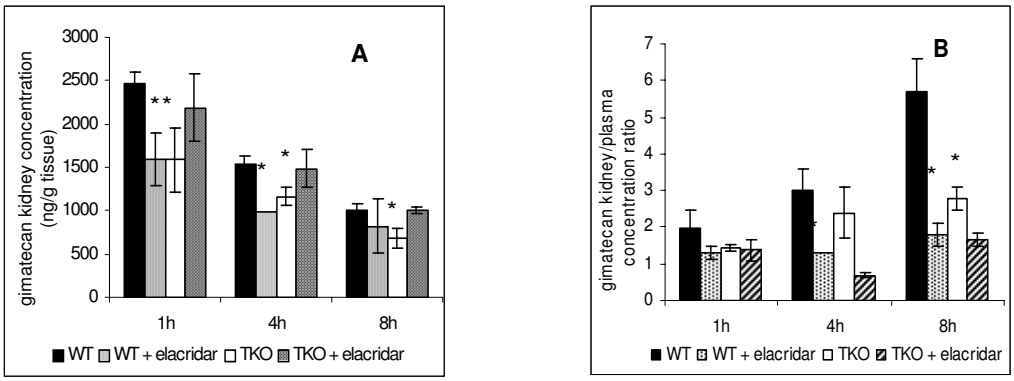

B

Figure 2. Gimatecan brain and kidney penetration in WT and Bcrp1/Mdr1a/Mdr1b$^{-/-}$ mice ± pre-treatment with elacridar. Elacridar (100 mg/kg) was given orally 2 h before i.v. gimatecan. At t = 1, 4 and 8 h blood, brain and kidneys were collected and concentrations of gimatecan were measured by HPLC. Results are expressed as the absolute amount of gimatecan (ng) detected per g tissue (BRAIN A and KIDNEY A) and as the tissue to plasma concentration ratio (BRAIN B and KIDNEY B) at t = 1, 4 and 8 h. Values shown are the means (columns) of 3 mice per group ± SD (bars), with the exception of few groups represented as columns (mean of two mice) without SD. *, $p < 0.05$ compared with WT mice.

Accumulation in other tissues

The distribution of i.v. gimatecan in mice to other tissues than brain was evaluated also. In the kidneys, at 1, 4 and 8 h after administration of i.v. gimatecan, absolute gimatecan concentrations were significantly reduced in Bcrp1/Mdr1a/1b$^{-/-}$ mice compared with WT mice ($p < 0.05$) (Fig. 2A Kidney). However, when corrected for the plasma concentration at t = 1 and 4 h, the accumulation of gimatecan in kidneys was not significantly different between Bcrp1/Mdr1a/1b$^{-/-}$ and control mice, suggesting that the kidney distribution at 1 and 4 h is a reflection of the elevated gimatecan plasma levels. In contrast, when corrected for the plasma concentration at t = 8 h after gimatecan administration the accumulation of gimatecan in the kidneys is reduced by ~2-fold in Bcrp1/Mdr1a/1b$^{-/-}$ compared with control mice ($p < 0.01$) (Fig. 2B Kidney). In addition, co-administration of elacridar in WT mice

lead to a significant reduction of the absolute concentration of gimatecan in kidneys to the level observed in Bcrp1/Mdr1a/1b$^{-/-}$ mice ($p > 0.05$ WT treated with elacridar versus Bcrp1/Mdr1a/1b$^{-/-}$ mice) (Fig. 2A Kidney). Similar results were obtained when absolute concentrations of gimatecan in the kidney were corrected for plasma levels at t = 4 and 8 h after i.v. administration (Fig. 2B Kidney). In the other tissues examined (liver, lung, heart and spleen) the absolute concentration of gimatecan was not significantly different in Bcrp1/Mdr1a/1b$^{-/-}$ compared with WT mice even when elacridar was co-administered (data not shown). However, after correction for the plasma concentration at t = 4 and 8 h after i.v. administration, we found that when elacridar was co-administered the accumulation of gimatecan was significantly reduced in all these organs of Bcrp1/Mdr1a/1b$^{-/-}$ and WT mice compared with control (WT and Bcrp1/Mdr1a/1b$^{-/-}$) mice treated with gimatecan alone (data not shown). Overall these results indicate that absence of Bcrp1 and P-gp increased the brain penetration of gimatecan whereas these drug transporters appear to slightly affect the distribution of gimatecan in the kidney. Furthermore, the impact of elacridar on the tissue distribution of gimatecan observed in knockout mice suggests the involvement of other drug transporters, besides BCRP and P-gp.

Discussion

We evaluated whether the absence of BCRP/Bcrp1 may affect the pharmacokinetics and the tissue distribution of gimatecan *in vivo*, employing WT and Bcrp1/Mdr1a/1b$^{-/-}$ mice. We chose the Bcrp1/Mdr1a/1b$^{-/-}$ (triple knockout) mouse model in order to exclude any potential effect of P-gp, also because some camptothecin derived top I inhibitors have low affinity for P-gp (6). No data are currently available on the affinity of gimatecan for mouse Mdr1a/Mdr1b; however, the results previously obtained by us and other authors with human MDR1 over-expressing cell lines support the evidence of a lack of affinity of gimatecan for MDR1 (2, 22). Therefore, the transport of gimatecan by murine Mdr1a/1b is unlikely and we believe that the effect of Mdr1a/1b gene deletion on gimatecan pharmacokinetics is negligible.

Results obtained after oral administration revealed a statistically significant effect of the absence of Bcrp1/Mdr1a/Mdr1b on the $AUC_{0\text{-}inf}$ as well as on the C_{max} of gimatecan. Considering the high contribution of the extrapolated area to the $AUC_{0\text{-}inf}$ observed in several mice treated we calculated also the $AUC_{0\text{-}24h}$ using the linear trapezoidal rule, which however did not lead to different results.

As expected, after i.v. administration no statistically significant difference was found between the curves of gimatecan in Bcrp1/Mdr1a/1b$^{-/-}$ versus WT mice. The apparent bioavailability of gimatecan in WT mice was 35 ± 2.9% and in Bcrp1/Mdr1a/1b$^{-/-}$ mice 48

± 4.4%, which difference is statistically significant ($p < 0.05$) and indicates that BCRP expressed in the gut limits oral uptake of gimatecan. In addition, deletion of Bcrp1 and Mdr1a/1b in mice resulted in significantly increased brain accumulation of gimatecan after i.v. administration compared with WT mice, thus suggesting that BCRP also limits the brain penetration of the drug.

In other experiments we tested the pharmacokinetics of p.o. and i.v. gimatecan when a P-gp and BCRP inhibitor (pantoprazole (6, 16, 17, 19) was co-administered. The results revealed that pre-treatment with 40 mg/kg pantoprazole did not affect the pharmacokinetics of oral neither i.v. gimatecan in this mouse model. The lack of the pharmacokinetic interaction between pantoprazole (which was applied at a high dose-level in our experiments) and gimatecan indicates that a clinical interaction between these two drugs is unlikely. In contrast, co-administration of elacridar significantly increased the $AUC_{0\text{-inf}}$ after oral and i.v. administration of the drug in WT as well as in the triple knockout mice. The additional effect on the AUC observed for elacridar in Bcrp1/Mdr1a/1b$^{-/-}$ mice suggests that besides BCRP/P-gp inhibition other mechanisms (such as interaction with other drug transporters or drug metabolizing enzymes) may contribute to this gimatecan-elacridar interaction and further experiments are warranted. Indeed, results obtained by Lee et al. suggested that elacridar most likely inhibits one or more transporters distinct from BCRP/P-gp (23) and in *in vitro* experiments, recently we found that elacridar inhibits efficiently the transport mediated by organic anion-transporting polypeptide 1B1 (OATP1B1) and organic cation transporter 1 (OCT1) (data submitted). In other *in vitro* experiments, we found also that gimatecan is a substrate for OATP1B1 (data submitted), whereas currently, no data are available regarding the affinity of gimatecan for OCT1 and other drug efflux transporters. The affinity of gimatecan for OATP1B1 may be clinically relevant, considering that lately Nozawa et al. demonstrated that OATP1B1 transports SN-38, the active metabolite of the camptothecin irinotecan (24) and OATP1B1-polymorphisms have been reported to affect irinotecan-pharmacokinetics and clinical outcome of cancer patients (25). In contrast, the lack of significant effect of elacridar on the brain penetration of gimatecan in WT and Bcrp1/Mdr1a/1b$^{-/-}$ mice might be explained, at least in part, by the expression at the blood brain barrier, besides P-gp/BCRP, of other transporters involved in gimatecan brain penetration and not inhibited by elacridar. Such transporters might counteract the activity of Bcrp1/P-gp. Indeed, it has been recently reported that in vitro gimatecan is a relatively modest and a good substrate for MRP1 and MRP4, respectively, two drug efflux transporters expressed at the blood brain barrier and potentially able to affect the brain penetration of substrate drugs (26). Leggas M et al. recently reported enhanced accumulation after i.v. administration of topotecan in brain tissue and cerebrospinal fluid of Mrp4$^{-/-}$ compared with Mrp4$^{+/+}$ mice (27). No data are

currently available about the effect of elacridar on MRP4 activity, whereas elacridar was not able to inhibit MRP1 and MRP2 in several in vitro experiments (16). Furthermore, in the evaluation of our results, it cannot be excluded that as a consequence of P-gp and Bcrp1 gene deletion other transporters and/or drug metabolizing enzymes involved in absorption, metabolism, distribution and elimination of gimatecan are over-expressed in knockout mice thus reducing the impact of Bcrp1/P-gp deletion on gimatecan pharmacokinetics. Moreover, potential species differences in expression and localization of transporters should be taken into account in extrapolating our results from animal models to the human situation. Clearly, our results obtained in the mouse model need to be confirmed in the clinic.

Conclusions

In mice absence of Bcrp1/Mdr1a/1b significantly affected the oral pharmacokinetics and the brain penetration of gimatecan, but had little effect on the i.v. pharmacokinetics. This means that most likely only the plasma pharmacokinetics of oral gimatecan is affected by endogenous epithelial BCRP in humans. Implications of BCRP expression in the gut for the oral development of gimatecan may be limited but need to be explored. Furthermore, a clinically relevant pharmacokinetic interaction between gimatecan and benzimidazole proton pump inhibitors is unlikely. In contrast, the *in vivo* interaction between elacridar and gimatecan appears to be partly mediated by other drug transporters than BCRP/Bcrp1. The increased CNS accumulation of gimatecan observed by concomitant administration of elacridar might be of therapeutic benefit in patients with primary CNS tumors and it is of interest to investigate that concept. Further clinical investigations about the interaction between oral gimatecan and other BCRP substrate drugs and/or inhibitors are warranted.

References

1. EMEA/COMP 1536/03 Rev 1. Public summary of positive Opinion for orphan designation of gimatecan for the treatment of glioma. CHMP, London 22 February 2007.
2. Marchetti S, Oostendorp RL, Pluim D, et al. In vitro transport of gimatecan (7-t-butoxyiminomethylcamptothecin) by breast cancer resistance protein, P-glycoprotein, and multidrug resistance protein 2. Mol Cancer Ther 2007;6:3307-3313.
3. Borst P, and Oude Elferink R. Mammalian ABC Transporters in Health and Disease. Annu Rev Biochem 2002;71:537-593.
4. Kruh GD, and Belinsky MG. The MRP family of drug efflux pumps. Oncogene 2003;22:7537-7552.
5. Schinkel AH, and Jonker JW. Mammalian drug efflux transporters of the ATP binding cassette (ABC) family: an overview. Adv Drug Deliv Rev 2003;55:3-29.
6. Maliepaard M, van Gastelen MA, Tohgo A, et al. Circumvention of breast cancer resistance protein (BCRP)-mediated resistance to camptothecins in vitro using non-substrate drugs or the BCRP inhibitor GF120918. Clin Cancer Res 2001;7:935-941.
7. Maliepaard M, van Gastelen MA, de Jong LA, et al. Overexpression of the BCRP/MXR/ABCP gene in a topotecan-selected ovarian tumor cell line. Cancer Res 1999;59:4559-4563.
8. Schellens JH, Maliepaard M, Scheper RJ, et al. Transport of topoisomerase I inhibitors by the breast cancer resistance protein. Potential clinical implications. Ann N Y Acad Sci 2000;922:188-194.

9. Jonker JW, Smit JW, Brinkhuis RF, et al. Role of breast cancer resistance protein in the bioavailability and fetal penetration of topotecan. J Natl Cancer Inst 2000;92:1651-1656.
10. Kruijtzer CM, Beijnen JH, Rosing H, et al. Increased oral bioavailability of topotecan in combination with the breast cancer resistance protein and P-glycoprotein inhibitor GF120918. J Clin Oncol 2002;20:2943-2950.
11. de Vries NA, Zhao J, Kroon E, et al. P-glycoprotein and breast cancer resistance protein: two dominant transporters working together in limiting the brain penetration of topotecan. Clin Cancer Res 2007;13:6440-6449.
12. Sparreboom A, Loos WJ, Burger H, et al. Effect of ABCG2 genotype on the oral bioavailability of topotecan. Cancer Biol Ther 2005;4:650-658.
13. de Jong FA, Marsh S, Mathijssen RH, et al. ABCG2 pharmacogenetics: ethnic differences in allele frequency and assessment of influence on irinotecan disposition. Clin Cancer Res 2004;10:5889-5894.
14. van Herwaarden AE, Jonker JW, Wagenaar E, et al. The breast cancer resistance protein (Bcrp1/Abcg2) restricts exposure to the dietary carcinogen 2-amino-1-methyl-6-phenylimidazo[4,5-b]pyridine. Cancer Res 2003;63:6447-6452.
15. Schinkel AH, Smit JJ, van Tellingen O, et al. Disruption of the mouse mdr1a P-glycoprotein gene leads to a deficiency in the blood-brain barrier and to increased sensitivity to drugs. Cell 1994;77:491-502.
16. Evers R, Kool M, Smith AJ, van Deemter L, de Haas M, and Borst P (2000) Inhibitory effect of the reversal agents V-104, GF120918 and Pluronic L61 on MDR1 Pgp-, MRP1- and MRP2-mediated transport. Br J Cancer 83:366-374.
17. Breedveld P, Zelcer N, Pluim D, et al. Mechanism of the pharmacokinetic interaction between methotrexate and benzimidazoles: potential role for breast cancer resistance protein in clinical drug-drug interactions. Cancer Res 2004;64:5804-5811.
18. de Bruin M, Miyake K, Litman K, et al. Reversal of resistance by GF120918 in cell lines expressing the half-transporter, MXR. Cancer Lett 1999;146:117-126.
19. Pauli-Magnus C, Rekersbrink S, Klotz U, and Fromm MF. Interaction of omeprazole, lansoprazole and pantoprazole with P-glycoprotein. Arch Pharmacol 2001;364:551-557.
20. Kuppens IE, Breedveld P, Beijnen JH, and Schellens JH. Modulation of oral drug bioavailability: from preclinical mechanism to therapeutic application. Cancer Invest 2005;23:443-464.
21. Breedveld P, Beijnen JH, and Schellens JH. Use of P-glycoprotein and BCRP inhibitors to improve oral bioavailability and CNS penetration of anticancer drugs. Trends Pharmacol Sci 2006;27:17-24.
22. De Cesare M, Pratesi G, Perego P, et al. Potent antitumor activity and improved pharmacological profile of ST1481, a novel 7-substituted camptothecin. Cancer Res 2001;61:7189-7195.
23. Lee YJ, Kusuhara H, Jonker JW, et al. Investigation of efflux transport of dehydroepiandrosterone sulfate and mitoxantrone at the mouse blood-brain barrier: a minor role of breast cancer resistance protein. J Pharmacol Exp Ther 2005;312:44-52.
24. Nozawa T, Minami H, Sugiura S, et al. Role of organic anion transporter OATP1B1 (OATP-C) in hepatic uptake of irinotecan and its active metabolite, 7-ethyl-10-hydroxycamptothecin: in vitro evidence and effect of single nucleotide polymorphisms. Drug Metab Dispos 2005;33:434-439.
25. Han JY, Lim HS, Shin ES, et al. Influence of the organic anion-transporting polypeptide 1B1 (OATP1B1) polymorphisms on irinotecan-pharmacokinetics and clinical outcome of patients with advanced non-small cell lung cancer. Lung Cancer 2008;59:69-75.
26. Koshiba S, Ito T, Shiota A, et al. Development of polyclonal antibodies specific to ATP-binding cassette transporters human ABCG4 and mouse Abcg4: site-specific expression of mouse Abcg4 in brain. J Exp Ther Oncol 2007;6:321-333.
27. Leggas M, Adachi M, Scheffer GL, et al. Mrp4 confers resistance to topotecan and protects the brain from chemotherapy. Mol Cell Biol 2004;24:7612-7621.

CHAPTER 3.3

OATP1B1 mediates transport of gimatecan and BNP1350 and can be inhibited by several classical BCRP and/or P-gp inhibitors

Roos L. Oostendorp, Evita van de Steeg, Cornelia M.M. van der Kruijssen,
Jos H. Beijnen, Kathryn E. Kenworthy,
Alfred H. Schinkel, Jan H.M. Schellens

Submitted for publication

Abstract

Organic anion transporting polypeptides (OATPs) are important uptake transporters that can have a profound impact on the systemic pharmacokinetics, tissue distribution and elimination of several drugs. Previous *in vivo* studies of the pharmacokinetics of the lipophilic camptothecin analogue, gimatecan, suggested that the P-glycoprotein (P-gp) and/or Breast Cancer Resistance Protein (BCRP) inhibitors elacridar and pantoprazole could inhibit transporters other than P-gp and BCRP. In this study, we tested the possible role of OATP1B1 in this interaction by screening a number of camptothecin analogues for their transport affinity by human OATP1B1 *in vitro*. Additionally, the impact of several widely used P-gp and/or BCRP modulators on this OATP1B1-mediated transport was assessed. We identified two novel camptothecin anticancer drugs, gimatecan and BNP1350, as OATP1B1 substrates, whereas irinotecan, topotecan and lurtotecan were not transported by OATP1B1. Interestingly, transport of 17β estradiol 17β-D-glucuronide (control), gimatecan and BNP1350 by OATP1B1 could be completely inhibited by the classical P-gp and/or BCRP inhibitors elacridar, valspodar, pantoprazole and, to a lesser extent, zosuquidar and verapamil. The effect of these P-gp and BCRP modulators on the plasma pharmacokinetics of gimatecan and BNP1350 (and possibly also other OATP1B1 substrates) may therefore be partly due to inhibition of OATP1B1 besides inhibition of P-gp and/or BCRP. The findings of this study suggest that OATP1B1 polymorphisms, or co-administration with one of the P-gp/BCRP inhibitors could affect drug uptake, tissue distribution and elimination of some camptothecin anticancer drugs, thereby modifying their efficacy and/or safety profile.

Introduction

Uptake transporters belonging to the superfamily of organic anion transporting polypeptides (rodents: Oatps, human: OATPs) are nowadays recognized as important transporters that can have a profound impact on the systemic pharmacokinetics, tissue distribution and elimination of a wide range of drugs. Among these OATPs, human OATP1B1 (previously called OATP-C, LST-1 or OATP2; gene symbol: SLCO1B1) is found to be specifically and highly expressed at the basolateral (sinusoidal) plasma membrane of hepatocytes and is considered to be one of the most important hepatic uptake transporters (1-3). The clinical importance of OATP1B1 in the plasma pharmacokinetics and elimination of substrate drugs has been confirmed by several studies focusing on commonly occurring SNPs in OATP1B1. In particular, the SLCO1B1*15 allele (c.388A>G and c.521T>C) has been associated with strongly reduced transport functionality and markedly increased plasma levels of pravastatin, pitavastatin, simvastatin acid, and sometimes resulting in fatal toxicity (4).

With the exception of methotrexate and SN-38 (5, 6), information about anticancer drugs being transported by OATP1B1 is limited. Therefore, we investigated a number of (novel) camptothecin analogues as possible substrates for human OATP1B1. Camptothecin (CPT) was originally isolated from the Chinese tree *Camptotheca acuminata* by Wall et al., (7). The molecular mechanism of CPT has been established to be inhibition of the nuclear enzyme DNA topoisomerase I, in which the intactness of the lactone ring of CPT plays a dominant role (8). This lactone moiety, however, is chemically unstable and undergoes pH-dependent reversible hydrolysis to a hydroxyl carboxylate form. Under acidic conditions (pH < 4) the lactone structure predominates, whereas at pH values > 10 the carboxylate form is exclusively present (9, 10). Since CPT itself is poorly water-soluble, the initial approach in camptothecin analogue development focussed on increasing water solubility. This resulted in the development of irinotecan (CPT-11, water soluble precursor of the more lipophilic and potent SN-38) and topotecan (TPT), which are nowadays important and widely used anticancer drugs (11, 12). However, a significant limitation of CPT-11, SN-38 and TPT is their affinity for the ATP-binding cassette (ABC) drug efflux transporters Breast Cancer Resistance Protein (BCRP; gene symbol: ABCG2) and P-glycoprotein (P-gp; gene symbol: ABCB1), often resulting in tumor resistance (13-15). Therefore, there is an increasing interest in the more recently developed highly lipophilic camptothecin derivatives such as lurtotecan (GI147211, NX211), gimatecan (ST1481, LBQ707) and BNP1350 (Karenitecin). These drugs have been suggested to be less affected by multidrug resistance. For example, lurtotecan has less affinity for BCRP than topotecan and SN-38,

while BNP1350 could be classified as a poor BCRP substrate (16). Furthermore, we recently showed that gimatecan was not a substrate for P-gp or Multidrug Resistance Protein 2 (MRP2; gene symbol: ABCC2), but our data did show that gimatecan is transported by BCRP (17). The *in vivo* role of BCRP in gimatecan pharmacokinetics was further assessed by our group using BCRP/P-gp knockout mice (submitted data). Interestingly, these data revealed that co-administration of elacridar (GF120918, an effective P-gp and BCRP inhibitor (18, 19) and pantoprazole (specific BCRP inhibitor (20)) also increased the area under the plasma concentration-time curve (AUC) of gimatecan in BCRP/P-gp knockout mice. This suggests that the interaction between gimatecan and elacridar or pantoprazole is partly mediated by drug transporters other than BCRP and P-gp. In the present study we tested the possible role of human OATP1B1 in this drug-drug interaction.

The aim of this study was to establish whether human OATP1B1 could transport the camptothecin analogues CPT-11, SN-38, TPT, lurtotecan, gimatecan and BNP1350. We also tested the pH-dependency of the OATP1B1-mediated transport of these compounds. Furthermore, several P-gp and/or BCRP inhibitors, including elacridar, zosuquidar, verapamil, valspodar and pantoprazole, were screened as possible OATP1B1 modulators.

Material and Methods

Chemicals and Reagents

[^{3}H]inulin (0.78 Ci/mmol) and [^{14}C]inulin carboxylic acid (54 mCi/mmol) were purchased from Amersham Biosciences (Little Chalfont, United Kingdom). [^{3}H]17β estradiol 17β-D-glucuronide (E_2G; 44 Ci/mmol) was purchased from PerkinElmer Life Science Products (Boston, MA). Topotecan (Hycamtin) and [^{14}C]topotecan (48 mCi/mmol) were obtained by SmithKline Beecham Pharmaceuticals (King of Prussia, PA). [^{3}H]Gimatecan (40 µCi/mg), valspodar and cyclosporin A were provided by Novartis Pharmaceuticals, Inc. Lurtotecan (NX211) was kindly provided by Gilead Sciences, Inc. (Foster City, CA), BNP1350 by BioNumerik Pharmaceuticals, Inc. (San Antonio, TX), zosuquidar trihydrochloride by Dr. P. Multani of Kanisa Pharmaceuticals (San Diego, CA) and elacridar by GlaxoSmithKline Pharmaceuticals (Research Triangle Park, NC). SN-38 was purchased from Sequoia Research Products (Pangbourne, UK). Pantoprazole (Pantozol® 40 mg, Altana Pharma, Zwanenburg, The Netherlands) and CPT-11 (Campto®; Pfizer BV, Capelle a/d Ijssel, NL) were obtained from the pharmacy of the Netherlands Cancer Institute/Slotervaart Hospital. Other chemicals and drugs were of analytical grade or better and were purchased from Sigma (St Louis, MO) or Invitrogen (Breda, The Netherlands).

Cell lines and culture conditions

Polarized Madin-Darby Canine Kidney II (MDCKII) epithelial cells, parental and stably expressing functional human OATP1B1, were kindly provided by Dr Y Sugiyama and were cultured as described previously (21).

Transport assays

Transcellular transport studies were performed as described previously (22), with minor modifications. Briefly, MDCKII-parental, and -OATP1B1 cells were grown on microporous polycarbonate membrane filters (3.0 μM pore size, 24 mm diameter; Transwell 3414; Costar, Corning, NY) at a density of 1.5 x 10^6 cells/well for 3 days. The expression level of OATP1B1 was induced with 5 mM sodium butyrate for 24 h prior to the start of the transport study. As control, in all transport experiments [^{3}H]E_2G (1 μM) was used as OATP1B1 substrate (21) and rifampicin (10 μM) as OATP1B1 inhibitor (23). When inhibitors were used, cells were incubated with one of the respective inhibitors for 2 hours prior to the start and throughout the transport experiments.

First, the camptothecins CPT-11 (5 μM), SN-38 (5 μM), [^{14}C]TPT (5 μM), lurtotecan (5 μM), [^{3}H]gimatecan (1 μM) and BNP1350 (0.2 μM) were tested for OATP1B1-mediated transport. After 2 and 4 h, aliquots of medium were taken and the amount of the tested drugs appearing in the compartment (apical (A) or basal (B)) opposite to which the drug was added was measured. Radiolabeled drugs were analyzed by liquid scintillation counting (Tri-Carb 2100 CS Liquid Scintillation Analyzer, Canberra Packard) and the non-radiolabeled drugs by fluorescence measurements at specific excitation/emission wavelengths of 370/480 (CPT-11), 380/535 (SN-38), 380/420 (lurtotecan) or 370/420 (BNP1350) using a microplate reader (Infinite® M200, Tecan Trading AG, Switzerland). The tested concentrations of the non-radiolabeled camptothecins were chosen within the linear range of the calibration curve of the fluorescence measurements, and the concentrations of the radiolabeled drugs were based on our experience with these compounds (24, 17).

Secondly, cellular accumulation of 1 μM [^{3}H]E_2G in MDCKII-OATP1B1 cells 4 h after BA (basal to apical) directed transport in the absence and presence of different concentrations of the camptothecin analogues CPT-11 (10 and 100 μM), SN-38 (10 and 100 μM), TPT (10 and 100 μM), lurtotecan (1, 10 and 100 μM), gimatecan (1 and 4 μM) and BNP1350 (1 and 10 μM) were tested.

Thirdly, the effect of extracellular pH 6.5 and 8.0 on the cellular accumulation of 1 μM [^{3}H]E_2G and several camptothecins in MDCKII-OATP1B1 cells 4 h after BA directed transport was investigated. Herein, the (serum-free) Opti-MEM medium (Life

Technologies) was adjusted to pH 6.5 or 8.0 by the addition of HCl (37% w/w) and NaOH (5 mM), respectively, immediately before addition of the (non-) radiolabeled drug.
Finally, the BCRP and/or P-gp inhibitors elacridar (5 µM), zosuquidar (5 µM), verapamil (10 µM), valspodar (5 µM) and pantoprazole (500 µM) were tested in this assay for the inhibition of OATP1B1 mediated transport of E_2G and camptothecins. The concentrations we used for the different P-gp/BCRP inhibitors are based on our comprehensive experience with these inhibitors (25, 26).

Statistical analysis

Statistical evaluation was performed using the two-sided unpaired Student's *t*-test to assess the statistical significance of difference between two sets of data. Differences were considered to be statistically significant when $P < 0.05$.

Results

Transport of several camptothecins across MDCKII-parental and MDCKII-OATP1B1-overexpressing monolayers

Transport of E_2G (control), TPT, CPT-11, SN-38, lurtotecan, gimatecan and BNP1350 by OATP1B1 was studied in MDCKII-OATP1B1 and MDCKII-parental cells. We found an increased transport of 1 µM gimatecan and 0.2 µM BNP1350 from the basal-to-apical (BA) compartments compared with the transport in the opposite direction (AB) in MDCKII-OATP1B1 cells (ratio BA/AB after 4 h is 2.7 ± 0.6 and 2.7 ± 0.1, respectively, Fig. 1, Table 1), whereas the parental cell line did not show transport (ratio BA/AB after 4 h is 1.1 ± 0.02 and 1.0 ± 0.2, respectively; Fig.1, Table 1). These ratios are within the same order of magnitude (or even slightly higher) as the positive control E_2G (ratio BA/AB = 2.4, Fig. 1, Table 1), demonstrating that gimatecan and BNP1350 are efficiently transported by OATP1B1. Moreover, like for E_2G, gimatecan and BNP1350 transport was completely inhibited in MDCKII-OATP1B1 monolayers in the presence of the OATP1B1-inhibitor rifampicin (10 µM; Fig. 1). SN-38 showed complex transport behavior, with increased BA directed transport by OATP1B1 compared to parental cells, however, AB directed transport was dominant, presumably due to the presence of an apical uptake transporter or a basolateral efflux transporter for SN-38 (Fig. 1). Addition of rifampicin resulted in inhibition of the BA directed (OATP1B1-mediated) transport, but it also increased the AB directed transport and the transport of SN-38 in the parental cells (Fig. 1). It may be that reduction of basolateral SN-38 re-uptake by inhibiting OATP1B1 (and possibly a related endogenous basolateral SN-38 uptake system in parental cells) with rifampicin results in higher net AB directed transport by the endogenous basolaterally directed SN-38 transport

system. Indeed, a qualitatively similar shift (increased basolaterally directed transport) was seen upon inhibiting OATP1B1-mediated gimatecan transport with rifampicin (Fig. 1; see also Table 1). No net transport was found for CPT-11, TPT and lurtotecan in MDCKII-OATP1B1 and parental cell line monolayers (data not shown).

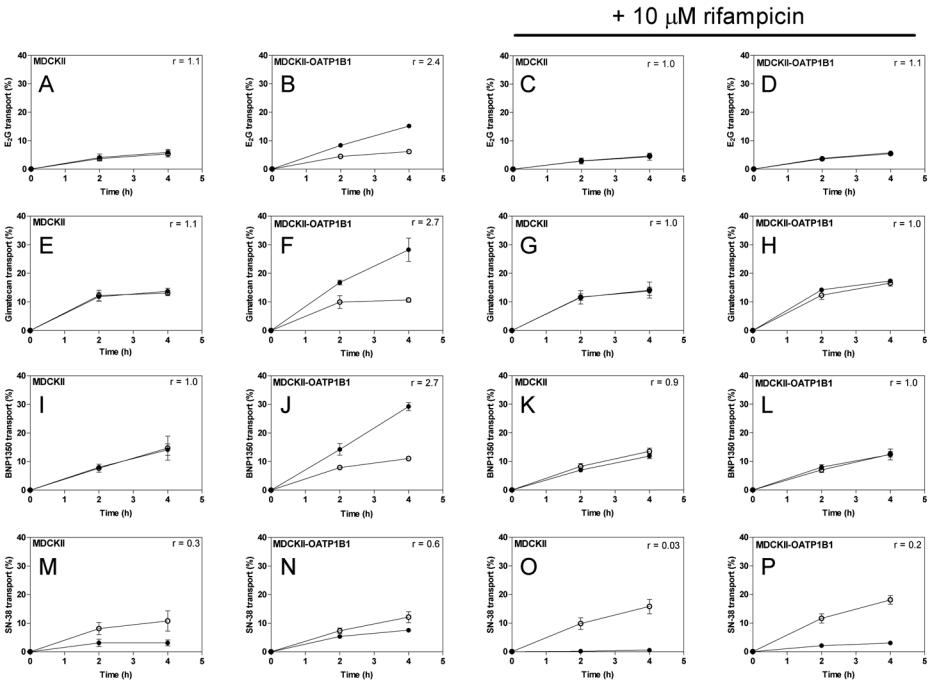

Figure 1. Transport of E_2G (1 μM) (A-D), gimatecan (1 μM) (E-H), BNP1350 (0.2 μM) (I-L) and SN-38 (5 μM) (M-P) in the absence or presence of rifampicin (10 μM) in MDCKII-parental and MDCKII-OATP1B1 cells. [^{3}H]E_2G, [^{3}H]gimatecan, BNP1350, or SN-38 were applied at t = 0 to the basal (B) or apical (A) side and the amount of drug appearing in the opposite apical (A) compartment (BA; closed symbols) or basal (B) compartment (AB; open symbols) was determined. Samples were taken at t = 2 and 4 h. Results are shown as % of total added dose. Symbols, mean of each experiment in triplicate ± SD; r = ratio BA versus AB.

Table 1. Inhibitory effect of BCRP/P-gp and control inhibitors on OATP1B1-mediated transport of E_2G, gimatecan and BNP1350

Inhibitors	E_2G (1 µM)			Gimatecan (1 µM)			BNP1350 (0.2 µM)		
	BA (%)	AB (%)	Ratio BA/AB	BA (%)	AB (%)	Ratio BA/AB	BA (%)	AB (%)	Ratio BA/AB
-	15.1 ± 0.7	6.2 ± 0.7	2.4	28.2 ± 4.1	10.7 ± 0.8	2.6	28.5 ± 1.9	8.4 ± 3.6	3.4
rifampicin (10 µM)	5.7* ± 0.6	5.4 ± 0.6	1.1	17.4* ± 0.2	16.6 ± 1.1	1.1	12.4* ± 1.9	12.5 ± 1.0	1.0
elacridar (5 µM)	5.5* ± 1.0	5.2 ± 1.0	1.1	13.5* ± 1.3	12.1 ± 0.8	1.1	17.2* ± 1.4	16.1 ± 0.6	1.1
zosuquidar (5 µM)	9.1* ± 1.4	6.3 ± 1.1	1.4	18.2* ± 0.4	16.3 ± 0.04	1.1	14.4* ± 0.8	11.1 ± 0.7	1.3
verapamil (10 µM)	7.9* ± 0.1	4.3 ± 0.5	1.8	22.3* ± 3.6	14.2 ± 1.7	1.6	29.9 ± 1.9	9.3 ± 2.5	3.2
valspodar (5 µM)	8.5* ± 1.4	8.3 ± 0.4	1.0	15.0* ± 0.4	16.2 ± 2.1	0.9	11.7* ± 1.8	9.7 ± 2.3	1.2
pantoprazole (500 µM)	4.6* ± 0.5	4.1 ± 0.3	1.1	15.6* ± 1.3	17.0 ± 1.0	0.9	11.1* ± 1.7	12.4 ± 1.5	0.9

Note: Data are mean ± SD, n = 3. Abbreviations: BA, transport from the basal to apical compartments; AB, transport from the apical to basal compartments; % total transport after 4 h. * $P < 0.05$, compared with OATP1B1-mediated transport of E_2G, gimatecan and BNP1350 without inhibitor.

The effects of several camptothecins on the OATP1B1-mediated transport of E_2G

The inhibitory effect of two concentrations of the camptothecin analogues CPT-11, SN-38, TPT, lurtotecan, gimatecan and BNP1350 on the OATP1B1-mediated transport of E_2G was assessed. Our aim was not to establish IC_{50} values, this might be part of future studies.

MDCKII-OATP1B1 cells showed a 2.4-fold ($P<0.05$) increased BA transport of 1 µM E_2G after 4 h compared with AB directed transport (Table 1), whereas parental cells did not show any transport of E_2G. The effects of various camptothecins on the uptake of E_2G by MDCKII-OATP1B1 cells are presented in figure 2, which shows the cellular accumulation of E_2G in MDCKII-OATP1B1 cells 4 h after addition of E_2G to the basal compartment without (i.e. control) and with addition of several camptothecins (presented as % of control). The first bar, however, represents the cellular accumulation of E_2G in parental cells. This bar shows that complete inhibition will maximally result in ~35% of control E_2G accumulation values. Indeed, the addition of rifampicin (10 µM), an

established OATP1B1 inhibitor that we used as a control, resulted in ~40% of control E_2G accumulation in MDCKII-OATP1B1 cells. This illustrates that rifampicin can virtually completely inhibit E_2G uptake by OATP1B1, as it resulted in cellular accumulation levels of E_2G roughly similar to that in parental cells. Lurtotecan and BNP1350 were identified as strong inhibitors of OATP1B1-mediated transport of E_2G, since at 1 μM these compounds significantly inhibited cellular accumulation of E_2G ($P < 0.001$). Initially, lurtotecan was tested at a concentration of 10 and 100 μM, which did show inhibition but not a concentration dependency. We therefore tested an additional concentration of 1 μM. In contrast, 1 μM gimatecan did not inhibit cellular accumulation of E_2G, however, at a concentration of 4 μM, it significantly inhibited the cellular accumulation of E_2G in MDCKII-OATP1B1 cells ($P < 0.01$). Gimatecan precipitated at concentrations > 4 μM, which was therefore the highest testable concentration. Furthermore, 10 μM SN-38 had only a minimal (but significant) inhibitory effect ($P < 0.05$), whereas at a higher concentration (100 μM) inhibition was more profound (~50% of control, $P < 0.001$). CPT-11 and TPT could be classified as less potent OATP1B1 inhibitors, only inhibiting E_2G transport by MDCKII-OATP1B1 cells at a concentration of 100 μM ($P < 0.05$ and $P < 0.001$, respectively). No effect of the tested camptothecins was seen on the transport of E_2G in parental cells (data not shown).

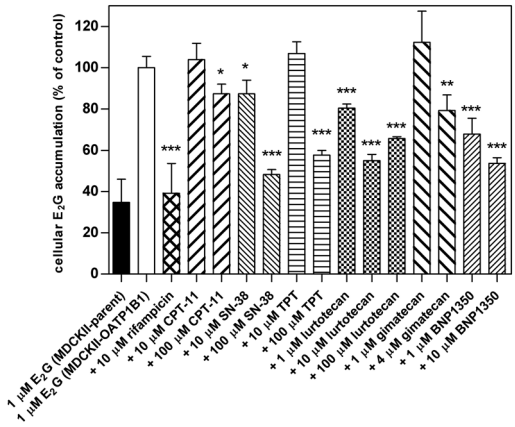

Figure 2. Cellular accumulation of 1 μM [^{3}H]E_2G in MDCKII-OATP1B1 cells 4 h after BA (basal to apical) directed transport in the absence (control) and presence of 10 μM rifampicin and different concentrations of the camptothecin analogues CPT-11 (10 and 100 μM), TPT (10 and 100 μM), SN-38 (10 and 100 μM), lurtotecan (1, 10 and 100 μM), gimatecan (1 and 4 μM) and BNP1350 (1 and 10 μM). The respective modulators were present throughout the experiments. The first bar shows cellular accumulation of 1 μM [^{3}H]E_2G in MDCKII-parental cells 4 h after BA directed transport. All bars represent the mean of each experiment in triplicate ± SD. $^{*}P < 0.05$; $^{**}P < 0.01$; $^{***}P < 0.001$.

pH-dependent uptake of E_2G, gimatecan and BNP1350 by human OATP1B1

We tested whether the OATP1B1-mediated transport of gimatecan and BNP1350 differed between the carboxylate and lactone form of these camptothecin analogues. Therefore, the effect of acidic (pH 6.5) and basic (pH 8.0) conditions on the OATP1B1-mediated uptake of gimatecan, BNP1350 and E_2G (used as a control) was investigated. Cellular accumulation of gimatecan and BNP1350 was not changed between these different pH values (data not shown). However, cellular uptake of E_2G, the molecular shape of which is chemically not affected by the tested pH values (Nghiem, et al., 2004), was significantly higher at acidic pH (pH 6.5) compared to control pH (pH 7.2) as shown in figure 3 (0.58 ± 0.13 versus 0.34 ± 0.04% of totally added E_2G accumulation 4 h after BA directed transport in MDCKII-OATP1B1 cells at pH 6.5 and 7.2, respectively; $P < 0.05$). This shows that OATP1B1 transports E_2G more efficiently at acidic pH, illustrating a pH dependency of OATP1B1. No effect of the different pHs was seen on cellular accumulation of E_2G in parental cells (Fig. 3).

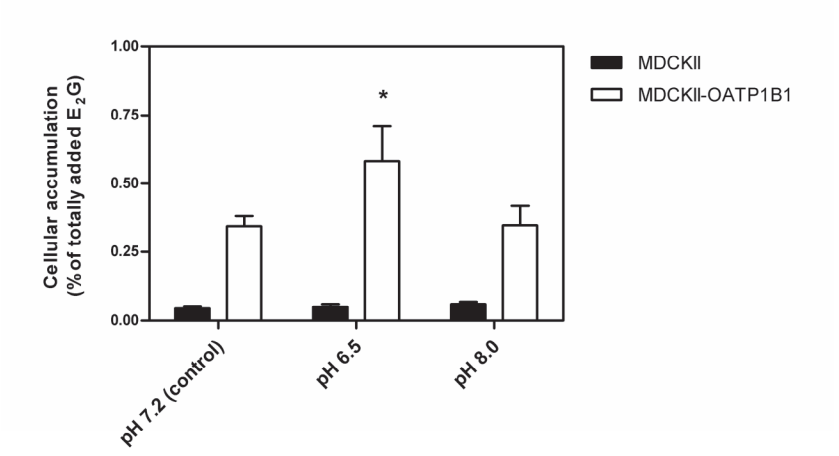

Figure 3. Cellular accumulation of 1 µM [^{3}H]E_2G in MDCKII-parental and -OATP1B1 cells 4 h after BA (basal to apical) directed transport at pH 7.2 (control), pH 6.5 and pH 8.0. Results are shown as percentage of totally added E_2G. All bars represent the mean of each experiment in triplicate ± SD. $^*P < 0.05$.

The effects of several classical BCRP/P-gp inhibitors on the transport of E_2G, gimatecan and BNP1350 by OATP1B1

Employing MDCKII-parental and -OATP1B1 monolayers we investigated whether the classical BCRP and/or P-gp inhibitors elacridar (5 µM), zosuquidar (5 µM), verapamil (10 µM), valspodar (5 µM) and pantoprazole (500 µM) were capable of inhibiting the transport of E_2G, gimatecan and BNP1350 by OATP1B1. OATP1B1 expression resulted in a 2.4-, 2.6- and 3.4-fold ($P < 0.05$) increased transport of E_2G, gimatecan and BNP1350, respectively, from BA compared with the transport from AB (Table 1). Interestingly, the tested BCRP and/or P-gp inhibitors, elacridar, valspodar and pantoprazole fully inhibited the OATP1B1-mediated transport of E_2G, gimatecan and BNP1350 (Table 1). Zosuquidar completely inhibited gimatecan but to a minor extent E_2G and BNP1350 transport by OATP1B1. Verapamil only had a minimal (but significant) inhibitory effect on the OATP1B1-mediated transport of E_2G and gimatecan, but had no inhibitory effect on the transport of BNP1350 (Table 1). No effect of the tested BCRP and/or P-gp inhibitors was found on the disposition of E_2G by parental cells (Table 1).

Discussion

We have identified two novel camptothecin analogue anticancer drugs, gimatecan and BNP1350, as substrate drugs for human OATP1B1. Interestingly, OATP1B1-mediated transport of these compounds could be efficiently inhibited by elacridar, valspodar, pantoprazole, and to a lesser extent also by zosuquidar and verapamil, which were originally developed and classified as P-gp and/or BCRP inhibitors.

In order to study the role of OATP1B1 in the disposition of several camptothecin analogues we made use of MDCKII cells stably expressing OATP1B1. In these cells, which were previously established and validated by Sasaki et al. (21), we showed that gimatecan, BNP1350 and SN-38 are substrate drugs for OATP1B1. CPT-11, TPT and lurtotecan could not be identified as OATP1B1 substrates. Concerning CPT-11 and SN-38, our results were in line with previously described data (27). In this study by Nozawa et al., SN-38 (but not CPT-11) was identified as a substrate for human OATP1B1, using HEK293 cells and *Xenopus* oocytes expressing OATP1B1. Our results revealed increased BA directed transport of SN-38 in MDCKII-OATP1B1 cells compared to parental MDCKII cells, but AB directed transport was dominant in both cell lines. From this we could conclude that SN-38 is transported by OATP1B1, but it also suggested that MDCKII cells express one or more unidentified endogenous apical uptake transporters (or basolateral active efflux transporters) with affinity for SN-38. The existence of an apical uptake transporter for SN-38 has been observed before, though these studies were only focussing

on a human intestinal cell line (Caco-2) and hamster or human intestinal epithelial cells, respectively (28, 29). Furthermore, inhibition experiments indicated that the reduced transport of SN-38 in MDCKII-OATP1B1 cells by rifampicin is related to more complex mechanisms, since it also affected AB directed transport of SN-38 and the transport of SN-38 by parental cells.

Several independent studies confirmed the *in vivo* importance of OATP1B1 in systemic pharmacokinetics and elimination of several drugs (i.e. several statins, fexofenadine, atrasentan, torsemide and irinotecan) by investigating SNPs. Especially the commonly occurring SLCO1B1*15 allele (c.388A>G and c.521T>C) is associated with reduced transport capacity and increased plasma AUC (4). Nozawa et al. (27), showed that OATP1B1*15 displayed 50% decreased transport activity for SN-38 *in vitro*. Importantly, OATP1B1*15 has also been associated with higher systemic exposure to SN-38, lower clearance of this compound and even severe toxicity in patients treated with irinotecan (30). Together, this demonstrates that genetic polymorphisms of OATP1B1 may contribute to the interpatient variability in the efficacy and toxicity of several drugs, including camptothecins. This might therefore also have clinical implications for the (highly toxic) anticancer drugs gimatecan and BNP1350. It would be interesting and of high importance to further investigate this *in vivo*.

Recently, additional novel camptothecins have been developed to improve oral uptake, intracellular accumulation, lactone stability, drug-target interaction and lipophilicity (31). This has led to the development of seven-position modified lipophilic camptothecin derivatives (e.g. gimatecan and BNP1350 (32)), and stable 5-membered E-ring ketone camptothecins (33). In the present study we show that gimatecan and BNP1350 are both transported by human OATP1B1. Interestingly, De Cesare et al. reported that gimatecan was more potent than TPT against liver metastasis in mice, suggesting the importance of Oatp-mediated hepatic uptake (34). It will be interesting to investigate whether other newly developed camptothecins, besides BCRP and P-gp, are also OATP1B1 substrate drugs.

Our group previously showed that BCRP transports substrate drugs more efficiently at low pH (24). Here we also demonstrate a pH-sensitive activity of human OATP1B1, which was shown by increased transport of E_2G at acidic pH (pH 6.5) compared to control pH (pH 7.2). In contrast to gimatecan and BNP1350, whose structures can change from the lacton to the carboxylate form upon pH changes, the chemical structure of E_2G is not chemically affected by this pH difference, since the pK_a of E_2G is 10.4 (35). No effect of different pH values was found on the transport of gimatecan and BNP1350 by OATP1B1. This is possibly masked by a difference in affinity between the lactone and the carboxylate form of gimatecan and BNP1350, since the molecular conversion of camptothecins is pH-dependent.

pH-sensitivity of OATP1B1 has not been reported before, however transport of estrone-3-sulfate by human OATP2B1 and OATP1A2 has been reported to be increased by low pH as well (36, 37). Unlike OATP2B1 and OATP1A2, the expression of human OATP1B1 is liver-specific (2, 38) and is therefore not found at the intestinal epithelial cells, where the luminal pH ranges from 4 to 7 (37). Consequently, the physiological impact of pH-sensitivity of OATP1B1 might be limited, as the extracellular pH around hepatocytes is neutral.

Based on our previous *in vivo* results (39), we found that elacridar and pantoprazole, two well-known BCRP and P-gp modulators, most likely inhibit one or more transporters distinct from BCRP and P-gp. In the present study, we hypothesized that the inhibitory effect of elacridar and pantoprazole could be partly due to modulation of the uptake transporter OATP1B1. The effect of several classical BCRP and/or P-gp modulators, elacridar, zosuquidar, verapamil, valspodar and pantoprazole was tested. Our data show, to our knowledge, for the first time that elacridar, valspodar, pantoprazole, and to a lesser extent zosuquidar and verapamil, are besides BCRP and P-gp inhibitors also OATP1B1 inhibitors (at levels of exposure that are commonly applied to inhibit BCRP and P-gp). This most likely explains our previous *in vivo* results regarding the effects of elacridar and pantoprazole in BCRP and P-gp knockout mice (39). Co-administration of camptothecins, or other drugs that are substrates for OATP1B1, and one of these well-known BCRP/P-gp inhibitors could affect drug uptake, tissue distribution and/or elimination, thereby modifying the efficacy and/or safety profile of these drugs. Pantoprazole, for example, belongs to the class of proton pump inhibitors (PPIs) that have emerged as the most important class of drugs for the management of a variety of acid-related disorders of the upper gastrointestinal tract, including gastric and duodenal ulcers, and gastroesophageal reflux disease accompanied by esophagitis (40). Pantoprazole is clinically a widely used drug and intake of this drug is rarely discontinued before treatment with other (anticancer) drugs. Although in this study we used high concentrations of pantoprazole, this might indicate that this combined treatment could lead to drug-drug interactions at the level of OATP1B1, possibly resulting in increased plasma levels of the drug, which could lead to undesirable side effects.

In conclusion, in the present study we show that gimatecan and BNP1350 are novel OATP1B1 substrate drugs. Since the clinical importance of OATP1B1 polymorphisms has been widely established nowadays, these might therefore have marked implications for these (highly toxic) anticancer drugs in patients. Additionally, the OATP1B1-mediated transport of gimatecan and BNP130 could be inhibited by several classical P-gp and/or BCRP modulators. The effect of these P-gp and/or BCRP modulators on the plasma pharmacokinetics of these camptothecin analogues (and possibly also other

OATP1B1 substrate drugs) may therefore not be solely ascribed to inhibition of P-gp and/or BCRP. The results of this study add to a better insight into the pharmacokinetic behaviour of camptothecin analogues, including drug-drug interactions which can affect the efficacy and/or safety profile of these drugs.

References

1. Hsiang B, Zhu Y, Wang Z, et al. A novel human hepatic organic anion transporting polypeptide (OATP2). Identification of a liver-specific human organic anion transporting polypeptide and identification of rat and human hydroxymethylglutaryl-CoA reductase inhibitor transporters. J Biol Chem 1999;274:37161-37168.
2. König J, Cui Y, Nies AT and Keppler D. A novel human organic anion transporting polypeptide localized to the basolateral hepatocyte membrane. Am J Physiol Gastrointest Liver Physiol 2000;278:G156-G164.
3. Abe T, Kakyo M, Tokui T, et al. Identification of a novel gene family encoding human liver-specific organic anion transporter LST-1. J Biol Chem 1999; 274:17159-17163.
4. Maeda K and Sugiyama Y. Impact of genetic polymorphisms of transporters on the pharmacokinetic, pharmacodynamic and toxicological properties of anionic drugs. Drug Metab Pharmacokinet 2008;23:223-235.
5. König J, Seithel A, Gradhand U and Fromm MF. Pharmacogenomics of human OATP transporters. Naunyn Schmiedebergs Arch Pharmacol 2006;372:432-443.
6. Hagenbuch B and Meier PJ. Organic anion transporting polypeptides of the OATP/ SLC21 family: phylogenetic classification as OATP/ SLCO superfamily, new nomenclature and molecular/functional properties. Pflugers Arch 2004;447:653-665.
7. Wall ME, Wani MC, Cook CE, et al. Plant antitumor agents. I. The isolation and structure of camptothecin, a novel alkaloidal leukemia and tumor inhibitor from Camptotheca acuminata. J Am Chem Soc 1966;88:3888-3890.
8. Adams DJ, Dewhirst MW, Flowers JL, et al. Camptothecin analogues with enhanced antitumor activity at acidic pH. Cancer Chemother Pharmacol 2000;46:263-271.
9. Fassberg J and Stella VJ. A kinetic and mechanistic study of the hydrolysis of camptothecin and some analogues. J Pharm Sci 1992; 81:676-684.
10. Underberg WJ, Goossen RM, Smith BR and Beijnen JH. Equilibrium kinetics of the new experimental anti-tumour compound SK&F 104864-A in aqueous solution. J Pharm Biomed Anal 1990;8:681-683.
11. Takimoto CH, Wright J and Arbuck SG. Clinical applications of the camptothecins. Biochim Biophys Acta 1998;1400:107-119.
12. Douillard JY, Cunningham D, Roth AD, et al. Irinotecan combined with fluorouracil compared with fluorouracil alone as first-line treatment for metastatic colorectal cancer: a multicentre randomised trial. Lancet 2000;355:1041-1047.
13. Mattern MR, Hofmann GA, Polsky RM, et al. In vitro and in vivo effects of clinically important camptothecin analogues on multidrug-resistant cells. Oncol Res 1993;5:467-474.
14. Lalloo AK, Luo FR, Guo A, et al. Membrane transport of camptothecin: facilitation by human P-glycoprotein (ABCB1) and multidrug resistance protein 2 (ABCC2). BMC Med 2004;2:16.
15. Hendricks CB, Rowinsky EK, Grochow LB, et al. Effect of P-glycoprotein expression on the accumulation and cytotoxicity of topotecan (SK&F 104864), a new camptothecin analogue. Cancer Res 1992;52:2268-2278.
16. Maliepaard M, van Gastelen MA, Tohgo A, et al. Circumvention of breast cancer resistance protein (BCRP)-mediated resistance to camptothecins in vitro using non-substrate drugs or the BCRP inhibitor GF120918. Clin Cancer Res 2001;7:935-941.
17. Marchetti S, Oostendorp RL, Pluim D, et al. In vitro transport of gimatecan (7-t-butoxyiminomethylcamptothecin) by breast cancer resistance protein, P-glycoprotein, and multidrug resistance protein 2. Mol Cancer Ther 2007;6:3307-3313.
18. Hyafil F, Vergely C, Du Vignaud P and Grand-Perret T. In vitro and in vivo reversal of multidrug resistance by GF120918, an acridonecarboxamide derivative. Cancer Res 1993;53:4595-4602.
19. Jonker JW, Smit JW, Brinkhuis RF, et al. Role of breast cancer resistance protein in the bioavailability and fetal penetration of topotecan. J Natl Cancer Inst 2000;92:1651-1656.

20. Breedveld P, Zelcer N, Pluim D, et al. Mechanism of the pharmacokinetic interaction between methotrexate and benzimidazoles: potential role for breast cancer resistance protein in clinical drug-drug interactions. Cancer Res 2004;64:5804-5811.
21. Sasaki M, Suzuki H, Ito K, et al. Transcellular transport of organic anions across a double-transfected Madin-Darby canine kidney II cell monolayer expressing both human organic anion-transporting polypeptide (OATP2/SLC21A6) and Multidrug resistance-associated protein 2 (MRP2/ABCC2). J Biol Chem 2002;277:6497-6503.
22. Schinkel AH, Wagenaar E, van Deemter L, et al. Absence of the mdr1a P-Glycoprotein in mice affects tissue distribution and pharmacokinetics of dexamethasone, digoxin, and cyclosporin A. J Clin Invest 2005;96:1698-1705.
23. Vavricka SR, Van Montfoort J, Ha HR, et al. Interactions of rifamycin SV and rifampicin with organic anion uptake systems of human liver. Hepatology 2002;36:164-172.
24. Breedveld P, Pluim D, Cipriani G, et al. The effect of low pH on breast cancer resistance protein (ABCG2)-mediated transport of methotrexate, 7-hydroxymethotrexate, methotrexate diglutamate, folic acid, mitoxantrone, topotecan, and resveratrol in in vitro drug transport models. Mol Pharmacol 2007;71:240-249.
25. Bardelmeijer HA, Ouwehand M, Beijnen JH, et al. Efficacy of novel P-glycoprotein inhibitors to increase the oral uptake of paclitaxel in mice. Invest New Drugs 2004;22:219-229.
26. Breedveld P, Pluim D, Cipriani G, et al. The effect of Bcrp1 (Abcg2) on the in vivo pharmacokinetics and brain penetration of imatinib mesylate (Gleevec): implications for the use of breast cancer resistance protein and P-glycoprotein inhibitors to enable the brain penetration of imatinib in patients. Cancer Res 2005;65:2577-2582.
27. Nozawa T, Minami H, Sugiura S, et al. Role of organic anion transporter OATP1B1 (OATP-C) in hepatic uptake of irinotecan and its active metabolite, 7-ethyl-10-hydroxycamptothecin: in vitro evidence and effect of single nucleotide polymorphisms. Drug Metab Dispos 2005;33:434-439.
28. Itoh T, Itagaki S, Sumi Y, et al. Uptake of irinotecan metabolite SN-38 by the human intestinal cell line Caco-2. Cancer Chemother Pharmacol 2005;55:420-424.
29. Kobayashi K, Bouscarel B, Matsuzaki Y, et al. pH-dependent uptake of irinotecan and its active metabolite, SN-38, by intestinal cells. Int J Cancer 1999;83:491-496.
30. Kweekel D, Guchelaar HJ and Gelderblom H. Clinical and pharmacogenetic factors associated with irinotecan toxicity. Cancer Treat Rev 2008 (in press).
31. Teicher BA. Next generation topoisomerase I inhibitors: Rationale and biomarker strategies. Biochem Pharmacol 2008;75:1262-1271.
32. Huang M, Gao H, Chen Y, et al. Chimmitecan, a novel 9-substituted camptothecin, with improved anticancer pharmacologic profiles in vitro and in vivo. Clin Cancer Res 2007;13:1298-1307.
33. Lansiaux A, Leonce S, Kraus-Berthier L, et al. Novel stable camptothecin derivatives replacing the E-ring lactone by a ketone function are potent inhibitors of topoisomerase I and promising antitumor drugs. Mol Pharmacol 2007;72:311-319.
34. De Cesare M, Pratesi G, Perego P, et al. Potent antitumor activity and improved pharmacological profile of ST1481, a novel 7-substituted camptothecin. Cancer Res 2001;61:7189-7195.
35. Nghiem LD, McCutcheon J, Schafer AI and Elimelech M. The role of endocrine disrupters in water recycling: risk or mania? Water Sci Technol 2004;50:215-220.
36. Kobayashi D, Nozawa T, Imai K, et al. Involvement of human organic anion transporting polypeptide OATP-B (SLC21A9) in pH-dependent transport across intestinal apical membrane. J Pharmacol Exp Ther 2003;306:703-708.
37. Badagnani I, Castro RA, Taylor TR, et al. Interaction of methotrexate with organic-anion transporting polypeptide 1A2 and its genetic variants. J Pharmacol Exp Ther 2006;318:521-529.
38. Tamai I, Nozawa T, Koshida M, et al. Functional characterization of human organic anion transporting polypeptide B (OATP-B) in comparison with liver-specific OATP-C. Pharm Res 2001;18:1262-1269.
39. Oostendorp RL, Buckle T, Beijnen JH, et al. The effect of P-gp (Mdr1a/1b), BCRP (Bcrp1) and P-gp/BCRP inhibitors on the in vivo absorption, distribution, metabolism and excretion of imatinib. Invest New Drugs 2008 (in press).
40. Jungnickel PW. Pantoprazole: a new proton pump inhibitor. Clin Ther 2000;22:1268-1293.

CHAPTER 3.4

Bioequivalence study of a new oral topotecan formulation relative to the current topotecan formulation in patients with advanced solid tumors

Roos L. Oostendorp, Jill Loftiss, Sanjay Goel, Deborah A. Smith, Mohammed M. Dar, Petronella O. Witteveen, Roger B. Cohen, Lionel D. Lewis, Sobha Kurian, Amita Patnaik, Hilde Rosing, Jos H. Beijnen, Emile E. Voest, Howard Burris, Jan H.M. Schellens

International Journal of Clinical Pharmacology and Therapeutics
(in press)

Abstract

The aims of this study were to investigate the bioequivalence of a new oral topotecan formulation (i.e., proposed commercial formulation) relative to the current oral formulation (formulation used in previous clinical trials), the effect of food on the absorption and disposition of the new oral topotecan and its safety and tolerability in patients with advanced solid tumors. This was a multi-center, pharmacological phase I, multiple-dose, randomized, open-label, cross-over bioequivalence study. In the bioequivalence part, 85 patients were randomized to receive either a 4 mg (4 x 1 mg) dose of the new or current formulation on Days 1 or 8. In the food-effect part, 23 patients received a 4 mg (4 x 1mg) dose of the new formulation in a fasted and fed state. Total topotecan and topotecan lactone were determined and pharmacokinetic data were analyzed by non compartmental method. Bioequivalence was demonstrated as the 90% confidence intervals of the ratio of the new to current formulation for both the area under the plasma concentration-time curve (AUC) and the maximal drug concentration (C_{max}) for topotecan lactone were contained within the 0.8 to 1.25 boundary. The AUC and C_{max} were similar in the fed and fasted state whilst food delayed the t_{max} for topotecan lactone and total topotecan. Safety data were collected on all subjects enrolled (N = 108) and were consistent with observations from previous studies of oral topotecan. All subjects experienced at least one adverse event, the majority of which were graded as mild to moderate in severity. The new oral topotecan formulation demonstrated bioequivalence to the current formulation and can be administered to patients with solid tumors in the fed or fasting state with equal systemic exposure.

Introduction

Topotecan (9-dimethylaminomethyl-10-hydroxycamptothecin), a well-known semisynthetic analog of the alkaloid camptothecin, is a cytotoxic agent and a specific inhibitor of DNA topoisomerase-I (1, 2). Inhibition of this enzyme results in lethal DNA damage during DNA replication. Intravenous (i.v.) topotecan (Hycamtin®) is approved for the treatment of metastatic carcinoma of the ovary after failure of initial or subsequent chemotherapy, small cell lung cancer (SCLC) in subjects with potentially sensitive disease after failure of first-line chemotherapy (3-5). In 2006, i.v. topotecan was granted approval in the USA in combination with cisplatin for the treatment of stage IV-B recurrent or persistent carcinoma of the cervix. Studies have investigated the efficacy and safety of oral topotecan in malignant solid tumors (SCLC, NSCLC, breast cancer, advanced ovarian cancer and colorectal carcinoma) (6-14). To date, similar response rates of 18.3% (oral) and 21.9% (i.v.) have been observed using 2.3 mg/m^2/day and 1.5 mg/m^2/day topotecan regimens, respectively, for 5 days every 21 days in patients with relapsed SCLC (10, 12, 13). Safety and efficacy studies of oral topotecan in combination with other chemotherapy agents are currently ongoing (15, 16).

The oral topotecan formulation produced by the new manufacturing process (i.e. proposed commercial formulation) was tested to define whether it was bioequivalent to the current oral topotecan formulation used in earlier clinical trials. The primary aim of this study was to examine the bioequivalence of the new versus the current oral topotecan capsule formulation in subjects with advanced solid tumors. Secondly, the effect of food on the bioavailability of the new formulation was assessed in order to meet the requirements for registration and marketing of this new formulation. In addition, the safety and tolerability of the new and current formulations of oral topotecan were assessed.

Materials and Methods

Eligibility Criteria

Patients were eligible for the study if they had a histologically or cytologically confirmed advanced solid tumor who had failed conventional therapy for their tumor type or had a tumor type for which no standard effective therapy existed or for whom single agent topotecan therapy was appropriate. Other eligibility criteria included the following: age ≥ 18 years; Eastern Cooperative Oncology Group (ECOG) performance status ≤ 2; estimated life expectancy ≥ 3 months; no previous anticancer therapy for ≥ 4 weeks (patients had to be free of post-treatment side effects). All patients were required to have adequate bone

marrow function, defined as a white blood cell count (WBC) ≥ 3.5 x 10^9/L; absolute neutrophil count (ANC) ≥ 1.5 x 10^9/L; platelets ≥ 100 x 10^9/L and haemoglobin ≥ 9.0 g/dL (5.5 mmol/L); acceptable liver function as evidenced by serum bilirubin ≤ 2.0 mg/dL (34 µmol/L) and AST/ALT/Alkaline Phosphatase ≤ 2 times the upper limit of normal (ULN) or ≤ 5 times ULN if liver metastases were present and adequate renal function as defined by an estimated creatinine clearance ≥ 60 mL/min. Patients were excluded if they had uncontrolled emesis regardless of etiology; active infection; a history of upper gastrointestinal (GI) surgery or clinical evidence of a GI disease that might influence GI motility or drug absorption; a history of allergic reactions to compounds chemically related to topotecan; a Body Surface Area (BSA) less than 1.4 m^2 or greater than 2.2 m^2. In addition, women who were pregnant or lactating were also excluded. The study protocol was approved by the Medical Ethics Committee of the participating hospitals or its equivalent. All study paticipants provided written informed consent prior to study enrollment.

Treatment Plan and Study Design

This was a multi-center, pharmacological phase I, multiple-dose, randomized, open-label, cross-over bioequivalence study in subjects with advanced solid tumors. Randomization in Course 1, Days 1 and 8 was stratified by gender. To study the bioequivalence of the new oral topotecan formulation compared with the current oral formulation, all patients fasted from midnight on the day prior to treatment on Days 1 and 8 of Course 1. While in the fasting state in the morning of Days 1 and 8 of Course 1, all patients received a 4 mg (4 x 1 mg) dose of either the new or current formulation in a randomized fashion (Table 1). On Days 1 and 8, fluid intake was restricted for 1 h before and 2 h following ingestion of oral topotecan, while food was restricted for 4 h following ingestion of oral topotecan. Dosing with either current or new topotecan was continued on Days 9 through 11 to complete the 5-day dosing course. The topotecan dose was adjusted on Day 9 of Course 1 based on BSA (the total daily dose did not to exceed 5.5 mg) and, if necessary, on subsequent days so that the total cumulative topotecan dose for Course 1 was the same as for the standard oral dosing regimen (2.3 mg/m^2/day x 5 days). Prior to the completion of the bioequivalence portion of the study, an optional food-effect portion of the study was available for participating sites. For those sites participating in this food-effect portion, patients who elected to enroll in the optional food-effect portion of the study first completed the bioequivalence portion of the study during Course 1 and then on Day 1 of Course 2 received 4 mg (4 x 1 mg) of new topotecan formulation fed (see details below). Subsequent doses with either current or new oral topotecan were administered on Days 2-5 in Course 2

to complete the standard 5-day course. Once the bioequivalence portion of the study was completed, the previous optional food-effect portion (conducted during Day 1 or Day 8 of Course 1 and Day 1 of Course 2) was closed and the effect of food on the pharmacokinetic parameters of the new topotecan formulation was now evaluated in the food-effect only portion of the study conducted on Day 1 of Course 1 after fasting from midnight the prior night, patients received a 4 mg (4 x 1 mg) dose of the new formulation of oral topotecan (Table 1). An identical 4 mg oral topotecan dose was administered on Day 8 after fasting from midnight the prior night and within five minutes after completing the ingestion of a high-fat breakfast (i.e. approximately 800 to 1000 calories with approximately 50% of the total caloric content comprised by fat). On Days 1 and 8 fluid intake was restricted for 1 h before and 2 h following ingestion of oral topotecan, while food was restricted for 4 h after ingestion of oral topotecan. Subsequent doses with either current or new oral topotecan were adjusted on Day 9 to 11 so that the total cumulative dose for Course 1 was the same as the standard oral dosing regimen (2.3 mg/m^2/day, Days 1 through 5, every 21 days). Subsequent treatment courses (i.e. after all pharmacokinetic samples were collected) used the standard, 21-day, 5 consecutive dose day regimens (Days 1 through 5) with topotecan administered either orally (current or new formulation) or intravenously. In these subsequent treatment courses, all patients were instructed to take oral topotecan with a glass of water, on an empty stomach, the same time each day, at least 30 min before a meal. Subjects were also instructed to remain in a sitting position for at least 30 min after taking the study drug. Subjects remained on study until occurrence of unacceptable toxicities, disease progression, withdrawal of consent, investigator discretion, or a treatment delay for more than 2 weeks.

Table 1. Study design of the bioequivalence and the food effect parts of Course 1.

Bioequivalence	**Course 1**		
	Day 1	**Day 8**	**Day 9-11**
Randomization: AB	A: 4 mg current formulation, fasted	B: 4 mg new formulation, fasted	2.3 mg/m^2 or Compensated Dose (CD) of new or current formulation
Randomization: BA	B: 4 mg new formulation, fasted	A: 4 mg current formulation, fasted	2.3 mg/m^2 or CD of new or current formulation
Food effect	**Course 1**		
	Day 1	**Day 8**	**Day 9-11**
	4 mg new formulation, fasted	4 mg new formulation, high fat meal	2.3 mg/m^2 or CD of new or current formulation

Patient Evaluation, Toxicity and response evaluation

Pre-treatment evaluation occurred within 21 days of the first topotecan treatment on Day 1 of Course 1 and included a complete medical history and physical examination, assessment of performance status (World Health Organization (WHO)), history of prior treatments, documentation of any residual toxicity relating to prior treatments, review of concomitant medications, vital signs, BSA determination, 12-lead electrocardiogram (ECG), and tumor evaluation using appropriate radiographic imaging. Within 7 days prior to Day 1 of Course 1, a serum pregnancy test, hematology, blood chemistry, and urinalysis were obtained. Hematology, blood chemistry, urinalysis, urine pregnancy test (only for women of childbearing potential), vital signs, BSA determination, adverse event (AE) assessment, and concomitant medications were checked within 5 days prior to Day 1 for subsequent courses. Only if clinically indicated, a 12-lead ECG was performed on Day 1 for subsequent treatment courses. AEs including both qualitative and quantitative toxicities measures were graded according to the National Cancer Institute (NCI) Common Toxicity Criteria (CTC) Version 2.0 (17). The next treatment course could begin if there was no clinical evidence of disease progression and the following criteria were met by the last day of the previous treatment course: haemoglobin $\geq$ 9 g/dL (5.5 mmol/L) after transfusions, if needed; ANC $\geq$ 1.5 x 10^9/L; platelets $\geq$ 100 x 10^9/L; and no clinically significant non-haemotologic drug related toxicities. If a patient failed to meet these criteria, the next treatment course was delayed until the criteria were met. If treatment was delayed more than two weeks beyond the last day of the previous treatment course, the patient would be withdrawn from the study. A dose reduction of 0.4 mg/m^2/d for oral topotecan treatment or a 0.25 mg/m^2/d dose reduction with iv topotecan treatment was required at the start of each new treatment cycle if a patient experienced any of the following: Grade 4 neutropenia (neutrophils < 500/mm^3) associated with either fever/infection or lasting $\geq$ 7 days; neutrophils $\leq$ 900/mm^3 lasting beyond Day 21; platelets $\leq$ 25,000/mm^3; or Grade 3/4 non-hematologic toxicity excluding Grade 3 nausea and Grade 3/4 vomiting. The minimum dose permitted during study was 1.5 mg/m^2/d for oral topotecan and 1.0 mg/m^2/d for i.v. topotecan. Delays of more than 2 weeks at this dose resulted in withdrawal from the study. Disease assessments of tumour burden were performed at baseline and every other cycle as clinically indicated, using the same radiological imaging method used at baseline. Responses to therapy were not collected during this study, and investigators were allowed to use the prevailing response assessment guidelines at their site (e.g., WHO or RECIST criteria). Approximately 28 days following the last dose of topotecan or discontinuation from treatment, patients returned for a final study evaluation.

Study Drug Description

Oral topotecan was supplied by GlaxoSmithKline as capsules containing topotecan hydrochloride, equivalent to either 0.25 or 1.0 mg of the anhydrous free base. Supplies included both the current and new topotecan formulations. Intravenous topotecan was supplied to the site as needed in vials containing 4 mg of topotecan as the free base.

Pharmacokinetic sample collection, processing and analysis

Whole blood samples of 5 mL were collected in lithium-containing tubes in Course 1, on Days 1 and 8 and if appropriate during Course 2, on Day 1. Topotecan blood sample collection occurred before dosing and at 0.25, 0.5, 1.0, 1.5, 2, 3, 4, 6, 8, 12 and 24 h after oral topotecan dosing. Blood samples were collected and processed as previously described (18). Briefly, blood samples were centrifuged at 4ºC for 10 minutes and plasma separated, aliquoted, and then frozen and stored at -30ºC until analyzed. One mL aliquot of plasma was added to two mL of ice-cold methanol, mixed, and centrifuged. The methanol supernate was separated and stored at -30ºC to maintain the ratio between the lactone and carboxylate forms of topotecan ex vivo. The plasma concentrations of total topotecan (lactone + carboxylate) and topotecan lactone were determined using a previously published, validated high performance liquid chromatography (HPLC) assay using good laboratory practice (18).

Pharmacokinetic analyses

The following pharmacokinetic parameters were derived for each patient from the observed plasma concentration-time data of total topotecan and topotecan lactone using standard non-compartmental analysis with WinNonLin software (version 4.1a, Pharsight Corporation, Mountain View, CA). The primary pharmacokinetic endpoints for bioequivalence were the area under the plasma concentration-time curve for time zero to infinity ($AUC_{(0-\infty)}$) and the maximal drug concentration (C_{max}) for topotecan lactone. The primary endpoints for the food-effect component of the study were $AUC_{(0-\infty)}$ and C_{max} for topotecan lactone and total topotecan. The secondary endpoints were the terminal elimination half-life ($t_{1/2}$), time to maximum drug concentration (t_{max}) and area under the plasma concentration-time curve for time zero to the last quantifiable time point ($AUC_{(0-t)}$) for topotecan lactone and C_{max}, $t_{1/2,}$ t_{max}, $AUC_{(0-t)}$, and $AUC_{(0-\infty)}$ for total topotecan. C_{max} and t_{max} were determined directly from the observed plasma concentration data. $AUC_{(0-t)}$ and $AUC_{(0-\infty)}$ were calculated using the linear trapezoidal rule for all incremental trapezoids arising from increasing concentrations and the logarithmic trapezoidal rule for those arising from decreasing concentrations. $AUC_{(0-\infty)}$ was estimated as the sum of $AUC_{(0-t)}$ and C_t

divided by the elimination rate constant, where C_t was the observed concentration value at the last measurable time point. Half-life was calculated as $0.693/\lambda_z$ (where λ_z is the calculated terminal elimination rate constant).

Statistical analysis

A four-stage group-sequential design with three interim analyses was used after approximately 50%, 65%, and 80% of the maximum information available, respectively. O'Brien-Fleming stopping boundaries for early stopping to accept or reject bioequivalence were used to control the overall error probabilities. No adjustments for multiple endpoints were made (19). The final target sample size was based on an information scale using EaSt software's *Information Based* approach [EaSt Cytel Software Corporation]. With a final target sample size of 106 subjects, driven by the largest intra-subject coefficients of variation (CVw = 45.5%) from the previous studies, Canadian regulatory guidance, the use of interim analysis, and the assumption of a true ratio of unity, this study design would provide at least 90% power to demonstrate bioequivalence of the new and the current formulation, based on the FDA criteria.

To demonstrate bioequivalence, a two-one sided testing procedure (20) of new to current formulation for $AUC_{(0-\infty)}$ and C_{max} of topotecan lactone was used on the basis of mixed-effect analysis of variance model, fitting the terms for sequence, regimen, and gender as the fixed effects, and the term for patients within sequences as the random-effect, using SAS (Version 8.2) Mixed Linear Models procedure. Bioequivalence between the new and current formulation would be demonsrated, if the 90% confidence intervals of the ratio of both parameters of the new to the current formulation were contained within the range 0.8 to 1.25. Based on Canadian regulatory guidance, bioequivalence was tested for $AUC_{(0-\infty)}$ and C_{max} of topotecan lactone utilizing adjusted 95% CIs for the comparisons of interest.

An estimation approach was to be used to evaluate the effect of food on the new formulation of oral topotecan, in which point estimates and associated 90% CIs for the ratio of fed to fasted status were constructed to provide a plausible range of values for the comparisons of interest. Based on the largest of the % CVw estimates (45.5% for C_{max} for topotecan lactone) and a sample size of 24 subjects completing the fed arm of the study, it was estimated that the half-width of the 90% CI for the fed:fasted comparison would be no more than 24% for C_{max}. This calculation was based on a symmetric two-tailed procedure and a type I error rate of 10%.

The final analysis was based on all the data collected. The 'buy-back boundary' method (21) was applied to analyze the primary and secondary endpoints after a properly stopped sequential trial. They were statistically analyzed using the same model described above, except t_{max}. Wilcoxon Method (22) as a non-parametric approach was used to provided the point estimate and 90% and 95% CIs for the median difference "fed-fasted" in t_{max}. Safety data were descriptively summarized with no formal statistical analysis.

Results

Patient Characteristics

Patients were recruited from cancer centers in the United States (n = 6) and the Netherlands (n = 2). Between October 2004 and December 2006, a total of 108 patients were recruited and enrolled in the study. Patient demographics are presented in Table 2. The population used for this pharmacokinetic study consisted of 85 subjects randomized to the bioequivalence study and 23 subjects randomized to the food-effect study. Seven subjects who were initially treated in the bioequivalence component of the study also participated in the food-effect component. Subjects were considered to have completed the study if they received study drug on all 5 planned dosing days of Course 1 and had a complete set of pharmacokinetic samples collected on Days 1 and 8. As detailed in Table 2, the median age of the patients was 57.5 years (range, 28 to 80 years) and the median ECOG performance status was 1 (range, 0 to 2). The majority of subjects (96%) had received prior chemotherapy. The most common tumor types enrolled in the study were ovary (n = 26), SCLC (n = 14) and prostate (n = 10). All 108 subjects received concomitant medications during the study. These medications included, but were not limited to nutritional supplements, pain medications, and treatments for adverse events (AEs).

Table 2. Patient Demographics.

		Number of Patients (n)	% of patients
No. of patients entered	Included in safety analysis	108	100
	Randomized to bioequivalence study	85	79
	Randomized to food-effect study	23	21
	Bioequivalence patients who also participated in food-effect	7	6
Completion status	No. of patients completed[1]	103	95
	No. of patients prematurely withdrawn	5	5
Primary reason for withdrawal of completed subjects	Disease Progression	64	59
	Adverse Event	13	12
	Subject Decided to Withdraw from study	11	10
	Death	7	6
	Other-General Deterioration	6	6
	Missing	2	2
Primary reason for withdrawal of prematurely withdrawn subjects	Adverse event	2	2
	Subject decided to withdraw	2	1
	Disease progression	1	1
Gender	Male	39	36
	Female	69	64
Age	Median years	57.5	
	Range	28-80	
Race	African American/African Heritage	15	14
	White-Arabic/North African Heritage	2	2
	White-White/Caucasian/European Heritage	91	84
Tumor types	Ovary	26	24
	Small Cell Lung	14	13
	Prostate	10	9
	Pancreas	7	6
	Non-Small Cell Lung	6	6
	Colon/Rectum	6	6
	Other	39	36
ECOG performance status at Baseline	0	31	29
	1	63	58
	2	14	13
Previous therapy (subjects could have more than one prior therapy)	Chemotherapy	104	96
	Radiotherapy	45	42
	Hormonal therapy	13	12
	Biological therapy	9	8
	Immunotherapy	2	2

[1] Subjects were considered to have completed the study if they received study drug on all 5 planned dosing days of Course 1 and completed Course 1 PK sampling on Days 1 and 8

Pharmacokinetics

Bioequivalence study

The first planned interim analysis was performed on plasma concentration-time data from 56 patients to evaluate bioequivalence and to re-estimate the final target study sample size. Bioequivalence was demonstrated with data from 56 patients, as the 90% and 95% CIs of the ratio of the new to current formulation for $AUC_{(0-\infty)}$ and C_{max} for topotecan lactone were completely contained within the range of 0.80 to 1.25. A final sample size in the bioequivalence portion of the study given enrollment was not interrupted during the interim analysis was 85 patients. Of these, 78 subjects contributed data to the final statistical analysis of bioequivalence, only those subjects with pharmacokinetic values for both treatment days were included. The mean plasma total topotecan and topotecan lactone concentration versus time data for the two topotecan formulations are shown in Fig. 1A. The primary ($AUC_{(0-\infty)}$ and C_{max} for topotecan lactone) and secondary ($AUC_{(0-\infty)}$, C_{max}, $AUC_{(0-t)}$ and $t_{1/2}$ for total topotecan and $AUC_{(0-t)}$ and $t_{1/2}$ for topotecan lactone) pharmacokinetic parameters, point estimates, 90 and 95% CIs, and within-subject variabilities for the new versus the current formulation are summarized in Table 3. Bioequivalence was demonstrated, as the adjusted 90 and 95% CIs of the ratio of the new formulation to current formulation for $AUC_{(0-\infty)}$ and C_{max} for topotecan lactone were completely contained within the range of 0.80 to 1.25. The secondary pharmacokinetic endpoints, $AUC_{(0-t)}$ and $t_{1/2}$ for topotecan lactone and $AUC_{(0-\infty)}$, C_{max}, $AUC_{(0-t)}$ and $t_{1/2}$ for total topotecan, also demonstrated bioequivalence (Table 3).

Food effect Part

Of the 108 patients enrolled, 23 patients participated in the food-effect component only. Seven subjects participated in both the bioequivalence and food-effect parts of the study. Four of the 23 patients were not included in the statistical analysis of the food-effect due to dosing errors or incomplete high-fat meal consumption. The mean plasma topotecan and topotecan lactone concentration versus time data for the fed and fasting states are shown in figure 1B. Pharmacokinetic parameter values for topotecan lactone and total topotecan are listed in Table 3. In the presence of a high-fat meal, there was a mean increase of approximately 10% in $AUC_{(0-\infty)}$ of topotecan lactone and $AUC_{(0-\infty)}$ and C_{max} of total topotecan. Food increased the median t_{max} from 1.5 to 3 h for topotecan lactone and from 3.0 to 4.0 h for total topotecan.

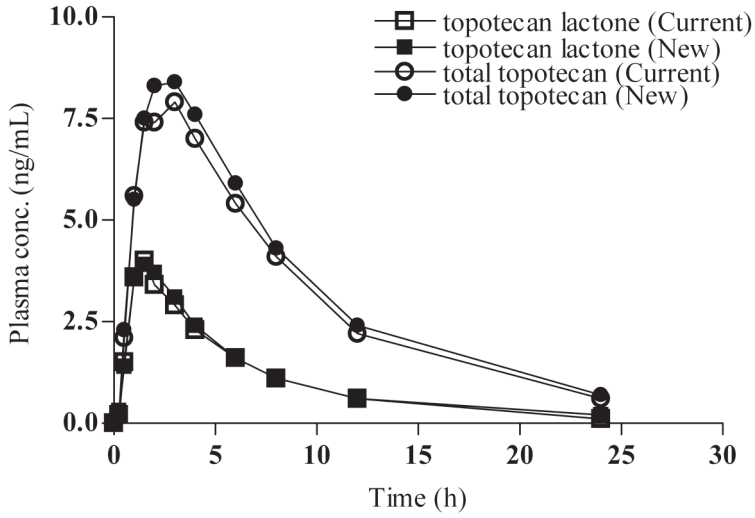

A

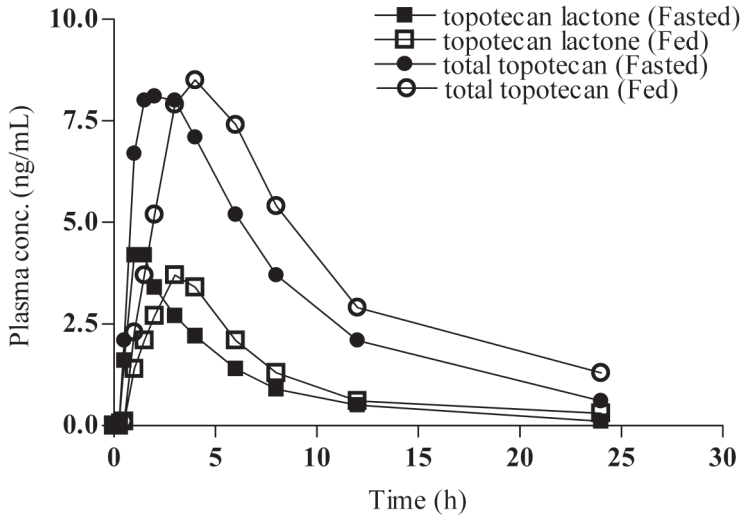

B

Figure 1. Mean plasma concentration-time profiles of topotecan lactone and total topotecan of the new (■ and ●, respectively) and current (□ and ○, respectively) formulation (A) and toptocan lactone and total topotecan of the new formulation under fed (■ and ●, respectively) or fasted (□ and ○, respectively) conditions

Table 3. Geometric mean ± SD pharmacokinetic parameters of topotecan lactone and total topotecan for the new versus the current formulation.

Bioequivalence						
parameter	**formulation**	**Geom. Mean (SD)**	**Ratio new:current**	**90% CI**	**95% CI**	**CVw (%)**
$AUC_{(0-\infty)}$ (h.ng/mL)						
topotecan lactone	new	23.2 (12.8)	1.04	0.98-1.11	0.97-1.13	24.22
	current	22.3 (12.5)				
total topotecan	new	73.9 (37.4)	1.06	1.00-1.12	0.99-1.13	21.37
	current	69.7 (37.7)				
C_{max} (ng/mL)						
topotecan lactone	new	4.4 (4.0)	1.01	0.91-1.11	0.90-1.13	37.01
	current	4.4 (3.6)				
total topotecan	new	8.9 (6.0)	1.06	0.99-1.14	0.98-1.16	27.71
	current	8.4 (5.1)				
$AUC_{(0-t)}$ (h.ng/mL)						
topotecan lactone	new	21.1 (12.4)	1.05	0.98-1.12	0.96-1.13	25.89
	current	20.2 (11.9)				
total topotecan	new	68.6 (33.5)	1.06	1.00-1.12	0.99-1.14	21.62
	current	64.5 (34.4)				
$t_{1/2}$ (h)						
topotecan lactone	new	4.9 (2.0)	1.03	0.96-1.11	0.95-1.13	27.44
	current	4.7 (2.0)				
total topotecan	new	5.7 (1.5)	1.02	0.98-1.06	0.97-1.07	15.06
	current	5.6 (1.5)				
Food-Effect Part						
parameter	**Fasted/Fed**	**Geom. Mean (SD) (ng.h/mL)**	**Ratio fed:fasted**	**90% CI**	**95% CI**	**CVw (%)**
$AUC_{(0-\infty)}$ (h.ng/mL)						
topotecan lactone	fed	24.8 (10.8)	1.10	0.97-1.24	0.95-1.27	25.22
	fasted	21.9 (10.1)				
total topotecan	fed	76.3 (43.4)	1.05	0.94-1.18	0.91-1.21	23.57
	fasted	68.6 (41.2)				
C_{max} (ng/mL)						
topotecan lactone	fed	4.1 (2.6)	0.97	0.79-1.20	0.75-1.26	46.92
	fasted	4.2 (3.4)				
total topotecan	fed	9.3 (5.4)	1.11	0.96-1.29	0.93-1.33	31.2
	fasted	8.4 (5.2)				
t_{max} (h)[1]						
topotecan lactone	fed	3.0 (1.0 to 8.0)	1.76	1.00-2.51	0.84-2.75	-
	fasted	1.5 (0.5 to 6.0)				
total topotecan	fed	4.0 (1.0 to 12.0)	1.76	1.01-2.73	0.98-2.76	-
	fasted	3.0 (0.5 to 6.0)				

[1] t_{max} is median and range and the stats are differences (fed-fasted) not ratio

Safety Results

All 108 subjects enrolled experienced at least one AE, the majority of events were assessed as grade 1 or 2 in severity (Table 4). The most common drug-related AEs were neutropenia (59%), nausea (59%), anemia (58%), fatigue (50%), thrombocytopenia (45%), and leucopenia (40%). The most frequent grade 3 haematological AEs were anemia (24%), neutropenia (22%), thrombocytopenia (18%), leucopenia (15%), while the most frequent grade 4 haematological AEs were neutropenia (22%) and leukopenia (8%). Febrile neutropenia was reported for 5% of all subjects with 3% assessed as grade 3 and 2% as grade 4. The most frequently reported grade 3 non-hematological AE was dyspnea (6%). grade 4 non-haematological AEs were reported for < 5% of the patients.

Death was reported for 16 study subjects. Of these, death in 15 subjects was assessed as related to disease progression. In one subject, death was attributed to dyspnea that was considered unrelated to study drug. This subject had metastatic follicular thyroid cancer with lung, pleural, and lymph node involvement at baseline. For eleven of the 15 subjects who died, fatal serious adverse events (SAEs), none assessed as related to study drug, were reported with the death. Non-fatal SAEs were reported for 34% of patients. The most frequently reported SAEs, regardless of causality, were dyspnea (total 7%; 3% fatal), anemia (6%) and thrombocytopenia (5%). All SAEs of dyspnea were experienced by subjects who had either a primary lung tumor or metastatic involvement of the lung and pleura and none were considered related to topotecan. All other SAEs were reported in ≤ 5% of subjects. Drug-related SAEs were reported for 11% of subjects, including anemia (6%), thrombocytopenia (5%), febrile neutropenia (4%), neutropenia (4%), and dehydration (3%). Other drug-related SAEs were each reported in < 1% of subjects and included pancytopenia, neutropenic infection, pneumonia, and vomiting.

AEs leading to permanent discontinuation of study drug or early withdrawal from the study were experienced by 13% of patients. Of these, 7% of subjects experienced AEs assessed as drug-related that led to discontinuation/withdrawal including anemia, leucopenia, thrombocytopenia, pancytopenia, fatigue, nausea, vomiting, pneumonia and dizziness. In total, 31% of subjects had their dose of study drug interrupted or reduced due to an AE, most often a hematological toxicity.

The most common treatment-emergent clinical chemistry laboratory abnormalities (inclusive of all grades) were hyperglycemia, hypoalbuminemia, hypocalcemia, hyponatremia, increased alkaline phosphatase, increased AST, and increased ALT. The most common grade 3 and 4 clinical chemistry laboratory abnormality was elevated gamma-glutamyl transferase affecting 16% of all subjects. The most common treatment-emergent hematological laboratory abnormalities (including all grades) were leucopenia,

anemia, neutropenia, and thrombocytopenia. The most common grade 3 or 4 hematological laboratory abnormalities were leucopenia and neutropenia affecting 54% and 51% of all subjects, respectively.

Table 4. Summary of treatment related and unrelated non-hematological and hematological Adverse Events (AEs) in patients treated with oral topotecan capsules of the new and current formulation.

Most frequent Adverse Events (AEs)	Study drug related	Regardless of relationship		
Any AE	101 (94%)	108 (100%)		
Any AE related to investigational product				
Most Common AEs (≥ 10% of patients):			Grade 3	Grade 4
Non-hematological				
Nausea	64 (59%)	71 (66%)	3 (3%)	0
Fatigue	54 (50%)	65 (60%)	4 (4%)	1 (<1%)
Diarrhea	38 (35%)	54 (50%)	4 (4%)	0
Vomiting	39 (36%)	48 (44%)	3 (2%)	1 (<1%)
Alopecia	33 (31%)	35 (32%)	0	0
Constipation	18 (17%)	35 (32%)	2 (2%)	0
Anorexia	29 (27%)	34 (31%)	0	0
Dyspnea	3 (3%)	22 (20%)	6 (6%)	3 (3%)
Abdominal pain	2 (2%)	20 (19%)	3 (3%)	0
Pyrexia	4 (4%)	20 (19%)	0	0
Headache	5 (5%)	16 (15%)	0	0
Dizziness	4 (4%)	15 (14%)	0	0
Cough	1 (<1%)	14 (13%)	1 (<1%)	0
Dyspepsia	7 (6%)	11 (10%)	0	0
Hematological[1]				
Anemia	63 (58%)	66 (61%)	26 (24%)	1 (<1%)
Neutropenia	64 (59%)	64 (59%)	24 (22%)	24 (22%)
Thrombocytopenia	49 (45%)	50 (46%)	19 (18%)	4 (4%)
Leucopenia	43 (40%)	44 (41%)	16 (15%)	9 (8%)
Febrile neutropenia	5 (5%)	5 (5%)	3 (3%)	2 (2%)

[1]The frequency of hematologic adverse events reported here are based on AEs reported by investigators. These results differ from frequencies of hematologic toxicities based on laboratory data alone reported in the Discussion section.

Discussion

In this study a new oral topotecan formulation, synthesized by a new process, was compared to the current oral topotecan formulation to assess bioequivalence. The current

oral topotecan formulation was used in previous efficacy and safety clinical trials (6-11, 13, 14, 23). In addition, the effect of food on the new formulation was determined.

To assess bioequivalence and the effect of food on the new formulation, all patients received the same dose (4 mg, 4 x 1 mg capsule) on Day 1 and Day 8 of Course 1 and if appropriate on Day 1 of Course 2. The topotecan dose was subsequently adjusted on Days 9-11 for Course 1 and, if appropriate, on Days 2-5 for Course 2, to ensure that the total cumulative dose for each course was the same as for the standard dosing regimen (2.3 mg/m^2/day x 5 days). By requiring all patients receive a standard dose of 4 mg (4 x 1 mg capsule) on pharmacokinetic sampling days 1 and 8, the study was designed to assess bioequivalence of the 1 mg capsule. Bioequivalence was successfully demonstrated at the first interim analysis based on data from 56 patients. Since enrollment continued while data from the interim analysis was obtained and analyzed, the final number of patients enrolled for the bioequivalence component of the study was 85 of which 78 patients were included in the final analysis.

A previously published study assessed the effect of a high-fat meal on the absorption and disposition of the current oral topotecan formulation (14). Results from that prior study were similar to the current study data indicating an approximate 10% increase in $AUC_{(0-\infty)}$ (topotecan lactone and total topotecan) and C_{max} (total topotecan) and similar C_{max} values (topotecan lactone) in the presence of a high-fat meal. As in this study, the median t_{max} in the previous food-effect study was also increased in the presence of a high-fat meal from 1.0 to 3.0 h (topotecan lactone) and 2.0 to 3.0 h (total topotecan). Food, particularly fat, slows down gastric emptying and therefore the changes in t_{max} are not unexpected.

In the current study, important grade 3/4 hematologic laboratory abnormalities of neutropenia, thrombocytopenia, and anemia occurred in 51%, 29%, and 22% of patients, respectively (data not shown). This is consistent with the incidence of hematological toxicity observed during previous oral topotecan studies (13, 22). Diarrhea was reported in 50% of the patients in this study, including 4% assessed as grade 3 with none assessed as grade 4. In comparison with other studies of the daily x 5 schedule of oral topotecan, diarrhea has been reported in 21% to 58% of patients (in each study $\leq$ 16% grade 3, $\leq$ 4% grade 4) (7, 11, 13, 23).

In studies of the approved commercial i.v. formulation of topotecan (Hycamtin®), diarrhea was reported less frequently in 20% patients (2.7% grade 3 or 4) (13). Other common gastrointestinal-related AEs in this study (Table 4) were assessed mostly as grade 1-2 in severity and were reported at a frequency comparable to the i.v. formulation nausea 64%, vomiting 45%, and constipation 29% (16). Alopecia was reported for 31% of patients in

this study compared to a 20% to 53% incidence in previous studies of daily x 5 schedule of oral topotecan (7, 11, 13, 23) and 49% incidence in studies of the approved commercial i.v. formulation of topotecan (16).

Conclusion

In conclusion, bioequivalence was demonstrated, as the 90% and 95% CIs of the ratio of the new to current formulation for both C_{max} and $AUC_{(0-\infty)}$ for topotecan lactone were completely contained within the range of 0.80 to 1.25. Following a high-fat meal, the extent of systemic exposure was similar in the fed and fasted state while food delayed the t_{max}. The most common drug-related AEs observed during this study included hematological (i.e., neutropenia, anemia, thrombocytopenia) and gastrointestinal (nausea, vomiting, diarrhea, anorexia) toxicities as well as fatigue and alopecia. Based on these study results, the new oral topotecan capsule formulation is bioequivalent to the current formulation and could be used for clinical application according to the labeled indications.

References

1. Hsiang YH, Liu LF. Identification of mammalian DNA topoisomerase I as an intracellular target of the anticancer drug camptothecin. Cancer Res 1988;48:1722-1726.
2. Kingsbury WD, Boehm JC, Jakas DR, et al. Synthesis of water-soluble (aminoalkyl)camptothecin analogues: inhibition of topoisomerase I and antitumor activity. J Med Chem 1991;34:98-107.
3. Von Pawel J, Schiller JH, Shepherd FA, et al. Topotecan versus cyclophosphamide, doxorubicin, and vincristine for the treatment of recurrent small-cell lung cancer. J Clin Oncol 1999;17:658-667.
4. Ten Bokkel Huinink W, Gore M, Carmichael J, et al. Topotecan versus paclitaxel for the treatment of recurrent epithelial ovarian cancer. J Clin Oncol 1997;15:2183-2193.
5. Ardizzoni A, Hansen H, Dombernowsky P, et al. Topotecan, a new active drug in the second-line treatment of small-cell lung cancer: a phase II study in patients with refractory and sensitive disease. The European Organization for Research and Treatment of Cancer Early Clinical Studies Group and New Drug Development Office, and the Lung Cancer Cooperative Group. J Clin Oncol 1997;15:2090-2096.
6. Gerrits CJ, Burris H, Schellens JH, et al. Oral topotecan given once or twice daily for ten days: a phase I pharmacology study in adult patients with solid tumors. Clin Cancer Res 1998;4:1153-1158.
7. Creemers GJ, Gerrits CJ, Eckardt JR, et al. Phase I and pharmacologic study of oral topotecan administered twice daily for 21 days to adult patients with solid tumors. J Clin Oncol 1997;15: 1087-1093.
8. Gerrits CJ, Schellens JH, Burris H, et al. A comparison of clinical pharmacodynamics of different administration schedules of oral topotecan (Hycamtin). Clin Cancer Res 1999;5:69-75.
9. Schellens JH, Creemers GJ, Beijnen JH, et al. Bioavailability and pharmacokinetics of oral topotecan: a new topoisomerase I inhibitor. Br J Cancer 1996;73:1268-1271.
10. Von Pawel J, Gatzemeier U, Pujol JL, et al. Phase ii comparator study of oral versus intravenous topotecan in patients with chemosensitive small-cell lung cancer. J Clin Oncol 2001;19:1743-1749.
11. Gerrits CJ, Burris H, Schellens JH, et al. Five days of oral topotecan (Hycamtin), a phase I and pharmacological study in adult patients with solid tumours. Eur J Cancer 1998;34:1030-1035.
12. Gralla R, Eckardt JR, von Pawel J. Quality of life with single agent oral topotecan vs intravenous topotecan in patients with chemosensitive small cell lung cancer (SCLC): An international phase III study. Lung Cancer 2003;41.
13. Eckardt JR, von Pawel J, Pujol JL, et al. Phase III study of oral compared with intravenous topotecan as second-line therapy in small-cell lung cancer. J Clin Oncol 2007;25:2086-2092.
14. Herben VM, Rosing H, Bokkel Huinink WW, et al. Oral topotecan: bioavailablity and effect of food co-administration. Br J Cancer 1999;80:1380-1386.

15. Kuppens IE, Witteveen EO, Jewell RC, et al. A phase I, randomized, open-label, parallel-cohort, dose-finding study of elacridar (GF120918) and oral topotecan in cancer patients. Clin Cancer Res 2007;13:3276-3285.
16. Eckardt JR, von Pawel J, Papai Z, et al. Open-label, multicenter, randomized, phase III study comparing oral topotecan/cisplatin versus etoposide/cisplatin as treatment for chemotherapy-naive patients with extensive-disease small-cell lung cancer. J Clin Oncol 2006;24:2044-2051.
17. Ajani JA, Welch SR, Raber MN, et al. Comprehensive criteria for assessing therapy-induced toxicity. Cancer Invest 1990;8:147-159.
18. Rosing H, Doyle E, Davies BE, et al. High-performance liquid chromatographic determination of the novel antitumour drug topotecan and topotecan as the total of the lactone plus carboxylate forms, in human plasma. J Chromatogr B Biomed Appl 1995;668:107-115.
19. Jennison C and Turnbull B. Group sequential methods with applications to clinical trials. Chapman & Hall 2000.
20. Schuirmann DJ. A comparison of the two one-sided tests procedure and the power approach for assessing the equivalence of average bioavailability. J Pharmacokinet Biopharm 1987;15:657-680.
21. Lan KK, Lachin JM and Bautista O. Over-ruling a group sequential boundary-a stopping rule versus a guideline. Stat Med 2003;22:3347-3355.
22. Steinijans VW, Diletti E. Statistical analysis of bioavailability studies: parametric and nonparametric confidence intervals. Eur J Clin Pharmacol 1983;24:127-136.
23. O'Brien ME, Ciuleanu TE, Tsekov H, et al. Phase III trial comparing supportive care alone with supportive care with oral topotecan in patients with relapsed small-cell lung cancer. J Clin Oncol 2006;24:5441-5447.

CHAPTER 4

Preclinical and clinical pharmacological studies on taxanes

CHAPTER 4.1

Co-administration of ritonavir strongly enhances the apparent oral bioavailability of docetaxel in patients with solid tumors

Roos L. Oostendorp, Alwin Huitema, Hilde Rosing, Robert S. Jansen, Rob ter Heine, Marianne Keessen, Jos H. Beijnen, Jan H.M. Schellens

Submitted for publication

Abstract

The oral bioavailability of docetaxel is very low, which is due to affinity for P-glycoprotein (P-gp) and metabolism of docetaxel by cytochrome P450 (CYP) 3A4. The purpose of this study was to enhance the systemic exposure to oral docetaxel by co-administration of ritonavir (RTV), an efficacious inhibitor of CYP 3A4 with minor P-gp inhibiting effects. A proof-of-concept study was carried out in 12 patients with solid tumors. The first cohort of patients (n = 4) received 10 mg and the subsequent cohort (n = 8) 100 mg of oral docetaxel, co-administered with 100 mg oral RTV randomized simultaneous or with a 60 minutes time interval on day 1 and 8. On day 15 or 22, patients received 100 mg intravenous (i.v.) docetaxel. The area under the plasma concentration-time curve (AUC) in patients who received 10 mg oral docetaxel in combination with RTV was low and the dose could safely be increased to 100 mg. The AUC in patients who received 100 mg oral docetaxel combined with RTV simultaneous or with a 60 minutes time interval was 2.4 ± 1.5 and 2.8 ± 1.4 mg.h/L, respectively, compared to 1.9 ± 0.4 mg.h/L after i.v. docetaxel. The apparent oral bioavailability of docetaxel combined with RTV simultaneous or 60 minutes time interval was 131% ± 90% and 161% ± 91%, respectively. The oral combination of docetaxel and RTV was well tolerated. Co-administration of RTV significantly enhanced the apparent oral bioavailability of docetaxel. There was no significant difference between the AUC of docetaxel when taken simultaneous with RTV or with a 60 min time interval. These data are promising and form the basis for further development of a clinically applicable oral formulation of docetaxel combined with RTV.

Introduction

There is an increasing interest in the development of oral treatment regimens of anticancer drugs. Patient convenience, practicality and pharmacoeconomics are major arguments in favor of oral therapy (1-3). In addition, weekly schedules of docetaxel are increasingly being used (4, 5). The oral route facilitates the use of more chronic treatment regimens, which results in more frequent exposure of tumor cells to the cytotoxic agent while lower maximal plasma concentration (C_{max}) values are reached (6). For the taxane docetaxel, an anticancer agent widely applied against numerous tumors, the low and variable oral bioavailability has limited the development of oral treatment regimens. This is, at least in part, due to the high affinity of docetaxel for the multidrug efflux pump P-glycoprotein (P-gp) (7). Preclinical and clinical studies in our group showed that co-administration of oral cyclosporin A, a strong inhibitor of P-gp and a substrate for the cytochrome P450 (CYP) 3A4 metabolic enzyme, significantly enhanced the oral bioavailability of docetaxel (8, 9). However, the development of this combination was terminated because preclinical and clinical research showed that first-pass elimination by CYP3A4 in the liver and/or gut wall contributed much more to the low oral bioavailability of docetaxel than blockade by P-gp (10-12). Clinical studies have demonstrated that less than 10% of administered docetaxel is excreted unchanged in the urine, suggesting an important role for hepatic metabolism (9). This has been supported by *in vivo* experiments in mice (12). Pre-clinical experiments, conducted in P-gp knockout and wild-type mice, have shown a significant increase in systemic exposure when docetaxel was co-administered orally with ritonavir (RTV) (12). The pre-clinical dosages (docetaxel 10-30 mg/kg; RTV 12.5 mg/kg) were, however, far higher than normally used in humans. RTV is a HIV protease inhibitor, with strong CYP3A4 inhibiting properties and with only minor P-gp inhibiting effects (13). Furthermore, the enhancement of the systemic exposure of CYP3A4 substrates by RTV is already standard practice in the treatment of HIV patients with protease inhibitors (14, 15). Recently, van Herwaarden et al (16) demonstrated that the absence of Cyp3a activity in mice alone increased the systemic exposure of docetaxel after oral administration *in vivo* 17.7-fold. They also indicated that RTV most likely is highly efficacious in inhibiting CYP3A and has high specificity for CYP3A4. We hypothesized that the systemic exposure of orally administered docetaxel could be increased by co-administration of RTV in patients, although the preclinically used dosages were far higher than considered safe in humans. To investigate this, we initiated a proof-of-concept study with low dosages of docetaxel in patients with solid tumors.

Patients and Methods

Patient Population

Patients for whom no standard therapy of proven benefit existed and with a histologically confirmed cancer refractory to current therapies were eligible for the study. Other eligibility criteria included the following: age ≥ 18 years; life expectancy ≥ 3 months; previous radiotherapy or chemotherapy was allowed, provided that the last treatment was at least 3 weeks before study entry and any resulting toxicities were resolved; hormonal therapy should be stopped at least one week prior to start of the study. Eligibility criteria included acceptable bone marrow function (WBC count > 3.0 x 10^9/L; platelet count > 100 x 10^9/L), liver function (serum bilirubin level ≤ 20 μmol/L; serum albumin level ≥ 25 g/L), and renal function (serum creatinine level ≤ 160 μmol/L or clearance ≥ 50 mL/min) and a World Health Organization (WHO) performance status ≤ 2. Patients were not eligible if they suffered from uncontrolled infectious disease, neurologic disease, bowel obstructions, or symptomatic brain metastases, alcoholism, drug addiction, psychotic disorders leading to inadequate follow-up or pregnancy. Other exclusion criteria were concomitant use of known P-gp inhibitors and chronic use of H_2-receptor antagonists or proton pump inhibitors. The study protocol was approved by the medical ethics committee of the institute, and all patients had to give written informed consent prior to start of the study.

Study design

A proof-of-concept study was carried out in 12 patients with advanced solid malignancies. In the first part of the study, 4 patients were randomized to receive 10 mg of oral docetaxel co-administered with a 100 mg oral dose of RTV simultaneously or with a 60 min time interval on day 1 and 8 of cycle one. On day 15 of cycle one, patients received 100 mg i.v. docetaxel. In the second part of the study, 8 patients were randomized to receive 100 mg of oral docetaxel co-administered with a 100 mg oral dose of RTV simultaneous or with a 60 min time interval on day 1 and 8 of cycle one. On day 22 of cycle one, patients received 100 mg i.v. docetaxel. If it was considered to be in their best interest, patients continued on a 3-weekly schedule of i.v. docetaxel (100 mg/m^2) (cycle 2, 3 etc.). In the first part, an oral docetaxel dose of 10 mg was selected for safety reasons because nonclinical data in mice revealed that co-administration of RTV resulted in a 50-fold increase in the systemic exposure to orally applied docetaxel (12). In the second cohort, a dose increase to 100 mg of oral docetaxel was considered justified, based on the pharmacokinetic and safety data obtained in the first part of this study and an earlier study conducted by Malingré et al. (9).

Drug administration

The i.v. formulation of docetaxel (Taxotere; Rhone-Poulenc Rorer/Aventis, Antony, France) was used for both i.v. and oral administration. RTV (Abbott, Illinois, USA) was given immediately before or 60 min before oral docetaxel administration. Oral drugs were taken with 100 mL of tap water after an overnight fast. Patients remained fasted until 1.5 h after docetaxel administration. Standard docetaxel pretreatment was given during all cycles and consisted of oral dexamethasone 4 mg 1 h before drug administration and 4 mg every 12 h (two times) after drug administration. One hour before oral docetaxel administration, patients received 1 mg of oral granisetron.

Patient evaluation

Pretreatment evaluation included a complete medical history and complete physical examination. Before each course, an interim history including concomitant drugs taken, toxicities, and performance status were registered, and a physical examination was performed. Hematology, blood chemistries, including liver and renal function, serum electrolytes, total protein, albumin and glucose levels, were checked weekly. All toxicities observed were graded according to the National Cancer Institute Common
Toxicity Criteria for Adverse Events (NCI CTCAE) version 3.0. Dose-limiting toxicity was defined as grade 4 granulocytopenia lasting more than 5 days, grade 4 thrombocytopenia of any duration, or any grade 3 or 4 nonhematologic toxicity except alopecia and untreated nausea and vomiting. Tumor measurements were performed every other cycle but initially after the first two i.v. cycles. Responses were evaluated according to the RECIST criteria (17).

Pharmacokinetic sample collection and sample analysis

Pharmacokinetic monitoring was performed during cycle one day 1, 8, and 15 or 22 for docetaxel and on day 1 and 8 for RTV. For plasma docetaxel and RTV concentrations, blood samples of 5 mL each were collected in heparinized tubes. After oral or i.v. administration, samples were obtained before dosing, and at 15, 30, 45, 60, 75 and 90 min, 2, 3, 4, 6, 8, 10, 24, 36, and 48 h after docetaxel. Blood samples were centrifuged, plasma was separated, and docetaxel and RTV samples were immediately stored at -20ºC until analysis. Docetaxel and RTV concentrations in plasma were determined using validated liquid chromatography coupled with tandem mass spectrometry methods (18, 19).

Pharmacokinetic and statistical analysis

Pharmacokinetic parameters were calculated by the noncompartmental trapezoidal method using the software package WinNonlin Professional (version 5.0, Pharsight, Mountain View, CA, USA). The area under the plasma concentration-time curve (AUC) was calculated from time 0 to 48 h and with extrapolation to infinity using the terminal rate constant k. The apparent oral bioavailability (F) was calculated by the formula $F = (AUC_{oral} \times dose_{i.v.})/(AUC_{i.v.} \times dose_{oral}) \times 100\%$. Other parameters to be assessed were the maximal plasma concentration (C_{max}), the time to maximal plasma concentration (t_{max}), the plasma clearance (Cl) after i.v. administration, and the volume of distribution (V_d) during the elimination phase. Statistical analysis of the data was performed using nonparametric Mann-Whitney *U* test. The level of significance was set at $P < 0.05$.

Results

Patient characteristics

A total of 12 patients (11 males and 1 female) were enrolled (Table 1). At study entry, the median age of the patients was 51 years (range, 37 to 69 years), and the median WHO performance status was 1 (range, 0 to 2). Primary tumor types included bladder carcinoma (n = 2), non-small-cell lung cancer (NSCLC) (n = 3), esophagus cancer (n = 1), penis cancer (n = 1), colorectal cancer (n = 2), cardiacarcinoma (n = 2) and gastric carcinoma (n = 1). Patients had received prior surgical therapy (n = 8), radiotherapy (n = 7), and/or chemotherapy (n = 12).

Table 1. Patient characteristics.

No. of patients	12
Sex	
Female	1
Male	11
Age (years)	
median	51
range	37 - 69
WHO performance status	
median	1
range	0 - 2
Tumor type	
bladder	2
non-small-cell lung (NSCL)	3
esophagus	1
penis	1
colorectal	2
cardia carcinoma	2
gastric carcinoma	1
Prior treatment	
Surgical therapy	7
Chemotherapy	12
Surgical therapy and chemotherapy	8
Radiotherapy and chemotherapy	7
Surgical therapy, radiotherapy, and chemotherapy	4

Pharmacokinetics

The mean plasma pharmacokinetic parameters of orally administered docetaxel (10 or 100 mg) with oral RTV (100 mg) simultaneously or with a 60 min time interval and i.v. docetaxel (100 mg) are presented in Table 2. Systemic exposure to 10 mg docetaxel was 0.11 ± 0.05 mg.h/L administered simultaneously and 0.16 ± 0.06 mg.h/L with a 60 min time interval. Compared to the systemic exposure to docetaxel after administration of a dose of 100 mg i.v. docetaxel, which was 1.9 ± 0.4 mg.h/L this was considered very low (Table 2; Fig. 1). The apparent oral bioavailability of docetaxel, calculated as the ratio of the AUC after oral and after i.v. administration with a correction for the difference in dose, was relatively high, 47.3 ± 22.4% in combination with 100 mg RTV co-administered simultaneously and 62.8 ± 34.4% with a 60 min time interval. The very low plasma concentrations of docetaxel may have limited optimal assessment of the AUC and specifically may have underestimated the oral AUC. Based on these pharmacokinetic and safety data, a dose increase to 100 mg oral docetaxel in combination with 100 mg RTV was considered justified in the second part of this study. The data showed a pronounced increase in the mean AUC value of orally administered docetaxel of 2.4 ± 1.5 mg.h/L (n = 7) with RTV co-administered simultaneously and 2.8 ± 1.4 mg.h/L with a 60 min time interval compared to i.v. docetaxel (1.9 ± 0.4 mg.h/L) (Table 2; Fig. 1). There was no significant difference between the mean oral AUC value of docetaxel co-administered with RTV simultaneously or with a 60 min time interval. The apparent oral bioavailability of docetaxel was strongly enhanced to 131% ± 90% (n = 8) with RTV co-administered simultaneous and 161% ± 91% (n = 8) with a 60 min time interval. The coefficient of variation of the AUC after oral docetaxel administration in combination with RTV simultaneously or with a 60 min time interval was 62.5% and 50%, respectively, (n = 8) and after i.v. administration 22% (n = 8). Overall, these data are promising and the basis for further development of a clinically useful oral formulation of docetaxel in combination with RTV.

Table 2. Main pharmacokinetic parameters of docetaxel after oral administration (10 or 100 mg) with or without ritonavir (RTV; 100 mg) and i.v. administration of docetaxel (100 mg). Data are mean ± SD.

Patient no.	T_{max} (h)	C_{max} (mg/L)	$AUC_{0-\infty}$ (mg*h/L)	F (%)	CV% of $AUC_{0-\infty}$
10 mg docetaxel					
oral docetaxel + RTV simultaneous	0.75 ± 0.20	0.02 ± 0.01	0.11 ± 0.05	47.3 ± 22.4	42.6
oral docetaxel + RTV 1 h interval	0.56 ± 0.24	0.02 ± 0.01	0.15 ± 0.07	62.8 ± 34.4	50.8
100 mg docetaxel					
oral docetaxel + RTV simultaneous	2.9 ± 1.1	0.32 ± 0.2	2.4 ± 1.5	131 ± 90	62.5
oral docetaxel + RTV 1 h interval	2.5 ± 0.9	0.47 ± 0.3	2.8 ± 1.4	161 ± 91	50
intravenous docetaxel	0.9 ± 0.1	1.4 ± 0.2	1.9 ± 0.4		22

Abbreviations: T_{max}, time to maximal concentration; C_{max}, the maximal plasma concentration; $AUC_{0-\infty}$, area under the plasma concentration-time curve from 0 to infinity (dose corrected AUC values); F, apparent bioavailability; CV%, coefficient of variation.

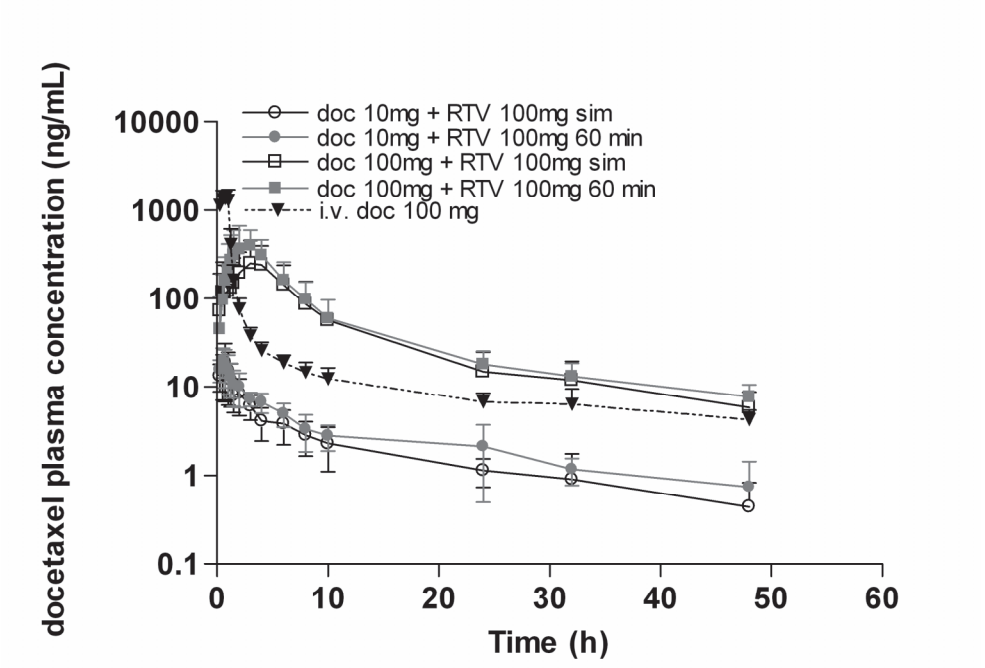

Figure 1. Plasma concentration-time curves of i.v.-administered docetaxel (100 mg) and oral docetaxel (10 or 100 mg) with RTV simulatenous (sim) or with a 60 min time interval (60 min) represented as mean ± SD.

Hematological and non-hematological toxicities

Docetaxel administered orally was well tolerated. In one of the patients no toxicity data was available. In none of the eleven patients any grade 1-4 hematological toxicity (anemia, leukocytopenia, neutropenia and thrombocytopenia) was observed after oral docetaxel administration in combination with RTV. Table 3 summarizes the non-hematologic toxicities that were observed after oral docetaxel combined with RTV and after the first i.v. administration on day 15 or 22. The main non-hematological toxicities after oral intake of docetaxel were diarrhea (seven patients), vomiting (five patients), fatigue (five patients), abdominal pain (three patients) and nausea (two patients). Most of the toxicities did not exceed grade 2 in severity except in five patients short lasting grade 3 events were observed (Table 3). Three patients developed grade 3 diarrhea after oral docetaxel that was considered to be probably related to oral docetaxel combined with RTV. Furthermore, one patient developed grade 3 stomatitis and one patient an allergic reaction grade 3 (Table 3). The principal non-hematologic toxicities during the first cycle of i.v. administered docetaxel were nausea (one patient), alopecia (one patient), diarrhea (2 patients), anorexia (one patient) and elevated alkaline phosphatase (AP) (one patient) (Table 3). The non-hematologic toxicities were mild (grade 1 or 2). In next i.v. cycles the principal non-hematological toxicities were grade 1 or 2 fatigue, alopecia, myalgia, nausea, diarrhea, infections, and skin reactions. In none of the patients treated with i.v. docetaxel any grade 1-4 hematological toxicity was observed.

Antitumor activity

In total six out of the eleven patients (three NSCLC, one bladder, one cardia and one esophagus cancer) were documented with partial responses. Two out of the six patients developed adverse events after three/four courses, such as radiation pneumonitis and neurotoxicity, both CTC grade 3. The other four patients showed stable disease and received a median of six courses (4–10 courses). The remaining five patients developed progressive disease after one or two courses.

Table 3. Non-hematologic toxicities observed after oral docetaxel administration in combination with RTV and the first i.v. course of docetaxel.

non-hematological toxicities	oral docetaxel + RTV simultaneous	oral docetaxel + RTV 60 min time interval	i.v. docetaxel 100 mg
Patients No.	11	11	11
Nausea			
Grade 1/2	1	1	1
Vomiting			
Grade 1/2	1	4	0
Diarrhea			
Grade 1/2	2	2	2
Grade 3/4	1	2	0
Abdominal pain			
Grade 1/2	1	2	0
Alopecia			
Grade 1/2	1	0	1
Fatigue			
Grade 1/2	3	2	0
Fever			
Grade 1/2	0	0	1
Anorexia			
Grade 1/2	0	0	1
Allergic reaction			
Grade 1/2	0	0	0
Grade 3/4	1	0	0
Elevated gamma-GT			
Grade 1/2	0	1	0
Stomatitis			
Grade 1/2	0	1	0
Grade 3/4	0	1	0
Infection			
Grade 1/2	1	0	0
Hiccup			
Grade 1/2	1	0	0
AP elevated			
Grade 1/2	0	0	1
Hyperkalemia			
Grade 1/2	1	0	0
Dizziness			
Grade 1/2	0	1	0

Discussion

The results presented here show that co-administration of oral RTV, an effective inhibitor of CYP3A4, strongly enhanced the systemic exposure to orally administered docetaxel in patients. Oral docetaxel dosed at 100 mg in combination with RTV resulted in an apparent bioavailability of 131% ± 90% and 161% ± 91% when given simultaneously or with a 60 min time interval, respectively. No significant differences were found between docetaxel and RTV administration simultaneously or with a 60 min time interval and the interpatient

variability in the systemic exposure after oral docetaxel was higher than after i.v. docetaxel, but comparable to other clinical studies with oral docetaxel (9).

Preclinical data obtained in wild-type mice, P-gp knockout and Cyp3a knockout mice combined with these first clinical data indicate that RTV reduced the elimination of orally administered docetaxel by effectively blocking docetaxel metabolism by CYP3A4 in the gut wall and/or liver (9, 12, 16). This is the major explanation for the substantially increased apparent oral bioavailability (more than 100%) of docetaxel with RTV in patients. This indicates that RTV also inhibited the elimination of systemic docetaxel after oral administration.

The apparent oral bioavailability after administration of 10 mg of oral docetaxel was much lower compared to the 100 mg dose. The very low plasma concentrations of docetaxel after treatment with 10 mg of oral docetaxel may have limited optimal assessment of the AUC and specifically may have underestimated the oral AUC. Recently, van Herwaarden et al. (16) illustrated in transgenic mice, with human CYP3A4 expression in intestine or liver, a dominant effect of intestinal CYP3A4 on the first-pass metabolism of docetaxel over liver CYP3A4. In addition, RTV inhibition of P-gp in the gastrointestinal tract may contribute to a minor extent to the increased systemic exposure.

Preclinical and clinical studies showed that the metabolism of docetaxel by CYP3A4 was the main factor for the low oral bioavailability of docetaxel, thus oral docetaxel in combination with RTV could be an advantage over CsA because RTV inhibits efficiently CYP3A4 and to a minor extent P-gp. Moreover, boosting with RTV may even reduce the costs of therapy, because lower doses of docetaxel can be used. No significant immunosuppressive effects of CsA are to be expected at the applied schedule (9), however the drug was considered unfavorable, compared with RTV as a high number of seven capsules of CsA need to be taken. At this moment in our institute a dose escalation study in patients with oral docetaxel and RTV is being executed to determine the maximum tolerated dose, dose limiting toxicities, and optimal dose of docetaxel that can safely be administered in combination with RTV in a weekly schedule.

The time span between docetaxel and RTV administered simultaneously or with a 60 min time interval was also investigated. There was no significant difference between the two treatment methods, thus simultaneous intake appears to be feasible. The C_{max} of oral docetaxel in combination with RTV was significantly lower than after i.v. docetaxel. This is probably an advantage for the safety of oral docetaxel over i.v. docetaxel.

The oral combination of docetaxel and RTV was well tolerated. However, some of the patients complained of an unpalatable and unpleasant taste of the drinking docetaxel solution, probably due to the polysorbate and ethanol excipients. The main side effects

were diarrhea, vomiting, fatigue, abdominal pain and nausea, which were mild to moderate for most of the toxicities, except for diarrhea (grade 3) in three out of twelve patients. CYP3A4/P-gp inhibition could cause an increase in the docetaxel levels in liver and the intestinal wall and may therefore enhance the risk of liver/intestinal toxicities (16, 20). However, we did not observe any signs or symptoms of liver toxicities in our study and only short lasting grade 3 diarrhea in three out of the eleven patients. After the first i.v. course of docetaxel, a similar pattern of toxicities was observed as after oral drug administration. However, diarrhea seemed to occur more often after oral administration in combination with RTV than after i.v. administration. This may be related to the inhibition of CYP3A4 in the gastrointestinal tract by RTV or unabsorbed docetaxel.

In summary, co-administration of oral RTV strongly enhanced the apparent oral bioavailability of docetaxel. The safety of the combination of docetaxel and RTV was good. These data are promising for the further development of this combination.

Acknowledgement

We are indebted to Brigitte Dufourny for data management, to the medical and nursing staff of the Netherlands Cancer Institute and to the patients who took part in this study.

References

1. DeMario MD and Ratain MJ. Oral chemotherapy: rationale and future directions. J Clin Oncol 1998;16:2557-2567.
2. Liu G, Franssen E, Fitch MI and Warner E. Patient preferences for oral versus intravenous palliative chemotherapy. J Clin Oncol 1997;15:110-115.
3. Schellens JH, Malingre MM, Kruijtzer CM, et al. Modulation of oral bioavailability of anticancer drugs: from mouse to man. Eur J Pharm Sci 2000;12:103-110.
4. Hainsworth JD, Burris HA, III, Erland JB, et al. Phase I trial of docetaxel administered by weekly infusion in patients with advanced refractory cancer. J Clin Oncol 1998;16:2164-2168.
5. Tabernero J, Climent MA, Lluch A, et al. A multicentre, randomised phase II study of weekly or 3-weekly docetaxel in patients with metastatic breast cancer. Ann Oncol 2004;15:1358-1365.
6. Di Maio M, Perrone F, Chiodini P, et al. Individual patient data meta-analysis of docetaxel administered once every 3 weeks compared with once every week second-line treatment of advanced non-small-cell lung cancer. J Clin Oncol 2007;25:1377-1382.
7. Wils P, Phung-Ba V, Warnery A, et al. Polarized transport of docetaxel and vinblastine mediated by P-glycoprotein in human intestinal epithelial cell monolayers. Biochem Pharmacol 2004;48:1528-1530.
8. van Asperen J, van Tellingen O, Sparreboom A, et al. Enhanced oral bioavailability of paclitaxel in mice treated with the P-glycoprotein blocker SDZ PSC 833. Br J Cancer 1997;76:1181-1183.
9. Malingre MM, Richel DJ, Beijnen JH, et al. Coadministration of cyclosporine strongly enhances the oral bioavailability of docetaxel. J Clin Oncol 2001;19:1160-1166.
10. Marre F, Sanderink GJ, de Sousa G, et al. Hepatic biotransformation of docetaxel (Taxotere) in vitro: involvement of the CYP3A subfamily in humans. Cancer Res 1996;56:1296-1302.
11. Shou M, Martinet M, Korzekwa KR, et al. Role of human cytochrome P450 3A4 and 3A5 in the metabolism of taxotere and its derivatives: enzyme specificity, interindividual distribution and metabolic contribution in human liver. Pharmacogenetics 1998;8:391-401.
12. Bardelmeijer HA, Ouwehand M, Buckle T, et al. Low systemic exposure of oral docetaxel in mice resulting from extensive first-pass metabolism is boosted by ritonavir. Cancer Res 2002;62:6158-6164.

13. Huisman MT, Smit JW, Wiltshire HR, et al. P-glycoprotein limits oral availability, brain, and fetal penetration of saquinavir even with high doses of ritonavir. Mol Pharmacol 2001;59:806-813.
14. Kempf DJ, Marsh KC, Kumar G, et al. Pharmacokinetic enhancement of inhibitors of the human immunodeficiency virus protease by coadministration with ritonavir. Antimicrob Agents Chemother 1997;41:654-660.
15. Kappelhoff BS, Huitema AD, Sankatsing SU, et al. Population pharmacokinetics of indinavir alone and in combination with ritonavir in HIV-1-infected patients. Br J Clin Pharmacol 2005;60:276-286.
16. van Herwaarden AE, Wagenaar E, van der Kruijssen CM, et al. Knockout of cytochrome P450 3A yields new mouse models for understanding xenobiotic metabolism. J Clin Invest 2007;117:3583-3592.
17. Therasse P, Arbuck SG, Eisenhauer EA, et al. New guidelines to evaluate the response to treatment in solid tumors. European Organization for Research and Treatment of Cancer, National Cancer Institute of the United States, National Cancer Institute of Canada. J Natl Cancer Inst 2000;92:205-216.
18. Kuppens IE, van Maanen MJ, Rosing H, et al. Quantitative analysis of docetaxel in human plasma using liquid chromatography coupled with tandem mass spectrometry. Biomed Chromatogr 2005;19:355-361.
19. ter Heine R, Alderden-Los CG, Rosing H, et al. Fast and simultaneous determination of darunavir and eleven other antiretroviral drugs for therapeutic drug monitoring: method development and validation for the determination of all currently approved HIV protease inhibitors and non-nucleoside reverse transcriptase inhibitors in human plasma by liquid chromatography coupled with electrospray ionization tandem mass spectrometry. Rapid Commun Mass Spectrom 2007;21:2505-2514.
20. Schinkel AH. The physiological function of drug-transporting P-glycoproteins. Semin Cancer Biol 1997;8:161-170.

CHAPTER 4.2

Paclitaxel in self-microemulsifying formulations: oral bioavailability study in mice

Roos L. Oostendorp, Tessa Buckle, Gregory Lambert, Jean S. Garrigue, Jos H. Beijnen, Jan H.M. Schellens, Olaf van Tellingen

Submitted for publication

Abstract

The anticancer drug paclitaxel is formulated for i.v. administration in a mixture of Cremophor EL and ethanol. Its oral bioavailability is very low due to the action of P-glycoprotein in the gut wall and CYP450 in gut wall and liver. However, proof-of-concept studies using the i.v. formulation diluted in drinking water have demonstrated the feasibility of the oral route as an alternative when given in combination with inhibitors of P-glycoprotein and CYP450. Because of the unacceptable pharmaceutical properties of the drinking solution, a better formulation for oral application is needed. We have evaluated the suitability of various self-microemulsifying oily formulations (SMEOF's) of paclitaxel for oral application using wild-type and P-glycoprotein knockout mice and cyclosporin A (CsA) as P-glycoprotein and CYP450 inhibitor. The oral bioavailability of paclitaxel in all SMEOF's without concomitant CsA was low in wild-type mice, showing that this vehicle does not enhance intestinal uptake by itself. Paclitaxel (10 mg/kg) in SMEOF#3 given with CsA resulted in plasma levels that were comparable to the Cremophor EL-ethanol containing drinking solution plus CsA. Whereas the AUC increased linearly with the oral paclitaxel dose in P-glycoprotein knockout mice, it increased less than proportional in wild-type mice given with CsA. In both strains more unchanged paclitaxel was recovered in the feces at higher doses. This observation most likely reflects more profound precipitation of paclitaxel within the gastro-intestinal tract at higher doses. The resulting absolute reduction in absorption of paclitaxel from the gut was concealed by partial saturation of first-pass metabolism when P-glycoprotein was absent. In conclusion, SMEOF's maybe a useful vehicle for oral delivery of paclitaxel in combination with CsA, although the stability within the gastro-intestinal tract remains a critical issue, especially when applied at higher dose levels.

Introduction

Paclitaxel is a widely used anticancer agent that is administered by an intravenous (i.v.) infusion (1, 2). Because the drug is poorly soluble in most pharmaceutical solvents it is formulated at a concentration of 6 mg/ml in a 1:1 mixture of Cremophor® EL (CrEL) and ethanol. Consequently, substantial amounts of these excipients are co-infused at the standard dose level of 175 mg/m^2. However, CrEL has been associated with sometimes severe hypersensitivity reactions (3) and non-linear pharmacokinetic behaviour of i.v. administered paclitaxel (4-6).

The oral route for the administration of drugs is more attractive than the i.v. route because it is more convenient for patients and because of pharmacoeconomic advantages (7, 8). In addition, the oral route would facilitate the use of more chronic treatment regimens, allowing a prolonged exposure to cytotoxic agents while avoiding high peak plasma concentrations (C_{max}). Unfortunately, paclitaxel has a very low oral bioavailability. This is mainly due to the action of the drug efflux transporter P-glycoprotein (P-gp) that is highly expressed in gastrointestinal tract and limits the uptake of paclitaxel from the intestinal lumen. Studies in mice have shown that whereas 87% of an orally administered dose of paclitaxel was recovered as unchanged drug in the feces of wild-type mice, excretion was reduced to 2% in P-gp knockout mice (9) indicating complete uptake from the gastro-intestinal tract when P-gp is absent. However, paclitaxel that does enter into the body is subjected to extensive first-pass metabolism by the gut and liver cytochrome P450 (CYP) enzymes (CYP2C8 and CYP3A4) (10), rendering the oral bioavailability in P-gp knockout mice about 40% (9). In line with these results, concomitant administration of agents that block the function of P-gp and/or CYP, e.g. cyclosporin A (CsA), have successfully been used to increase the systemic exposure to the i.v. paclitaxel formulation after oral administration in mice and patients (11-13).

The design of an oral formulation of paclitaxel for use in patients remains a critical issue. So far, studies in patients have been conducted with the marketed formulation for i.v. administration, which is diluted with water before administration to yield an oral drinking solution (12, 14, 15). Although these studies have shown that oral administration of paclitaxel is feasible and associated with antitumor efficacy (14-16), there are issues with the oral drinking solution that preclude its more widespread implementation in clinical practice. One of these concerns is the presence of substantial amounts of CrEL, which, when given at higher doses, antagonizes the absorption of paclitaxel from the GI tract (17-19) and for that reason, higher dose intensities can only be delivered by repeated administration. However, CrEL gives the drinking solution an appalling taste resulting in

intolerance, nausea and vomiting, especially when administered repeatedly. Novagali Pharma has investigated possible solutions to this issue by developing self-microemulsifying oily formulations (SMEOF) in which paclitaxel is encapsulated into 1-10 nm size oily droplets. The formulations consist of isotropic mixtures of oils and surfactants, which solubilize paclitaxel and spontaneously form a microemulsion upon contact with water. In a previous *in vitro* study the choice of the excipients was motivated by the particle size, physical and chemical stability as well as cytotoxicity of different self-emulsing drug delivery system formulations of paclitaxel (20). In the different SMEOF formulations tyloxapol and TPGS (d-alpha-tocopheryl polyethylene glycol 1000 succinate) have been chosen for their ability to solubilize paclitaxel (20-23). As compared to the commercial paclitaxel (Taxol®) formulation tested orally, the SMEOF formulations are CrEL-free and have a significantly lower ethanol to paclitaxel ratio.

The purpose of this preclinical study was to test the suitability of SMEOFs to serve as an oral delivery formulation of paclitaxel. We selected the most appropriate candidate for further investigations. In particular, we addressed the issue of the linearity of the relationship between the oral dose of paclitaxel and the systemic exposure.

Material and Methods

Chemicals and reagents

SMEOF#1 (1.5%), SMEOF#2 (3.0%), SMEOF#3 (1.5 or 3.0%), SMEOF#4 (1.5%) (contents of paclitaxel between parenthesis; see Table 1 for compositions) were prepared by Novagali Pharma SA, (Evry Cedex, France). SMEOF#4 is identical to SMEOF#3, except that this formulation already contains cyclosporine A at a concentration of 1.5%. Cyclosporin A (Sandimmune) originated from Novartis (Basel, Switzerland), Taxol® from Bristol-Meyers Squibb (München, Germany) and pure paclitaxel was obtained from Novagali. Polysorbate 80 was purchased from Brocacef B.V. (Maarssen, The Netherlands). All other chemicals were of analytical or lichrosolv gradient grade and originated from E. Merck (Darmstadt, Germany). Drug-free human plasma was obtained from the Central Laboratory of the Blood Transfusion Service (Sanquin, Amsterdam, The Netherlands).

Table 1. Composition of the different SMEOF formulations.

Formulation	Component	Percentage % (w/v)		Function
SMEOF#1 (1.5%)		Phase A	Phase B	
	Paclitaxel	-	1.5	Active substance
	Vitamin E	5.00	-	Oil
	TPGS	14.24	14.25	Surfactant, co-solvent
	Tyloxapol	15.75	15.75	Surfactant, co-solvent
	Ethanol	15.25	15.25	Solvent
	Doc-Na	3.00	-	
	Total	53.24	46.75	
SMEOF#2 (3.0%)		Phase A	Phase B	
	Paclitaxel	-	3.0	Active substance
	Vitamin E	5.00	-	Oil
	TPGS	14.00	14.00	Surfactant, co-solvent
	Tyloxapol	15.50	15.50	Surfactant, co-solvent
	Ethanol	15.00	15.00	Solvent
	Doc-Na	3.00	-	
	Total	52.50	47.50	
SMEOF#3 (1.5% and 3.0%)		(1.5%)	(3.0%)	
	Paclitaxel	1.5	3.0	Active substance
	Vitamin E	5.00	5.00	Oil
	TPGS	29.95	29.45	Surfactant, co-solvent
	Tyloxapol	33.05	32.55	Surfactant, co-solvent
	Ethanol	30.5	30.0	Solvent
	Total	100	100	
SMEOF#4 (1.5%)				
	Paclitaxel	1.5		Active substance
	Cyclosporin A	1.5		P-gp inhibitor
	Vitamin E	5		Oil
	TPGS	29.45		Surfactant, co-solvent
	Tyloxapol	32.55		Surfactant, co-solvent
	Ethanol	30		Solvent
	Total	100		

Abbreviations: TPGS: d-alpha-tocopheryl polyethylene glycol 1000 succinate; DOC-Na: Sodium desoxycholate.

Animals

Mice were housed and handled according to institutional guidelines complying with Dutch legislation. Animals used in all experiments were female Mdr1a/1b$^{-/-}$ (P-gp knockout) and wild-type (WT) mice of FVB genetic background between 10 and 16 weeks of age. Animals were kept in a temperature-controlled environment with a 12-hour light/12-hour dark cycle. They received a standard diet (AM-II, Hope Farms, Woerden, The Netherlands) and acidified water *ad libitum.*

Drug solutions

SMEOF#1, SMEOF#2 are two-phase formulations that were quantitatively mixed just prior to 10-fold dilution in sterile water while SMEOF#4 working solution was also prepared by 10-fold dilution in water. Final paclitaxel concentrations were 1.5, 3.0, and 1.5 mg/mL for SMEOF# 1, 2 and 4, respectively. SMEOF#3 (1.5%) was diluted 5 and 10-fold, while SMEOF#3 (3.0%) was diluted 10 and 20-fold with water for injection to yield final concentrations of 3.0 and 1.5 mg/mL of paclitaxel, respectively. Cyclosporin A (CsA) 50 mg/mL was diluted 25-fold with water for injection. Taxol® (paclitaxel; 6 mg/ml in CrEL:Ethanol 1:1; v/v) was diluted 4-fold with water for injection. Paclitaxel (6 mg/ml) in polysorbate/ethanol (1:1; v/v) was prepared at our institute and was diluted 4-fold with saline for injection.

Plasma pharmacokinetics and oral bioavailability

In the first part of the study, cohorts of WT mice were treated orally with one of the four different SMEOF working solutions and Taxol® as a reference at a dose level of 10 mg/kg of paclitaxel. Separate cohorts of mice received paclitaxel (formulated in Polysorbate 80: ethanol) i.v. in order to calculate the absolute bioavailability. Polysorbate 80-ethanol and not the standard i.v. formulation of CrEL-ethanol was used to avoid the CrEL mediated nonlinear plasma pharmacokinetics of paclitaxel (4, 5). Oral drug administrations were given by gavage into the stomach. The SMEOF solutions were aliquoted in small portions in order to have fresh and clear drug solutions for all animals. By working this way we avoided precipitation from the formulation that sometimes occurred within minutes after the gavage. The animals were treated with or without concomitant administration of CsA (10 mg/kg), given at 20 min prior to oral paclitaxel or 30 min prior to i.v. paclitaxel. No concomitant CsA was given to animals receiving SMEOF#4 as this formulation already contains CsA. In the second part, WT and P-gp knockout mice received paclitaxel in SMEOF#3 at dose levels of 10, 30 and 60 mg/kg. The WT mice also received oral CsA (10

mg/kg), 20 min prior to oral paclitaxel. An additional cohort of P-gp knockout mice received i.v. paclitaxel formulated in Polysorbate 80: ethanol (1:1; v/v). In the third part, the properties of SMEOF#3 (containing 30 mg/ml (3%, w/w) of paclitaxel) was investigated in P-gp knockout mice. These animals received dose levels of 10, 30 and 60 mg/kg. In all these pharmacokinetic experiments, five animals per time point were euthanized for blood sampling by cardiac puncture at 1, 2, 4, and 8 h after administration. The plasma fraction of the blood samples was collected after centrifugation at 5,000 x *g* for 10 min at 4°C, and stored at -20°C until analysis.

Fecal excretion

WT and P-gp knockout mice were individually housed in Ruco Type M/1 metabolic cages (Valkenswaard, The Netherlands). They were first accustomed to the cages for 2 days before receiving paclitaxel in SMEOF#3 (1.5%) working solution at dose levels of 10, 30 and 60 mg/kg (five animals per dose). The WT mice also received CsA (10 mg/kg), 20 min prior to oral paclitaxel. Additionally, P-gp knockout mice received paclitaxel orally in SMEOF#3 (3.0%) paclitaxel at dose levels of 10, 30 and 60 mg/kg (five animals per dose). The feces were collected every 24 h for up to 96 h. Feces were pooled per animal and homogenized in 4% (w/v) BSA in water. The samples were stored at -20°C until analysis.

Drug analysis

Amounts of paclitaxel in all biological samples were determined using a previously described validated high-performance liquid chromatography assay (24, 25) with a lower limit of quantification of 25 ng/ml using 250 µl of sample.

Pharmacokinetic and statistical analysis

Pharmacokinetic parameters were calculated by non-compartmental methods using the software package Quattro Pro (Corel Corp., 1996; version 6.02). The area under the plasma concentration-time curve (AUC) was calculated using the linear trapezoidal rule without extrapolation to infinity using the formula:

$$AUC = \sum^{n}_{i=2} \text{concentration}_i \cdot \frac{(\Delta\text{time}_{i-1} + \Delta\text{time}_i)}{2}$$

With $\Delta\text{time}_n = 0$

The standard error (SE) of the AUC was calculated with the law of propagation of errors using the formula:

$$SE_{AUC} = \sqrt{\left(\sum^{n}_{i=2} SE_i \cdot \frac{(\Delta\text{time}_{i-1} + \Delta\text{time}_i)^2}{4}\right)}$$

The maximal plasma concentration (C_{max}) and the time at which the maximal plasma level was reached (T_{max}) were determined graphically. The oral bioavailability (F) was calculated using the formulas:

$F = (AUC_{oral}/AUC_{i.v.}) * 100\%$

The $SE_{(F)}$ was calculated using:

$SE_{(F)} = F \cdot (SE_{(AUC, oral)}/AUC_{oral})^2 + (SE_{(AUCi.v.)}/AUC_{i.v.})^2$

The unpaired Student's t-test (two-tailed) was used to compare the pharmacokinetic parameters. P-values < 0.05 were considered statistically significant.

Results

Plasma pharmacokinetics of oral paclitaxel formulated in different SMEOFs in wild-type and P-gp knockout mice

We first compared the oral bioavailability of paclitaxel in the four different SMEOF working solutions using the standard Taxol® solution as reference. To determine the systemic exposure after i.v. injection we used paclitaxel formulated in polysorbate 80-ethanol instead of the standard CrEL-ethanol formulation in order to avoid the nonlinear pharmacokinetic behavior of paclitaxel in this vehicle (4, 5). As expected, the paclitaxel plasma levels were low with all tested oral SMEOF working solutions when administered without CsA (Table 2 and Fig. 1). In combination with CsA, SMEOF#1 and SMEOF#2 resulted in a lower paclitaxel exposure when compared with the standard Taxol® formulation. Moreover, some turbidity of the diluted SMEOF#1 and #2 paclitaxel formulations started to occur within minutes after the first administration. For these reasons, and because these two-Phase systems were less convenient, the development of SMEOF#1 and #2 was discontinued. The administration of paclitaxel formulated in SMEOF#3 in combination with CsA and of SMEOF#4 (which contains CsA) resulted in systemic exposures that were similar to those obtained with the standard Taxol® formulation (Table 2 and Fig. 1). The oral bioavailability ranged from 18.4 to 21.7%. Turbidity was not observed in these samples. In conclusion, the results of this study showed that the formulations SMEOF#3 and SMEOF#4 in combination with CsA are promising alternatives to the standard Taxol® formulation. In the next mice experiments we have chosen to further explore the SMEOF#3 paclitaxel formulation in combination with CsA.

Table 2. Plasma pharmacokinetic parameters of paclitaxel (10 mg/kg) after oral treatment of the different SMEOF formulations (SMEOF#1 - SMEOF#4, 1.5% w/w paclitaxel) and Taxol® or after i.v. administration of paclitaxel in a Polysorbate 80: ethanol solution in wild-type mice with or without co-administration of Cyclosporin A (10 mg/kg). Data are mean ± Standard error (SE), oral and i.v. administration (n = 5).
$AUC_{0-\infty}$ Area under the concentration time curve from 0 to infinity, F oral bioavailability, n/a not applicable.

Paclitaxel formulation	Paclitaxel concentration, administration route	Cyclosporin A, administration route	$AUC_{0-\infty}$ (ng/mL*h)	F (%)
SMEOF#1	10 mg/kg, p.o.	-	306 ± 46	5.2 ± 0.8
SMEOF#1	10 mg/kg, p.o.	10 mg/kg, p.o.	1652 ± 181	12.0 ± 1.4
SMEOF#2	10 mg/kg, p.o.	-	173 ± 40	2.9 ± 0.7
SMEOF#2	10 mg/kg, p.o.	10 mg/kg, p.o.	1480 ± 160	10.8 ± 1.3
SMEOF#3	10 mg/kg, p.o.	-	108 ± 17	1.8 ± 0.3
SMEOF#3	10 mg/kg, p.o.	10 mg/kg, p.o.	2534 ± 177	18.4 ±1.6
SMEOF#4	10 mg/kg, p.o.	10 mg/kg, p.o.	2769 ± 307	20.1 ± 2.7
Taxol®	10 mg/kg, p.o.	-	417 ± 64	7.1 ± 1.2
	10 mg/kg, p.o.	10 mg/kg, p.o.	2984 ± 173	21.7 ± 1.6
Polysorbate 80	10 mg/kg, i.v.	-	5862 ± 366	n/a
EtOH	10 mg/kg, i.v.	10 mg/kg, p.o.	13754 ± 670	n/a

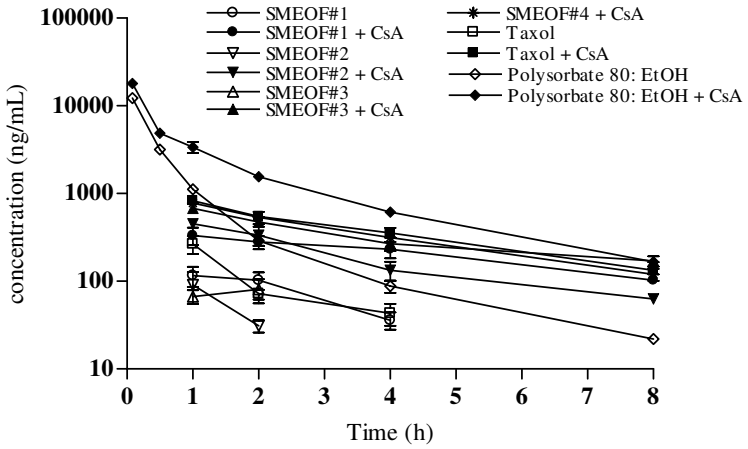

Figure 1. Paclitaxel plasma concentration versus time curves after oral administration of different SMEOF (SMEOF#1 – SMEOF#4, 1.5% w/w paclitaxel) formulations and Taxol® or i.v. administration of paclitaxel in a Polysorbate 80: ethanol solution in wild-type with or without co-administration of Cyclosporin A (10 mg/kg). Plasma levels of paclitaxel were determined by a validated HPLC method with lower limit of quantification (25 ng/mL). Data points are expressed as mean concentrations for oral and i.v. (n= 5) administration; error bars indicate Standard Errors (SEs).

Systemic exposure of paclitaxel formulated in SMEOF#3 in wild-type and P-gp knockout mice

When P-gp knockout mice received SMEOF#3 (1.5%) orally at doses of 10, 30, or 60 mg/kg of paclitaxel, the exposure (AUC) increased in a dose-proportional manner (Table 3 and Fig. 2). The mean oral bioavailability of paclitaxel ranged from 29.9 to 38.6%. Figure 3 reveals that the T_{max} is longer at higher dose levels, suggesting delayed gastric emptying. When WT mice received SMEOF#3 at 10, 30, or 60 mg/kg of paclitaxel in combination with CsA (10 mg/kg), the increase in the exposure to paclitaxel was not proportional with dose. Consequently, the absolute bioavailability decreased at higher dose levels (Table 3; Fig. 2). Overall, the exposure to paclitaxel in WT mice treated at a dose of 10 mg/kg of paclitaxel in combination with CsA was similar as in P-gp knockout mice treated with 10 mg/kg of paclitaxel in SMEOF#3. Since the concomitant administration of CsA (10 mg/kg) also increased the exposure of i.v. administered paclitaxel, the oral bioavailability in WT mice was lower. Similar as observed in P-gp knockout mice the T_{max} was delayed at the higher dose levels.

When P-gp knockout mice received the SMEOF#3 with a higher load of paclitaxel (SMEOF#3 (3%) the oral bioavailability at 10 mg/kg was similar to that observed using SMEOF#3 (1.5%) (Table 3; Fig. 2). However, the oral bioavailability decreased markedly when higher dose levels were administered. Moreover, turbidity was also observed in the diluted formulations within 5 to 15 min after the first administration.

Table 3. Plasma pharmacokinetic parameters of paclitaxel after oral treatment of the SMEOF#3 formulation (with 1.5% w/w and 3.0% w/w paclitaxel) at different doses of 10, 30, or 60 mg/kg or after i.v. administration of paclitaxel in a Polysorbate 80: ethanol solution in P-gp knockout and/or wild-type mice co-administered with or without Cyclosporin A (10 mg/kg). Data are mean ± Standard error (SE), oral and i.v. administration (n = 5).

Paclitaxel formulation	Paclitaxel	Cyclosporin A	$AUC_{0-\infty}$ (ng/mL*h)	F (%)
P-gp knockout mice				
SMEOF#3, (1.5%)	10 mg/kg, p.o.	-	1841 ± 166	29.9 ± 3.1
SMEOF#3, (1.5%)	30 mg/kg, p.o.	-	7110 ± 382	38.6 ± 2.8
SMEOF#3, (1.5%)	60 mg/kg, p.o.	-	11220 ± 1131	30.4 ± 3.4
Polysorbate 80:EtOH	10 mg/kg, i.v.	-	6147 ± 291	n/a
Wild-type mice				
SMEOF#3, (1.5%)	10 mg/kg, p.o.	10 mg/kg, p.o.	2090 ± 174	15.2 ± 1.5
SMEOF#3, (1.5%)	30 mg/kg, p.o.	10 mg/kg, p.o.	3835 ± 430	9.3 ± 1.1
SMEOF#3, (1.5%)	60 mg/kg, p.o.	10 mg/kg, p.o.	5916 ± 765	7.2 ± 1.0
P-gp knockout mice				
SMEOF#3, (3.0%)	10 mg/kg, p.o.		1710 ± 131	27.8 ± 2.5
SMEOF#3, (3.0%)	30 mg/kg, p.o.		3871 ± 621	21.0 ± 3.5
SMEOF#3, (3.0%)	60 mg/kg, p.o.		1764 ± 168	4.8 ± 0.5

$AUC_{0-\infty}$ Area under the concentration time curve from 0 to infinity, F oral bioavailability, n/a not applicable

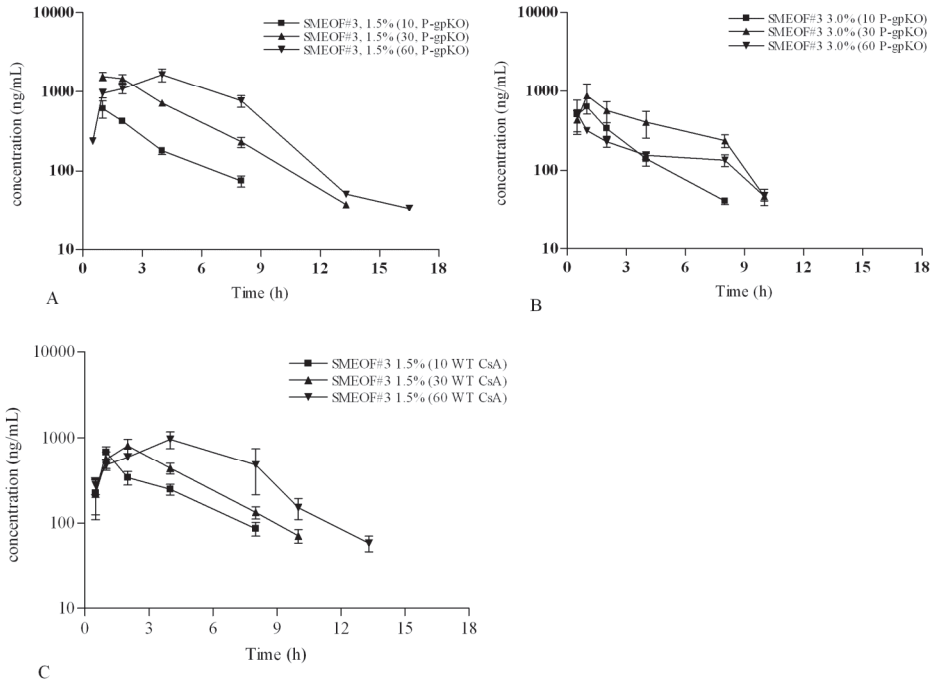

Figure 2. Paclitaxel plasma concentration versus time curves after oral administration of the SMEOF#3 formulation with 1.5% w/w and 3.0% w/w paclitaxel at different doses of 10, 30, or 60 mg/kg in P-gp knockout (A and B) and wild-type mice (C) co-administered with Cyclosporin A (10 mg/kg). Plasma levels of paclitaxel were determined by a validated HPLC method with lower limit of quantification (25 ng/mL). Data points are expressed as mean concentrations for oral (n = 5) administration; error bars indicate Standard Errors (SEs).

Fecal excretion of the paclitaxel formulated in SMEOF#3 in Wild-type and P-gp knockout mice

When SMEOF#3 (1.5%) was administered orally at doses of 10, 30, or 60 mg/kg of paclitaxel to P-gp knockout mice, the recovery of unchanged paclitaxel in the feces increased with dose from 27.9% ± 2.4% to 56.4% ± 5.3% of the administered dose, whereas the recovery ranged up to 84.7% ± 5.2% when using SMEOF#3 (3%) (Fig. 3). Thus, the fecal recovery of paclitaxel in P-gp knockout mice was considerably higher with SMEOF#3 (3.0%) than with SMEOF#3 (1.5%), which is in line with the finding that the plasma concentration and oral bioavailability of paclitaxel in SMEOF#3 (3%) was lower. This result may be due to more extensive precipitation of paclitaxel in the gastro-intestinal tract with higher loads of paclitaxel in SMEOF#3. The fecal excretion of paclitaxel in WT mice receiving SMEOF#3 (1.5%) in combination with CsA, increased with dose from 60.1 to 95.0% (Fig. 3), indicating that intestinal P-gp was not completely inhibited by CsA.

Furthermore, this could also be due to precipitation of paclitaxel in the gastrointestinal tract.

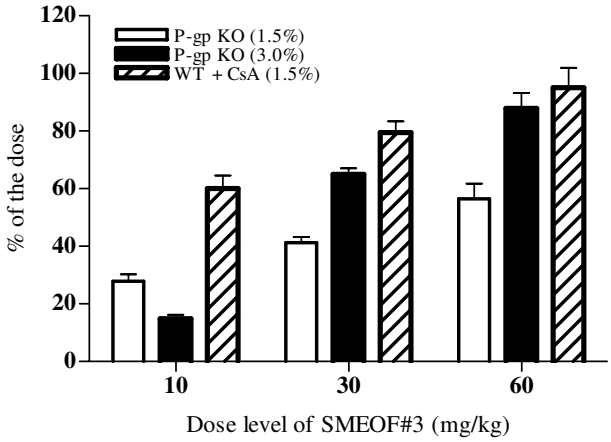

Figure 3. Fecal excretion of paclitaxel in P-gp knockout and Wild-type mice co-administered with CsA (10 mg/kg). The mice were housed in metabolic cages and were treated with an oral administration of SMEOF#3 (with 1.5% w/w or 3.0% w/w paclitaxel) at different doses of 10, 30, or 60 mg/kg. Paclitaxel levels were measured in feces excreted between 0-96 h using a validated HPLC method. Results are expressed as percentage of the given dose; Bars ± SE (n = 5).

Discussion

The present study shows that SMEOFs are potentially suitable as delivery vehicles for oral administration of paclitaxel when administered in combination with a P-gp inhibitor such as CsA. We selected SMEOF#3 for more extensive studies because the systemic exposure and bioavailability of paclitaxel after oral administration of SMEOF#3 was comparable to the standard drinking solution containing Cremophor EL:ethanol (Taxol®). SMEOF#1 and #2 are less practical since they are two-phase solutions that require mixing prior to administration. Moreover, it appeared that they were less stable, which resulted in lower exposures when compared to SMEOF#3. SMEOF#4 is identical to SMEOF#3, except that it already contains CsA and was at least as good as SMEOF#3. Although such a combination of paclitaxel and a P-gp/CYP450 inhibitor in one formulation holds attractive perspectives for future clinical implementation, it was considered more appropriate to use the single drug formulation in this preclinical-mechanistic investigation.

There are two major issues that need to be addressed in order to achieve adequate exposure of paclitaxel after oral administration. The first issue is that it is essential to block and/or bypass the action of P-gp in the intestinal wall as this drug transporter is mainly responsible for the negligible uptake of paclitaxel by the enterocytes (9). Changing the

formulation from a system of co-solvents to a SMEOF was not sufficient to bypass P-gp as the exposure of paclitaxel in WT mice receiving paclitaxel in various SMEOF's without concomitant CsA was very low. Consequently, a combination of paclitaxel in SMEOFs with a P-gp inhibitor is mandatory to yield acceptable oral bioavailabilities.

The second issue concerns the composition and stability of the formulation in the gastro-intestinal tract, as this determines the rate at which paclitaxel will be released from the carrier and becomes available for uptake through the intestinal wall. If degradation of the carrier occurs too slowly, as with CrEL, a substantial fraction of the dose will leave the body without having had the opportunity for uptake by enterocytes (17). On the other hand, if the release from the carrier occurs too rapidly, there is a chance of irreversible precipitation of the liberated and water-insoluble paclitaxel molecules within the intestinal lumen. By using P-gp knockout mice we were able to study this latter issue without having to take into account the action of P-gp.

The plasma pharmacokinetics and fecal excretion of paclitaxel were evaluated at three different dose levels in P-gp knockout mice. At the lowest dose level of 10 mg/kg the plasma AUC is very similar to the AUC achieved in patients receiving oral paclitaxel in the CrEL containing drinking solution (19), although the direct comparison is somewhat tricky because the shape of the curves in mice and humans differ with higher C_{max}, shorter T_{max} and shorter elimination half-life in mice. When patients receive increasing doses of oral paclitaxel, the plasma AUC increases only marginally because of entrapment of paclitaxel in CrEL micelles in the intestinal lumen (17, 18). Although the finding that the plasma AUC of paclitaxel in mice increased proportional with dose when using SMEOF#3 suggested that the uptake by the intestines was also independent of the dose, this was not the case. The fecal excretion of unchanged drug at the 10 mg/kg dose was already much higher than the less than 2% previously observed with the CrEL drinking solution (9) and the fecal excretion further increased with dose. Because the fecal excretion of unchanged drug was even more pronounced when the amount of carrier relative to paclitaxel was reduced as in SMEOF#3 (3%), it is most likely that a rapid degradation of the carrier is responsible for the reduced intestinal uptake. Apparently, this formulation may not be stable enough to contain paclitaxel at this concentration in order to protect paclitaxel from precipitation in the gastro-intestinal tract. Moreover, gastric emptying in mice was delayed at the higher dose levels, as indicated by the longer T_{max}, leaving even more time for degradation of the carrier before the drug enters into the intestines. In view of this, the finding that the plasma level of paclitaxel increased dose-proportionally, in spite of the fact that the uptake at higher dose levels occurs less efficiently, is most likely coincidental and caused by saturation of first-pass metabolism at the higher doses. In a previous pilot study with SMEOF#3 (1.6%) in patients, it was observed that the AUC was similar, but that the

T_{max} was shorter and the C_{max} was higher than with the CrEL drinking solution (26). This finding is consistent with the idea that paclitaxel becomes more readily available for uptake when given in SMEOF#3. As the load of paclitaxel in SMEOF#3 appears to be an important determinant for the rate of release, future clinical studies aimed at establishing the dose-AUC proportionality of oral paclitaxel with SMEOF#3 should include the testing of different loads.

As expected, the fecal recovery was higher in WT mice due to reduced intestinal uptake because of incomplete inhibition of P-gp by CsA. We have used a dose level of 10 mg/kg of CsA because we previously found that increasing the dose to 50 mg/kg did not further increase the oral bioavailability (12). Moreover, this lower dose was preferred because we wanted to avoid as much as possible an interaction between the SMEOF and CrEL that is present in the CsA formulation. For this reason there was also a 20 min lag time between the two subsequent oral administrations. Incomplete inhibition of P-gp was more pronounced at higher dose levels of SMEOF#3. Whereas it is possible that the dose level of CsA was too low to compete for the higher quantities of paclitaxel, it is also likely that it is a consequence of the delayed gastric emptying. Due to this effect, CsA that was given 20 min prior to paclitaxel had already moved to lower parts of the intestinal tract when a substantial fraction of the dose of paclitaxel was still present in the stomach. Both the dose and the timing issues would be addressed when the formulation would hold both paclitaxel and the inhibitor as in SMEOF#4 and this is certainly an option to test in future clinical studies.

In conclusion, our preclinical mechanistic studies with oral administration of paclitaxel in novel SMEOFs showed that SMEOF#3 is a potentially suitable vehicle for oral delivery of paclitaxel when given in combination with a P-gp inhibitor such as CsA. Our results revealed that the bioavailability and the systemic exposure to paclitaxel after a single oral administration of SMEOF#3 were comparable to the standard Cremophor EL: ethanol formulations. The load of paclitaxel in the formulation appears to be important with respect to the stability of paclitaxel in the gastro-intestinal tract and can be used to optimize the bioavailability and dose-proportionality of systemic drug exposure after oral administration in future clinical studies.

References

1. Huizing MT, Misser VH, Pieters RC, et al. Taxanes: a new class of antitumor agents. Cancer Invest 1995;13:381-404.
2. Rowinsky EK, Wright M, Monsarrat B and Donehower RC. Clinical pharmacology and metabolism of Taxol (paclitaxel): update 1993. Ann Oncol 1994;5 Suppl 6:S7-16.
3. Dorr RT. Pharmacology and toxicology of Cremophor EL diluent. Ann Pharmacother 1994;28:S11-S14.
4. Sparreboom A, van Tellingen O, Nooijen WJ and Beijnen JH. Nonlinear pharmacokinetics of paclitaxel in mice results from the pharmaceutical vehicle Cremophor EL. Cancer Res 1996;56:2112-2115.
5. van Tellingen O, Huizing MT, Panday VR, et al. Cremophor EL causes (pseudo-) non-linear pharmacokinetics of paclitaxel in patients. Br J Cancer 1999;81:330-335.
6. Sparreboom A, van Zuylen L, Brouwer E, et al. Cremophor EL-mediated alteration of paclitaxel distribution in human blood: clinical pharmacokinetic implications. Cancer Res 1999;59:1454-1457.
7. Liu G, Franssen E, Fitch MI and Warner E. Patient preferences for oral versus intravenous palliative chemotherapy. J Clin Oncol 1997;15:110-115.
8. Schellens JH, Malingre MM, Kruijtzer CM, et al. Modulation of oral bioavailability of anticancer drugs: from mouse to man. Eur J Pharm Sci 2000;12:103-110.
9. Sparreboom A, van Asperen J, Mayer U, et al. Limited oral bioavailability and active epithelial excretion of paclitaxel (Taxol) caused by P-glycoprotein in the intestine. Proc Natl Acad Sci U S A 1997;94:2031-2035.
10. Sonnichsen DS, Liu Q, Schuetz EG, et al. Variability in human cytochrome P450 paclitaxel metabolism. J Pharmacol Exp Ther 1995;275:566-575.
11. van Asperen J, van Tellingen O, Sparreboom A, et al. Enhanced oral bioavailability of paclitaxel in mice treated with the P-glycoprotein blocker SDZ PSC 833. Br J Cancer 1997;76:1181-1183.
12. van Asperen J, van Tellingen O, Van Der Valk MA, et al. Enhanced oral absorption and decreased elimination of paclitaxel in mice cotreated with cyclosporin A. Clin Cancer Res 1998;4:2293-2297.
13. Meerum Terwogt JM, Beijnen JH, Bokkel Huinink WW, et al. Co-administration of cyclosporin enables oral therapy with paclitaxel. Lancet 1998;352:285.
14. Kruijtzer CM, Schellens JH, Mezger J, et al. Phase II and pharmacologic study of weekly oral paclitaxel plus cyclosporine in patients with advanced non-small-cell lung cancer. J Clin Oncol 2002;20:4508-4516.
15. Kruijtzer CM, Boot H, Beijnen JH, et al. Weekly oral paclitaxel as first-line treatment in patients with advanced gastric cancer. Ann Oncol 2003;14:197-204.
16. Helgason HH, Kruijtzer CM, Huitema AD, et al. Phase II and pharmacological study of oral paclitaxel (Paxoral) plus ciclosporin in anthracycline-pretreated metastatic breast cancer. Br J Cancer 2006;95:794-800.
17. Malingre MM, Schellens JH, van Tellingen O, et al. The co-solvent Cremophor EL limits absorption of orally administered paclitaxel in cancer patients. Br J Cancer 2001;85:1472-1477.
18. Bardelmeijer HA, Ouwehand M, Malingre MM, et al. Entrapment by Cremophor EL decreases the absorption of paclitaxel from the gut. Cancer Chemother Pharmacol 2002;49:119-125.
19. Malingre MM, Terwogt JM, Beijnen JH, et al. Phase I and pharmacokinetic study of oral paclitaxel. J Clin Oncol 2000;18:2468-2475.
20. Gursoy N, Garrigue JS, Razafindratsita A, et al. Excipient effects on in vitro cytotoxicity of a novel paclitaxel self-emulsifying drug delivery system. J Pharm Sci 2003;92:2411-2418.
21. Gershanik T and Benita S. Self-dispersing lipid formulations for improving oral absorption of lipophilic drugs. Eur J Pharm Biopharm 2000;50:179-188.
22. Chang T, Benet LZ and Hebert MF. The effect of water-soluble vitamin E on cyclosporine pharmacokinetics in healthy volunteers. Clin Pharmacol Ther 1996;59:297-303.
23. Boudreaux JP, Hayes DH, Mizrahi S, et al. Use of water-soluble liquid vitamin E to enhance cyclosporine absorption in children after liver transplant. Transplant Proc 1993;25:1875.
24. Sparreboom A, van Tellingen O, Nooijen WJ and Beijnen JH. Determination of paclitaxel and metabolites in mouse plasma, tissues, urine and faeces by semi-automated reversed-phase high-performance liquid chromatography. J Chromatogr B Biomed Appl 1995;664:383-391.
25. Huizing MT, Sparreboom A, Rosing H, et al. Quantification of paclitaxel metabolites in human plasma by high-performance liquid chromatography. J Chromatogr B Biomed Appl 1995;674:261-268.
26. Veltkamp SA, Thijssen B, Garrigue JS, et al. A novel self-microemulsifying formulation of paclitaxel for oral administration to patients with advanced cancer. Br J Cancer 2006;95:729-734.

CHAPTER 4.3

Dose-finding and pharmacokinetic study of orally administered indibulin (D-24851) to patients with advanced solid tumors

Roos L. Oostendorp, Petronella O. Witteveen, Brian Schwartz, Liia D. Vainchtein, Margaret Schot, Annemarie Nol, Hilde Rosing, Jos H. Beijnen, Emile E. Voest, Jan H.M. Schellens

Submitted for publication

Abstract

Indibulin (ZIO-301/D-24851) is an orally applied small molecule with antitumor activity based upon destabilization of microtubule polymerization. The purpose of this phase I study was to determine the maximum tolerated dose (MTD) as well as the dose limiting toxicity (DLT), the pharmacokinetics, safety and tolerability of orally administered indibulin as capsule formulation in patients with advanced solid tumors.

Patients received a single dose of indibulin. Seven dose-levels were evaluated: 100, 150, 250, 350 and 600 mg once daily (QD), 450 and 600 mg twice daily (BID). After a washout period, patients received indibulin at the pre-defined daily dose for 14 days every 3 weeks (multiple dose part). A total of twenty-eight patients entered the study. Indibulin administered as capsules was generally well tolerated. The MTD was not reached. There was a disproportionate increase of the area under the plasma concentration-time curve (AUC) with dose, with declining AUC corrected for dose starting at the 250 mg dose-level. Twice daily dosing instead of once daily schedule had no significant effect on the increase of the systemic exposure to indibulin. There was no significant difference in AUC of indibulin after multiple dosing (day 1-14) compared to single administration (day-4). Inter-patient variability in AUC (102% CV) was high.

A plateau in drug exposure was observed prior to reaching the MTD. Continued dose-escalation was unlikely to yield any increase in exposure of indibulin. A plausible explanation for the low systemic exposure is the low solubility of indibulin in its current formulation. This formulation may not be suitable to protect indibulin from precipitation in the gastro-intestinal tract. The formulation needs optimization to increase the systemic exposure upon oral administration.

Introduction

Indibulin (ZIO-301; D-24851; (N-(pyridine-4-yl)-[1-(4-chlorbenzyl)-indol-3-yl]-glyoxyl-amid)) is a novel, orally applied, synthetic, small molecule with antitumor activity based upon destabilization of microtubules (1). Indibulin induces accumulation of cells with condensed nuclei and abnormal mitotic spindles, and arrests cells at metaphase. This antimitotic drug is active against a wide range of human tumor cell lines and xenografts, including multidrug resistant tumor cells and taxane refractory tumors (2, 3). In preclinical studies indibulin lacks neurotoxicity typically associated with other tubulin binding drugs such as the taxanes and vinca alkaloids (4-7). Furthermore, good bioavailability after oral application and curative treatment at almost non-toxic doses were shown (2, 3). Thus, the novel tubulin binding agent indibulin was predicted to have a significantly improved therapeutic index compared to other microtubule inhibiting compounds, such as paclitaxel and vincristine (8, 9). Previously, an oral drinking solution of indibulin in 10% lactic acid was selected from a number of formulations for further clinical testing in a phase I trial (3, 10). During this phase I study (10), a schedule of once daily administration on 14 consecutive days was chosen based upon preclinical studies, wherein a higher efficacy after prolonged oral daily dosing was found. Furthermore, the effect of food was investigated in that study and administration of indibulin in patients in fasting or fed condition did not reveal differences in efficacy or tolerability. However, in this previously published phase I study (10) it became evident that an increase in the occurrence of nausea and vomiting occurred with continued dosing of indibulin, clearly correlated to the formulation of indibulin. Patients complained about the bad taste of the formulation, which was probably related to the lactic acid in the drinking solution. Therefore, a new capsule formulation was prepared to improve the tolerability of the formulation. Indibulin formulated in capsules was investigated in a dose-escalation study with the primary objective to determine the maximum tolerated dose (MTD) of orally administered indibulin on a once or twice daily schedule for 14 days every 3 weeks in subjects diagnosed with advanced solid tumors. Secondary objectives were the determination of the dose-limiting toxicity (DLT), characterization of the profile of adverse reactions, the pharmacokinetics after single and multiple administrations at different dose-levels, and preliminary antitumor activity.

Patients and Methods

Patient selection/ Eligibility Criteria

Patients with histological proof of cancer for whom no standard therapy of proven benefit existed were eligible for the study. Previous radiotherapy or chemotherapy was allowed but

treatment had to be stopped at least four weeks prior to study entry and any resulting toxicities had to be resolved. Patients had to have acceptable bone marrow, liver and renal function evidenced by the following parameters: WBC ≥ 3.0 x 10^9/L, platelets ≥ 100 x 10^9/L, ANC ≥ 1.5 x 10^9/L, hemoglobin > 6.0mM, total bilirubin < 1.5 x ULN, liver enzymes SGOT/ASAT and SGPT/ALAT ≤ 2.5 x ULN unless related to liver metastases then ≤ 5 x ULN was accepted and serum creatinine ≤ 135 μmol/L or clearance ≥ 50 mL/min, calculated according to Cockcroft and Gault. All patients had to have an Eastern Cooperative Oncology Group (ECOG)/World Health Organization (WHO) performance status (PS) ≤ 2, had to be ≥ 18 years of age, had to have a life expectancy of more than 3 months, and were not allowed to have previous anticancer therapy for ≥ 4 weeks. Patients were excluded if they suffered from uncontrolled infectious disease, neurologic disease, psychiatric disease that could interfere with proper completion of the protocol assignment, or from bowel obstruction or motility disorders that could influence the absorption of the study drug. Patients with symptomatic brain metastases were not eligible. Further exclusion criteria were: concomitant use of H_2-receptor antagonists or proton pump inhibitors. The trial was approved by the Medical Ethics Committee of both institutes where the study was performed, The Netherlands Cancer Institute and the University Medical Center Utrecht. All study participants provided written informed consent prior to study enrollment.

Treatment Plan and Study Design

This was an open label, non-controlled, multicenter dose-finding and pharmacokinetic phase I study with single- and multiple-dose pharmacokinetics and inter-subject dose-escalation. A starting dose of 100 mg indibulin capsules in the dose-escalation study was derived under consideration of the non toxic effect level in the previous phase I study published by Kuppens et al. (10). The indibulin capsules were administered orally once daily (QD), after an overnight fast of at least ten hours, in the morning after breakfast, together with 100 mL tap water on day -4 (single dose) followed by a washout of 3 consecutive days (Fig. 1). From the dose-escalation step 900 mg/day onwards, the daily dose was split into two equal daily doses (BID), starting at 450 mg BID. The schedule of the multiple dose part was daily administration of indibulin in the morning after breakfast for 14 days without interruption (Fig. 1). No fluid intake for 1 hour post-dose and no food were allowed for at least 2 hours post-dose. Cycles were repeated every 21 days and if subjects had recovered from signs of toxicity. Subjects remained on study until occurrence of unacceptable toxicities, disease progression, withdrawal of consent, investigator discretion, or a treatment delay for more than 3 weeks.

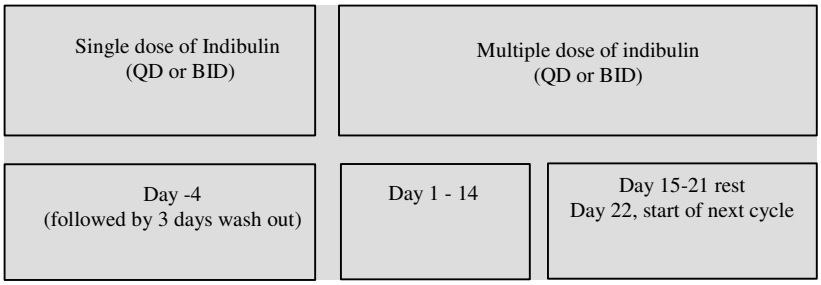

Figure 1. Study design of the dose-escalation.

A minimum of three patients with at least 1 evaluable cycle in each patient had to be entered at each dose-level. At a given dose-level, at least 14 days should pass between the entry of the first and the following two patients. If a DLT was observed in one out of three patients at a given dose-level in the first cycle, up to three additional patients were to be treated at that dose-level. Dose-escalation steps were depending upon the type and grade of observed toxicity. In case of CTC grade 0-1 hematological and/or non-hematological toxicity (except for alopecia and anemia) the dose was escalated by 100%. In case of grade 2 hematological toxicity (except anemia) doses were increased by 50%. Doses were increased by 33% in case of non-hematological CTC grade 2 toxicity (except alopecia, non-treated nausea and/or vomiting) or in case of CTC grade 3 hematological toxicity (except anemia). No new patients were recruited at the same or a higher dose-level if two or more patients at a given dose-level experienced a DLT. A DLT was an adverse event (AE) of the following types for which the relation to the study treatment was likely or not assessable: non-hematological toxicity of CTC grade ≥ 3 (except alopecia and/or nausea and/or vomiting in the absence of appropriate anti-emetic treatment) or hematological toxicity CTC grade 4 (if thrombocytopenia; or if neutropenia for more than 7 days) or neutropenia of CTC grade 3 plus fever or non reversible neurotoxicity of CTC grade > 2 or appropriately treated drug related nausea and/or vomiting preventing drug intake for more than three consecutive days.

The MTD was defined as the dose which produced DLT in two or more patients in the first cycle at a given dose-level. The recommended dose for future (phase II) trials, which is below the MTD, was to be defined on the basis of tolerance of the dose schedule administered repetitively.

All used and unused trial supplies were completed on a medication accountability list and also patients were asked to keep a diary to document the quantity and administration of indibulin by date.

Patient Evaluation, Toxicity and response evaluation

Baseline evaluation prior to study entry included a complete medical history and physical examination, ECG, slit lamp ophthalmoscopic examination, clinical blood parameters, including blood count and differentiation, blood chemistry, tumor evaluation, serum tumor markers and the evaluation of the extent of the tumor using appropriate radiographic imaging. Slit lamp ophthalmoscopic examinations were performed because in one monkey a mild cataract was observed at the end of treatment although that was most probably related to the animal's age.

Evaluation of PS, body weight, clinical laboratory parameters and patient compliance were assessed on day -4, day 14 and 21 of the dose-escalation study, and on day 1 of every following cycle. AEs were assessed continuously. Assessments in patients with measurable disease followed RECIST criteria (response evaluation criteria in solid tumors) (11). Response to therapy was assessed on day 21 of a cycle (day-1 of the consecutive cycle). If retreatment was postponed, the data obtained immediately prior to retreatment served as day-1 data for the next cycle. AEs were graded according to the National Cancer Institute-Common Toxicity Criteria (NCI-CTC) version 3.0.

Study Drug Description

The indibulin capsules consisted of hard gelatin capsules containing, 50 or 100 mg indibulin active substance and as excipients 50 mg Corn Starch C Pharma, 45 mg Avicel, 5.5 mg Aerosil, 5.0 mg Tween 80, 2.5 mg Gelatin, 2.0 mg Magnesium stearate (non-bovine) and purified water. The capsules were stored at room temperature.

Pharmacokinetic sample collection and analysis

The pharmacokinetics of indibulin were studied on day -4 and 14 of the dose-escalation study. Heparinized blood samples 5 mL each were collected before administration and at 1, 2, 3, 4, 5, 7, 10, 12, 24, 32, 48, 96 h after drug intake. Samples were centrifuged at 3,000 g for 10 minutes at room temperature and plasma was stored at -20°C until analysis. Indibulin was stable at -20°C in plasma over the time-period stored and analyzed, and not influenced by freeze-thawing (12). Indibulin plasma concentrations were measured by a validated LC-MS/MS method (12). The lower limit of quantitation was 1.00 ng/mL for plasma.

Statistical analysis

Pharmacokinetic parameters were calculated by the noncompartmental trapezoidal method using the software package WinNonlin Professional (version 5.0, Pharsight, Mountain View, CA, USA). The area under the plasma concentration-time curve (AUC) was

calculated from time 0 to 24 h and with extrapolation to infinity using the terminal rate constant k. Other parameters to be assessed were the terminal half-live ($t_{1/2}$), the maximal plasma concentration (C_{max}) and the time to maximal concentration (T_{max}). Statistical analyses of the data were performed using paired sample t-tests. A significance level of 0.05 was used for analyses. The statistical analyses were performed using SPSS for Windows (version 15.0).

Results

Patient Characteristics, dose-levels and main drug-related toxicities

A total of twenty-eight subjects (fourteen males and fourteen females) were enrolled into the study and their characteristics are presented in Table 1. The following dose levels of indibulin were tested: 100, 150, 250, 350, and 600 mg QD, 450, and 600 mg BID. All patients were evaluable for safety and indibulin as capsule was generally well tolerated. Twenty-eight subjects reported adverse events (AEs) and twenty-one out of the twenty-eight subjects reported AEs with causality likely to be related to the study medication. The drug related hematological and non-hematological toxicities displayed by dose-level and toxicity grade are presented in Table 2. Almost all hematological and non-hematological toxicities started during the first cycle and were resolved or improved within 1-14 days. Toxicities did not significantly increase in number and/or severity after multiple cycles of therapy. Thus, no signs of cumulative toxicity were observed. The most frequently indibulin related non-hematological toxicities in all cycles were nausea (39% of patients), fatigue (36% of patients), and vomiting (32% of patients). The hematological toxicity was mild and did not exceed CTC grade 2. Most AEs were reversible and rated as either CTC grade 1 and 2. Of the total 34 CTC grade 3 and 4 AEs, only 6 AEs were considered likely related to the study medication, such as fatigue, increased aspartate aminotransferase (AST), alanine aminotransferase (ALT), alkaline phosphatase (AP), and gamma-glutamyltransferase (γ-GT). No neurotoxicity has been observed.

A total of twenty-two serious adverse events (SAEs) were experienced by fourteen patients. One out of these fourteen patients (100 mg dose group) reported SAEs (increased AST/ALT), considered likely related to the study medication. Study treatment in this patient was stopped due to liver function tests with the AST/ALT values normalizing after discontinuation of study medication. By the time of final evaluation/follow-up eight subjects had died. Six out of these eight patients died from malignant/progressive disease (one in the 100 mg, two in the 250 mg, and three in the 1200 mg dosage group), one from cardiovascular disease (100 mg dosage group), and one from unknown cause (1200 mg dosage group). No deaths were considered to be related to study medication.

Table 1. Patient characteristics.

No. of patients	28
Sex	
Female	14
Male	14
Age (years)	
median	59
range	44 – 82
WHO performance status	
median	1
0	3
1	23
2	2
Tumor type	
Adrenal cortex	1
Cervix	1
Colorectal	8
Esophagus	1
Gastric cancer	1
Head and neck	1
Melanoma	1
Mesothelioma	1
Non-small cell lung cancer (NSCLC)	3
Ovarian Cancer	1
Pancreatic cancer	3
Prostate	1
Small-cell lung cancer (SCLC)	1
Soft tissue sarcoma	2
Urothelial cancer	2
Vulva cancer	1
Number of subjects completing cycles	
Pre-Cycle 1	28 (100%)
Cycle 1	21 (75%)
Cycle 2	13 (46.4%)
Cycle 3	6 (21.4%)
Cycle 4	4 (14.3%)
Cycle 5	1 (3.6%)
Cycle 7	1 (3.6%)
Prior treatment	
Surgery	16
Radiotherapy	13
Hormone therapy	1
Chemotherapy	25
Other	5

Five observations in patients meet the criteria for DLT of indibulin. One patient at dose level 100 mg had CTC grade 3 elevated AST/ALT levels in cycle 6 and 7. This event was considered likely related to the study drug and the patient was discontinued from the study due to repeated elevated AST/ALT levels. In another patient, at dose level 100 mg CTC grade 3 supraventricular tachycardia in cycle 1 was observed which was considered likely non-related to the study medication. The patient died, however, it was not confirmed that cardiovascular disease was the cause of the death. Furthermore, at dose level 150 mg, one patient showed CTC grade 3 fatigue in cycle one, considered likely related to the study drug, and CTC grade 3 increased ALT in cycle one, considered non-related. In another patient at the 150 mg dose level CTC grade 3 hypophosphatemia was observed in cycle two and was considered not related to study drug. The last patient in whom DLT was observed (at dose level 250 mg) showed CTC grade 3 increased AP and CTC grade 4 increased γ-GT

in cycle two, both considered likely related to the study drug. However, there was no apparent relationship between dose-level and frequency or intensity of treatment-emergent AEs. To date the MTD with the oral capsules dosed up to 600 mg BID (1200 mg total/day) was not reached in this study on the basis of the observed DLTs. Dose-escalation was stopped at that level, because of the low and variable systemic exposure to indibulin without a significant increase with dose (as shown in the pharmacokinetics paragraph).

Table 2. Hematological and non-hematological toxicities (AEs) per dose-level related to the study drug.

Toxicity type	**Dose capsules (mg)**	**100**	**150**	**250**	**350**	**600**	**900**	**1200**	**Total**
	No. of pts. with at least one AE	3	3	3	3	1	3	5	21
Hematological	**CTC grade**								
anemia	2	0	0	0	0	1	0	0	1
Non-hematological									
Photophobia	1	0	1	0	0	0	0	0	1
Blurred vision	1	1	0	0	0	0	0	0	1
Visual acuity reduced	1	0	0	1	0	0	0	0	1
Abdominal pain	1	0	0	0	1	0	1	0	2
	2	0	0	0	1	0	0	0	1
Constipation	1	0	0	0	1	0	0	0	1
Diarrhea	1	1	1	0	0	0	1	0	3
Dry mouth	1	0	0	0	0	1	0	0	1
Dyspepsia	1	0	0	1	0	0	0	0	1
Nausea	1	1	1	1	2	0	1	3	9
	2	1	0	1	0	0	0	0	2
Reflux gastritis	1	1	0	0	0	0	0	0	1
Stomatitis	1	0	0	0	0	1	0	0	1
Vomiting	1	1	0	2	1	0	1	3	8
	2	1	0	0	0	0	0	0	1
Chills	1	1	0	0	0	0	0	0	1
fatigue	1	0	0	0	0	0	0	0	0
	2	1	1	1	0	1	1	1	6
	3	0	2	1	0	0	1	0	4
nasopharyngitis	1	0	0	0	0	0	1	0	1
Muscle strain	1	1	0	0	0	0	0	0	1
ALT increased	2	1	1	1	0	0	0	0	3
	3	1	0	0	0	0	0	0	1
AST increased	1	0	0	1	0	0	0	0	1
	2	0	0	0	0	0	0	0	0
	3	1	0	0	0	0	0	0	1
AP increased	1	1	0	0	0	0	0	0	1
	2	0	0	0	0	0	0	0	0
	3	0	0	1	0	0	0	0	1
LDH increased	1	1	0	0	0	0	0	0	1
γ-GT increased	1	1	0	0	0	0	0	0	1
	2	0	0	0	0	0	0	0	0
	3	0	0	0	0	0	0	0	0
	4	0	0	1	0	0	0	0	1
Weight decreased	1	0	1	0	0	0	0	0	1
	2	1	0	0	0	0	0	0	1
anorexia	1	0	1	1	1	0	0	0	3
	2	1	0	0	0	0	1	0	2
dizziness	1	1	0	0	0	0	0	0	1
dysgeusia	1	0	1	1	0	1	0	0	3
headache	1	1	0	0	0	0	0	0	1
hyposmia	1	0	1	0	0	0	0	0	1
paraesthesia	1	0	1	0	0	0	0	0	1
Peripheral sensory neuropathy	1	0	1	0	0	0	0	0	1

Abbreviations: ALT, alanine aminotransferase; AST, aspartate aminotransferase; ALP, alkaline phosphatase; LDH, lactate dehydrogenase; γ-GT, gamma-glutamyltransferase.

Pharmacokinetics

Blood sampling for pharmacokinetic analysis was performed in twenty-eight patients on day -4 and in twenty-three patients on day 14. The plasma concentration versus time curves for indibulin on day -4 and day 14 at all dose-levels are depicted in figure 2 and the related pharmacokinetic parameters of indibulin are presented in Table 3. Indibulin was absorbed relatively slowly and variably and the maximal plasma concentration was reached between 1 to 12 h after administration. Systemic exposure to indibulin was low and variable at all dose-levels and a non-linear relationship between dose and $AUC_{0\text{-}24h}$ was found on day -4 and day 14 (Table 3; Fig. 3). There was a disproportionate increase of the $AUC_{0\text{-}24h}$ with dose with declining AUC corrected for dose starting at 250 mg dose-level (Table 3; Fig. 3). The inter-patient variability in AUC was high (variable from 5 to 102% CV) on both days (Table 3). The systemic exposure to oral indibulin did not increase with twice daily instead of once daily dosing. Furthermore, it was determined whether accumulation of the drug occurred. A paired sample t-test for day -4 vs day 14 was performed for the $AUC_{0\text{-}24h}$ and C_{max} at the different dose levels. Higher $AUC_{0\text{-}24h}$ levels were observed after multiple dosing (day 14), but these were not statistically significant compared with single dosing (day -4) (Fig. 3). There was no significant difference between the C_{max} on day -4 and day 14 at all dose levels. The terminal half-life at the highest tested dose of 600 mg BID (100 mg capsules) was 34 ± 9.5 h and 27 ± 17 h on day -4 and day 14, respectively. No difference in pharmacokinetics between the 50 mg and 100 mg indibulin capsules was observed at dose-level 600 mg BID. A plateau in drug exposure was observed with the oral indibulin capsule formulation prior to reaching the MTD. Therefore, it was decided to discontinue this study.

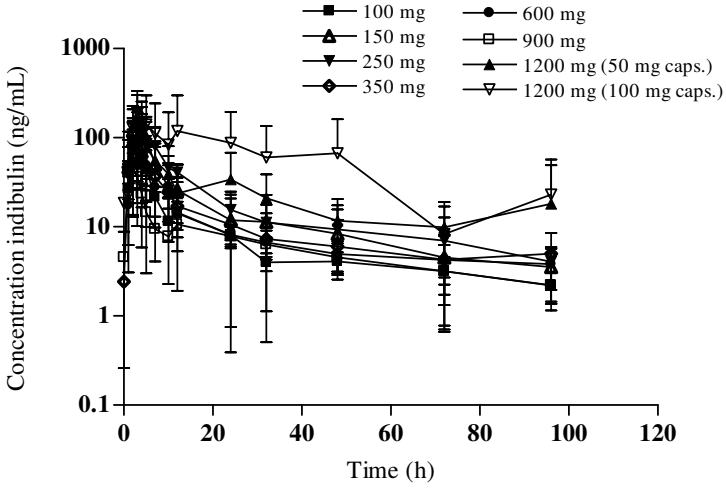

A

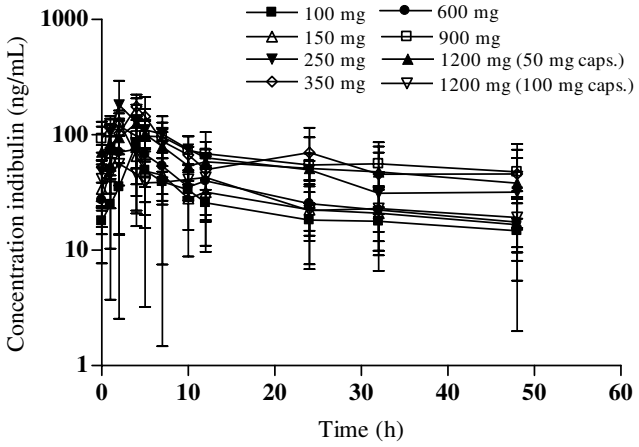

B

Figure 1. Plasma concentration-time curves of indibulin at different dose-levels on day -4 (A) and after multiple dosing from day 1 – 14 (B) represented as mean ± SD.

Table 3. Main pharmacokinetic parameters of indibulin in the dose escalation study, day -4 and day 14. Data are mean ± SD.

Dose (mg) day -4	**N**	**AUC $_{0\text{-}24}$ ng*h/mL (mean ± SD)**	**AUC/ Dose**	**C_{max} ng/mL (mean ± SD)**	**T_{max} (h)**	**$t_{1/2}$ (h)**	**%CV of $AUC_{0\text{-}24}$**
100 QD	3	426 ± 346	4.3	65 ± 51	3.0 (2-5)	75 ± 73	81
150 QD	4	1064 ± 693	7.1	202 ± 109	3.0 (1-4)	29 ± 2.8	65
250 QD	4	1253 ± 707	5.0	280 ± 139	2.5 (2-3)	23 ± 3.6	56
350 QD	3	691 ± 711	2.0	102 ± 97	3.0 (2-3)	31 ± 3.8	102
600 QD	3	597 ± 268	1.0	95 ± 89	4.0 (3-5)	24 ± 8.3	45
450 BID	3	339 ± 17	0.4	47 ± 8	3.0 (2-4)	49 ± 28	5
600 BID (50 mg caps)	5	1049 ± 570	0.9	141 ± 66	4.5 (2-7)	35 ± 12	54
600 BID (100 mg caps)	3	3180 ± 2288	2.6	182 ± 155	6.0 (3-12)	34 ± 9.5	72
Dose (mg) day 14	**N**	**AUC $_{0\text{-}24}$ ng*h/mL (mean ± SD)**	**AUC/ Dose**	**C_{max} ng/mL (mean ± SD)**	**T_{max} (h)**	**$t_{1/2}$ (h)**	**%CV of $AUC_{0\text{-}24}$**
100 QD	3	760 ± 304	7.6	84 ± 62	4.0 (4)	59 ± 31	40
150 QD	3	977 ± 395	6.5	130 ± 32	2.0 (2)	54 ± 16	41
250 QD	2	1942 ± 194	7.8	194 ± 95	3.5 (2-5)	30 ± 20	10
350 QD	3	1895 ± 527	5.4	187 ± 43	3.5 (2-5)	75 ± 86	28
600 QD	3	1038 ± 721	1.7	81 ± 59	6.0 (2-12)	32 ± 10	69
450 BID	3	1875 ± 553	2.1	135 ± 25	3.3 (1-7)	45 ± 4.2	30
600 BID (50 mg caps)	3	1648 ± 1161	1.4	135 ± 86	3.0 (1-4)	37 ± 19	70
600 BID (100 mg caps)	3	909 ± 475	0.8	62 ± 37	5.3 (2-10)	27 ± 17	52

Abbreviations: $AUC_{0\text{-}24h}$ area under the plasma concentration-time curve from 0 to 24 h after administration; C_{max}, the maximal plasma concentration; T_{max}, time to maximal concentration; $t_{1/2}$, terminal half-life; %CV, coefficient of variation; QD, once daily dosing; BID, twice daily dosing.

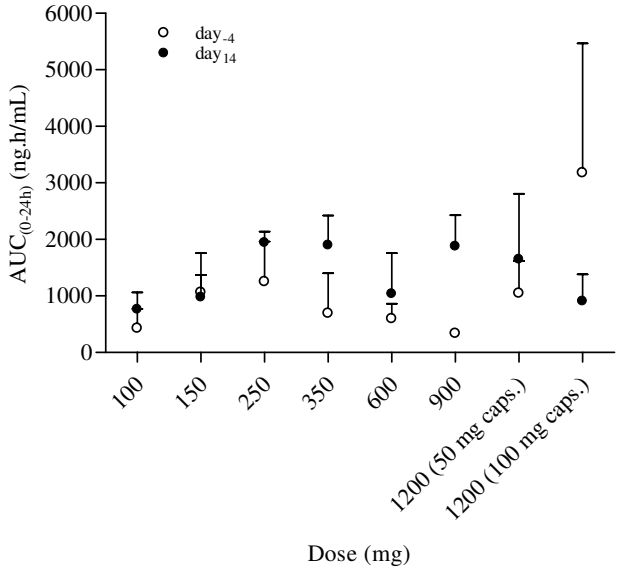

Figure 2. $AUC_{(0\text{-}24h)}$ of indibulin versus dose om day -4 and 14.

Antitumor activity

Out of the twenty-eight patients, twenty-two subjects discontinued the study because of disease progression, four because of lack of tolerability of study medication and two patients withdrew consent due to subject's wish. A best overall response of stable disease (SD) was reported for four subjects (two sigmoid, one non-small cell lung cancer (NSCLC) and one colon cancer), which lasted for 68 to 87 days prior to disease progression (i.e. 3 to 4 cycles of treatment). Fifteen subjects developed progressive disease (PD), which developed between 34 to 87 days after start of entry into the study.

Discussion

The present phase I dose escalation study shows that orally administered indibulin formulated as capsules was well tolerated at the tested doses in patients with advanced solid tumors. However, prior to reaching MTD, a plateau in drug exposure was observed starting at dose-levels above approximately 250 mg QD. Twice daily instead of once daily dosing did not significantly further increase the systemic exposure to indibulin. There was no significant difference in AUC of indibulin after multiple dosing (day 1-14) compared to single administration (day-4). Inter-patient variability in AUC was high. No neurotoxicity has been observed with the indibulin capsules.

Indibulin was selected for testing in patients with advanced solid tumors based on preclinical data that showed high activity of indibulin in preclinical models and good safety profile (2). An indibulin drinking solution in 10% lactic acid plus glucose was selected for the previously published phase I study (3, 10). However, an increase in the incidence and severity of nausea and vomiting occurred at continued dosing of indibulin in patients, clearly correlated to the lactic acid in the solution. Therefore, in this study the new formulation of indibulin administered as capsules was tested. The formulation consists of a mixture of surfactants, Cornstarch, microcrystalline cellulose, aerosil, polysorbate and magnesium stearate, that solubilise indubulin and is used as filling agent for the gelatin hard capsules. The indibulin capsules were well tolerated by the patients. The MTD, with the oral capsules dosed up to 600 mg BID (1200 mg total/day), was not reached in this study. Six CTC grade 3 and 4 AEs (fatigue and increased AST, ALT, AP and γ-GT) were considered likely related to the study medication and five observations met the criteria for DLT as specified in the protocol. However, each case was discussed and there was no apparent relationship between dose-level and frequency or intensity of treatment-emergent toxicities. Prior to reaching the MTD, a plateau in drug exposure with the oral indibulin capsule formulation was observed with declining AUC values corrected for dose starting at 250 mg dose-level (Table 3; Fig. 3). The protocol was modified to twice daily dosing in an attempt to further increase the systemic exposure to indibulin. However, this strategy had no beneficial effect on the systemic exposure to indibulin. Furthermore, there was a high inter-patient variability in AUC and a relatively slow and variable absorption of the indibulin capsules. Continued dose-escalation was unlikely to yield any increase in exposure of indibulin, therefore it was decided to discontinue this study.

A plausible explanation for the low systemic exposure is the low solubility of indibulin in its current oral formulation. This formulation may not be suitable to protect indibulin from precipitation in the gastro-intestinal tract. The formulation needs optimization to increase the systemic exposure upon oral administration of indibulin. This is a common problem in the development of oral formulations of taxanes such as paclitaxel (13-15). Several clinical studies were described with new oral paclitaxel formulations, however, so far no clinically applicable oral paclitaxel formulation has been developed (13-15).

In this study determination of antitumor activity of indibulin was a secondary endpoint. Stable disease in four patients suffering from progressive sigmoid carcinoma, NSCLC and colon cancer, who received treatment at doses varying from 100 to 900 mg/day for three to four cycles of treatment, has been observed.

In conclusion, indibulin was well tolerated at the tested doses. A plateau in drug exposure was observed prior to observing the MTD. Therefore, it was decided to

discontinue this study. Continued dose-escalation was unlikely to yield any further increase in systemic exposure to indibulin. A plausible explanation for the low systemic exposure is the low solubility of indibulin in its current formulation. The formulation needs optimization to increase the systemic exposure upon oral administration.

Acknowledgement

We thank the medical and nursing staff of the Netherlands Cancer Institute and the University Medical Center Utrecht for the support of the patients in this study.

References

1. Jordan MA. Mechanism of action of antitumor drugs that interact with microtubules and tubulin. Curr Med Chem Anticancer Agents 2002;2:1-17.
2. Bacher G, Nickel B, Emig P, et al. D-24851, a novel synthetic microtubule inhibitor, exerts curative antitumoral activity in vivo, shows efficacy toward multidrug-resistant tumor cells, and lacks neurotoxicity. Cancer Res 2001;61:392-399.
3. Baxter. Investigator's Brochure Indibulin 2005.
4. Hussain M, Wozniak AJ, Edelstein MB. Neurotoxicity of antineoplastic agents. Crit Rev Oncol Hematol 1993;14:61-75.
5. Hilkens PH, Verweij J, Vecht CJ, et al. Clinical characteristics of severe peripheral neuropathy induced by docetaxel (Taxotere). Ann Oncol 1997;8:187-190.
6. Freilich RJ, Balmaceda C, Seidman AD, et al. Motor neuropathy due to docetaxel and paclitaxel. Neurology 1996;47:115-118.
7. Windebank AJ. Chemotherapeutic neuropathy. Curr Opin Neurol 1999;12:565-571.
8. Rowinsky EK. The development and clinical utility of the taxane class of antimicrotubule chemotherapy agents. Annu Rev Med 1997;48:353-374.
9. Schiller JH. Role of taxanes in lung-cancer chemotherapy. Cancer Invest 1998;16:471-477.
10. Kuppens IE, Witteveen PO, Schot M, et al. Phase I dose-finding and pharmacokinetic trial of orally administered indibulin (D-24851) to patients with solid tumors. Invest New Drugs 2007;25:227-235.
11. Therasse P, Arbuck SG, Eisenhauer EA, et al. New guidelines to evaluate the response to treatment in solid tumors. European Organization for Research and Treatment of Cancer, National Cancer Institute of the United States, National Cancer Institute of Canada. J Natl Cancer Inst 2000;92:205-216.
12. Stokvis E, Nan-Offeringa LG, Ouwehand M, et al. Quantitative analysis of D-24851, a novel anticancer agent, in human plasma and urine by liquid chromatography coupled with tandem mass spectrometry. Rapid Commun Mass Spectrom 2004;18:1465-1471.
13. Veltkamp SA, Rosing H, Huitema AD, et al. Novel paclitaxel formulations for oral application: a phase I pharmacokinetic study in patients with solid tumours. Cancer Chemother Pharmacol 2007;60:635-642.
14. Veltkamp SA, Alderden-Los C, Sharma A, et al. A pharmacokinetic and safety study of a novel polymeric paclitaxel formulation for oral application. Cancer Chemother Pharmacol 2007;59:43-50.
15. Veltkamp SA, Thijssen B, Garrigue JS, et al. A novel self-microemulsifying formulation of paclitaxel for oral administration to patients with advanced cancer. Br J Cancer 2006;95:729-734.

Chemical structures of investigated molecules in this thesis

Chemical structures

Imatinib and GCP74588

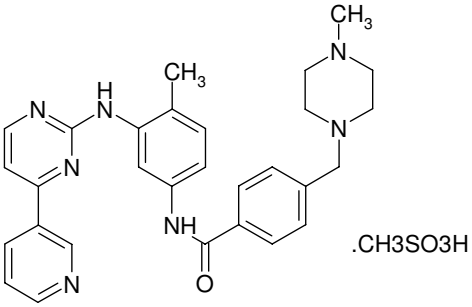

Imatinib

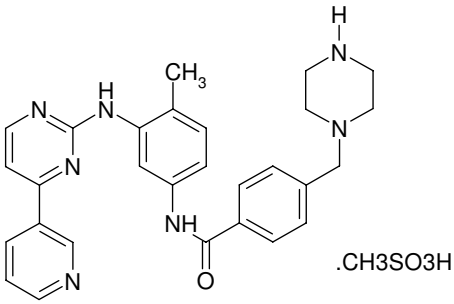

CGP74588

Camptothecins

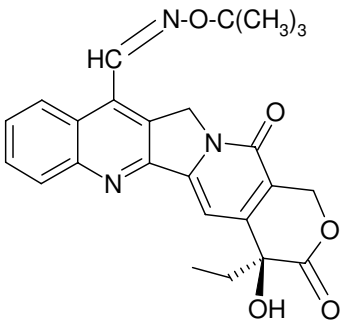

Gimatecan

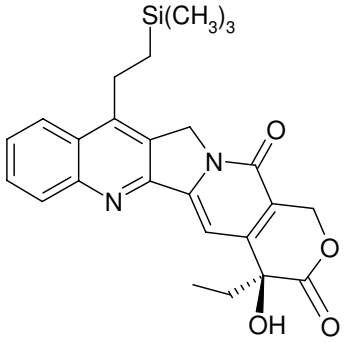

BNP1350

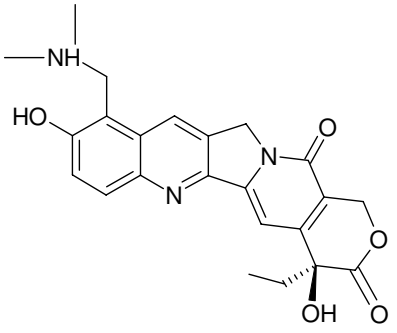

Topotecan

Taxanes

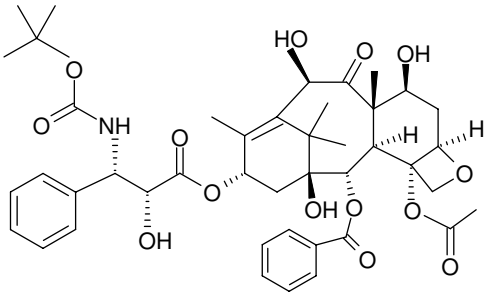

Docetaxel

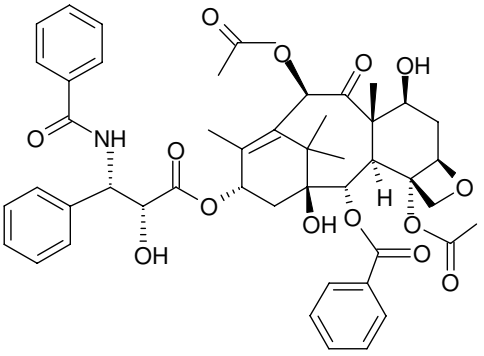

Paclitaxel

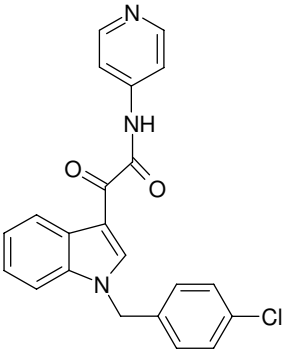

Indibulin (D-24851)

Conclusions and Perspectives

Conclusions and Perspectives

The studies described in this thesis show that ATP-Binding Cassette (ABC) drug transporters, solute carrier (SLC) transporters, metabolic cytochrome P450 enzymes and the drug formulation all can largely affect the (pre)clinical pharmacology of orally applied anticancer drugs. This concerns drugs primarily developed for the oral route, such as most tyrosine kinase inhibitors, and drugs primarily developed for i.v. administration, but now under review for oral application, such as the taxanes docetaxel and paclitaxel. By using sophisticated preclinical models the role of drug transporters and CYP enzymes in the absorption, distribution, metabolism and/or elimination (ADME) of orally administered drugs and drug-drug interactions in the clinic can be better predicted. Furthermore, concomitant use of transporter and/or CYP enzyme inhibitors and oral drugs could be an effective and safe strategy that probably is at least as effective as standard i.v. therapy. Besides the transport proteins and CYP enzymes, the impact of the drug formulation could be important to deliver the oral drug with an adequate oral bioavailability.

Nowadays, new oral anticancer drugs are developed to have favourable pharmacological profiles and negligible affinity for drug efflux transporters and metabolic degradation enzymes. However, in clinical studies limited oral bioavailability, high inter-individual variability in pharmacokinetics, enzyme induction/inhibition, genetic polymorphisms and unwanted drug-drug interactions have been observed with new oral anticancer drugs. In this thesis, comprehensive preclinical studies with imatinib and gimatecan have been described and results showed that ABC/SLC transporters and CYP enzymes play a significant role in the ADME and drug-drug interactions of these drugs.

Even though imatinib has an oral bioavailability of around 98%, however a reduced systemic exposure to imatinib over prolonged time periods and wide inter-individual variability in the systemic exposure is observed in patients. Besides drug metabolizing enzymes, preclinical studies have shown that imatinib interacts with Breast Cancer Resistance Protein (BCRP) and P-glycoprotein (P-gp), however, the exact impact of these transporters on ADME of imatinib was not fully understood due to incomplete data. We found that BCRP and P-gp had only a modest effect on the ADME of imatinib *in vivo* in comparison to metabolic elimination. Co-administration of the BCRP/P-gp inhibitor elacridar significantly increased the systemic exposure to imatinib in the presence or absence of BCRP/P-gp in mice. Although compensatory mechanisms in knockout mice may conceal some of the effects of the absence of these transporters, we showed non-selective inhibitory effects of elacridar. We hypothesized that elacridar inhibited elimination pathways besides BCRP and P-gp such as other efflux or uptake transporters.

We demonstrated *in vitro* that elacridar inhibited the uptake transporters Organic Cation Transporter 1 (OCT1) and Organic Anion Transporter Protein 1B1 (OATP1B1), but not Multidrug Resistance Protein 2, 4 (MRP2, 4) and Organic Anion Transporter 1 (OAT1). We showed in OCT1/2 knockout mice that OCT1/2 has a modest, albeit statistically significant, effect on the systemic exposure but not on the hepatobiliary excretion and liver accumulation of imatinib. The considerable drug-drug interaction observed with elacridar is only partly mediated by inhibition of OCT1/2 and furthermore by other pathways, however imatinib is *in vitro* not transported by OATP1B1. Drug-drug interactions with imatinib wherein OCT1 is inhibited could have an effect on the response of imatinib therapy, since OCT1 transript levels are lower in imatinib non-responders than in imatinib responders. These uptake/elimination pathways can probably be important to explain the observed changes/variability in the pharmacokinetics of imatinib that may compromise therapeutic efficacy in patients. The complexity in the pharmacology of imatinib is also shown in combination therapy of imatinib plus hydroxyurea, which is associated with remarkable antitumor activity in patients with recurrent glioblastoma multiforme. We demonstrated that hydroxyurea did not interact with imatinib by inhibition of P-gp/BCRP mediated transport or CYP3A mediated metabolism of imatinib. There are several other possible mechanisms of action that warrant further investigation and underlie the positive activity of this regimen.

Besides imatinib, the new camptothecin analogue, gimatecan, was developed to have negligible affinity for BCRP and P-gp, however, in this thesis we showed *in vitro* and *in vivo* that gimatecan was transported by BCRP. BCRP affected the oral pharmacokinetics and brain penetration of gimatecan *in vivo*. The P-gp/BCRP inhibitor elacridar also showed non-selective inhibitory effects *in vivo*. We demonstrated *in vitro* that gimatecan is a substrate for OATP1B1 and can be inhibited by elacridar, whereas gimatecan was not transported by P-gp, MRP2, MRP4, OCT1, and OAT1. The affinity of gimatecan for OATP1B1 may be clinically relevant since we demonstrated that also other camptothecins were transported by OATP1B1, such as SN38 and BNP1350. Since the clinical importance of OATP1B1 polymorphisms has been widely established contributing to the inter-patient variability in the efficacy and toxicity of several drugs, this might therefore also have clinical implications for gimatecan. Furthermore, we showed *in vitro* that besides elacridar other widely applied P-gp and/or BCRP inhibitors valspodar, pantoprazole, zosuquidar and verapamil were also non-selective inhibitors since they could also inhibit OATP1B1-mediated transport. These findings suggest that co-administration of camptothecins, or other drugs that are substrates for OATP1B1, and one of these well-known P-gp/BCRP

inhibitors could affect drug uptake, tissue distribution and elimination and probably modify the efficacy and safety profile of drugs.

Our preclinical results demonstrate the importance of comprehensive ADME studies with new oral anticancer drugs to better estimate the pharmacological profile in the clinic. Although it is a useful way to pre-screen new test drugs *in vitro* with affinity for well known ABC transporters and CYP enzyme substrates or inhibitors, it is recommended to enlarge this screen with SLC transporters. In addition, sophisticated *in vitro* models, such as drug transporter assays and biotransformation assays (highly expressing one of the drug transporters or CYP enzymes of interest) are valuable tools to better understand the role of drug transporters and CYP enzymes in the clinical pharmacology of oral anticancer drugs. Furthermore, single or combined drug efflux/uptake transporters and CYP enzyme knockout mice models are required, to investigate the exact role of the identified *in vitro* transporters and CYP enzymes in the ADME of drugs. Moreover, potential species differences in expression and localization of transporters should be taken into account in extrapolating results from animal models to the human situation.

That preclinically designed concepts could successfully be translated to the clinic is shown for oral docetaxel in combination with ritonavir. Oral administration of docetaxel is hampered by its low bioavailability, due to liver and/or gut wall metabolism by CYP3A and to a minor extent by extrusion by P-gp. Co-administration of ritonavir, a CYP3A/P-gp inhibitior strongly enhanced the apparent oral bioavailability of docetaxel in mice and in patients. The combination was well tolerated. This is one of the first clinical examples that concomitant use of transporter and/or CYP enzyme inhibitors with oral anticancer drugs is an effective and safe strategy. Future studies should address the activity and efficacy of this oral treatment approach in comparison with standard i.v. therapy. A dose escalation study in patients with oral docetaxel and ritonavir is being executed to determine the maximum tolerated dose (MTD), dose limiting toxicities (DLT) and optimal dose of docetaxel that can safely be administered in combination with ritonavir in a weekly schedule. These data are promising and form the basis for further development of a clinically applicable oral formulation containing both compounds.

Thus far no clinically applicable oral formulation of paclitaxel has been developed. Oral administration of paclitaxel is hampered by its low bioavailability, due to proficient P-gp in the gut wall and CYP3A enzyme in gut wall and liver. In addition it has been reported that cremophor® EL (CrEL) which is used as solubilizer for paclitaxel in the i.v. paclitaxel (Taxol®) formulation, limits absorption of paclitaxel from the gastro intestinal (GI) tract. This thesis described a novel oral formulation of paclitaxel without the cosolvent CrEL co-

administered with the P-gp/CYP inhibitor cyclosporine A (CsA). This self-microemulsifying oily formulation (SMEOF) of paclitaxel co-administered with CsA is potentially suitable as delivery vehicle and demonstrated equal systemic exposure to paclitaxel comparable to orally administered Taxol®. Changing the formulation from a system of co-solvents to a SMEOF was not sufficient to bypass P-gp. The load of paclitaxel in the SMEOF formulation appears to be important with respect to the stability of paclitaxel in the GI tract and can be used to optimize the bioavailability and dose-proportionality of systemic drug exposure after oral administration in future clinical trials. The design of novel taxanes with a low affinity for P-gp seems to be promising to improve oral bioavailability and penetration multidrug resistant tumors. We tested indibulin, a novel oral tubulin binding agent, which was highly active against human tumor cell lines and xenografts, including multidrug resistant tumor cells and taxane refractory tumors. The indibulin capsules were well tolerated by the patients. However, a plateau in drug exposure was observed prior to reaching the MTD. Twice-daily dosing instead of once daily had no beneficial effect on the systemic exposure to indibulin. Furthermore, there was a high inter-patient variability in the systemic exposure to indibulin following oral administration of the capsules. Continued dose-escalation was unlikely to yield any increase in exposure to indibulin, therefore it was decided to discontinue this study. A plausible explanation for the low systemic exposure is the low solubility of indibulin in its current oral formulation. This formulation may not be suitable to protect indibulin from precipitation in the gastro-intestinal tract. The oral indibulin formulation needs optimization to increase the systemic exposure upon oral administration. It remains a challenge to successfully deliver taxanes orally and to further increase the bioavailability of this drug. The formulation is at least as critical as the affinity for P-gp. It is important that the antitumor activity and oral bioavailability of new taxanes is determined in comprehensive preclinical models, including multidrug resistant models and P-gp knockout mice. Slow progress has been made over the last years in the development of alternative paclitaxel oral formulations. Several new drug carrier systems, such as liposomes, polymeric micelles and (albumin) nanoparticles, are in development. Besides promising antitumor activity, new taxanes might cause less toxicity than the currently used taxane formulations.

The studies described in this thesis show that besides metabolizing enzymes and ABC drug transporters, SLC carrier transporters may potentially play an important clinical role in the ADME of oral drugs and drug-drug interactions. This emphasizes the importance of incorporating SLC drug transporter kinetics and polymorphisms into screening of test drugs, ADME studies and subsequent mechanism-based PK/PD modelling of several

(anticancer) drugs. Recognition of the importance of transporters, CYP enzymes and drug formulations could guide the design and development of novel oral drugs. Preclinical and clinical studies have shown that the oral bioavailability of drugs can be improved substantially by temporary inhibition of drug transporters or CYP enzymes. Concomitant use of transporter and/or CYP enzyme inhibitors with oral drugs is a boosting concept and hopefully an effective and safe way that is at least as effective as standard i.v. therapy. However, the originally developed and classified P-gp and/or BCRP inhibitors showed non-selective inhibitory effects, which has to be taken into account in future (pre)clinical studies. It is of interest to develop inhibitors that interact more specifically. The communication between preclinical and clinical research is of high importance to understand better the pharmacology of drugs. This can probably prevent termination of drug development at later stage and accelerate the development of new oral drugs.

Summary
Samenvatting

Summary

Nowadays, more than 25% of all anticancer drugs are developed as oral formulations. Oral administration of drugs has several advantages over intravenous (i.v.) administration. It will on average be more convenient for patients, because they can take oral medication themselves, there is no need for frequent hospitalization, and the discomfort of an injection or infusion and risk for injection or infusion associated adverse events is absent. However, limited oral bioavailability, high inter-individual variability in pharmacokinetics, enzyme induction/inhibition, and unwanted drug-drug interactions have been observed in clinical studies with new oral anticancer drugs. This thesis investigates the influence of multiple factors, such as the expression and activity of ATP-Binding Cassette (ABC) drug transporters, solute carrier (SLC) transporters, and metabolic cytochrome P450 (CYP) enzymes, and the type of drug formulation, on the absorption, distribution, metabolism and elimination (ADME) of orally administered anticancer drugs. By using sophisticated preclinical models (*in vitro* drug transporter/biotransformation assays and drug transporter/CYP enzyme knockout mice models), the influence of drug transporters and CYP enzymes in the ADME of oral drugs and drug-drug interactions in the clinic can be better predicted. In addition, the type of oral formulation (e.g. polymer, liposome) can be important in order to deliver a certain oral drug with an adequate oral bioavailability and low inter-individual variability. The communication between preclinical and clinical research is of high importance to better understand the pharmacology of drugs in humans.

ABC and SLC drug transporters

Over the past two decades, enormous progress has been made in understanding the pharmacological and physiological role of ABC and SLC drug transporters. **Chapter 1** presents a review on the impact of ABC and SLC drug transporters localized at the intestinal barrier on the absorption, and disposition of orally administered drugs. The outlined preclinical and clinical studies show that the oral bioavailability of drugs can be improved substantially by inhibition of ABC drug transporters. Concomitant use of inhibitors of ABC transporters with orally applied anticancer drugs is hopefully an effective and safe strategy that will at least be as effective as standard i.v. therapy in the treatment of patients with cancer. Pre-screening of anticancer drugs to assess whether they have affinity for ABC and SLC transporters is important to predict their intestinal absorption and this can guide the design and development of novel oral drugs.

Preclinical pharmacological studies on imatinib

Imatinib, an orally active tyrosine kinase inhibitor described in **Chapter 2,** is a drug which shows excellent anticancer activity in chronic myeloid leukemia (CML) and

gastrointestinal stromal tumor (GIST) patients. However, often patients develop resistance to imatinib therapy after chronic use especailly in the case of GIST. Several potential resistance mechanisms have been described. In addition, changes or variations in the pharmacokinetics of imatinib that may affect its therapeutic efficacy have also been observed. Despite the high oral bioavailability of imatinib of 98%, a reduced systemic exposure and a wide inter-individual variability in the systemic exposure to the drug has been observed in patients who used imatinib for prolonged periods of time. Preclinical studies have shown that imatinib interacts with the ABC drug transporters, P-glycoprotein (P-gp) and Breast Cancer Resistance Protein (BCRP; ABCG2), and the expression/activity of these transporters in tumor tissue probably influences the response to imatinib in patients. However, the exact impact of these transporters on the ADME of imatinib is not yet fully understood. The (pre)clinical findings were the basis for our comprehensive preclinical pharmacokinetic study (**Chapter 2.1**) in wild-type, P-gp and/or BCRP knockout mice to unequivocally establish the role of these drug transporters on the disposition of imatinib. Our results reveal that P-gp and BCRP only have modest effects on the ADME of imatinib in comparison to metabolic elimination in mice. Of these two drug transporters, P-gp is the most dominant factor for systemic clearance and the most important for limiting brain penetration of imatinib. Interestingly, co-administration of the P-gp/BCRP inhibitor, elacridar, in mice leads to a 3-fold significant increase in the systemic exposure to imatinib in the presence or absence of P-gp/BCRP. This suggests that elacridar also inhibits other elimination pathways than P-gp and BCRP. It is known from *in vitro* studies that the human Organic Cation Transporter 1 (OCT1) is involved in the cellular uptake of imatinib in a variety of leukaemia cells. Furthermore, in patients with CML it has been found that OCT1 transcript levels in leukemia tumor cells are lower in imatinib non-responders than in imatinib responders. **Chapter 2.2** shows that elacridar inhibits OCT1 *in vitro*. In addition, the research described in this chapter demonstrates that OCT1/2 has a significant effect on the pharmacokinetics of imatinib *in vivo* by using OCT1/2 knockout mice. This OCT1/2 double knockout mouse model was chosen by us as imatinib might have affinity both for OCT2 and OCT1. The considerable drug-drug interaction observed with elacridar and imatinib is only partly mediated by inhibition of OCT1/2. These uptake/elimination pathways can be important to explain the observed changes and variability in the pharmacokinetics of imatinib that may affect therapeutic efficacy in patients.

The complexity in the pharmacology of imatinib is also shown in the *in vitro* study described in **Chapter 2.3**. Imatinib plus hydroxyurea, a ribonucleotide reductase inhibitor, is associated with remarkable antitumor activity in patients with recurrent glioblastoma multiforme. We demonstrate that hydroxyurea and imatinib do not interact at the level of P-gp, BCRP and CYP3A4. Further research is needed to clarify the beneficial activity of this

regimen. **Chapter 2.4** describes the validation of a simple sensitive reversed-phase high performance liquid chromatographic (HPLC) method for the quantification of imatinib and its main metabolite N-desmethyl-imatinib (CGP74588) in human and mice. This method is applied to study the pharmacokinetics of imatinib and its main metabolite in microvolumes of human and mice plasma and a range of other biological matrices of mice.

Preclinical and clinical pharmacological studies on camptothecins

Chapter 3 describes preclinical and clinical pharmacological studies on the camptothecin derived topoisomerase I inhibitors. Camptothecins, such as topotecan and irinotecan, are important and widely used anticancer drugs. However, a significant limitation of these drugs is their affinity for BCRP and P-gp, often resulting in tumor resistance. Therefore, there is an increasing interest in new camptothecins with lower affinity for these drug efflux transporters, such as the highly lipophilic derivatives gimatecan, BNP1350 and lurtotecan. However, in **Chapter 3.1** and **3.2,** we clearly demonstrate that the new camptothecin analogue gimatecan is transported by BCRP, which affects the oral pharmacokinetics and brain penetration of gimatecan in mice. Elacridar also shows a pharmacokinetic interaction with gimatecan, partly mediated by other elimination pathways than BCRP. **Chapter 3.3** shows that gimatecan is a substrate for the Organic Anion Transporter Protein 1B1 (OATP1B1), which can be inhibited by elacridar. We also demonstrate that other camptothecins are transported by OATP1B1, such as SN38 (active metabolite of irinotecan) and BNP1350. Furthermore, we show *in vitro* that besides elacridar other widely applied P-gp and/or BCRP inhibitors are also non-selective inhibitors since they could also inhibit OATP1B1-mediated transport. These findings suggest that co-administration of camptothecins, or other drugs that are substrates for OATP1B1, and one of these well-known P-gp/BCRP inhibitors could affect drug uptake, tissue distribution and elimination and probably modify the efficacy and safety profile of drugs. **Chapter 3.4** describes a clinical study with a new oral topotecan capsule formulation which demonstrates bioequivalence to the current oral formulation and can be administered to patients with solid tumors without any effect of food on the apparent bioavailability. In this study, the requirements for registration and marketing of this new oral topotecan formulation are assessed and the new oral topotecan capsule formulation can be used for clinical applications according to the labelled indications.

Preclinical and clinical pharmacological studies on taxanes

In **Chapter 4** the preclincial and cinical pharmacology of the taxanes, docetaxel and paclitaxel, which are frequently used in a number of patients with solid tumors, such as lung, ovarian and breast tumors are described. These drugs were initially developed as i.v.

formulations, but are under review for oral application. **Chapter 4.1** demonstrates that co-administration of ritonavir, a CYP3A/P-gp inhibitor, strongly enhances the apparent oral bioavailability of docetaxel in patients. The combination is well tolerated and the safety profile is acceptable. These data are promising and form the basis for further development of a clinically applicable oral formulation containing both compounds. **Chapter 4.2** describes novel oral self-microemulsifying oily formulations (SMEOFs) of paclitaxel without the cosolvent Cremophor® EL (CrEL) in mice. CrEL is normally used as solubilizer for paclitaxel in the i.v. paclitaxel (Taxol®) formulation, but limits absorption of oral paclitaxel from the gastro-intestinal tract. We show that SMEOF#3 is a potentially suitable vehicle for oral delivery of paclitaxel when given in combination with the P-gp/CYP inhibitor cyclosporin A (CsA) and demonstrate equal systemic exposure to paclitaxel comparable to orally administered i.v. Taxol®. The design of novel taxanes with a low affinity for P-gp seems to be promising to improve oral bioavailability and penetration into multidrug resistant tumors. In **Chapter 4.3**, a clinical study with a novel oral tubulin binding agent, indibulin is described. It is shown that the indibulin capsule is well tolerated up to 1200 mg/day in patients with advanced solid tumors. However, a plateau in drug exposure is observed prior to observing the maximum tolerated dose. Twice-daily dosing instead of once daily had no beneficial effect on the systemic exposure to indibulin. Furthermore, there is a high inter-patient variability in the systemic exposure to indibulin following oral administration of the capsules. Continued dose-escalation is unlikely to yield any further increase in systemic exposure to indibulin. Therefore, it was decided to discontinue this study. A plausible explanation for the low systemic exposure is the low solubility of indibulin in its current formulation. The formulation needs optimization to increase the systemic exposure upon oral administration.

Conclusion

In conclusion, the (pre)clinical studies described in this thesis show that ABC/SLC transporters, metabolic CYP enzymes and the type of drug formulation all can have a significant impact on the ADME of orally administered anticancer drugs and drug-drug interactions. Recognition of the importance of transporters, CYP enzymes and drug formulations could guide the design and development of novel oral anticancer drugs. This can probably prevent termination of drug development at later stage and accelerate the development of new oral drugs.

Samenvatting

Vandaag de dag wordt meer dan 25% van alle antikankermiddelen ontwikkeld als orale formulering. Orale toediening (via de mond) van geneesmiddelen heeft verschillende voordelen boven intraveneuze (i.v.) toediening (via de ader). Op deze manier kunnen medicijnen in de thuissituatie zelf worden ingenomen, hetgeen patiëntvriendelijk is en de kwaliteit van leven van een grote groep patiënten met kanker kan verhogen. Ook hebben patiënten geen ongemak meer van een injectie of infuus en het risico op injectie en infuus geassocieerde bijwerkingen is afwezig. Helaas hebben de meeste geneesmiddelen, wanneer ze oraal worden toegediend, een lage dan wel zeer variabele biologische beschikbaarheid en worden ongewenste geneesmiddelen interacties waargenomen in klinische studies met nieuwe orale antikanker middelen. Dit proefschrift onderzoekt de invloed van verschillende factoren, zoals de expressie en activiteit van transporters die geneesmiddelen in of uit de cel kunnen pompen (efflux (ABC) of opname (SLC) transporters), metabolisme door cytochroom P450 (CYP) enzymen en de soort formulering, op de "absorptie, distributie, metabolisme en eliminatie" (ADME) van oraal toegediende antikanker middelen. Door het gebruik van ver ontwikkelde preklinische cel en/of muis modellen (*in vitro* geneesmiddel transporter/biotransformatie assays en *in vivo* geneesmiddel transporter/CYP enzym uitgeschakelde muis modellen), kan de invloed van deze transporters en CYP enzymen op de ADME van orale medicijnen en geneesmiddelen interacties in de kliniek beter worden voorspeld. Ook kan de soort formulering (bijv. polymeer, liposoom) van belang zijn om een oraal middel met een goede orale en lage variabele biologische beschikbaarheid af te leveren. De communicatie tussen preklinisch en klinisch onderzoek is van groot belang om de farmacologie van geneesmiddelen in mensen beter te begrijpen.

ABC en SLC geneesmiddelen transporters

Afgelopen twee decennia, is er een enorme vooruitgang gemaakt in het begrijpen van de farmacologische en fysiologische rol van ABC en SLC transporters. **Hoofdstuk 1** geeft een overzicht van de invloed van ABC en SLC transporters in het maagdarmstelsel op de absorptie en distributie van oraal toegediende geneesmiddelen. De preklinische en klinische studies, beschreven in dit hoofdstuk, laten zien dat de orale biologische beschikbaarheid van medicijnen aanzienlijk kan worden verhoogd door het remmen van transport van deze geneesmiddelen door ABC transporters. Een remmer voor één of meerdere ABC transporter(s) in combinatie met een oraal antikanker middel is mogelijk een effectieve en veilige strategie, die minstens zo effectief is als een standaard i.v. toediening, in de behandeling van patiënten met kanker. Het vooraf screenen van antikankermiddelen op affiniteit voor ABC en SLC transporters is belangrijk om de absorptie van het middel door

het maagdarmstelsel te kunnen voorspellen. Dit kan bijdragen aan de ontwikkeling van nieuwe orale antikankermiddelen.

Preklinische farmacologische studies met imatinib

Hoofdstuk 2 beschrijft studies met imatinib, een oraal toegediende tyrosine kinase remmer met uitstekende antitumor activiteit in patiënten met chronische myeloïde leukemie (CML) en gastrointestinale stromale tumoren (GIST). Desondanks, ontwikkelen voornamelijk GIST patiënten vaak resistentie tegen imatinib na langdurige behandeling. Verschillende potentiële resistentie mechanismen zijn beschreven. Daarnaast zijn er veranderingen en variaties in de farmacokinetiek van imatinib waargenomen, die mogelijk de therapeutische werkzaamheid van imatinib beïnvloeden. Ondanks dat imatinib een hoge orale biologische beschikbaarheid heeft van 98%, is er een afname in de systemische blootstelling aan imatinib waargenomen en is er een hoge variabiliteit in de systemische blootstelling tussen patiënten gezien in patiënten die imatinib langdurig gebruiken.

Preklinische studies hebben aangetoond dat imatinib affiniteit heeft voor de geneesmiddelen efflux transporters "P-glycoproteïn" (P-gp; MDR1) en "Breast Cancer Resistance Protein" (BCRP; ABCG2). De expressie en activiteit van P-gp en BCRP in tumorweefsel hebben mogelijk invloed op de respons in patiënten die worden behandeld met imatinib . Echter, de exacte invloed van deze transporters op de ADME van imatinib is nog onduidelijk. Deze (pre)klinische bevindingen zijn de basis voor de uitgebreide preklinische farmacokinetiek studie, beschreven in **Hoofdstuk 2.1**. Deze studie onderzoekt nauwkeurig de rol van P-gp en BCRP in de ADME van oraal toegediend imatinib door middel van het gebruik van muizen die geen P-gp en/of BCRP eiwit aanmaken en zogenaamde controle muizen die wel beide eiwitten aanmaken. Onze resultaten laten zien dat P-gp en BCRP nauwelijks effect hebben op de ADME van imatinib in vergelijking met de metabolische eliminatie in muizen. Van deze twee drug transporters, levert P-gp de grootste bijdrage in de systemische klaring en in de beperking van de hersenpenetratie van imatinib. Opmerkelijk is dat elacridar, een remmer van P-gp en BCRP, in combinatie met imatinib een drievoudige significante toename in systemische blootstelling aan imatinib laat zien in de aan- en afwezigheid van P-gp/BCRP. Dit suggereert dat elacridar naast P-gp en BCRP ook andere eliminatie routes remt. Uit de literatuur is bekend, dat de "Organic Cation Transporter 1"(OCT1) is betrokken bij de cellulaire opname van imatinib in verschillende leukemische cellijnen. Verder is gebleken dat de expressie van OCT1 in leukemische tumorcellen van patiënten met CML lager is in patiënten met een slechte respons dan in patiënten met een goede respons op imatinib. **Hoofdstuk 2.2** laat zien dat elacridar OCT1 remt *in vitro*. Ook wordt in dit hoofdstuk aangetoond dat OCT1/2 een significant effect heeft op de farmacokinetiek van imatinib *in vivo* door het gebruik van

muizen waarbij het gen dat codeert voor OCT1/2 is uitgeschakeld. Dit OCT1/2 muismodel is door ons gekozen omdat imatinib mogelijk affiniteit heeft voor zowel OCT1 als OCT2. De aanzienlijke farmacokinetische interactie tussen imatinib en elacridar is deels te verklaren door remming van OCT1/2. De genoemde opname en eliminatie routes kunnen de waargenomen veranderingen en variaties in de farmacokinetiek van imatinib in belangrijke mate verklaren en hebben mogelijk een effect op de therapeutische werking van imatinib in patiënten.

De complexe farmacologie van imatinib wordt ook duidelijk uit de preklinische studie beschreven in **Hoofdstuk 2.3**. De basis voor deze studie was het gegeven dat imatinib in combinatie met hydroxyurea, een ribonucleotide reductase remmer, geassocieerd is met een opmerkelijke antitumor activiteit in patiënten met terugkerende glioblastome multiforme. Wij laten in dit hoofdstuk zien dat P-gp, BCRP en CYP3A4 geen effect hebben op de interactie tussen hydroxyurea en imatinib. Meer onderzoek is nodig om het mechanisme van de effectiviteit van dit regime te achterhalen. **Hoofdstuk 2.4** beschrijft de validatie van een simpele gevoelige "reversed phase high-perfomance liquid chromatographic" (HPLC) detectie methode voor de bepaling van imatinib en belangrijkste metaboliet, N-desmethyl-imatinib (CGP74588), in mens en muis. Deze methode is gebruikt om de farmacokinetiek van imatinib en CGP74588 te bestuderen in kleine volumina plasma van mensen en muizen en een serie van andere biologische matrices van muizen.

Preklinische en klinische farmacologische studies met camptothecines.

Hoofdstuk 3 beschrijft preklinische en klinische farmacologische studies met camptothecine analoge topoisomerase I remmers. Camptothecines, zoals topotecan en irinotecan, zijn belangrijke en veel gebruikte antikankermiddelen. Desondanks, hebben deze geneesmiddelen een significante beperking voor toepassing in de kliniek, omdat ze affiniteit vertonen voor BCRP en P-gp, wat vaak resulteert in tumorresistentie. Hierdoor is er een toegenomen interesse voor nieuwe camptothecines, zoals de in hoge mate lipofiele derivaten gimatecan, BNP1350 en lurtotecan, die weinig tot geen affiniteit vertonen voor deze geneesmiddelen efflux transporters. Echter, in **hoofdstuk 3.1** en **3.2,** tonen wij duidelijk aan dat de nieuwe camptothecine analoog gimatecan getransporteerd wordt door BCRP en een effect heeft op de orale farmacokinetiek en hersenpenetratie van gimatecan in muizen. Elacridar heeft ook een farmacokinetische interactie met gimatecan, deels via interactie met BCRP en deels via interactie met een andere eliminatie route. In **Hoofdstuk 3.3** wordt beschreven dat gimatecan een substraat is voor de opname transporter "Organic Anion Transporter Protein 1B1" (OATP1B1) en dat elacridar transport van gimatecan door OATP1B1 remt. Ook tonen we in deze studie aan dat andere camptothecines, zoals SN-38 (actieve metaboliet van irinotecan) en BNP1350 affiniteit hebben voor OATP1B1. Verder

blijkt uit onze *in vitro* studies dat naast elacridar ook andere veel toegepaste P-gp en/of BCRP remmers niet selectief zijn, aangezien deze remmers ook OATP1B1-gedreven transport remmen. Deze bevindingen suggereren dat het combineren van camptothecines, of andere medicijnen die affiniteit hebben voor OATP1B1, met één van de veel gebruikte P-gp/BCRP remmers een effect kan hebben op de opname, distributie en eliminatie en mogelijk op de werking en veiligheid van geneesmiddelen. In **Hoofdstuk 3.4** wordt een klinische studie beschreven met een nieuwe orale topotecan formulering. Deze nieuwe topotecan capsule is bioequivalent aan de huidige orale topotecan capsule en kan veilig worden toegediend in patiënten met solide tumoren. Voedsel heeft geen effect op de orale biologische beschikbaarheid van topotecan. Met deze studie zijn de eisen voor het registreren en het op de markt brengen van de nieuwe orale topotecan formulering vastgesteld. De orale topotecan capsule kan nu in de kliniek worden toegepast voor de voorgeschreven indicatie(s).

Preklinische en klinische farmacologische studies met taxanen

In **Hoofdstuk 4** wordt de preklinische en klinische farmacologie van de taxanen, docetaxel en paclitaxel, beschreven. Deze geneesmiddelen worden veel gebruikt in patiënten met solide tumoren, zoals long-, eierstok- en borst-tumoren, en zijn aanvankelijk ontwikkeld voor i.v. toediening, maar nu in onderzoek voor orale toepassing. **Hoofdstuk 4.1** laat zien dat ritonavir, een CYP3A/P-gp remmer, de orale biologische beschikbaarheid van docetaxel sterk verhoogd. De combinatietherapie wordt goed verdragen en het veiligheidsprofiel is acceptabel. Deze resultaten zijn veelbelovend en vormen de basis voor verdere ontwikkeling van een klinisch toepasbare orale formulering die beide middelen bevat. **Hoofdstuk 4.2** beschrijft een studie in muizen met een nieuwe orale formulering van paclitaxel ("self-microemulsifying oily formulation", (SMEOF)) zonder cremophor® EL (CrEL). CrEL wordt gebruikt in de i.v. paclitaxel (Taxol®) formulering om paclitaxel in oplossing te houden, maar heeft als nadeel dat het de absorptie remt van paclitaxel vanuit de darm. Deze studie laat zien dat SMEOF#3 een potentieel bruikbare formulering is voor de orale toepassing van paclitaxel wanneer het in combinatie wordt gegeven met cyclosporine A (CsA), een remmer van P-gp en CYP3A. Deze combinatie leidde tot een vergelijkbare systemische blootstelling aan paclitaxel in vergelijking met orale toediening van i.v. Taxol®. De ontwikkeling van nieuwe taxanen met een lage affiniteit voor P-gp lijkt een veelbelovende methode om de orale biologische beschikbaarheid te verhogen en de doordringbaarheid van paclitaxel in "multidrug" resistente tumoren te verbeteren. In **Hoofdstuk 4.3** is een klinische studie met een nieuwe orale tubuline bindende stof, indibulin, beschreven. De indibulin capsule wordt goed verdragen in een dosering tot 1200 mg per dag in patiënten met vergevorderde solide tumoren. Desondanks, wordt er een

plateau in indibulin blootstelling waargenomen voordat de maximale tolereerbare dosis bereikt wordt. Tweemaal daagse toediening in plaats van eenmaal daags had geen positief effect op de systemische blootstelling van oraal toegediend indibulin. Ook is er een hoge variabiliteit in de systemische blootstelling aan indibulin tussen patiënten waargenomen. Het is onwaarschijnlijk dat verdere verhoging van de dosis leidt tot toename in de systemische blootstelling aan indibulin. Op basis van deze conclusies is besloten om niet verder te gaan met deze studie. Een logische verklaring voor de lage systemische blootstelling is de lage oplosbaarheid van indibulin in de huidige formulering.

Samenvattend, laten de (pre)klinische studies die in dit proefschrift worden beschreven zien dat ABC/SLC geneesmiddelen transporters, CYP enzymen en de formulering van het geneesmiddel, allemaal een significante invloed kunnen hebben op de ADME van oraal toegediende antikankermiddelen en op geneesmiddelen interacties. Vroegtijdig onderzoek naar transporters, CYP enzymen en de formulering van het geneesmiddel kan de ontwikkeling van nieuwe orale antikanker medicijnen bevorderen. Dit kan mogelijk voorkomen dat de ontwikkeling van een medicijn in een laat stadium moet worden beëindigd en kan de ontwikkeling van nieuwe orale geneesmiddelen versnellen.

Dankwoord
Curriculum Vitae
List of Publications

Dankwoord

Het is klaar!! Heerlijk!! Ik had niet gedacht dat het zo'n geweldig en gelukkig gevoel zou geven, maar toch voelt het ook een beetje dubbel. Nu ik dit zit te schrijven weet ik dat mijn tijd in het NKI/AvL er echt bijna op zit en dat vind ik ontzettend jammer. Ik besef maar al te goed dat ik zonder alle leuke, behulpzame, gezellige, slimme collega's nooit zoveel geleerd had, nooit zoveel lol in m'n werk zou hebben gehad en deze prestatie nooit waar had kunnen maken! Helaas kan ik niet iedereen uitgebreid bedanken, maar ik wil een aantal mensen in het bijzonder noemen.

Allereerst wil ik de patiënten bedanken die mee hebben gewerkt aan de klinische onderzoeken. Ik heb onbeschrijfelijk veel bewondering voor de kracht en het optimisme, waarmee zij in het leven staan en aan de onderzoeken hebben meegewerkt. Ik heb op persoonlijk vlak enorm veel geleerd van deze contacten. Het heeft er toe bijgedragen dat ik meer in het NU leef, in plaats van vooral vooruit te kijken zonder van de mooie momentjes van de dag te genieten.

Mijn proefschrift was natuurlijk nooit tot stand gekomen zonder mijn promotoren Jan Schellens en Jos Beijnen en mijn co-promotor Olaf van Tellingen.

Beste Jan, ik ben je zeer dankbaar voor de kans die ik heb gekregen om preklinisch en klinisch onderzoek te combineren. Ons overleg gaf me altijd een stimulerend en motiverend gevoel, waardoor ik weer fris en enthousiast aan de slag kon. Ik heb enorm veel geleerd van de vrijheid die je me gaf om zelfstandig te werken en je kritische blik was er op de juiste momenten. Ik heb veel bewondering voor de manier, waarop je de kliniek, wetenschap, management, OIO's, je gezin en vele andere dingen op de rit weet te houden. Ondanks alle drukte heb je me altijd het gevoel gegeven dat de deur open stond.

Beste Jos, heel erg bedankt voor je altijd snelle reactie en kritische, nuttige verbeteringen in mijn manuscripten. Ook heb ik veel waardering voor de wijze waarop je alles combineert, managet en draaiende houdt. Ik ben je zeer dankbaar voor de analytische ondersteuning die je me hebt gegeven tijdens het uitvoeren van de klinische studies.

Beste Olaf, ik weet nog goed dat ik als adoptie kind bij jou, Tessa en Nienke in de groep werd opgenomen en dat voelde vanaf het eerste moment heel erg goed! Bedankt dat je me wegwijs hebt gemaakt in de "HPLC, muizen en transporter" wereld. Jouw behulpzaamheid en kritische blik, maar ook de fijne werksfeer heb ik altijd enorm gewaardeerd.

Lieve Tess, zonder jouw geweldige muizenvingertjes waren al mijn experimentjes nooit zo snel en goed uitgevoerd. Ik zal onze gezellige ochtendjes in de depressief makende, radioactieve muizenkelder niet snel vergeten. Thanks voor alle mooie en goede gesprekken die we tijdens onze warme choco's gevoerd hebben. Lieve Nienke, ik weet nog goed dat we als twee "groentjes" aan onze OIO carrière begonnen. Wat hebben we een fijne tijd gehad. Succes met de allerlaatste loodjes! Dorothé, Tiny, Marianne en alle mensen van het klinisch lab, bedankt voor de interesse, bloedafnames en hulp die jullie me hebben gegeven.

Hilde, ik heb je gezellige praatjes, je hulp en ondersteuning bij de analyses zeer gewaardeerd. Alle SLZ labgenoten (in het bijzonder Ciska, Bas, Carolien, Dieuwke, Liande, Rianne, Liia) bedankt voor alle analyses en uitwerkingen. Als ik weer eens als totale SLZ vreemdeling bij jullie aan kwam waaien met m'n witte piepschuimen doos vol met opgespaarde samples en een stapel priklijsten, stonden jullie altijd klaar om me wegwijs te maken in de GLP. Roel, geweldig hoe je de GLP op het lab in goede banen leidt; bedankt voor alle "state voorzittersessies" en vragen die ik bij je kwijt kon. Alwin, bedankt voor je hulp in de wereld van de farmakokinetiek. Ik heb veel van je snelle en kritische blik op de PK geleerd.

Lieve NP-ers en (kinetiek)verpleegkundigen: de hulp die jullie me gaven als ik weer moest multi-tasken tussen kliniek, muisjes en celletjes, was fantastisch! Nog even in het bijzonder: Ans, jouw printpapier met gele marker, Thea, jouw geweldige dansmoves, Annette, jouw prachtige schaterlach en, Rens, ons nog steeds superhecht contact zal ik niet snel vergeten! Ik heb voor iedereen van 4C enorme bewondering hoe jullie het allemaal runnen. Jammer dat ik de laatste 2 jaar weinig kinetiek meer heb gehad, maar ik krijg altijd fijne, positieve energie als ik jullie weer tegen kom. Tussen al deze vrouwen hoort natuurlijk ook m'n kinetiek maatje David thuis! Respect hoe jij je handhaaft tussen de dames! Bedankt voor alle hulp en gezelligheid in het kinetiekhok; we waren een mooi team.

Lieve Marja, hoe houd je toch alle klinische studies op de rit? Bedankt voor alle interesse, lieve mailtjes en voor onze fijne samenwerking. Alle mensen van het trialbureau: de deur stond altijd open voor alle vraagjes die ik had omtrent de klinische studies. Bedankt voor de hulp! Cecile en Brigitte, jullie QA en GCP kennis is geweldig; daar heb ik veel van geleerd. Ik ben door jullie een stuk preciezer geworden! Lieve Jolanda, zonder jou waren veel regeldingen rond mijn promotie in de soep gelopen. Jouw altijd rustige houding, behulpzaamheid en luisterend oor heb ik erg kunnen waarderen. Lieve Dilsha, ik vind het super leuk dat we nog steeds af en toe afspreken en bijkletsen.

Hennie en Theo: een geweldig duo zijn jullie. Bedankt voor alle uurtjes die ik bij jullie in de kelder heb mogen doorbrengen; succes met de verhuizing! Alle proefdierverzorgers wil ik bedanken voor de verzorging van alle muisjes!

Mijn directe kamergenoten hebben mij een supertijd in het NKI bezorgd. Ik heb er veel zien komen en gaan, maar denk dat "Fieltcamp" en "de Dickmeister" de mannen zijn waar ik het langst mee heb doorgebracht. Sander, 3 jaar lang mijn rechter buurman: ik denk dat je weleens gek werd van m'n kletspraatjes; maar wat een goede tijd hebben we gehad, vol humor en een bizarre LA reis om nooit te vergeten. Ik ben je erg dankbaar voor de enorme hulp bij mijn promotie! Dick, jouw "grunningse" nuchterheid en humor vind ik geweldig! Je staat altijd voor iedereen klaar, zelfs voor mijn "dom blondje" computer vragen, die ik regelmatig stelde. Maarten, af en toe heb ik wel medelijden met je gehad tussen alle vrouwenpraat. Ik ben je slechte grappen steeds leuker gaan vinden; bedankt voor de gezellige tijd, succes met je laatste jaar; komt helemaal goed! Lot, ondanks dat we nog niet zolang collega's zijn, voelt het of we elkaar al jaren kennen. Ik heb heel veel aan je gehad in dit laatste halfjaar. Laten we de gezellige etentjes er in blijven houden! Monique, Marije en Stefan, bedankt dat jullie me wegwijs hebben gemaakt op H6. Het was een mooie tijd!

Serena, Suzanne, Valerie en Arthur, succes in de toekomst! Irma en Stefan, ook al zaten jullie in Utrecht, bedankt voor de kennis en de hulp die we af en toe konden uitwisselen.

Ik wil, naast de Schellens, uiteraard ook een klein woordje tot de Schinkeltjes richten, want zonder jullie transporter en CYP kennis was ik een stuk minder ver gekomen! Marijn, bedankt voor de geweldige LA tijd en fijne kletsjes; die houden we erin! Evita onze samenwerking was briljant. Ik zal ons "sexy" artikeltje niet snel vergeten. Jurjen en Robert, jullie onderbroeken-lol en interesse zijn zeker altijd gewaardeerd. Els, bedankt voor al je belangstelling en natuurlijk de hulp met de OCT muisjes! Corina, je hulp bij de transwell experimentjes was erg fijn. Beste Alfred, heel erg bedankt voor al je kennis, suggesties, snelle reacties en kritische blik op het onderzoek.

En dan, Kokkie!! Toch mooi dat we als OIO nichtjes op dezelfde afdeling terecht zijn gekomen. De biertjes in café "de Truffel" na de stafavonden waren geestverruimend. Haha, ik vind onze conversaties en familie onderonsjes altijd geweldig. Dat er nog maar veel mogen volgen!
Natuurlijk heb ik ook een mooie tijd met vele anderen van H6 gehad. Sari en Monique, laten we de Amsterdamse etentjes erin houden. Succes met jullie onderzoek! Richard en Hugo, jullie bulderende geschater zal ik niet snel vergeten! Saske, Marion, bedankt voor alle gezellige lunchjes. Dat we nog maar veel gaan hardlopen! Thea, jouw organisatorische brein achter veel dingen is onmisbaar! Hans te P, jouw inzet om H6 draaiende te houden is super. Alle andere Beggs, Stewarts, van 't Veer en v.d. Vijvers: bedankt voor alle gezellige lab-uitjes, squash-sessies, H6- borreltjes, kerstdiners!

Naast de H6-ers, wil ik ook een speciaal woordje aan de geweldige OIO's uit de Keet richten. Joehoe (speciaal voor Joost)!! Al voelde ik me af en toe een aanhangsel, ik baal er enorm van dat ik jullie moet verlaten. Wat een geweldig gezellig, energierijk stel zijn jullie! Bedankt voor de mooie hardloopwedstrijdjes, biertjes in "de Rooie", zeilweekendjes met de "Amstel Live cover band" en de honderden kopjes koffie!! Reken maar dat jullie nog niet van me af zijn!
Lytje, Roberto, Anthe, en Ronnie, het Zweedse weekendje, twee weken voor m'n deadline, was niet verstandig maar wel super! Ik zal de rendierworst, liederentafel en schnaps bij de Zweedse promotie, hoeree hoeree, niet snel vergeten!
Natuurlijk zijn veel promovendi, waar ik ook een super tijd mee heb gehad, mij voorgegaan. Tessa, Anthe, Jeany, Wandena, Suu, ik vind het leuk dat we elkaar af en toe nog zien en bijkletsen! Maartje en Annelies het "Dr.-Trio" is bijna rond. Tijd voor een etentje!

B7, helaas heb ik de tijd niet meer om jullie beter te leren kennen, maar jullie Nespresso apparaat hield mij op de been! Ik weet zeker dat we als groep goed terecht zijn gekomen!

Uiteraard heb ik de afgelopen jaren me niet alleen met collega's vermaakt, maar zijn vrienden en familie ook van groot belang geweest om Rosie, alias Dr. Vogel (in spé), door dit hele traject heen te trekken. Lieve Mo'tje en Boersie, ik had jullie graag als een soort ceremoniemeesters bij m'n promotie gehad, maar helaas laten de tradities dit niet toe. Thanks voor alle goede gesprekken en de enorme positieve energie die ik van jullie krijg. Maar ook niet te vergeten: alle ontspanningsavondjes en -feestjes. Jullie zijn Toppertjes!! Sannie, zonder jouw creatieve talent en geweldige lieve hulp was dit proefschrift veel

minder mooi geworden, je bent een schat! Roelsie, de komende twee maanden gaan de dametjes nog veel mooie ontspanningsmiddagen maken. Daar heb ik nu eindelijk tijd voor! De rest van m'n lieve cluppie wil ik persoonlijk bedanken met een handgeschreven noot voorin het proefschrift. Ik ben natuurlijk net zo blij met jullie allemaal. Dat we nog maar van veel moois mogen genieten met z'n allen! Alle andere lieve vriendinnen, vrienden en hockeyteam, thanks voor alle belangstelling voor de voor jullie vaak onbegrijpelijke "Rosie-materie". De ontspanning, afleiding, mooie feestjes, vakanties hebben er voor gezorgd dat ik altijd vol energie en enthousiasme dit traject heb gelopen!

Lieve Huub, ik ben bang dat jij misschien nog wel het meest van mijn promotiestress hebt meegemaakt. Desalniettemin hebben we samen een hele mooie en fijne tijd gehad. Hiervoor bedankt, het zal altijd in mijn herinnering blijven.
Lieve Inge, je interesse in het vakgebied van Jaap en mij moet voor jou wel eens een enorme opgave zijn. Respect!! Ik beloof je dat de promotiepraat achter slot en grendel gaat. Ik ben enorm blij met jou en nu als "echte Oostendorp" hoop ik dat we nog maar veel moois gaan beleven! Guido, alias willie wortel, heel erg bedankt voor alle hulp bij vele dingen. Jouw altijd positieve instelling kan ik enorm waarderen. Op naar jouw Dr. titel! Hopelijk kunnen Jaap en ik je dan een keer helpen.
Roelie, bedankt voor je belangstelling in mijn onderzoek.

En dan natuurlijk mijn paranimfen! Naast Dr. Japie hebben we nu ook bijna een Dr. Rosie. Ja, ja, je kleine zusje is je wederom gevolgd. Ik vind het super dat je mijn paranimf wilt zijn. Als "big brother" heb ik enorm veel aan je gehad en veel van je geleerd. En naast de serieuze dingen ben ik ook altijd enorm blij met de gemeenschappelijk "Oostendorp" humor, waar we zelf altijd het hardst om kunnen lachen! We maken er een topdag van!
Lieve Lytje T, "gekke" Vietnamees, wat hebben we mooie jaren gehad saampies, vol gezelligheid en serieuze momenten tijdens onze ontelbare koffietjes/ijsjes. Dat we samen nog maar veel fijne uren als promotie/hardloopmaatjes gaan beleven. Op naar jouw promotie en natuurlijk de marathon van NY!

Lieve Pap en Mam, een stelletje "bijzondere" kinderen hebben jullie op de wereld gezet. Wie had ooit gedacht dat jullie een Dr^2 zouden produceren!! Bedankt voor jullie enorme belangstelling, luisterend oor en steun in dit voor jullie onbekende, soms bizarre wereldje. Lieve Pap, ik kan de gezellige etentjes, zeilbootavonturen en je altijd verrassende krantenknipsels erg waarderen.
Lieve Mamsie, zonder jouw wijze raad, humor, vrolijkheid, geduld, steun en ontspanningsdagjes had dit afgelopen halfjaar nooit tot deze prestatie kunnen leiden. Mijn dank is groot!!!

Ik denk dat ik nu toch echt moet afsluiten. Mijzelf kennende, had deze kletskous nog uren door kunnen gaan. Nog éénmaal: voor iedereen, ook degene die ik vergeten ben, BEDANKT VOOR ALLES. Ik hoop dat we de 21ste met z'n allen een borrel kunnen drinken en kunnen proosten niet alleen op mij, maar ook op jullie. Want zonder jullie had ik deze klus nooit kunnen klaren!

Rosie

Amsterdam, November 2008

Roos Oostendorp werd op 6 juni 1978 geboren te Deventer. In 1997 behaalde ze haar VWO diploma aan het Overgelder College te Deventer. Vervolgens studeerde ze in Groningen en Farmacochemie aan de Vrije Universiteit van Amsterdam. Gedurende haar studie werden verschillende wetenschappelijke stages volbracht bij de afdeling Genetica, Erasmus Universiteit Rotterdam (Prof. J.H.J. Hoeijmakers); de afdeling moleculaire toxicologie, Vrije universiteit, Amsterdam (Prof. N.P.E. Vermeulen); de afdeling moleculaire farmacologie, Vrije Universiteit, Amsterdam (Prof. R. Leurs) en een farmaceutische industrie stage bij Pfizer Global, UK (Dr. R. Russel). In 2004 behaalde ze haar doctoraal. In dat zelfde jaar begon zij aan het promotieonderzoek dat is beschreven in dit proefschrift, onder begeleiding van Prof. Dr. J.H.M. Schellens, Prof. Dr. J.H. Beijnen en Dr. O. van Tellingen.

List of Publications

Articles marked with an asteric (*) relate to the work described in this thesis

1.* **Oostendorp RL**, Buckle T, Beijnen JH, van Tellingen O, Schellens JHM. The role of Organic Cation Transporter 1 and 2 in the *in vivo* pharmacokinetics of imatinib. *Submitted for publication*

2.* **Oostendorp RL**, van de Steeg E, Beijnen JH, Schinkel A, Schellens JHM. OATP1B1 mediates transport of gimatecan and BNP1350 and can be inhibited by several classical BCRP and/or P-gp inhibitors. *Submitted for publication*

3.* **Oostendorp RL**, Huitema A, Rosing H, Jansen RS, ter Heine R, Beijnen JH, Schellens JHM. Co-administration of ritonavir strongly enhances the apparent oral bioavailability of docetaxel. *Submitted for publication*

4.* Koolen SLW, **Oostendorp RL**, Beijnen JH, Schellens JHM, Huitema ADR. Population pharmacokinetics of intravenously and orally administered docetaxel with or without co-administration of ritonavir in patients with advanced cancer. *Submitted for publication*

5.* **Oostendorp RL**, Witteveen PO, Schwartz B, Beijnen JH, Voest EE, Schellens JHM. Dose-finding and pharmacokinetic study of orally administered indibulin (D-24851) to patients with advanced solid tumors. *Submitted for publication*

6.* Marchetti S, **Oostendorp RL**, Pluim D, van Tellingen O, et al. *In vivo* implications of BCRP/P-gp deletion on the pharmacokinetics of gimatecan (7-t-butoxyiminomethylcamptothecin). *Submitted for publication*

7* **Oostendorp RL**, Loftiss J, Goel S, Smith DA, et al. Bioequivalence study of a new oral topotecan formulation relative to the current topotecan formulation in patients with advanced solid tumors. *International Journal of Clinical Pharmacology and Therapeutics 2008 (in press)*

8* **Oostendorp RL**, Buckle T, Beijnen JH, van Tellingen O, Schellens JHM. The effect of P-gp (Mdr1a/1b), BCRP (Bcrp1) and P-gp/BCRP inhibitors on the *in vivo* absorption, distribution, metabolism and excretion of imatinib. *Invest New Drugs 2008 (in press)*

9* **Oostendorp RL**, Beijnen JH, Schellens JHM. The biological and clinical role of drug transporters at the intestinal barrier. *Cancer Treatment Reviews 2008 (in press); ABC transporters and Multi Drug Resistance. Edited by Bourmendjel A, Boutonnat J, Robert J; Medicinal Research Reviews series published by Willy 2008 (in press)*

10* Marchetti S, **Oostendorp RL**, Pluim D, van Eijndhoven M, van Tellingen O, et al. *In vitro* transport of gimatecan (7-t-butoxyiminomethylcamptothecin) by breast cancer resistance protein, P-glycoprotein, and multidrug resistance protein 2. *Mol Cancer Ther 2007 Dec;6:3307-13*

11* van Erp NP, **Oostendorp RL,** Guchelaar HJ, Schellens JH, Gelderblom H. Is rectal administration an alternative route for imatinib? *Cancer Chemother Pharmacol 2007 Sep;60(4):623-4*

12* **Oostendorp RL**, Beijnen JH, Schellens JH, Tellingen O. Determination of imatinib mesylate and its main metabolite (CGP74588) in human plasma and murine specimens by ion-pairing reversed-phase high-performance liquid chromatography. *Biomed Chromatogr 2007 Jul;21(7):747-54*

13* **Oostendorp RL**, Marchetti S, Beijnen JH, Mazzanti R, Schellens JH. The effect of hydroxyurea on P-glycoprotein/BCRP-mediated transport and CYP3A metabolism of imatinib mesylate. *Cancer Chemother Pharmacol 2007 May;59(6):855-60*

14 Niedernhofer LJ, Garinis GA, Raams A, Lalai AS, Robinson AR, Appeldoorn E, Odijk H, **Oostendorp R**, et al. A new progeroid syndrome reveals that genotoxic stress suppresses the somatotroph axis. Nature 2006 Dec 21;444(7122):1038-43.

15 Haringman JJ, **Oostendorp RL**, Tak PP. Targeting cellular adhesion molecules, chemokines and chemokine receptors in rheumatoid arthritis. *Expert Opin Emerg Drugs 2005 May;10(2):299-310. Review*